July 2016

Neoarchean Arc Magmatism, Subsequent Collisional Orogenesis, and Paleoproterozoic Disruption within the Western Churchill Province: Implications for the Growth and Modification of Lower Continental Crust

Sean P. Regan
University of Massachusetts - Amherst

NEOARCHEAN ARC MAGMATISM, SUBSEQUENT COLLISIONAL OROGENESIS, AND PALEOPROTEROZOIC DISRUPTION WITHIN THE WESTERN CHURCHILL PROVINCE: IMPLIACATIONS FOR THE GROWTH AND MODIFICATION OF LOWER CONTINENTAL CRUST

A Dissertation Presented

By

SEAN P. REGAN

Submitted to the Graduate School of
The University of Massachusetts Amherst in partial fulfilment
of the requirements for the degree of

DOCTOR OF PHILOSOPHY

May 2016

Geosciences

NEOARCHEAN ARC MAGMATISM, SUBSEQUENT COLLISIONAL OROGENESIS, AND PALEOPROTEROZOIC DISRUPTION WITHIN THE WESTERN CHURCHILL PROVINCE, CANADA: IMPLICATIONS FOR THE GROWTH AND MODIFCATION OF LOWER CONTINENTAL CRUST

A Dissertation Presented

By

SEAN P. REGAN

Approved as to style and content

_____
Michael L. Williams, chair

_____
Michael J. Jercinovic, member

_____
Sheila J. Seaman, member

_____
Kevin Mahan, member

_____
Laurie Brown, member

_____
Rolf Karlstrom, external member

_____
Julie Brigham-Grette, Department head
Geosciences

ACKNOWLEDGEMENTS

First and foremost, I would like to extend a special thanks to my advisor, Dr. Michael L. Williams for constant patience, support, and an undying enthusiasm for my education. He has been a phenomenal advisor and mentor, and has made a serious impact on both my personal and professional life. Dr. Michasel J. Jercinovic has aided in numerous ways and both facilitated much of the data acquired herein, and also taught me how to be a good analyst. The entire research group at the University of Massachusetts, Amherst has been a constant source of peer support and I have gained much insight in various discussions, interactions, and seminars. These people include: Dr. Chris Koteas, Dr. Julien Allaz, Jeffrey R. Webber, Amanda VanLankvelt, Calvin Mako, Phillip S. Geer, and Claire Pless. Dr. Kevin H. Mahan (CU Boulder) has been an excellent external mentor and impactful on my education despite his location approximately 2000 miles away. Greg Walsh (USGS) has contributed a great deal of time and resources in support of completion of the below work. Excellent field support and friendship is owed to Mark E. Holland, and Omero F. Orlandini.

This work was funded by several sources. Primary funding came from the National Science Foundation (NSF) research grants EAR-0948560 awarded to Kevin H. Mahan and Dr. Michael L. Williams, EAR-1045515 awarded to Laurie Brown. Other sources of funding were two student research grants awarded to Sean P. Regan. Also, five student research awards from the Department of Geosciences, University of Massachusetts, Amherst have supported various components of the presented research. Many others have contributed to this dissertation including best friends and colleagues Jeffrey Chiarenzelli and Mark Holland.

All the work presented herein is collaborative. Chapter 2 was published in the Canadian Journal of Earth Sciences with coauthors: Dr. Michael L. Williams, Shannon Leslie, Dr Kevin Mahan, Dr. Michael Jercionivic, and Mark Holland. Chapter 3 is currently being prepared for

submission to Geology with coauthors Michael L. Williams, Michael Jercinovic, and Matthew Wielicki (University of California, Los Angeles). The fourth chapter will be submitted in the next several months to Precambrian Research with coauthors Dr. Michael L. Williams, Dr. Kevin H. Mahan, Dr. Greg Dumond, Dr. Michael J. Jercinovic, and Omero Felipe Orlandini. The final chapter is a 'work in progress' but will likely be submitted to Precambrian Research with coauthors Dr. Jeffrey R. Chiarenzelli, Dr. Michael L. Williams, Dr. Lawrence Aspler, and Dr. Michael J. Jercionivc.

ABSTRACT

NEOARCHEAN ARC MAGMATISM, SUBSEQUENT COLLISIONAL OROGENESIS, AND PALEOPROTEROZOIC DISRUPTION WITHIN THE WESTERN CHURCHILL PROVINCE, CANADA: IMPLICATIONS FOR THE GROWTH AND MODIFICATION OF LOWER CONTINENTAL CRUST

MAY 2016

SEAN P. REGAN, B.S., ST. LAWRENCE UNIVERSITY

M.S., UNIVERSITY OF MASSACHUSETTS, AMHERST

Ph.D., UNIVERSITY OF MASSACHUSETTS, AMHERST

Directed by: Professor Michael L. Williams

The growth and modification of continental lithosphere are fundamental geologic processes that have had a profound effect on Earth's evolution. The lower continental crust can play a myriad of roles pertaining to these processes depending on the strength, age, temperature, and composition of the rocks present. However, the lower continental crust is impossible to sample in-situ, and thus observations of modern lower continental crust are limited to seismic studies and xenolith studies, which provide mere snap shots of the lower crust. High pressure granulite terranes provide 4 dimensional, and spatially resolvable, analogues of lower continental crust. The Athabasca granulite terrane (AGT), along the eastern margin of the Rae subprovince of the western Churchill Province, is underlain by >20,000 km^2 of high pressure granulite, and is arguably to be the largest intact exposure of lower continental crust in the North America. Work presented herein provides a detailed temporal and tectonic framework for interpreting rocks of the AGT, and evaluates rocks ca. 400 km along strike to test for spatial consistency. Results suggest that the Paleoproterozoic involved the juxtaposition of various lithotectonic blocks along major ductile shear zones that vary in metamorphic conditions, timing and kinematics. Sinistral kinematics within the Cora Lake shear zone within the AGT, for instance, are explained by accretion of the Lynn-Lake and La Ronge arcs along the southern periphery of the Churchill

Province at ca. 1.88 Ga at the waning phases of granulite-facies conditions. Ca. 1.9 Ga deformation involved upright folding, and the development of a regionally extensive dextral transpressive fabrics, and appears to be spatially related to the Chipman dike swarm. This event may have been driven by accretionary and collisional tectonics between the Slave and western Churchill Province. IN-SIMS micro zircon geochronology suggests a ca. 2.1 Ga emplacement age for the Chipman dikes, and may be indicative of an incipient rift, which was the locust for ca. 1.9 Ga reactivation. Preceding these events was a major crustal thickening event that occurred immediately after widespread arc-like magmatism interpreted to represent early subduction and subsequent collisional orogenisis. Rocks along strike, 400 km to the northeast of the AGT, share a similar Neoarchean history, and dike swarm, but contain little evidence of regionally extensive Paleoproterozoic granulite-facies reactivation. The reasoning for this is unknown at current, but perhaps it is due to an increasing distance from the bounding Paleoproterozoic orogens. These data provide a four dimensional framework to evaluate changes in lower crustal properties and behavior for greater than 600 my.

TABLE OF CONTENTS

Page

LIST OF TABLES

Table **Page**

LIST OF FIGURES

Figure **Page**

CHAPTER 1

INTRODUCTION

Introduction

The material properties of lower to middle continental crust exert fundamental controls on the growth and evolution of continental lithosphere (Rutter and Brodie, 1992; Beaumont et al., 2006). These properties influence melt production and transport, strain distribution and partitioning, and the height and geometry of mountain belts. However, the middle to lower continental crust is inherently impossible to sample in-situ, and observation techniques are limited to seismic interpretation (Holbrook et al., 1992), xenoliths (Percival, 1992; Rudnick and Fountain, 1995), numeric models (Beaumont et al., 2006), and exhumed granulite facies terranes (Mezger, 1992). All of these methods, except exhumed granulite terranes, are limited in that they provide mere "snap shots" of these inaccessible regions, and offer little information about how the material properties change through time. Granulite terranes, however, can preserve the spatial, structural, and geologic relationships that were present at depth. These attributes provide a four – dimensional window into the processes operating at levels currently inaccessible, and thus insight into how these properties evolve through time.

The Athabasca granulite terrane (AGT) in northern Saskatchewan is underlain by high pressure granulite (> 1.0 GPa) that extends over an area > 20,000 km^2 (Williams et al., 2009; Dumond et al., 2010). Located within the eastern Rae subprovince (or domain) of the western Churchill Province, the AGT has been argued that the region is the largest intact exposure of lower continental crust in North America (Dumond et al., 2013), and thus represents a natural laboratory to study lower continental crust (Mezger, 1992; Williams et al., 2009). Furthermore, given the age of all exposed rocks (Mesoarchean to Paleoproterozoic) within the Athabasca

granulite terrane, the region also provides an opportunity to study early styles of plate tectonics, and how these processes generated and modified continental crust through geologic time.

The AGT contains evidence of experiencing two phases of regionally extensive deformation at ca. 2.56 and 1.9 Ga (Mahan et al., 2006a,b; Williams et al., 2009; Dumond et al., 2010), both of which correspond to the development of granulite facies metamorphic assemblages and fabrics (Williams et al., 1995; Flowers et al., 2006a). Although portions of the western AGT contain evidence for ca. 2.1 Ga surficial exposure, and thus had to be uplifted between the two main phases of deformation (Bethune et al., 2012). Other regions, like the Tontato domain (after Gilboy, 1980; East Athabasca mylonite triangle of Hanmer et al., 1994) are interpreted to have remained within the lower continental crust in the interim (Williams et al., 2009). Therefore, these regions have been the focus of inquiry regarding the growth and modification of lower continental crust for over a decade (Williams et al., 2009)

The Snowbird Tectonic zone is a ca. 2800 km geophysically defined lineament that bisects the western Churchill Province (Ross, 1994). Initially interpreted as the boundary between Rae and Hearne subprovinces of the western Churchill Province, Hoffman (1988) tentatively interpreted the anomaly as a collisional suture between the two that formed at ca. 1.9 Ga. The Snowbird Tectonic Zone has remained an enigmatic albeit controversial geologic feature, and of relatively unrecognized significance. It has been interpreted as 1) a Paleoproterozoic suture (Hoffman, 1988; Berman et al., 2007), 2) an Archean intracontinental strike-slip shear system (Hanmer et al., 1994), and 3) an anastomosing tapestry of strike-slip and reverse-oblique shear zones active during the Paleoproterozoic (Mahan and Williams, 2005). Debate persists regarding these hypothesis, which are critical pieces of information pertaining to the geologic context of the AGT.

The aim of this dissertation is to understand the origin of the lateral heterogeneity within the Athabasca granulite terrane (Cora Lake shear zone), directly date the Chipman dike swarm, which has thought to be ca. 1.9 Ga and responsible for major Paleoproterozoic reactivation (Flowers et al., 2006a), integrate geochemistry with P-T-t-D paths to put Neoarchean magmatism and tectonism into a tectonic framework, and to assess the continuity of these features along strike to Angikuni Lake, Nunavut. Collectively, these data will provide a clear picture of how the rocks of the Athabasca granulite terrane formed and evolved during the Neoarchean, and how the rocks were modified during Paleoproterozoic tectonism. Furthermore, data will also add to ongoing work discerning plate-tectonic styles into the Neoarchean.

Purpose and General Approach

The work discussed below has been carried out within two main subdomains of the Athabasca granulite terrane: The northwestern and Chipman subdomains. Data ranges from structural analysis, quantitative thermobarometry, forward petrologic modelling, in-situ monazite U-Th-total Pb geochronology, whole rock major and trace element geochemistry, and U-Th-Pb zircon analysis including IN-SIMS (in-situ secondary ionization mass spectrometry) and LA-ICP-MS (Laser ablation inductively coupled plasma mass spectrometry) analyses. Collectively, these methods were designed to answer specific questions pertaining to the larger goal, and yield insight into the various structural, metamorphic, and tectonic features of the region.

Dissertation Organization

This dissertation is subdivided into four main chapters (Chapters 2-5), each of which provide insight into the temporal and spatial evolution of the region while it was in the lower continental crust. All chapters are organized as independent contributions designed to be, or have been already, submitted to peer-reviewed journals. Therefore, background and some descriptions will be repeated in each chapter.

Chapter 2 discusses work done along the Cora Lake shear zone, which subdivides the Northwestern and Chipman subdomains, and represents a major thermobarometric discontinuity (Mahan et al., 2008). Perhaps most interesting about the Cora Lake shear zone, however, are the pervasive sinistral kinematics, unlike immediately surrounding wall rock and other major shear zones. Work presented within Chapter 2 consists of field data, metamorphic petrology, microstructural analysis, thermobarometric analysis, and in-situ monazite geochronology of the Cora Lake shear zone and immediate wall rocks. Results suggest that the Cora Lake shear zone formed at the waning phases of granulite facies metamorphism and juxtaposed the Northwestern and Chipman subdomain at ca. 1.88 Ga. P-T paths of each subdomain converge within the shear zone. The anomalous kinematics present within the Cora Lake shear zone are interpreted in terms of evolving collisional events on the western and southern margins of the Churchill Province.

Chapter 3 discusses results from in-situ U-Pb geochronology of the Chipman dike swarm. Long considered as having been emplaced at ca. 1.9 Ga during transpressive, and widespread, deformation of the AGT, the Chipman dike swarm has remained undated. Owing to basic composition and a pervasive granulite-grade, and locally migmatitic, overprint, primary zircon is difficult to find, and has predominately been converted to metamorphic zircon. Sampling of coarse dike centers, pegmatitic regions, and relatively low strain Chipman dikes facilitated the identification of micro zircon in-situ. One grain contained igneous morphology and composition. Once drilled out of the thin section, several grains were analyzed via Secondary Ionization Mass Spectrometry (SIMS). Analysis yielded a ca. 2.12 Ga age, ca. 200 my older than initially thought. Similar in composition and isotopically identical to the ca. 2.11 Ga Griffin gabbros in the central Hearne subprovince, the Chipman dikes are interpreted as distal correlatives. The dikes may represent the extensional event recognized throughout the Churchill Province.

The tectonic setting of Neoarchean plutonic rocks and subsequent tectonism has persisted as enigmatic. Chapter 4 presents geochemical data from a transect across the ca. 2.6 Ga plutonic

rocks exposed throughout the Northwestern subdomain. Along with this data, in-situ monazite geochronology of rocks within the northwestern and Chipman subdomains is presented and linked to forward petrologic models. Collectively these results show that ca. 2.6 Ga plutonic rocks are arc related, and that arc construction was followed by a long period of high pressure granulite facies tectonism. Deformation involved crustal thickening and lateral flow of the lower continental crust (Dumond et al., 2010). This series of events is interpreted in terms of active margin processes, where early arc construction is followed by collisional orogenisis and the generation of syn-collisional leucogranites (migmatites).

The final chapter, Chapter 5, presents preliminary field and geochronologic data from Angikuni Lake, Nunavut. Also situated along boundary between Rae and Hearne subprovinces, Angikuni Lake is 200 km northeast of the AGT. The Angikuni Lake region is the location where the Hearne, Rae, and newly designated Chesterfield (Berman et al., 2007) sutures have been drawn, which is interpreted to represent a Neoarchean boundary between Rae-Chesterfield, and a Paleoproterozoic suture between Hearne and Rae-Chesterfield composite blocks (Berman et al., 2007). LA-ICP-MS zircon analysis of two plutonic, and two detrital samples paired with field and existing geochemical data suggest that the rocks of Angikuni Lake were host to both Neoarchean and Paleoproterozoic tectonism, but show little evidence for substantial crustal thickening during the Paleoproterozoic. Similar to rocks of the AGT, Paleoproterozoic strain is localized within, and perhaps reactivating, major shear zones that juxtapose individual crustal blocks (Aspler et al., 1999).

Summary

Analysis presented below combines several fields of geologic inquiry, and uses an integrated approach to address specific problems regarding geologic process including: 1) the processes that govern the growth and modification of lower continental crust; 2) the role of deformation at strengthening the lower continental crust; 3) the longevity of preexisting

weaknesses at focusing lithospheric-scale strain; 4) the recognition of horizontal plate-tectonic styles into the Neoarchean; and 5) the integration of field, structural, metamorphic, geochemical, and geochronologic datasets to constrain temporal evolution of Precambrian gneiss terranes. The AGT contains a block style architecture, and understanding when and at what conditions the juxtaposition of disparate lithotectonic took place is critical for constraining the initial geometries of the region, and of Precambrian gneiss terranes in general. Variations in kinematics, P-T conditions, and timing of shear zones can yield insight pertaining to the ongoing tectonic processes. Constraining the timing and tectonic setting of major igneous suites is a fundamental component of gneiss terranes, and can have a myriad of effects on host rocks. Lastly, the Snowbird Tectonic Zone is one of the major discontinuities within the Western Churchill Province, and remains of uncertain geologic significance. Work at Angikuni Lake and in the AGT provides insight testing current tectonic hypotheses. Furthermore, the research approached outlined below provides an example of how various types of datasets can yield critical information regarding the temporal and spatial evolution of large Precambrian gneiss terranes.

References

Beaumont, C., Jameison, R.A., Nguyen, M.H., and Medvedev, S., 2004, Crustal channel flows: 1. Numerical models with applications to the tectonics of the Himalayan-Tibetan orogen: Journal of Geophysical Research, v. 109, B06406, doi:10.1029.2003JB002809.

Berman, R.G., Davis, W.J., and Pehrsson, S., 2007, Collisional Snowbird tectonic zone resurrected: Growth of Laurentia during the 1.9 Ga accretionary phase of the Hudsonian orogeny: Geology, v. 35, n. 10, p. 911-914, doi:10.1130/G23771A.1.

Bethune, K.M., Berman, R.G., Rayner, N., and Ashton, K.E., 2013, Structural, petrological and U-Pb SHRIMP geochronological study of the western Beaverlodge domain: Implications for crustal architecture, multi-stage orogenesis and the extent of the Taltson orogen in the SW Rae craton, Canadian Shield: Precambrian Research, v. 232, p. 89-118.

Chapman, D.S., and Furlong, KI.P., 1992, Thermal state of the continental crust: Continental Lower Crust, Ed(s) D.M. Fountain et al., p. 179-198, Elsevier, Berlin.

Dumond, G., Goncalves, P., Williams, M.L., and Jercinovic, M.J., 2010, Subhorizontal fabric in exhumed continental lower crust and implication for lower crustal flow: Athabasca granulite terrane, Western Canadian Shield: Tectonics, v. 29, TC2006, doi:10.1029/2009TC002514.

Dumond, G., Mahan, K.H., Williams, M.L., and Jercinovic, M.J., 2013, Transpressive uplift and exhumation of continental lower crust revealed by synkinematic monazite reactions: Lithosphere, v. 5, n. 5, p. 507-512, doi: 10.1130/L292.1

Flowers, R., Bowring, S.A., Mahan, K.H., and Williams, M.L., 2006a, Timescales and significance of high pressure, high-temperature metamorphism and mafic dike anatexis, Snowbird tectonic zone, Canada: Contribution to Mineralogy and Petrology, v. 151, n. 5, p. 558-581, doi:10.1007/s00410-006-0066-7.

Dumond, G., Mahan, K.H., Williams, M.L., and Jercinovic, M.J., 2013, Transpressive uplift and exhumation of continental lower crust revealed by synkinematic monazite reactions: Lithosphere, v. 5, n. 5, p. 507-512, doi: 10.1130/L292.1

Gilboy, C.F., 1980, Bedrock compilation geology: Stony Rapids area (NTS 74p)-Prelimanary geological map, scale 1:250,000, Sask. Geol. Surv., Sask. Energy and mines, Regina.

Hanmer, S., Parrish, R., Williams, M., and Kopf, C., 1994, Striding-Athabasca Mylonite: Complex Archean deep crustal deformation in the East Athabasca mylonite triangle, N. Saskatchewan: Canadian Journal of Earth Sciences, v. 31, p. 1287-1300, doi:10.1139/e94-111.

Hoffman, P.F., 1988, United Plates of America, the birth of a craton: Early Proterozoic assembly and growth of Laurentia: Annual Review of Earth and Planetary Sciences, v. 16, p. 543-603, doi:10.1146/annurev.ca.16.050188.002551.

Mahan, K.H., and Williams, M.L., 2005, Reconstruction of a large deep-crustal terrane: Implication for the Snowbird tectonic zone and early growth of Laurentia: Geology, v. 33, n. 5, p. 385-388, doi:10.1130/G21273.1.

Mahan, K.H., Goncalves, P., Williams, M.L., and Jercinovic, M.J., 2006a, Dating metamorphic reactions and fluid flow: Application to exhumation of high-P granulites in a crustal-scale shear

zone, western Canadian Shield: Journal of Metamorphic Geology, v. 24, n. 3, p. 193-217, doi:10.1111/j.1525-1314.2006.00633.x.

Mahan, K.H., Williams, M.L., Flowers, R.M., Jercinovic, M.J., Baldwin, J.A., and Bowring, S.A., 2006b, Geochronological constraints on the Legs Lake shear zone with implications for regional exhumation of lower continental crust, western Churchill Province, Canadian Shield: Contributions to Mineralogy and Petrology, V. 152, n. 2, p. 223-242, doi:10.1007/s00410-006-0106-3.

Percival, J.A., 1992, Exposed crustal cross sections as windows on the lower crust: in Continental Lower Crust, ed(s): D.M. Fountain et al., pp. 317-362, Elsevier, Amsterdam.

Ross, G.M., Broome, J., and Miles, W., 1994, Potential fields and basement structure – western Canada sedimentary basin: *in* Geological Atlas of the Western Canada Sedimentary Basin, G.D. Mossop and I. Shetsen (comp.), Canadian Society of Petroleum Geologists and Alberta Research Council, URL <http://www.ags.gov.ab.ca/publications/wcsb_atlas/atlas.html>, [Date last accessed online].

Rudnick, R.L., and Fountain, D.M., 1995, Nature and composition of the continental crust: A lower crustal perspective: Reviews of Geophysics, v. 33, n. 3, p. 267-309.

Rutter, E.H., and Brodie, K.H., 1992, Rheology of the lower crust: Contental Lower Crust, Ed(s) D.M. Fountain et al., p. 201—267, Elsevier, Amsterdam.

Williams, M.L., Karlstrom, K.E., Dumond, G., and Mahan, K.H., 2009, Perspectives on the architecture of continental crust from integrated field studies of exposed isobaric sections: in Miller, R.B., and Snoke, A.W., eds., Crustal Cross Sections from the Western North American

Cordillera and Elsewhere: Implication for Tectonic and Petrologic Processes: GSA Special Paper 465, p. 219-241, doi:10.1130/2009.2456(08).

Williams, M.L., Hanmer, S., Kopf, C., and Darrach, M., 1995, Syntectonic generation and segregation of tonalitic melts from amphibolite dikes in the lower crust, Striding-Athabasca mylonite zone, northern Saskatchewan: Journal of Geophysical Research, V. 100, n. B8, p. 15,717-15,734, doi:10.1029/95JB00760.

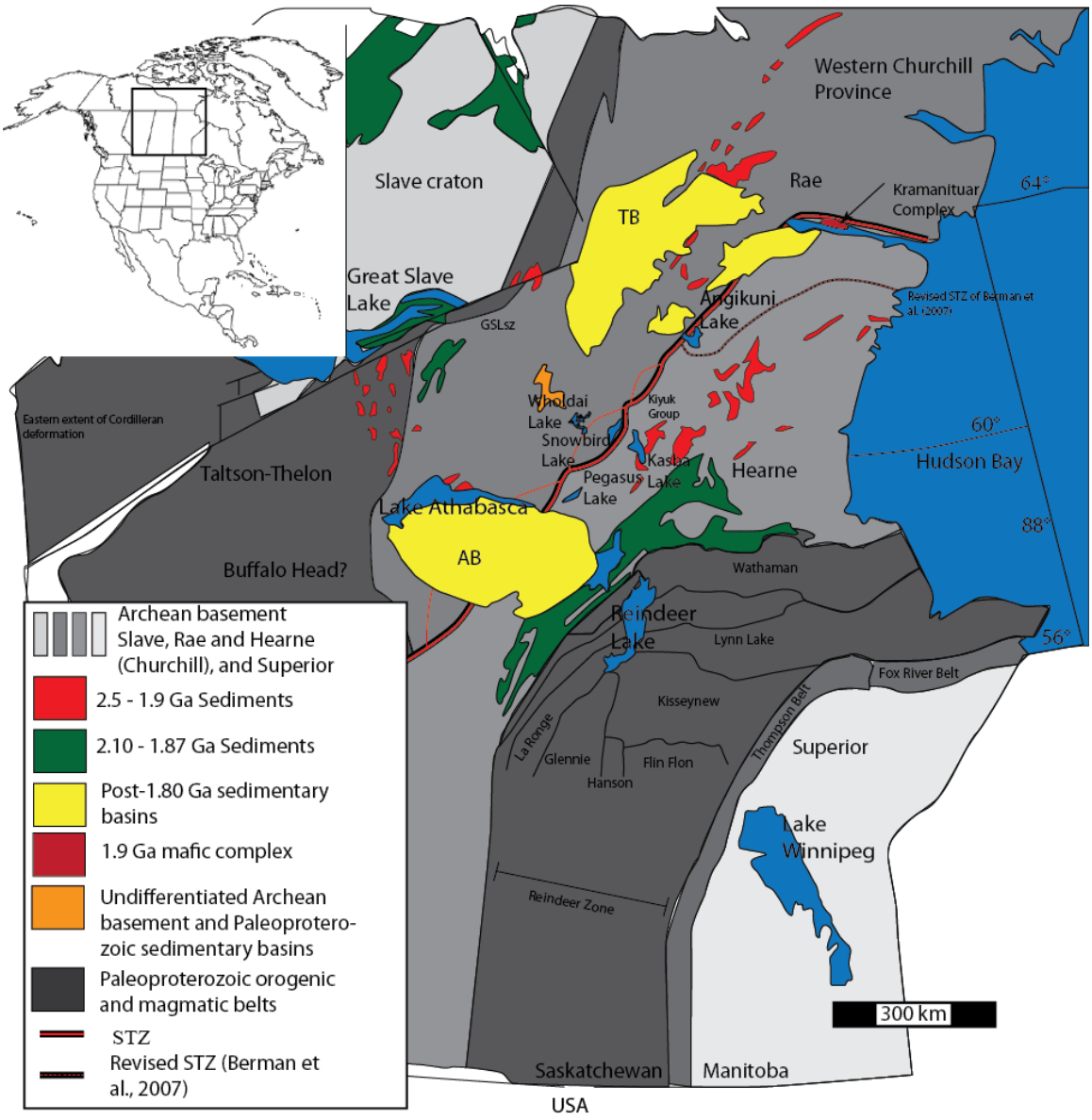

Figure 1: Lithotectonic map of the western Canadian Shield.

CHAPTER 2

THE CORA LAKE SHEAR ZONE, ATHABASCA GRANULITE TERRANE, AN INTRAPLATE RESPONSE TO FAR-FIELD OROGENIC PROCESSES DURING THE AMALGAMATION OF LAURENTIA

Introduction

Shear zones (high-strain zones) are common components of many metamorphic terranes. They typically divide larger regions into subdomains or lithotectonic blocks that contain primary structural and tectonic elements (Dumond et al., 2007; Karlstrom and Bowring, 1988; Klepeis et al., 2004). Interpretation of the geologic history and tectonic processes in these regions typically involves integrating the tectonic history of the shear zones with that of the blocks on either side (Dumond et al., 2007). Two end-member models might be considered. A shear zone may be a long-lived heterogeneity reflecting strain partitioning within the terrane, and thus, the history of the shear zone is essential to characterizing the structural style of the region. Alternatively, the shear zone might be a relatively late-stage feature and understanding the tectonic history involves reconstructing the pre-shear zone geometry of a larger more homogeneous region. Incorporating shear zones into the regional tectonic history is complicated because shear zones may record different stages of the history than their wall rocks and they may be significantly modified by fluids that were not present in the wall rocks. Relative and absolute timing constraints on deformational fabrics and metamorphic assemblages are essential for evaluating the temporal evolution of metamorphic terranes with respect to lithotectonic discontinuities.

The Athabasca Granulite Terrane, northern Saskatchewan, Canada is a large isobaric terrane, preserving pressures near 1.0 GPa over thousands of km^2. The region has been argued to preserve a snapshot of the geometry and character of the continental deep crust (Mahan and Williams, 2005; Williams et al., 2009). At the largest scale, the region is characterized by

lithothectonic blocks separated by thick ductile shear zones. The Cora Lake shear zone separates two of the largest blocks. The relationship between this shear zone and its wall rocks is critical to interpreting regional tectonics and to deep crustal behavior in general. If it represents a relatively early and periodically reactivated structure, then it may mark a rheological boundary and a zone of vertical coupling within the flowing deep crust. If it is a relatively late feature, then its anomalous kinematics within dextrally sheared wall rocks, is difficult to reconcile. The difference in vergence may be a response to shifts in plate-scale stresses, and thus may be important for larger-scale tectonic reconstructions (Whitmeyer and Karlstrom, 2007). Furthermore, if its deformation is late, it may record a portion of the P-T path not recorded in either wall rock, notably, the point where the independent P-T paths of the larger lithotectonic domains converge (Flowers et al., 2006a).

Structural, petrologic, and geochronological data have been used to characterize the Cora Lake shear zone (CLsz) in its type locality, and to place the shear zone into the regional tectonic evolution. The data suggest that the CLsz formed during the waning phases of granulite facies metamorphism (ca. 1.89-1.87Ga), and served to juxtapose contrasting lithotectonic domains or possibly crustal layers. The anomalous sinistral vergence of the CLsz corresponds to the cessation of eastward convergence along the western margin of Laurentia, and the development of strong northwestward convergence along the southern periphery of the Hearne Domain (Hildebrand et al., 2010; Corrigan et al., 2009; Andsell, 2005; Corrigan et al., 2005; *and references therein*). Furthermore, the Cora Lake shear zone is interpreted to have been a relatively weak zone within the Churchill craton, and thus, a sensitive monitor of regional (i.e. far-field) stress and tectonic events.

Geologic Setting

The East Athabasca mylonite triangle is a triangular shaped region within northern Saskatchewan that is defined by an area of anastomosing nested shear zones overprinting

dominantly Archean rocks. This region coincides with the Snowbird Tectonic Zone (STZ), a 2700 km long geophysically defined lineament within the Western Canadian Shield. It divides the Western Churchill Province into the northwestern Rae and southeastern Hearne domains (Hoffman, 1988). The central Snowbird Tectonic zone is underlain by abundant high pressure granulite, that are part of the Athabasca Granulite Terrane (Mahan and Williams, 2005; Dumond et al., 2008). The East Athabasca mylonite triangle is located in the Athabasca Granulite Terrane, and defines the southern portion of the central Snowbird Tectonic Zone (e.g. Williams et al., 2009; Mahan and Williams, 2005; Hanmer et al., 1995a,b; Gilboy, 1980). It has been hypothesized that the region was resident in the deep crust for the ca.650 million years (ie. 2560-1900 Ma; Mahan and Williams, 2005; Dumond et al., 2010; Williams et al., 2009), making the East Athabasca mylonite triangle a premier location to study lower crustal processes.

The East Athabasca mylonite triangleconsists of three structural and tectonic subdomains bounded by two major high strain zones: the Northwestern subdomain, the Chipman subdomain, and the Upper Deck subdomain (Figure 2)(Hanmer, 1994). The Legs Lake shear zone defines the southeastern boundary of the Chipman subdomain. This structure accommodated at least 15km of uplift of the Athabasca Granulite Terrane over the Hearne domain rocks to the southeast (Mahan et al., 2003; Mahan et al., 2006a; Dumond et al., 2013). The Grease River shear zone (Fig. 1) is the northern boundary of the Northwestern subdomain, and accommodated ca. 110 km of right-lateral strike slip motion at ca. 1800 Ma, subsequent to exhumation along the Legs Lake shear zone (Mahan and Williams, 2005). An earlier (ca. 1900 Ma) deformationevent in the Grease River shear zone has been suggested by Dumond et al. (2008). The Northwest subdomain and Chipman subdomain are separated by the Cora Lake shear zone (CLsz), a 4-6 km-wide zone of intense mylonite and ultramylonite that is entirely contained within the high-pressure terrane. The Northwest subdomain and Chipman subdomain are the CLsz's hangingwall and footwall, respectively.

The Cora Lake shear zone (CLsz) has been has been previously mentioned in Mahan et al. (2008; 2011) and Dumond et al. (2010). Mahan et al. (2008) suggested that Chipman dikes are highly strained within the CLsz region, and to a lesser extent further east, suggesting that the CLsz was active after emplacement of the dike swarm. Dumond et al. (2010) tentatively suggested a component of dextral shear along the CLsz at 1.9 Ga, but this suggestion came before widespread range fires led to extensive exposures of the shear zone and observation of abundant sinistral kinematic indicators (see below). With evidence of subhorizontal crustal flow to the northwest (Dumond et al., 2010), it has been speculated that the CLsz may have been a boundary or heterogeneity during flow, where tonalitic rocks to the southeast were too strong to flow. However, this assumes that the Cora lake discontinuity was already present in the Archean (see below). Furthermore, near Snowbird Lake to the north, the CLsz is thought to continue, dividing the Chipman Panel (after Martel et al., 2008) from orthopyroxene-bearing granitoids and overlying Paleoproterozoic sedimentary successions (Martel et al., 2008; Williams et al., 2012). However, no sedimentary rocks have been identified within the corresponding northwestern subdomain within the East Athabasca mylonite triangle suggesting a difference in Paleoproterozoic histories or exposed crustal levels.

Rock Types

The CLsz occurs along the boundary between the Northwestern and Chipman subdomains of the Athabasca Granulite Terrane (Fig. 2). Deformation related to the CLsz has not been identified outside of the shear zone. Because the CLsz dips steeply westward, the northwestern wall rocks will henceforth be called “hangingwall” and the southeastern wall rocks will be called “footwall”.

Hangingwall

The region north and west of the CLsz (“hangingwall”) is dominated by the ~2.6 Ga, composite Mary batholith (Fig. 4a)(Hanmer et al., 1994; Hanmer, 1997). The Mary batholith ranges from granitic to granodioritic in composition, and typically contains some combination of

plagioclase, quartz, orthopyroxene, clinopyroxene, garnet, biotite, and potassium feldspar (Fig. 4a). The original igneous protolith assemblage is interpreted to be orthopyroxene, plagioclase, K-feldspar, quartz, +/- biotite (Williams et al., 2000; Dumond et al., 2010). Commonly, this primary assemblage is heavily overprinted by a metamorphic assemblage consisting of plagioclase +clinopyroxene+ garnet +/- quartz +/- k feldspar +/- hornblende assemblage. The metamorphic assemblage observed throughout the Mary granite exposure is interpreted to be the product of (Williams et al., 2000):

$$Opx+Pl_1= Grt+Pl_2 + Qtz \quad (1)$$

The reaction, casually known as "the Mary Reaction", has been discussed in detail by Williams et al. (2000), Dumond et al. (2010), and Holland (2012), and is equivalent to the classic reaction separating intermediate and high pressure granulite fields of Green and Ringwood (1967) for basaltic compositions. $Plagioclase_1$ is relatively Ca rich (An_{32}) compared to $Plagioclase_2$(An_{22}). X_{An} content decreases by approximatelyten percent from core to the dynamically recrystallized rim across plagioclase grains (Williams et al., 2000).

Orthopyroxene bearing granitoids grade into the ca. 2.6 Ga Bohica mafic complex (Fig. 4b) and subordinate Beed granite in the northeastern portion of the hangingwall (Hanmer et al., 1994). The Bohica intermediate-mafic complex is lithologically heterogeneous, ranging in composition from amphibolite to clinopyroxene + garnet + plagioclase- mafic granulite to more intermediate, orthopyroxene-bearing variants. The petrologic complexity of this suite is currently under investigation. There are local thin (~10 m thick) layers of a megacrystic, Beed, granite interlayered with the Bohica complex, which are likely compositional and textural variants of the Mary batholith.

Footwall

The heterogeneous, ca. 3.2 Ga, Chipman tonalite gneiss is the dominant rock type in the southeastern footwall (Chipman subdomain)(Fig. 4c) (Macdonald, 1980; Hanmer, 1994). The tonalite contains layers and schlieren of amphibolite and mafic garnet granulite. Quartz is variable in abundance in the tonalite, and isolated exposures of anorthosite lenses occur within the field area. Tonalite layers range from garnet absent to garnet-rich (up to 15% mode), with varying crystal sizes.

Felsic granulite (diatexite) is typically exposed in thin, tens of meter wide screens (Hanmer, 1994). It has an assemblage of plagioclase + K-feldspar + quartz + garnet + silliminite +/- orthopyroxene +/- biotite +/- muscovite +/- kyanite. Garnet ranges in size from a few microns to 10's of centimeters in diameter, commonly displaying fractures perpendicular to penetrative foliation, locally infilled and replaced by biotite+/-cordierite (Mahan et al., 2006a,b). Garnet commonly contains distinctive, relatively large, round quartz inclusions. This rock type typically contains abundant monazite, making it suitable for geochronology. Felsic granulites have been interpreted as remnants of biotite dehydration melting of a granitic protolith (Baldwin et al., 2004; Dumond et al., 2010).

Mafic granulites (ca. 2.6 Ga) occur within the footwall and contain hornblende + clinopyroxene + plagioclase +/- orthopyroxene +/- ilmenite +/- rutile (Mahan et al., 2008; Flowers et al., 2008). They are generally exposed in meter to decimeter wide lozenges within the tonalite, and locally are associated with thick magnetite +garnet layersin and near the CLsz. The mafic granulite layers are differentiated from Chipman dikes by a coarser grain size, the presence of orthopyroxene, and characteristic boudins of coarse garnet + clinopyroxene + hornblende layers, which Mahan et al. (2008) interpreted to represent the first of two granulite grade metamorphic assemblages (events). The surrounding hornblende + plagioclase +orthopyroxene +/- garnet matrix anastomoses around these relict lenses.

The ca. 1.9 Ga Chipman dike swarm occurs throughout the footwall domain. Dikes range in width from <0.5 meters, to greater than 10 meters (Fig. 3d; Williams et al., 1995; Flowers et al., 2006a). Their composition ranges from a nearly pristine primary assemblage of hornblende and plagioclase, to garnet clinopyroxene granulites, and migmatitic members (Williams et al., 1995; Flowers et al., 2006a; 2008). The dikes almost exclusively intrude Chipman tonalite andfurther to the southeast, the Fehr granite (Koteas et al., 2010). Dikes are commonly slightly oblique to the NE-striking host fabric (Fig. 4d). The obliquity varies from clockwise to counterclockwise, and is generally no greater than a few degrees as previously reported in Hanmer et al. (1995).

Lithologies within the CLsz (Figure 6)

The CLsz contains a wide variety of rock types and assemblages including: tectonized megacrystic granites, ultramylonitic granitoids, felsic granulites, mafic granulites, and well banded intermediate orthogneiss (+/- garnet +/- orthopyroxene) ultramylonites (Fig. 4). The zone is particularly notable for its localized zones of grain size reduction, grain sizes on the micron scale, even when defined by relatively high-temperature assemblages. The shear zone fabric overprints rock types of both subdomains, and thus has been divided into components with hanging wall (northwestern subdomain and footwall (Chipman subdomain) affinity. Pseudotachylite and minor greenschist facies cataclastic zones occur within mafic and intermediate ultramylonites (Orlandini et al., 2013). They are parallel to the CLsz, and continuous for at least several kilometers. Hydrous assemblages are particularly common within reworked hangingwall rock types throughout the CLsz and range from synkinematic rims of biotite around garnet to randomly oriented chlorite pseudomorphs after garnet. Garnet within felsic granulites is commonly fractured, locally brecciated with biotite filling cracks.

Structural Geology

Northwestern wall rocks

The northwestern wall rocks contain two regionally pervasive fabrics that predate the CLsz (see table 1 for nomenclature). The earliest (S_{N1}) is defined by gneissic layering and a well developed subhorizontal layer-parallel foliation. Assemblages include quartz, feldspar, orthopyroxene, clinopyroxene, garnet +/- biotite, and hornblende. A relatively strong mineral lineation trends shallowly to the east-southeast. Kinematic indicators suggest top to the east-southeast shearing. Plagioclase porphyroclasts display classic "core and mantle" structure (White, 1976) suggesting dislocation creep as the dominant deformation mechanism (Passchier and Trouw, 2004; Williams et al., 2000). These core-mantle structures include both σ and δ- clast asymmetry and S-C-C' geometries consistent with top to the east-south-east relative motion on the shallow fabric (Passchier and Trouw, 2004). Work within the Beed Lake region confirmsthat the early gneissic layering is present further to the northeast.With a shallow enveloping surface and consistent kinematics, this fabric is interpreted to be correlative withS_1 of Dumond et al. (2010) further to the southwest where it was interpreted to represent subhorizontal flow of the lower crust.

The early gneissic foliation (S_{N1}) is folded by map scale upright folds with near vertical, SW-striking axial surfaces. The axial-planar S_{N2} cleavage ranges in intensity from a subtle mineral alignment (Figure 7a,b) to a mylonitic foliation with grain sizes approaching the sub mm scale. S_{N2} is most strongly developed in the limb domains of the large-scale folds whereas hinge regions tend to preserve the earlier S_1 fabric. Mineral lineations on S_{N2} plunge shallowly to the SW (12°=>242°). S-C-C' geometries and asymmetric σ-clasts indicate dextral shearing (Figure 7c). Feldspar porphyroclasts display core and mantle microstructures similar to those on S_{N1} suggesting a second phase of dislocation creep (Williams et al., 2000; Passchier and Trouw, 2004), but matrix grain sizes are significantly finer than those on S_{N1} (< 1 mm locally). All the structural aspects of D_{N2} suggest dextral transpression as the major stress regime.

Southeastern wall rocks

The Chipman tonalite is dominated by a NE-striking, steeply dipping gneissic fabric that varies in intensity. Older fabric generations are heterogeneously preserved, most typically as isolated fold hinges of an earlier gneissic fabric (Mahan et al., 2008; 2011). The relict folds have subhorizontal enveloping surfaces, suggesting that the earlier fabric (S_{C1}) may have also been subhorizontal, similar to S_1 in the northwestern subdomain (Figure 7d). S_{C2} is the dominant tectonic fabric within the footwall domain. It is upright, and defines the axial planes of open, upright meter-scaled folds preserved within low strain zones (Figure 7e).On a km-scale with, large crenulated regions are interpreted to define the map-scale hinge regions, where S_{C1} is preserved. Axes plunge shallowly to the SW (12° to 230°), parallel to the L_{2C}orientation. Kinematics vary, and may be partly inherited from S_{1C}, which was subsequently folded. However, dextral kinematics dominate where S_{C2} is well developed and also within migmatized Chipman dikes (Flowers et al., 2006a). S_{C2} is extremely planar, especially in the Chipman tonalite. The strong foliation parallel to compositional layering within the Chipman tonalite suggests that large-scale transposition occurred throughout the region.

In summary, pre-CLsz fabrics both in the northwest and to the southeast of the shear zone involve an early subhorizontal S_1 foliation, better developed in the northwest, which is folded and locally transposed into a northeast-striking upright S_2 cleavage that is more strongly developed in the southeast. Lineations have a similar shallow SW plunge in both domains and kinematic indicators suggest dextral shearing during the F_2 shortening.

Cora Lake shear zone (S3, M3, D3)

CLsz rocks appear to have the same protoliths as wall rocks, and rocks can be classified as having either hangingwall or footwall affinity. The shear zone strikes to the SW (~231°) and is moderately to steeply dipping to the northwest. The S_3 foliation is defined by alternating mafic and felsic layers, by leucosome vs. restite layering, and an intense mylonitic foliation. Awell-developed mineral lineation, L_3, plunges obliquely to the southwest(~19° to 238°). Locally, even

clinopyroxene forms elongate rods defining the lineation, particularly within the footwall affinity portion of the shear zone. Garnet is consistently fractured and dispersed along foliation planes.

Abundant asymmetric porphyroclasts and S-C-C' geometries (Passchier and Trouw, 2004) within the CLsz all suggest oblique-normal, sinistral sense of motion, with a dominant strike-slip component. This contrasts with the dextral kinematics preserved along S_2 in the hangingwall and footwall. Although the foliation and lineation orientations are similar, the distinct kinematics of the Cora Lake fabric suggests that it is a new deformation event rather than a localization and intensification of the D_2.Several zones of relatively intense ultramylonite occur throughout the width of the CLsz. For the purpose of description and sampling, the CLsz is subdivided into the following six structural zones from southeast to northwest (Fig. 7).

Zone 1: The southeastern segment of the CLsz is defined by S>L tectonites in protomylonitic to mylonitic rocks of the Chipman subdomain. Several highly magnetic mafic granulite bodies occur near the southeastern margin of the shear zone. D_3 (CLsz) fabrics are relatively weak.

Zone 2: This zone is characterized by ca. 100-200 metresof S=L tectonite ultramylonites with a distinctly glassy appearance due to their ultrafine grain sizes. Predominantly Chipman subdomain affinity rocks and a thick zone of biotite to garnetiferous (+clinopyroxene+orthopyroxene) anothosite ultramylonite are characteristic of this zone. Crosscutting carbonate and semi-concordant pseudotachylite veins have also been observed within this zone.

Zone 3: Zone 3 contains abundant grain size variations (strain gradients) and rock type changes and is approximately 1 km thick. Mylonitic orthopyroxene bearing intermediate orthogneiss ultramylonites grade into mafic and felsic granulite. Grain sizes, on a whole, are coarser than in Zone2. However, local strands, approximately 10-30 m in thickness, of extremely fine grained ultramylonites similar to zone 2 anastomose throughout Zone 3. Brittle faults, and less common

greenschist facies cataclasic zones (chlorite, plagioclase, biotite, and quartz) roughly 5-10 m wide are subparallel to the local fabric, but the continuity of lithologies across them suggests that the brittle structures did not contribute significantly to the exposed structural complexity. Both concordant and discordant zones of pseudotachylyte occur within the most strained rocks (i.e. fine grain sizes).

Zone 4: This region is defined by the transition from footwall affinity to hangingwall affinity rock types, and is dominated by interlayered mylonitic intermediate to felsic orthogneiss (no porphyroclasts) and diatexitic felsic granulite. Intermediate (orthopyroxene+plagioclase+quartz+/-garnet) granulites grade into semi-continuous sheets of diatexitic felsic granulite interlayered on a decimeter scale with L>S felsic orthogneiss. The felsic orthogneiss ultramylonites increase in abundance toward the northwest. Diatexitic felsic granulites commonly contain alternating feldspar- and quartz-rich domains with local biotite.

Zone 5: In Zone 5, porphyroclastic protomylonitic granitoids (+/- biotite) are intercalated with orthopyroxene bearing felsic granulite at varying scales, and minor amounts of megacrystic Beed Granite (Fig. 7d). Slivers of intermediate granulite and mafic dikes (Chipman dikes?) occur locally, suggesting possible tectonic emplacement of footwall blocks into the northwestern affinity hangingwall rock types. The megacrystic granitoids ultimately pinch out completely along strike to the northeast. Folds are variably preserved on a meter to submeter scale, always aligned in the CLsz fabric, and strongly overprinted by CLsz related shear.

Zone 6: Within this zone, the CLsz fabric is significantly less intense, ranging from protomylonitic to mylonitic. Charnockitic gneisses are interlayered on a 100 meter-scale with felsic granulites. Garnet is typically intact, and kinematic indicators are not as well developed as in Zones 2-5. Hornblende and anthophyllite are common throughout this zone, the latter likely reflecting post-kinematic hydration.

Metamorphic Petrology

Wavelength dispersive (WDS) compositional maps, and mineral analysis were acquired using a Cameca SX-50 electron microprobe at the University of Massachusetts, Amherst.High resolutionmaps of individual phases (ie. garnet, plagioclase, pyroxene) were collected using a 100 nA current, 100 ms dwell time, and a step size of 2 to 10 μm. Electron microprobe compositional maps (WDS) were utilized to characterize compositional zoning, and to choose domains for thermobarometric calculations. Quantitative mineral analyses were performed using a 20 nA current. Feldspar and hornblende analyses were performed using a slightly defocused beam (2 μm) at 15 KeV to prevent Na diffusion. A focused beam was utilitzed for garnet and pyroxene. Calibration was done using standards similar to phases analyzed. Matrix corrections were carried out using a PAP model (*Pouchou and Pichoir*, 1984).

Pressure and temperature estimates of major assemblage generations were calculated using TWQ 3.2 (Berman, 1994, updated in 2007). Deformation microstructures were correlated with metamorphic assemblages to determine mineral stability during fabric formation events. Electron microprobe compositional maps were utilized to identify any potential compositional zoning to evaluate P-T history and to select equilibrium domains. P-T conditions calculated by TWQ are qualitatively estimated to have an absolute error of 50° C and 0.1 GPa (Berman, 1991). Equilibria involving amphibole were calculated with TWQ version 1.02 with data from Mader et al. (1994). The feldspar solution model of Fuhrman and Lindsley (1988) was usedin both versions of the TWQ software. Solution models for garnet and pyroxene are from Berman and Aranovich (1996). Calculations were used for the following equilibria:

$$6En + 3An = Gr + 2Py + 3\beta Qz \quad (2)$$

$$3En + Alm = 3Fsl + Py \quad (3)$$

$$3An + 3Di = 3\beta Qz + Py + 2Gr \quad (4)$$

$$Alm + 3Di = Py + 3Hd \quad (5)$$

$$3Tsc + 12\alpha Qtz + 2Py + 4Gr = 12An + 3Tr \quad (6)$$

$$3Tr + 5Alm = 5Py + 3FeTr \quad (7)$$

Equilibria (2) and (3) are calculated using orthopyroxene + garnet + plagioclase + quartz (En: enstatite, An: anorthite, Gr: grossular, Py: pyrope, Qz: quartz, Alm: almandine, and Fsl: ferrosillite)while (4) and (5) are calculated with clinopyroxene instead of orthopyroxene (Di: diopside, Hd: hedenbergite). Clinopyroxene is the most common mafic phase, so wherever found, equilibria (4) and (5) were used. Employing the same two equilibria on as many samples as possible reduces the sources of error associated with evaluating relative differences (Dumond et al., 2007). Equilibria (6) and (7) were calculated using TWQ version 1.02 with amphibole + garnet + plagioclase + quartz (Tsc: tschermak, Tr: tremolite, FeTr: Fe-tremolite). All other equilibria were solved using TWQ version 2.32. These equilibria correspond to commonly used thermometers and barometers, and were chosen due to their relatively well constrained thermodynamic data (for discussion see Williams et al., 2000). Samples were chosen from regions of abundant outcrop and clear structural relationships. Although this led to a larger geographic spread, it facilitates a broader understanding of the P-T conditions within each wall rock.

Northwestern Hangingwall

11R-081

The earliest structural fabric within the northwestern hangingwall is a subhorizontal gneissic fabric (S_{N1}; sample 11R-081; East Hawkes Lake). Along this fabric, particularly well exposed in the Mary granodiorite, plagioclase porphyroclasts are dynamically recrystallized and contain blood red garnet along the edges of recrystallized feldspar tails. Primary orthopyroxene +/- ilmenite crystals and mineral aggregates are fractured in a bookshelf fashion, and contain asymmetric tails and corona of garnet +/- clinopyroxene consistently displaying top to the east

relative motion. Compositionally, plagioclase porphyroclasts smoothly grade from An_{37} in the core to An_{27} in dynamically recrystallized tails(Fig. 9). Garnet is generally unzoned and is consistently grossular- rich almandine (X_{Alm} = 0.70 , X_{Gr}= 0.20, X_{py}= 0.09). Clinopyroxene also displays little zonation, has Mg/Mg+Fe of ca. 0.45. Sharp increases in this ratio along the rims suggest minor diffusional exchange with garnet during cooling. X_{Di} is consistently 0.24 and X_{Hd} is 0.29.

96W-062g

The second metamorphic assemblage (M_{N2}) is developed along the second fabric generation (S_{2N}; sample 96W-62g). The mineral assemblage along this fabric is similar to M_{N1}, but containsa substantially greater amount of hornblende and smaller amounts of orthopyroxene was observed. Plagioclase porphyroclasts contain blood red garnet crystals in the dynamically recrystallized tails that extend along S_{N2}. Where present, orthopyroxene is commonly replaced by post-kinematic anthophyllite. This orthopyroxene is interpreted to be a primary igneous mineral, and is typically associated with tails of hornblende, garnet, +/- clinopyroxene. These observations suggest both a dynamic and a late stage static hydration with respect to M_{N2}. Plagioclase porphyroclasts that are interpreted to have recrystallized during M_{N2} (Fig. 9) are similar in composition to M_{N1} porphyroclasts. The composition varies smoothly from An_{47}in the core toAn_{33} in the recrystallized rim. Garnet is unzoned, and has a grossular-pyrope rich - almandine composition (X_{Al}=0.64, X_{Py}= 0.16, and X_{Gr}= 0.19). There is a substantial decrease in $X_{Mg/Mg+Fe}$ along the rim of garnet crystals from a core value of 0.21 down to 0.16. Although significantly less common within this fabric, clinopyroxene is locally present as small grains along foliation planes, typically within hornblende ribbons. It is interpreted to have resulted from orthopyroxene consumption (*see above*). The clinopyroxene is unzoned (X_{Di} of 0.343 and X_{Hd} of 0.191), and has a $X_{Mg/Mg+Fe}$ ratio of 0.642, quite different from that analyzed from M_{N1}, with a large increase at the edge of the crystal consistent with diffusional reequilibration with garnet

during cooling. Compositions for thermobarometric analysis were chosen from just inside the rims modified by Mg/Mg+Fe diffusional exchange.

Using equilibria (4) and (5), assemblages that formed on both S_{N1} and S_{N2} yield similar P-T conditions of 0.9 GPa and 725°C (11R-081 and 96W-062g, respectively). These data are in agreement with previously published results for P-T conditions within the region (Williams et al., 2000; Dumond et al., 2010). Even though the calculated conditions are similar, the conditions are interpreted to represent two distinct metamorphic events at widely different times (see below).

Southeastern footwall

Mafic granulites of the southeastern footwall domain contain evidence for three phases of metamorphism (Mahan et al., 2008). The texturally oldest assemblage occurs in folded to completely dismembered pods of garnet + clinopyroxene + ilmenite (ca. 1.35 GPa and 850°C). Garnet crystals contain orthopyroxene and plagioclase inclusions interpreted to be of igneous origin.These domains are folded and overprinted by an axial planar fabric defined by hornblende, plagioclase, and minor quartz (M_2 of Mahan et al. 2008). These in turn are overprinted by a peak assemblage consisting of orthopyroxene + plagioclase +/- garnet +/- hornblende. Garnet and hornblende crystals are texturally early, and were interpreted to have grown during the initial thermal reactivation (M_{3a} after Mahan et al., 2008;<1.1 GPa and >800°C), followed by plagioclase and orthopyroxene and clinopyroxene during Med-P granulite facies metamorphism (M_{3b} of Mahan et al., 2008; M_{C2} this study). For additional information, see Mahan et al. (2008).

The Chipman dikes have been previously analyzed for thermobarometry (Williams et al., 1995; Mahan and Williams, 2005; Martel et al., 2008). Dikes contain evidence for a single metamorphic cycle exemplified by both cauliflower textures and local partial melt (Williams et al., 1995; Flowers et al., 2006a). They commonly contain a granulite grade mineral assemblage of clinopyroxene and garnet that heterogeneously overprints the primary igneous assemblage of hornblende and plagioclase. Collectively, close to 20 Chipman dikes have been analyzed in an

attempt to decipher the metamorphic conditions, which consistently yield P-T data between 1.15 and 1.20 GPa and 800°C - 875°C (Williams et al., 1995; Mahan and Williams, 2005; Martel et al., 2008).

10W-094a

The Chipman dike swarm was emplaced prior to or during the second metamorphic event. Dikes preserve a clean record of peak conditions during the last metamorphic events peak conditions and place a tight timing constraint on several of the major structural elements within the region (10W-094a; S_{C2})(Fig. 10). The primary mineralogy consists of fine grained hornblende and plagioclase. This assemblage contains local corona and recrystallized rims of clinopyroxene and garnet, interpreted to represent the peak metamorphic assemblage. Hornblende and plagioclase occur locally along clinopyroxene and garnet grain boundaries, reflecting minor amounts of retrogression. The retrograde assemblage does not appear to have a shape preferred orientation, and is developed symmetrically around the peak assemblage suggesting retrograde metamorphism was static in nature.

One dike was analyzed during this study for comparison with those from Williams et al., (1995) and Mahan and Williams (2005). Plagioclase composition is uniformly An_{25}. However, a slight increase in An content (X_{An}=0.29) occurs immediately adjacent to the garnet overgrowths suggesting late plagioclase growth. Garnet is also compositionally unzoned, except for a thin domain immediately adjacent to the analyzed plagioclase, where X_{Gr} decreases. Garnet has a composition of pyrope-grossular rich – almandine (X_{Al} = 0.64, X_{Py} = 0.16, X_{Gr} = 0.18). Clinopyroxene composition does not vary, has a Mg/Mg+Fe ratio of 0.554, and has a composition of X_{Di} of 0.28 and X_{Hd} of 0.23. Using equilibria (4) and (5), the dike yielded peak P-T of 1.17 GPa and 800°C. Using TWQ version 1.02, a P-T calculation was made using the post-peakassemblage of plag+amphibole, and garnet rims within the mafic dike. The assemblage

associated with retrogressionyielded a P-T of 1.06 GPa and 725°C using equilibria (6) and (7), without substantial differences in plagioclase and garnet composition.

Cora Lake shear zone

10W-112b

The CLsz contains a wide variety of rock types and assemblages. Evidence for both dynamic and static hydration is widespread throughout the reworked hangingwall portion (Zones 4,5) of the shear zone. An orthopyroxene-bearing, porphyroclastic felsic granulitefrom Zone 5, also containing plagioclase, quartz, potassium feldspar, garnet, hornblende, and biotite, was targeted for thermobarometry due to little evidence for static retrogression (10W-112; Fig.9).Plagioclase porphyroclasts display core and mantle structures with dynamically recrystallized tails. Garnet crystals are fractured along discrete breaks, and show evidence for small amounts of displacement along the fractures suggesting a syn-kinematic relationship with respect to D_3. Orthopyroxene is boudinaged, fractured, and dispersed about the matrix along with hornblende, suggesting that it was in equilibrium with surrounding phases.

There is no compositional variation in the core or dynamically recrystallized tail of the core and mantle plagioclase. Cores and mantles have a uniform composition of X_{An} =0.34. X_{Gr}(garnet) ranges from 0.03 within the core to 0.07 in the innerrims and back to 0.03 in the outer rim. Overall, the garnet is a pyrope-rich almandine. A slight decrease in Mg/Mg+Fe ratios along the outerrim was observed. Orthopyroxene does not contain systematic zonation, but very slight, non systematic variations occur from point to point with X_{Al} ranging from 0.56 to 0.60 and X_{Py} ranging from 0.32 to0.38. Mg/Mg+Fe ratios range from 0.62 to 0.65. Also, Mg/Mg+Fe ratios in orthopyroxene outerrims increase slightly suggesting post kinematic diffusional reequilibration with garnet. This assemblage yielded P-T conditions of 0.87 GPa and 775°C using equilibria (2) and (3).

10W-100a

Mafic granulites from Zone 3 of the shear zone contain dynamically recrystallized clinopyroxene, fine grained red garnet, and extremely fine grained dynamically recrystallized plagioclase ribbons. Minor hornblende occurs along grain boundaries between clinopyroxene and garnet. Clinopyroxene is generally located between garnet and plagioclase domains. Garnet is subhedral, and clinopyroxene and plagioclase ribbons are deflected around the garnet crystals. Given the mineral assemblage, this rock likely shares a protolith with mafic granulites from the footwall domain. It is interesting that the M_3 assemblage mimics the earliest assemblage (M_1 after Mahan et al., 2008). Hornblende is interpreted to be syn to post kinematic and present along grain boundaries due to thin-section-scale variability in fluid availability.

Sample 10W-100a is typical of CLsz mylonitic mafic granulites (zone 3). Anorthite content ranges from An_{42} to An_{47} with higher An contents along the dynamically recrystallized rims. Garnet is slightly zoned with X_{Gr} ranging from 0.33 in the core down to 0.29 within the innerrims, with a slight increase back to core-like values along the outerrim. Mg/Mg+Fe ratio in garnet ranges from 0.12 to 0.14 with a slight decrease along the outer most rims (Fig. 11). The garnet grains analyzed are all grossular-rich almandine with an average composition X_{Alm} of 0.59, and X_{Pyr} of 0.09, with a slight increase in X_{Alm} rimward. Clinopyroxene is compositionally unzoned despite decreases in the $X_{Mg/Mg+Fe}$ along the very rim of the crystal consistent with post kinematic diffusional reequilibration. The most representative composition for the clinopyroxene has a $X_{Mg/Mg+Fe}$ value of 0.53, X_{Di} of 0.27, X_{Hd} of 0.24. Using equilibria (4) and (5), the mafic granulite mylonite yielded an equilibrium P-T of 0.95 GPa and 725°C, which is indistinguishable from the retrogression conditions yielded by the mafic dike outside of the shear zone (10W-094a).

10W-099

Ten meters away from 10W-100a is another mafic granulite (10W-099) but it is significantly finer grained (Fig. 12). Grain sizes range from 100 μm to less than 10 μm's. The

sample has very little garnet (< 1%). Clinopyroxene occurs as tails and corona around orthopryoxene. Clinopyroxene contains asymmetric tails of consisting predominately of ilmenite, but locally of magnetite. Othopyroxene grain size is bimodal and occurs as both microporphyroclasts and as fine matrix grains. Plagioclase is dynamically recrystallized into fine grained ribbons with grain textures difficult to investigate petrographically.

At such fine grain sizes, evaluating equilibrium becomes very difficult, due to the ease with which post-kinematic diffusional reequilibration can occur at the intergrain scale. Anorthite content varies little in this sample, X_{An} = 0.43. Clinopyroxene compositions vary systematically (Fig. 12). Away from garnet they consistently have lower $X_{Mg/Mg+Fe}$ ratios, and flat profiles. However, clinopyroxene crystals near garnet have elevated $X_{Mg/Mg+Fe}$ ratios, and U-shaped profiles. Because grain sizes are fine, clinopyroxene crystals away from garnet were chosen for P-T calculations to avoid diffusional exchange. Clinopyroxene compositions distal from garnet are consistently X_{Di} of 0.36 and X_{Hd} of 0.14. Garnet crystals are far less abundant in this rock type compared to neighboring lithologies; the pyroxene to garnet ratio is exceedingly high. The fine grained garnet crystals have a $X_{Mg/Mg+Fe}$ of 0.16 to 0.24 and are consistently grossular rich almandine (X_{Alm}=0.59, X_{Gr}=0.19, X_{Py}=0.18). $X_{Mg/Mg+Fe}$ has concave down profiles, compatible with diffusional exchange with neighboring clinopyroxene. Core compositions were chosen for thermobarometric analysis to minimize the effects of diffusional exchange. However, it is important to note that given the low modal abundance relative to pyroxene, and fine grain sizes of garnet crystals, it is likely that the composition was slightly reequilibrated.This high-strain mafic granulite ultramylonite yielded 0.80 GPa and 725°C using equilibria (4) and (5), interpreted to represent a minima due to the fine grain sizes.

P-T results confirm that a thermobarometric discontinuity exists across the CLsz. P-T estimates from the hangingwall are 0.9 GPa and 750°C, whereas peak metamorphic conditions in the southeastern footwall are 1.17 GPa and 800°C during D_2. However, P-T estimates from

hangingwall and footwall affinity rocks converge within the CLsz (ca. 0.9 GPa and 775°C), consistent with the interpretation that the shear zone juxtaposed the two, during footwall decompression.

Monazite Geochronology

Monazite geochronology was performed in-situ using the Cameca SX-100 "Ultrachron microprobe" at the University of Massachusetts, Amherst following the procedures outlined by Williams et al. (2006) and Dumond et al., (2008). Five spectrometers were used for measuring, U, Th, Pb, S, Ca, K, Sr, Si, Y and P and REE elements (see supplementary file). Lead was measured using two very large PET crystals (VLPET) simultaneously, and counts were aggregated in order to increase count resolution. Background measurements were performed once for each compositional domain. Then, successive peak measurements were made until errors stabilized at an acceptable level. Measurements were excluded when compositions were significantly outside the mean for the particular compositional domain, and when the values suggest overlap with adjacent domains. Background values for U, Th, and Pb were determined using the multipoint method (Allaz, in preparation), whereby eight to ten background intensities are measured at known points of no spectral interference both above and below peak values. The multipoint data are regressed using an exponential fit (Jercinovic et al., 2008; Allaz, in preparation), and the background intensity at the peak position is calculated. Typically, between four and eight peak measurements were made per monazite compositional domain. A single date is calculated for each domain based on one background intensity and the 4-8 peak analyses (a set of analyses yield a single "age"). Errors are calculated in several ways (Williams et al., 2006). Typically, a single weighted mean and error is calculated for each chemical component and then a single "date" is calculated for each domain.This allows the compositional homogeneity of each domain to be evaluated independent of dates. Individual errors are propagated through the age equation to yield a single error for the calculated date.

Calibration for monazite analysis was performed on natural and synthetic standards. $PbPO_4$ (Pyromorphite) was used for Pb, $ThPO_4$ (Barbanite) was used for Th, and UO_2 was used for U. An "in house" consistency standard (Moacyr) was analyzed prior to, and throughout, analytical sessions (506 +/- 1 Ma; *see discussion in* Williams et al., 2006; Dumond et al., 2008).Calibration was performed prior to every analytical session, and for long sessions, the calibration was checked and updated during the session. Peak positions were routinely updated for P, Ce, La, and Nd using synthetic phosphates prior to each analytical session.

Northwestern Hangingwall

Previous results

Dumond et al. (2008; 2010) described and interpreted both monazite and zircon U-Th-Pb geochronological data from the Northwestern subdomain. Geochronological constraints from the ca. 1800 Ma Grease River shear zone, suggest a punctuated history, involving dextral shearing at several times preceding the final phase of motion. Zircon and monazite from a synkinematic granitic dike yield a ca. 1900 Ma igneous age. Along the western exposure of the East Athabasca mylonite triangle on the northern shore of the Fond du Lac, Dumond et al. (2010) performed a transect across the Northwestern subdomain. These authors presented monazite geochronology suggesting that early subhorizontal gneissic layering, and top to the east southeast shearing occurred at ca. 2560 Ma. Upright folding, subtle axial planar mineral alignments, and localized shear zones developed at ca. 1900 Ma.

12R-054

The Beed granite is a distinctive megacrystic K-feldspar and plagioclase, biotite bearing (apatite+ ilmenite) granite (Fig. 13). It outcrops as a layer, approximately 300 m thick that is folded around map-scale F_{N2} folds. The S_{N1} and L_{N1} (layer-parallel) fabric and top to the east D_{N1} kinematic indicators are superbly developed with little to no S_{N2} fabric development. Monazite is abundant (up to 350μm in diameter); no garnet is present within the sample collected for monazite analysis. Twenty-four monazite grains were mapped and display complex

compositional zonation including innercores, outercores, innerrims, and outerrims. Innercores contain greater than 2.0 wt % Y_2O_3 and just less than 5.0 wt % ThO_2 and, on average, contain slightly lower UO_2 contents relative to innerrims.The remainder of the monazite generations (domains) contain ThO_2 contents approximately 6-8 wt %. These outercores to innerrims are aligned along L_{N1}. Outerrims contain less than 0.7 wt % Y_2O_3, whereas the cores and innerrims contain more than 1.0 wt %, and are texturally distinct. These outer rims only occur on the sides of grains aligned with foliation and perpendicular to L_{N1}, but parallel to the axial plane of large scale folds.

Inner cores yield an average age of 2608 +/- 8.4 Ma consistent with igneous zircon ages reported for other orthogneisses in the region (Hanmer et al., 1994), and this age is thus interpreted to be an approximation of the age of igneous crystallization, and their significance will be discussed in detail in a separate contribution. Outercores/innerrims, based on three sets of analyses, yield an average age of 2577 +/- 22 Ma interpreted to represent a period of dynamic recrystallization of kspar and corresponding development of the S_{N1} fabric. Low Y outerrims yield an average age of 1917 +/- 12 Ma (MSWD: 2.6) based on 3 sets of analyses, which is interpreted to represent initial layer parallel shortening prior to buckling (pre F_{N2}).

12R-057c

The Beed Lake region, located in the northeastern portion of the northwestern hangingwall (Fig. 3), contains several distinctive felsic granulite layers that are concordant to, but do not contain, an S_{N1}tectonic fabric. They are interpreted to be syn D_{N2} leucosomes, which were the result of anatexis along the base of the Beed granite (S_{N1} dominated).One sample, 12R-057c, was cut to fold profile view to look for any layer parallel fabric, but none was found. Sixteen monazite grains were mapped in-situ, and two distinct compositional domains are apparent. Cores are all uniformly low Y, with Y_2O_3 below 0.01 weight percent in all analyses. Most grains contain rims, which envelop the entire monazite crystal. Rims are characterized by a marked

increase in Y_2O_3 concentrationranging from 0.22 to over 1.0 weight percent. ThO_2 concentrationdecreases sharply (by >2 wt %) at the rims. The zonation is interpreted to represent initial anatexis during peritectic garnet growth and during F_{N2} folding. High Y rims are thus,interpreted to reflect hydration associated with retrograde biotite growth after garnet, with a increase in available Y associated with garnet breakdown. Biotite grains are randomly oriented, and locally occur as partial pseudomorphs of garnet. Rims are generally evenly developed and symmetrical around the monazite crystals. Most are interpreted to represent static retrograde metamorphism as a result of fluid influx after D_2 deformation.

Ten sets of analyses yield a well constrained 1895 +/- 3.2 Ma (MSWD: 1.5) age for the low Y, high Th core domains. This age is interpreted to correspond to the development of the strong S_{N2} fabric during prograde garnet growth and during F_{N2} folding. Excluding one statistical outlier, five sets of rim analyses yield an average age of 1882 +/- 4.8 Ma (MSWD: 0.28), which is interpreted to reflect the age of hydration and garnet breakdown. Rim dates spread more broadly than core dates, ranging from 1879 Ma upwards towards 1900 Ma. We suggest that hydration and replacement of garnet by biotite reactions may have begun during peak metamorphism, but continued long afterward.

Southeastern Footwall

Previous Results

Mahan et al. (2006a,b) performed systematic monazite geochronology from diatexitic felsic granulites of the Chipman subdomain, with focus on timing fluid flow away from the Legs Lake shear zone. These authors suggested that hydration from the Hearne domain footwall was syn-kinematic with dextral/thrust sense shear within the Legs Lake shear zone from ca. 1850-1830 Ma (Mahan et al., 2006b). Flowers et al. (2006a) presented ID-TIMS zircon results from melted Chipman dikes. Zircon from the tonalitic leucosome surrounding peritectic garnet yielded a precise age of 1896.2+/-0.3 Ma. Further zircon analyses on mafic granulites from the western Chipman subdomain presented in Flowers et al. (2008) produced an odd discordia array with an

upper intercept of ca. 2560 Ma, interpreted to represent peak metamorphism (Mahan et al., 2008), and a lower intercept of ca. 1900 Ma interpreted to represent thermal resetting, and some internal zircon deformation (Flowers et al., 2008).

10W-094g_2

Sample 10W-094g_2 is a folded felsic granulite migmatite with layering defined by alternating garnetite and plagioclase-porphryoclastic leucosome, located along the southwestern bay of Cora Lake. This sample was cut perpendicular to the fold axis, and obliquity between original gneissic layering (S_{C1}) and a strong axial planar fabric (S_{C2}) is well preserved. The two fabrics are also apparent in full section compositional maps (Fig. 14). Fourteen monazite grains were mapped. Innerrims have high Th content, and generally envelope the entire crystal. They are interpreted to have grown syn to post S_{C1}. They contain from 7.5 to >10 wt % ThO_2, and all have Y_2O_3 contents below 0.07 wt %. Several grains contains rims that are interpreted to be developed in extensional quadrants along the S_{C2} plane (Fig. 14c, d, and e), suggesting a syn-kinematic growth history. These outerrims contain 5.3-6.2 wt % ThO_2 and 0.18 wt % Y_2O_3.

Two sets of analyses of high Th innerrims yielded ages of 2557 +/- 19 Ma and 2461 +/- 53 Ma. The2461 Ma date is interpreted to have been partially altered based on the patchy texture(Williams et al., 2011). However, the 2557 Ma age is interpreted to represent the end of M_{1C}, and its high Th contents may correspond to the crystallization of partial melt that defines the compositional layering. Four sets of analyses on outerrims yield an average date of 1899 +/- 4 Ma (MSWD: 0.31), interpreted to represent syn-S_{C2} development NW-SE shortening, folding, and the development of the strong axial planar fabric, which ultimately led to large scale transposition in the footwall.

Cora Lake shear zone

11R-028b

Zone 4 of the CLsz contains one dominant, very intense fabric (*see Fig. 5)*. Sample 11R-028b, from Jeanotte Lake, is a felsic granulite that outcrops in a strain shadow of a decimeter-

scale mafic granulite boudin. It contains medium sized monazite grains (50 – 100 μm) Two domain types were identified from nine mapped monazite grains. Core domains are defined by weak oscillatory Th zonation; the oscillations vary in width and intensity. The rims are unzoned, and range from 10 μm overgrowths, to tails elongated along the lineation for greater than 50 μms, suggesting syn-kineamtic growth.

Results from 11R-028b yield two well constrained populations (Fig. 15). The cores have a weighted mean of 1906.2 +/- 7.0 Ma (MSWD: 1.3). Rims have a weighted mean age of 1875 +/- 6.4 Ma (MSWD: 0.6). Oscillatory zonation within cores suggests growth from a magma. These dates are interpreted to reflect D_{N2} partial melting. Rims are interpreted to represent syn-tectonic growths during CLsz related sinistral deformation. Similar Y_2O_3 contents suggest that garnet was still stable and the textural relationship of elongate monazite concordant with mineral lineation suggests that they are syn kinematic with respect to the CLsz.

10W-110

The northernmost portion of the CLsz, along the southeastern portion of Scharfe Lake is underlain by coarse, megacrystic, Beed granite, similar to that in the northwestern hangingwall (Zone 5). Monazite grains from this rock are large, ranging in size from 75 to 200 μms. Analyses show that the majority of grains, and their complex zonation, is Archean in age (Regan, unpublished data). There are however, several small tips on monazite crystals that yield Paleoproterozoic ages. M9 contains two symmetric high Th rims on either side of the crystal, each yielding a 1903 +/- 3 and 1904 +/-24 Ma ages. One monazite crystal (M2) is located within a sinistral shear band and has δ-type asymmetry on one side. The majority of the grain is Archean in age. However, a very thin (~3 μm) rim yielded an age of 1885 +/- 11 Ma.

10W-098a

Sample 10W-098 is a felsic granulite from Zone 3 of the CLsz and is immediately adjacent to 10W-099 (P-T sample above). Sinistral kinematic indicators at both outcrop and thin

section scale are apparent within this sample. Two monazite generations were identified based on morphology. Group 1 are typically equant whereas group 2 grains contain a shape preferred orientation with high aspect ratios (6:1). Group 2 grains are consistently aligned with the stretching lineation of the CLsz. Y contents in both generations are low, but group 1 grains contain, on average, less Y than group 2 grains.

Group 1 monazite yield a weighted mean of 1916 +/- 12 Ma (MSWD: 0.42), and are interpreted to reflect prograde metamorphism that coincided with the onset of D_{C2}, and garnet stability. Group 2 monazite grains yield a weighted mean of 1888 +/- 6 Ma (MSWD: 0.68). Given their textural setting, and slightly higher Y contents, it seems likely that group 2 grains represent CLsz related deformation, and perhaps, the onset of garnet breakdown, typically to biotite.

Discussion

Setting of the Cora Lake shear zone

Three periods of tectonism have been identified within the Cora Lake area. The oldest two are recognized in the northwest and southeast wall rocks outside of the shear zone. They are penetrative, pervasive, and regionally developed. Both hanging and footwall contain evidence of an Archean subhorizontal layering that underwent large amplitude folding at ca. 1900 Ma, with progressive development of a partitioned axial planar shear fabric. The Cora Lake shear zone represents the last event to affect the study area and is also the most localized. It is 4-6 km wide, strongly mylonitic throughout most of its width, and contains a sinistral-normal sense of shear with a dominant strike-slip component. There are abundant compositional variations and strain gradients throughout its width. Metamorphic assemblages include garnet, clinopyroxene, orthopyroxene, plagioclase, with variable amounts of hornblende and biotite within most rock types. Anthophyllite and randomly oriented chlorite (pseudomorphs of garnet and orthophyroxene) are post kinematic. Metamorphic conditions range from conditions similar to

peak P-T (Hangingwall: 0.9 GPa and 750°C; Footwall: 1.17 GPa and 800°C) to 0.82 GPa and 700°C (10W-099) from Chipman domain affinity rocks.

Figure 17 is a composite P-T-t-D path for both hanging and footwall, including deformation within the CLsz. Deformation and metamorphism in both hangingwall and footwall were nearly synchronous although the structural style and metamorphic grade differ.D_1 involved a subhorizontal fabric and, at least in the hanging wall, top-to-the-east flow (Dumond et al., 2010). Monazite geochronology suggests that D_1 fabric on both sides of the shear zone formed during ca. 2.570-2.560 Ga tectonism. Hanging and footwall developed upright, open folds, with a strong axially planar fabrics during the peak metamorphic conditions (D_2) at ca. 1.900 Ga. Shortly after the D_2 event, the CLsz became active with a sinistral-normal sense of shear. Progressive uplift of footwall rocks relative to hangingwall mylonites accommodated the juxtaposition of the two lithotectonic domains during cooling from ca. 1.890-1.875Ga.

No piercing point has been recognized in order to place a precise measure of offset across the CLsz. However, there is a P-T difference of just under 0.3 GPa and 100°C. Reworked hangingwall and footwall rocks within the shear zone yield converging P-T paths, suggesting that the subdomains were juxtaposed by the end of CLsz deformation. Provided an average stretching lineation (slip vector) of 19° to 238° within an average foliation of 231°, 71°assuming a geobaric gradient of 37 km/GPa, the discontinuity across the CLsz would be consistent with approximately 10 km of dip slip and 35 km of left-lateral strike-slip motion.

Distinctly different rock types are juxtaposed across the CLsz, tonalite to the southeast and charnockite/granitoid to the northwest. This juxtaposition could have been the result of the horizontal component of motion, although 35 km may be too small for such a change in rock types, and the truncation of the Chipman dike swarm. Furthermore, the Chipman batholith continues northeastward along strike for 100s of km (Martel et al., 2008; Mahan et al., 2008), and

should be present within the immediate hangingwall if horizontal motion alone took place. An alternative interpretation is that the major heterogeneity defined by the CLsz came about due to the vertical component of displacement. The vertical component (~10km) of offset may have juxtaposed different crustal layers. By this interpretation, granitoids of the northwestern hangingwall may be underlain by the tonalite, similar to southeastern footwall rock types. This is supported by the presence of a several-km-wide subdomain of Chipman-like tonalite (*see Fig. 3*), with mafic (Chipman?) dikes at Father Lake in the northwestern domain;this anomalous tonalite occuranceis currently under investigation.

Localization

Localization is a process by which strain is continually partitioned into smaller regions of even higher finite strain, which suggests that strain is accommodated by a decreasing volume through time (Gerbi et al., 2010; De Brasser et al., 2001). The CLsz represents a highly localized deformation event within the Athabasca granulite terrane, and corresponds to a major lithotectonic discontinuity. Of particular interest is the fact that the CLsz seems to have initiated immediately after peak metamorphic conditions, as early as 1890 Ma, but was localized, with no CLsz related deformation identified outside of the shear zone. Therefore, the CLsz represents a major period of localization within the Athabasca granulite terrane and given abundant high strain zones and systematic variation of P-T with decreasing grain size, likely represents progressive localization within the shear zone similar to that observed by Hanmer (1997) in the Grease River shear zone.

Pressure-temperature estimates from within the reworked footwall of the CLsz document a systematic decrease in pressure associated with increasing strain (finer grain sizes). Relatively coarser mafic granulite mylonites within Zone 3 yield pressure estimates of 1.06 GPa, while extremely fine grained rocks of a similar rock type yield pressure estimates just above 0.8 GPa. Given the kinematics of the shear zone, this outcome suggests that higher strain rocks,

equilibrated at lower pressures. These results imply that localization continued within the CLsz while it was active. Furthermore, these results are in good agreement with titanite data presented in Flowers et al. (2006b), who suggested that the northwestern hangingwall and southeastern footwall were at a similar crustal level (i.e. similar pressure) by approximately 1880 Ma.

The Cora Lake shear contains strain gradients, fine and unannealed crystals, and as noted above, strain localization. Although temperature estimates suggest some cooling during CLsz deformation (ca. 100°C), the lowest temperature of 700°C seems sufficient to accommodate both dynamic and static recovery (Nicolas and Poirier, 1976). Sustained high strain rates have been determined to inhibit crystal coarsening (De Brasser et al., 2001; Hanmer et al., 1995), but this does not explain the preservation of such fine grain sizes. As localization proceeded, segments within the CLsz were abandoned, but remained at temperatures exceeding those expected to result in static coarsening. Yet, the zone is generally unaffected by common post-kinematic processes. Although the reasons for the lack of dynamic or static coarsening are not fully known at present, locally pervasive carbonate veins and the lack of abundant syn-kinematic hydrous phases are consistent with CO_2-rich and H_2O poor conditions during shear, which may have inhibited recovery (Manktelow and Pennacchioni, 2004).

Kinematic evolution of the Athabasca granulite terrane

The western Churchill Province is bounded by two major Paleoproterozoic orogenic belts: the Taltson-Thelon orogen on its western margin and the Trans-Hudson orogen on its southern margin (Fig. 17; modified from Aspler et al.(2002)(Hoffman, 1988)). The Athabasca granulite terrane is located approximately equidistant from both. The Taltson-Thelon orogen defines the boundary between Slave and Churchill Provinces of the Canadian Shield, and was active from ca. 1980-1910 Ma, exemplified by the 1930-1910 Ma Great Slave Lake shear zone, that accommodated major indentation of the Slave craton into the Churchill Province (Hanmer et al., 1992; Hildebrand et al., 2010; Bethune et al., 2012; *and references therein*). The southern

margin of the Churchill Province is defined by the Reindeer Zone (Corrigan et al., 2009; Corrigan, 2005; Chiarenzelli et al., 1998), which represents the orogenic internides of the Trans Hudson orogen between Churchill, Sask, and Superior cratons. This protracted, Himalayan-scale collision culminated at ca. 1820 Ma (Corrigan et al., 2009).

The coalescence and ultimate evolution of the Laurentian craton occurred during several periods of collisional and accretionary events along both the western and southern margin of the Churchill Province (Hildebrand et al., 2010; Corrigan et al., 2009; Hoffman, 1988). Initially, the collision of the Slave craton with the Rae Province caused E-W shortening during the ca. 1980-1910 Ma Taltson-Thelon orogen (Bethune et al., 2013; Hildebrand et al., 2010; Hoffman, 1988), and subsequent indentation of the Slave into the Rae Province (Hanmer et al., 1992). Following this phase of E-W shortening, convergence along the western margin ended, while the Lynn-Lake and La Ronge arcs were accreted along the southern periphery of the Hearne domain during the Reindeer Orogeny (Corrigan et al., 2009). This accretionary phase may have caused NW-SE directed shortening within the Churchill Province from ca. 1890-1870 Ma (Corrigan et al., 2009; *and references therein*). Following this accretionary phase along the southern margin of the Churchill Province, E-W convergence rejuvenated along the western margin (Wopmay orogen) at approximately 1860 Ma (Hildebrand et al., 2010). In conjunction with rejuvenated convergence along the western flank of the continguous Churchill-Slave craton was extensional rollback tectonics along the southern Churchill Province (Corrigan et al., 2009). This period of E-W shortening coincides with reactivation of the Great Slave Lake shear zone, which accommodated approximately 70-125 km of right lateral offset during this latter phase of convergence (Hanmer et al., 1992).

The events outlined above correspond remarkably well with observed kinematic changes within the study region. Large amplitude folding, Chipman dike emplacement, and synchronous dextral shear at ca. 1900 Ma coincides with the latter phases of the Slave craton's initial

indentation into the Churchill craton, and associated E-W shortening (Hanmer et al., 1992). Sinistral shear within the CLsz corresponds remarkably well with accretion of Lynn-Lake and La Ronge arcs along the southern margin of the craton (Corrigan et al., 2009), and cessation of convergence along the western margin (Hildebrand et al., 2010). Following this phase of sinistral shear and further cooling within the lower crust of the Athabasca granulite terrane, dextral kinematics within the Legs Lake shear zone accommodated contractional uplift of the entire region on a similarly oriented stretching lineation at ca. 1850 Ma (Mahan et al., 2003; 2006a). This may be associated with E-W directed shortening along the western margin within the Wopmay orogen post 1860 Ma, and reactivation of the Great Slave Lake shear zone (Hanmer et al., 1992)(Fig. 17).

Peak metamorphic conditions at ca. 1900 Ma are synchronous with the widespread Chipman dike swarm, and pervasive dextral transpression. We propose that the source for the regional thermal perturbation may be a mafic underplate at the base of the crust (Williams et al., 2009; Williams et al., 1995). Based on published and new thermobarometric estimates, regional cooling took place over ~50 my, (Flowers et al., 2006b; Mahan et al., 2003; 2006a,b; 2008; Dumond et al., 2008). We suggest that the thermally weakened region of the lower crust, remained anomalously warm relative to surrounding rocks for 10s of m.y., and as such, was the locus for several periods of localized deformation during the progressive growth of Laurentia on both western and southern margins. The region was, in essence, amonitor to the tectonic processes leading up to the construction of Nuna.

Implications for the Snowbird Tectonic Zone

The CLsz and surrounding rocks coincides with the geophysically defined central Snowbird Tectonic zone (Gilboy, 1980; Hoffman, 1988). Within the Athabasca granulite terrane, the strong correlation between geophysical, magmatic and gravity anomalies represents an array ofnested shear zones that overprint highly deformed granulites. These shear zones juxtapose

crustal blocks of distinctive heritage (Dumond et al., 2013; Hanmer et al., 1994). The largest magnetic anomaly within the region coincides with the southeastern margin of the CLsz (Brown et al., in press), within the western Chipman subdomain. The source of this anomalous magnetism may be mafic granulite bodies with large amounts of magnetite that define the southeastern margin of the CLsz (Brown et al., in press).

The Snowbird tectonic zone has had varied tectonic interpretations over the last three decades including a Paleoproterozoic suture between Rae and Hearne domains of the western Churchill Province (Hoffman, 1988; Berman et al., 2007), an Archean intracontinental shear zone (Hanmer et al., 1995), and an anastomosing series of cross cutting thrust and strike slip shear zones (Mahan and Williams, 2005; Dumond et al., 2013). Most recently, the Snowbird tectonic zone has been suggested to represent a suture between two isolated continents (Rae and Hearne), that were divided by an ocean basin that closed at ca. 1900 Ma (Berman et al., 2007). However, work presented herein suggests that deformation at ca. 1900 Ma is pervasive, but does not represent the hinterland of a continental collision. There is no magmatic arc that preceded Paleoproterozoic deformation indicative of subduction and peak metamorphic conditions were rather short lived (Flowers et al., 2006b). Furthermore, there has been no evidence of foredeep sedimentation typical of collisional sutures within upper stratigraphic positions of the Paleoproterozoic sediments within the vicinity of the study region (Aspler et al., 2002; Aspler and Chiarenzelli, 1996; Ashton et al., 2013). These observations suggest an intracontinental setting during Paleoproterozoic reactivation within the Athabasca granulite terrane.Circa 1.9 Ga deformation is related to a majorintracontinental thermal perturbation of the lower continental crust, exemplified by the widespread Chipman dike swarm, and associated dextral transpression.

The observed structural and lithologic discontinuities are interpreted to reflect episodic pulses of localized deformation that juxtapose varying metamorphic grade and structural history from 1900-1820 Ma (Mahan et al., 2006a; Mahan and Williams, 2005; Dumond et al., 2008,

2013; Flowers et al., 2006b; *among others*). Therefore, the Paleoproterozoic history of the central Snowbird tectonic zone is interpreted to reflect intracontinental deformation caused by thermal weakening, expressed by the widespread Chipman dike swarm (Flowers et al., 2006a). The zone remained weak as the terrane slowly cooled, and was reactivated during the several periods of orogenisis along the craton margins.

References

Andsell, K.M., 2005, Tectonic evolution of the Manitoba-Saskatchewan segment of the Paleoproterozoic Trans-Hudson Orogen, Canada: Canadian Journal of Earth Sciences, v. 42, p. 741-759.

Aranovich, L.Y., and Berman, R.G., 1997, A new garnet-orthopyroxene thermometer based on reversed Al_2O_3 solubility in FeO-Al_2O_3-SiO_2 orthopyroxene: American Mineralogists, v. 97, p. 331-342.

Aspler, L.B., Chiarenzelli, J.R., and McNicoll, V.J., 2002, Paleoproterozoic basement-cover infolding and thick-skinned thrusting in Hearne domain, Nunavut, Canada: intracratonic response to Trans-Hudson orogen: Precambrian Research, v. 116, p. 331-354

Baldwin, J.A., Bowring, S.A., Williams, M.L., and Williams, I.S., 2004, Eclogites of the Snowbird tectonic zone: Petrologic and U-Pb geochronological evidence for Paleoproterozoic high-pressure metamorphism in the western Canadian Shield: Contributions to Mineralogy and Petrology, v. 147, n. 5, p. 528-548, doi: 10.10007/s00410-004-0572-4.

Berman, R.G., Davis, W.J., and Pehrsson, S., 2007, Collisional Snowbird tectonic zone resurrected: Growth of Laurentia during the 1.9 Ga accretionary phase of the Hudsonian orogeny: Geology, v. 35, n. 10, p. 911-914, doi:10.1130/G23771A.1.

Berman, R.G., 2006, Thermobarometry with Estimation of Equilibration State (TWEEQU): An IBM Compatible Software Package: Geological Survey of Canada, Open file 5408, Ottawa.

Berman, R.G., and Aranovich, L.Y., 1996, Optimized standard state and solution properties of minerals I. Model calibration for olivine, orthopyroxene, cordierite, garnet, and ilmenite in the system FeO-MgO-CaO-Al_2O_3-TiO_2-SiO_2: Contributions to Mineralogy and Petrology, v. 119, p. 30-42.

Berman, R.G., 1991, Thermobarometry using multi-equilibrium calculations: A new technique with petrological applications: Canadian Mineralogists, v. 29, p. 833-855.

Bethune, K.M., Berman, R.G., Rayner, N., and Ashton, K.E., 2013, Structural, petrological and U-Pb SHRIMP geochronological study of the western Beaverlodge domain: Implications for crustal architecture, multi-stage orogenesis and the extent of the Taltson orogen in the SW Rae craton, Canadian Shield: Precambrian Research, v. 232, p. 89-118.

Brown, L.L., Webber, J., Williams, M.L., Regan, S., Seaman, S., *in review*, Magnetism of the Lower Crust: observations from the Chipman Domain, Athabasca Granulite Terrain, northern Canada: Tectonophysics

Brown, M., Korhonen, F.J., and Siddoway, C.S., 2011, Organizing melt flow through the crust: Elements: When the Continental Crust Melts, Ed(s) E.W. Sawyer et al., p. 261-288.

Chiarenzelli, J.R., Aspler, L., Villeneuve, M., and Lewry, J.,1998, Early Proterozoic evolution of the Saskatchewan craton and its allochthonous cover, Trans-Hudson orogen: Journal of Geology, v. 106, p. 247-267.

Corrigan, D., Hajnal, Z., Nemeth, B., and Lucas, S.B., 2005, Tectonic framework of a Paleoproterozoic arc-continent to continent-continent collisional zone, Trans-Hudson Orogen, from geological and seismic reflection studies: Canadian Journal of Earth Sciences, v. 42, p. 421-434, doi: 10.1139/05-025.

Corrigan, D., Pehrsson, S., Wodicka, and de Kemp, E., 2009, The Paleoproterozoic Trans-Hudson Orogen: a prototype of modern accretionary processes: in Ancient Orogens and Modern Analogues, Ed(s) Murphy et al., Geological Society of London, Special Publications, v. 327, p. 457-479, doi:10.1144/SP327.19.

Cousens, B.L., Aspler, L.B., Chiarenzelli, J.R., Donaldson, J.A., Sandeman, H., Peterson, R.D., LeCheminant, A.N., 2001, Enriched Archean lithospheric mantle beneath western Churchill Province tapped during Paleoproterozoic orogenesis: Geology, v. 29, n. 9, p. 827-830.

De Bresser, J.H.P., Ter Heege, J.H., and Spiers, C.J., 2001, Grain size reduction by dynamic recrystallization: can it result in major rheological weakening?: International Journal of Earth Sciences, v. 90, p. 28-45.

Dumond, G., McLean, N., Williams, M.L., Jercinovic, M.J., and Bowring, S.A., 2008, High resolution dating of granite petrogeneisis and deformation in a lower crustal shear zone: Athabasca granulite terrane, western Canadian Shield: Chemical Geology, v. 16, n. 4, p. 175-196, doi:10.1016/j.chemgeo.2008.04.014.

Dumond, G., Goncalves, P., Williams, M.L., and JHercinovic, M.J., 2010, Subhorizontal fabric in exhumed continental lower crust and implication for lower crustal flow: Athabasca granulite terrane, Western Canadian Shield: Tectonics, v. 29, TC2006, doi:10.1029/2009TC002514.

Dumond, G., Mahan, K.H., Williams, M.L., and Jercinovic, M.J., 2013, Transpressive uplift and exhumation of continental lower crust revealed by synkinematic monazite reactions: Lithosphere, v. 5, n. 5, p. 507-512, doi: 10.1130/L292.1

Dumond,G., Mahan, K.H., Williams, M.L., and Karlstrom, K.E., 2007, Crustal segmentation, composite looping pressure-temperature paths, and magma-enhanced metamorphic fi eld gradients: Upper Granite Gorge, Grand Canyon, USA: GSA Bulletin, v. 119, p. 202-220, doi: 10.1130/B25903.1

Flowers, R., Bowring, S.A., Mahan, K.H., and Williams, M.L., 2006a, Timescales and significance of high pressure, high-temperature metamorphism and mafic dike anatexis, Snowbird

tectonic zone, Canada: Contribution to Mineralogy and Petrology, v. 151, n. 5, p. 558-581, doi:10.1007/s00410-006-0066-7.

Flowers, R.M., Mahan, K.H., Bowring, S.A., Williams, M.L., Pringle, M.S., and Hodges, K.V., 2006b,Multistage exhumation and juxtaposition of lower continental crust in the western Canadian Shield: linking high resolution U-Pb and $^{40}Ar/^{39}Ar$ thermochronometry with pressure-temperature-deformation paths: Tectonics, v. 25, TC4003, doi:10.1029/2005TC001912.

Flowers, R.M., Bowring, S.A., Mahan, K.H., Williams, M.L., and Williams, I.S., 2008, Stabilization and reactivation of cratonic lithosphere from the lower crustal record in the western Canadian shield: Contributions to Mineralogy and Petrology, v. 156, n. 4, p. 529-549, doi:10.1007/s00410-008-0301-5.

Furhman, M. L. and Lindsley, D. H., 1988. Ternary-feldspar modeling and thermometry: American Mineralogist, v. 73, p. 201–216.

Gerbi, C., Culshaw, N., and Marsh, J., 2010, Magnitude of weakening during crustal-scale shear zone development: Journal of Structural Geology, v. 32, p. 107-117.

Gilboy, C.F., 1980, Bedrock compilation geology: Stongy Rapids area (NTS 74p)-Prelimanary geological map, scale 1:250,000, Sask. Geol. Surv., Sask. Energy and mines, Regina.

Green, D. H. and Ringwood, A. E., 1967, An experimental investigation of the gabbro to eclogite transformation and its petrological applications: Geochimica et Cosmochimica Acta, v. 31, p. 767–833

Hanmer, S., Bowring, S.A., Van Breeman, O., and Parrish, R.R., 1992, Great Slave Lake shear zone, northwest Canada: mylonitic record of Early Proterozoic convergence, collision, and indentation: Journal of Structural Geology, v. 14, p. 757-773.

Hanmer, S., 1994, Geology, East Athabasca mylonite triange, Saskatchewan, Map 1859A, scale 1:100,000, Geol. Surv. Of Can., Ottawa.

Hanmer, S., 1997, Geology of the Striding-Athabasca mylonite zone, northern Saskatchewan and southeastern District of Mackenzie, Northwest Territories: Pap. Geol. Surv., of Can., Ottawa.

Hanmer, S., Parrish, R., Williams, M., and Kopf, C., 1994, Striding-Athabasca Mylonite: Complex Archean deep crustal deformation in the East Athabasca mylonite triangle, N. Saskatchewan: Canadian Journal of Earth Sciences, v. 31, p. 1287-1300, doi:10.1139/e94-111.

Hanmer, S., Williams, M., and Kopf, C., 1995, Modest movements, spectacular fabrics in an intracontinental deep-crustal strike-slip fault: Striding-Athabasca mylonite zone, NW Canadian Shield: Journal of Structural Geology, v. 17, n. 4, p. 493-507, doi:10.1016/0191-8141(94)00070-G.

Hildebrand, R.S., Hoffman, P.F., and Bowring, S.A., 2010, the Calderian orogeny in Wopmay orogen (1.9 Ga), northwestern Canadian Shield: Geological Society of America Bulletin, v. 122, p. 794-814, doi: 10.1130/B26521.1

Hoffman, P.F., 1988, United Plates of America, the birth of a craton: Early Proterozoic assembly and growth of Laurentia: Annual Review of Earth and Planetary Sciences, v. 16, p. 543-603, doi:10.1146/annurev.ca.16.050188.002551.

Holland, M.E., Williams, M.L., and Regan, S.P., 2012, The mary reaction: timing deep crustal deformation and metamorphism with implications for strengthening and stabilization of flowing lower crust: NEGSA 47th abstracts with programs.

Jercinovic, M.J., Williams, M.L., and Lane, E.D., 2008, In-situ trace element analysis of monazite and other fine-grained accessory minerals by EPMA: Chemical Geology, v. 254, p. 197-215.

Karlstrom, K.E., and Bowring, S.A., 1988, Early Proterozoic assembly of tectonostratigraphic terranes in south-western North America: The Journal of Geology, v. 96, p. 561–576.

Klepeis, K. A., G. L. Clarke, G. Gehrels, and J. Vervoort (2004), Processes controlling vertical coupling and decoupling between the upper and lower crust of orogens: Results from Fiordland, New Zealand, Journal of Structural Geology, v. 26, n. 4, p. 765–791, doi:10.1016/j.jsg.2003.08.012

Koteas, G.C., Williams, M.L., Seaman, S.J., and Dumond, G., 2010, Granite genesis and mafic-felsic magma interaction in the lower crust: Geology, v. 38, p. 1067-1070, doi:10.1130/G31017.1.

Leslie, S., 2012, Contrasts in sillimanite deformation in felsic tectonites from anhydrous granulite- and hydrous amphibolite-facies shear zones, western Canadian Shield [M.S.: University of Colorado, 69 p.

Macdonald, R., 1980, New edition of the geological map of Saskatchewan, Precambrian Shield area, in Summary of Investigations, Misc. Rep. 01-4.2, p. 19-21, Sask. Geol. Surv., Sask. Ind. And Resour, Regina.

Mader, U., Percival, J.A., and Berman, R.G., 1994, Thermobarometry of garnet-clinopyroxene-hornblende granulites from the Kapuskasing structural zone: Canadian Journal of Earth Sciences, v. 31, p. 1134-1145.

Mahan, K.H., Williams, M.L., and Baldwin, J.A., 2003, Contractional uplift of deep crustal rocks along the Legs Lake shear zone, western Churchill Province, Canadian Shield: Canadian Journal of Earth Sciences, v. 40, n. 8, p. 1085-1110, doi:10.1139/e03-039.

Mahan, K.H., and Williams, M.L., 2005, Reconstruction of a large deep-crustal terrane: Implication for the Snowbird tectonic zone and early growth of Laurentia: Geology, v. 33, n. 5, p. 385-388, doi:10.1130/G21273.1.

Mahan, K.H., Goncalves, P., Williams, M.L., and Jercinovic, M.J., 2006a, Dating metamorphic reactions and fluid flow: Application to exhumation of high-P granulites in a crustal-scale shear zone, western Canadian Shield: Journal of Metamorphic Geology, v. 24, n. 3, p. 193-217, doi:10.1111/j.1525-1314.2006.00633.x.

Mahan, K.H., Williams, M.L., Flowers, R.M., Jercinovic, M.J., Baldwin, J.A., and Bowring, S.A., 2006b, Geochronological constraints on the Legs Lake shear zone with implications for regional exhumation of lower continental crust, western Churchill Province, Canadian Shield: Contributions to Mineralogy and Petrology, V. 152, n. 2, p. 223-242, doi:10.1007/s00410-006-0106-3.

Mahan, K.H., Goncalves, P., Flowers, R., Williams, M.L., and Hoffman-Setka, D., 2008, The role of heterogeneous strain in the development and preservation of a polymetamorphic record in high-P granulites, western Canadian Shield: Journal of metamorphic geology, v. 26, n. 6, p. 669-694, doi:10:111/j.1525-1314.2008.00783.x.

Mahan, K.H., Smit, C.A., Williams, M.L., Dumond, G., and Van Reenan, D.D., 2011, Heterogeneous strain and polymetamorphism in high-grade terranes: Insight into crustal processes from the Athabasca Granulite Terrane, western Canada, and the Limpopo Complex, southern Africa: in van Reenen, D.D., Kramers, J.D., McCourt, S., and Perchuk, L.L., eds., Origin and evolution of Precambrain High-Grade Gneiss terranes, with Special Emphasis on the Limpopo Complex of Southern Africa: GSA Memoir, V. 207, p. 269-287, doi:10.1130/2011.1207(14).

Mancktelow, N. S., and G. Pennacchioni (2004), Theinfluence of grain boundary fluids on the micro- structure of quartz-feldspar mylonites,Journal of Structural Geology, v. 26, n.1, p. 47–69, doi:10.1016/S0191-8141(03)00081-6

Martel, E., van Breeman, O., Berman, R.G., and Pehrsson, S., 2008, Geochronology and tectonometamorphic history of the Snowbird Lake area, Northwest Territories, Canada: New insights into the architecture and significance of the Snowbird tectonic zone: Precambrian Research, v. 161, n. 3-4, p. 201-230, doi:10.1016/j.precamres.2007.07.007.

Maxeiner, R.O., and Rayner, N., 2010, Continental arc magmatism along the southeast Hearne Craton margin in Saskatchewan, Canada: Comparison of the 1.92-1.91 Ga Porter Bay Complex and the 1.86-1.85 Ga Wathaman Batholith: Precambrian Research, v. 184, p. 93-120, doi:10.1016/j.precamres.2010.10.005.

Nicolas, A., and Poirier, J.P., 1976, Crystalline plasticity and solid state flow in metamorphic rocks: Selected Topics in Geological Sciences, ed. M.H.P. Bott, John Wiley and Sons, p. 444

Orlandini, O.F., Mahan, K.H., Regan, S., Williams, M.L., and Leite, A., 2013, Microstructure of deep crustal pseudotachylyte-bearing mylonites: GSA annual meeting, Denver CO

Passchier, C.W., and Trouw, R.A.J., 2005, Microtectonics, 2nd edition, 366 pp. Springer, Berlin.

Percival, J.A., 1992, Exposed crustal cross sections as windows on the lower crust: in Continental Lower Crust, ed(s): D.M. Fountain et al., pp. 317-362, Elsevier, Amsterdam.

Pouchou, J.L., and Pichoir, F., 1984, Possibilités d'analyse en profondeur à la microsonde électronique: *Recherche Aérospatiale, v. 5, p. 349-351.*

Regan, S.P., Williams, M.L., Mahan, K.H., Dumond, G., Jercinovic, M.J., and Orlandini, O.P., in prep, Neoarchean arc magmatism and subsequent collisional orogenisis within the eastern Athabasca granulite terrane: implications for the early growth of the western Churchill Province: to be submitted to Precabrian Research

Spear, F.S., 1993, Metamorphic phase equilibria and Pressure-Temperature-Time paths: 2nd edition, Mineralogical Society of America, Washington D.C., p. 799.

White, S.H., 1976, The effects of strain on the microstructures, fabrics, and deformation mechanisms in quartzites: Philosophical Transactions of the Royal Society of London A, v. 283, p. 69-86.

Whitmeyer, S.J., Karlstrom, K.E., 2007, Tectonic model for the Proterozoic growth of North America: Geosphere, v. 3, n. 4, p. 220-259.

Williams, M.L., and Hanmer, S., 2006, Structural and metamorphic processes in the lower crust: Evidence from a deep-crustal isobarically cooled terrane, Canada: Evolution and Differentiation of the Continental Crust, ed(s) M. Brown and T. Rushmer, p. 231-267, Cambridge University Press, Cambridge.

Williams, M.L., and Jercinovic, M.J., 2002, Microprobe monazite geochronology: putting absolute time into microstructural analysis: Journal of Structural Geology, v. 24, p. 1013-1028, doi:10.1016/S0191-8141(01)00088-8.

Williams, M.L., Hanmer, S., Kopf, C., and Darrach, M., 1995, Syntectonic generation and segregation of tonalitic melts from amphibolite dikes in the lower crust, Striding-Athabasca mylonite zone, northern Saskatchewan: Journal of Geophysical Research, V. 100, n. B8, p. 15,717-15,734, doi:10.1029/95JB00760.

Williams, M.L., Melis, E.A., Kopf, C.F., and Hanmer, S., 2000, Microstructural tectonometamorphic processes and the development of gneissic layering: A mechanism for metamorphic segregation: Journal of Metamorphic Geology, v. 18, p. 41-57, doi:10.1046/j.1525-1314.2000.00235.x.

Williams, M.L., Jercinovic, M.J., Goncalves, P., and Mahan, K., 2006, Format and philosophy for collecting, compiling, and reporting microprobe monazite ages: Chemical Geology, v. 225, n. 1-2, p. 1-15

Williams, M.L., Jercinovic, M.J., Harlov, D.E., Budzyn, B., and Hetherington, C.J., 2011, Resetting monazite ages during fluid-related alteration: Chemical Geology, v. 283, p. 218-225, doi:10.1016/j.chemgeo.2011.01.019.

Williams, M.L., Karlstrom, K.E., Dumond, G., and Mahan, K.H., 2009, Perspectives on the architecture of continental crust from integrated field studies of exposed isobaric sections: in Miller, R.B., and Snoke, A.W., eds., Crustal Cross Sections from the Western North American Cordillera and Elsewhere: Implication for Tectonic and Petrologic Processes: GSA Special Paper 465, p. 219-241, doi:10.1130/2009.2456(08).

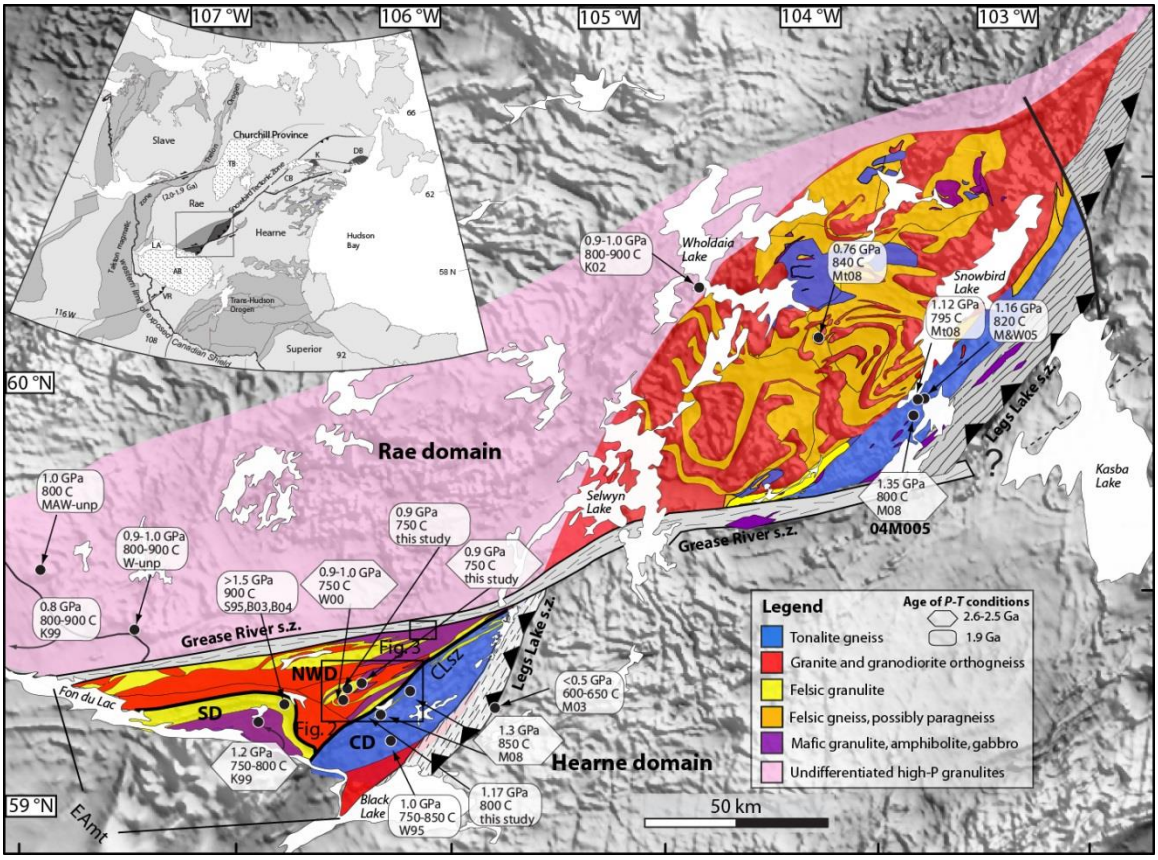

Figure 2: (a) Simplified geological and tectonic map of the western Churchill Province. AB, Athabasca basin; CB, Chesterfield block; DB, Daly Bay complex; K, Kramanituar complex; TB, Thelon basin; VR, Virgin River shear zone, (b) Simplified geology of the the high-P Athabasca granulite terrane. The pink shading approximates that part of the Rae domain (undifferentiated) thought to be underlain by high-P (~1.0 GPa) rocks based on reconnaissance mapping. East Athabasca mylonite triangle (EAmt) divided in Chipman domain (CD), Southern Domain (SD), North-western domain (NWD), and Cora Lake shear zone (CLsz). Dark outline in the east Athabasca mylonite triangle shows the location of Fig. 2 and 3.Modified from *Mahan et al. (2008) and references therein*,i

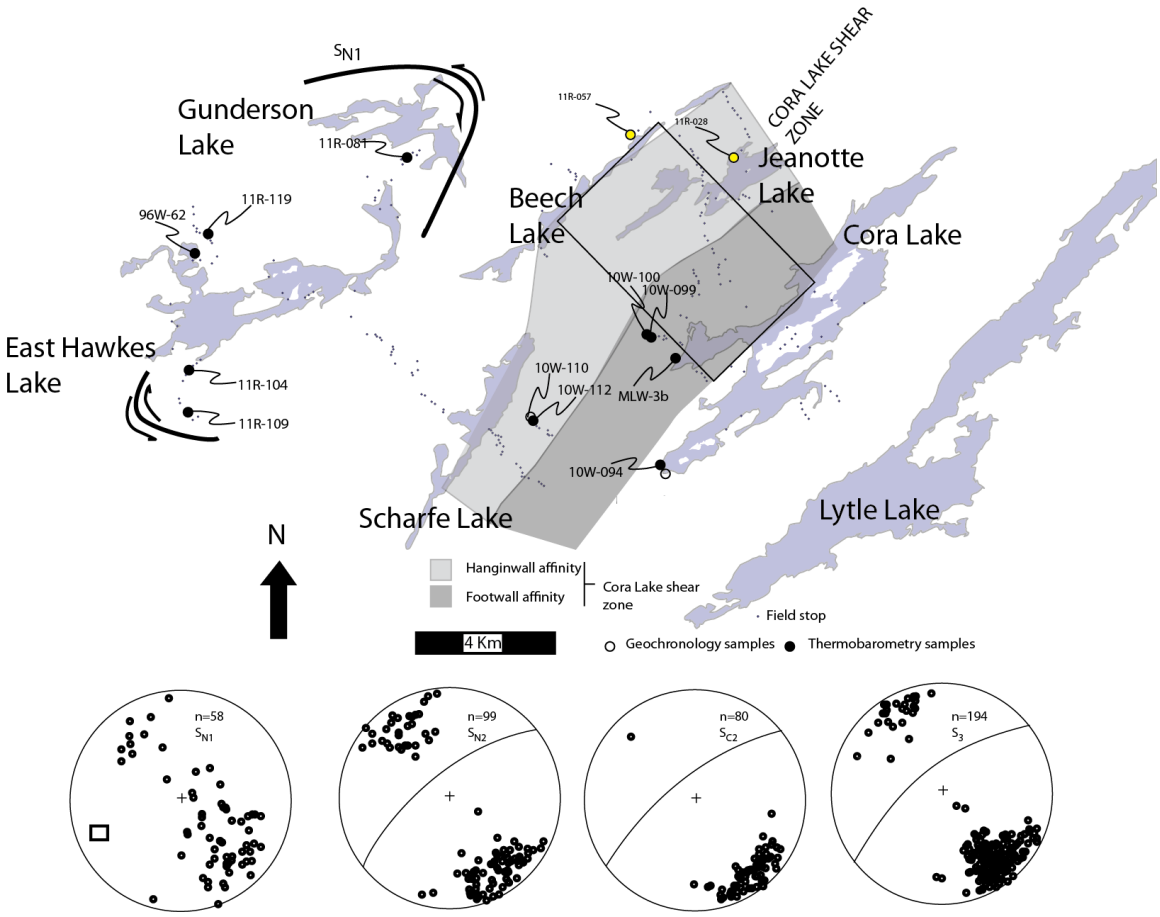

Figure 3: Simplified map of the central CLsz (this study) showing the shear zone, and as well as the location of hangingwall and footwall affinity rocks. Sample locations are shown, with color indicating the type of data ascertained.

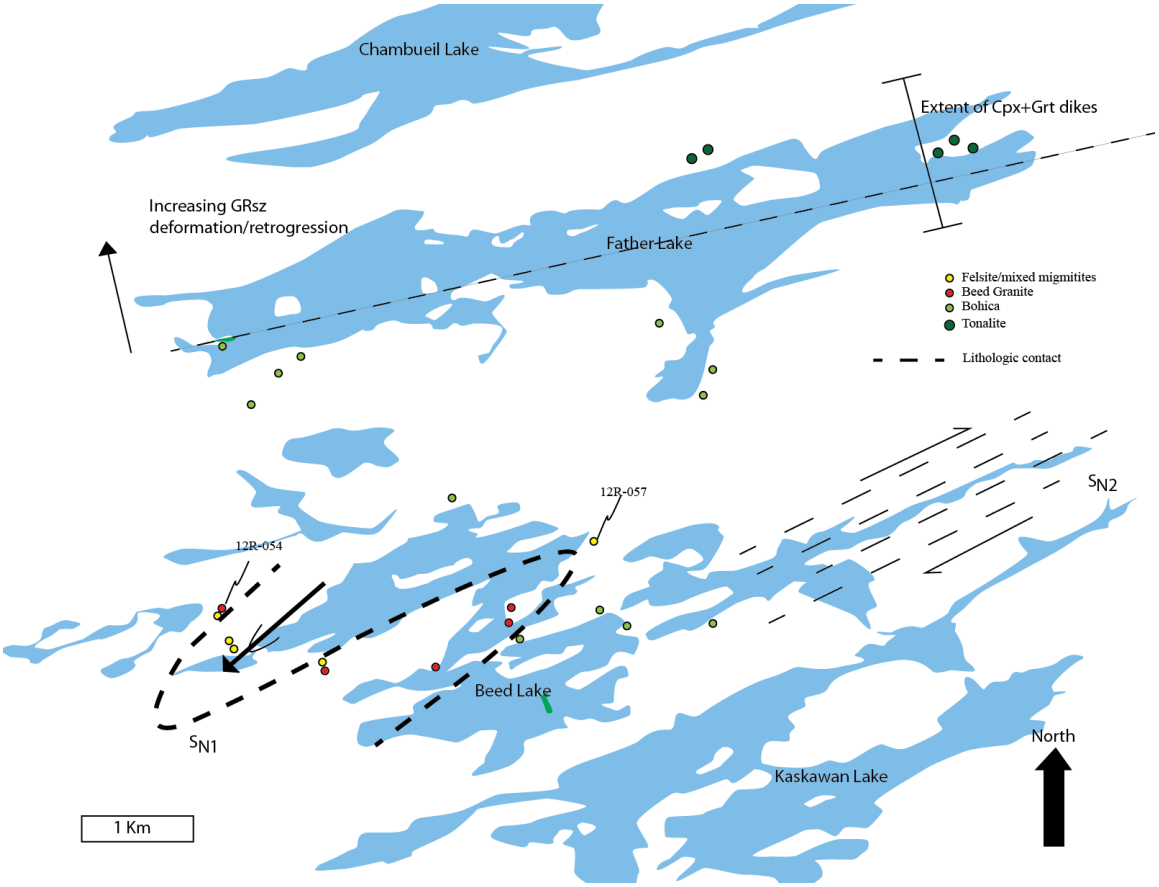

Figure 4: Sample locations within the Beed Lake region in the northwestern hangingwall. Compositional contact between Beed Granite, and diatexitic units drawn with adashed line. Samples discussed in text are labeled. GRsz: Grease River shear zone.

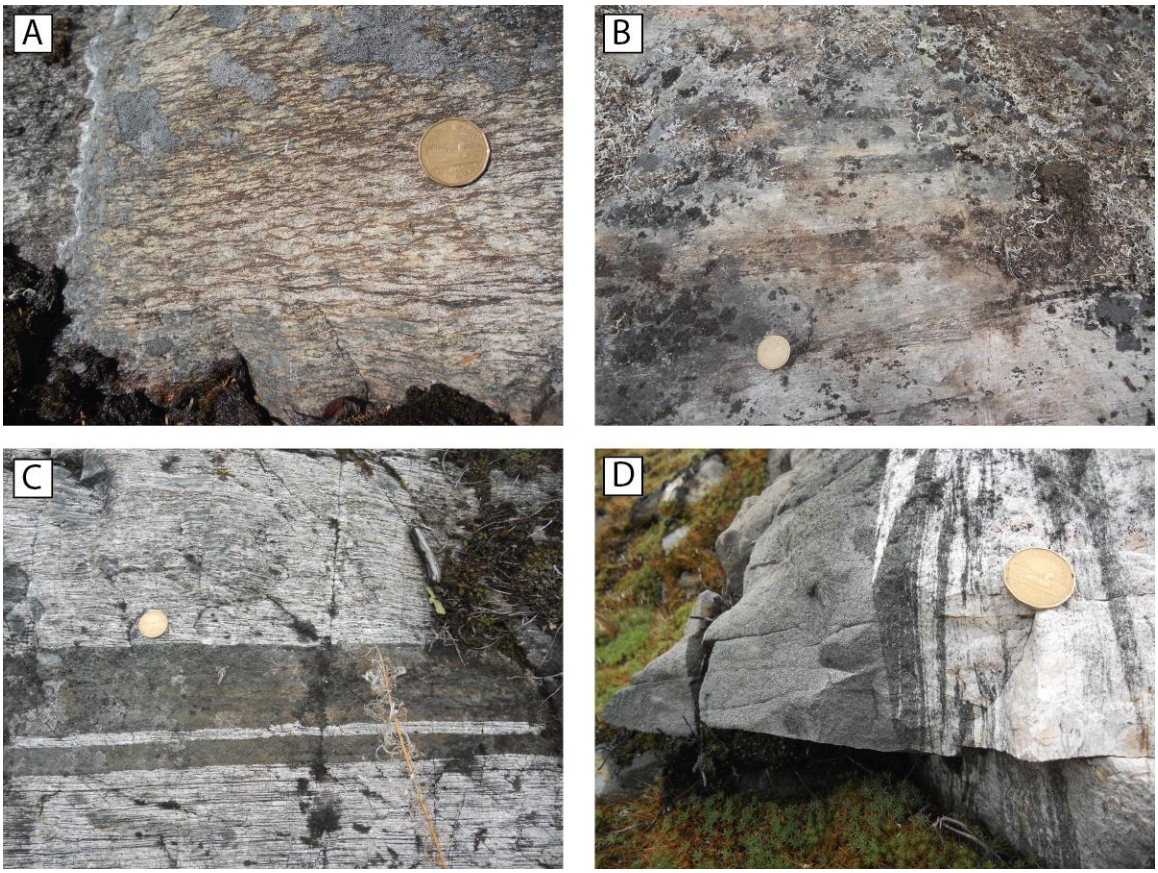

Figure 5: Representative field photographs of common lithologies (Canadian dollar for scale). Northwestern hangingwall: (A) the Porphyroclastic Mary Granodiorite; (B) The Bohica intermediate to mafic suite; Southeastern footwall: (C) the ~3.2 Ga Chipman tonalite straight gneiss with characteristic mafic granulite and tonalite banding; (D) a ~1.9 Ga Chipman dike with characteristic obliquity to Chipman tonalite.


A


B

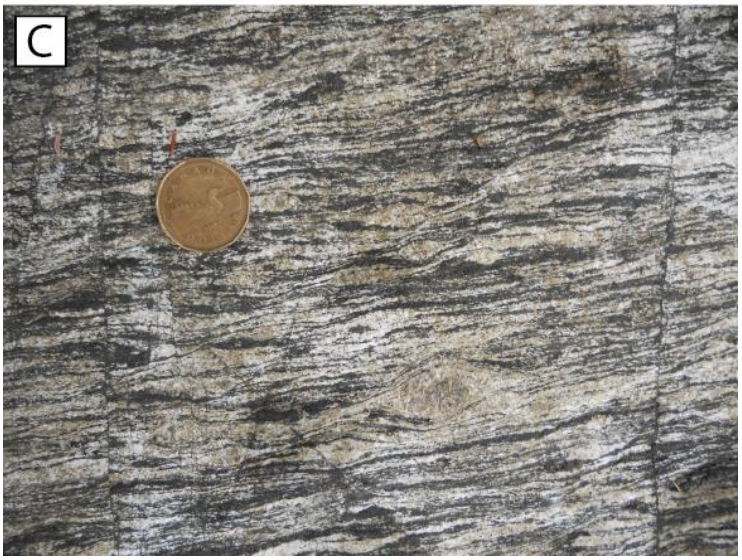
C

Figure 6: Common rock types of the CLsz (Canadian dollar for scale): (A) Felsic granulite with brecciated lilac garnet porphyroblasts; (B) Orthopyroxene bearing intermediate granulite with intrafolial folds; (C) biotite bearing megacrystic k-feldspar granitoid w sinistral shear bands.

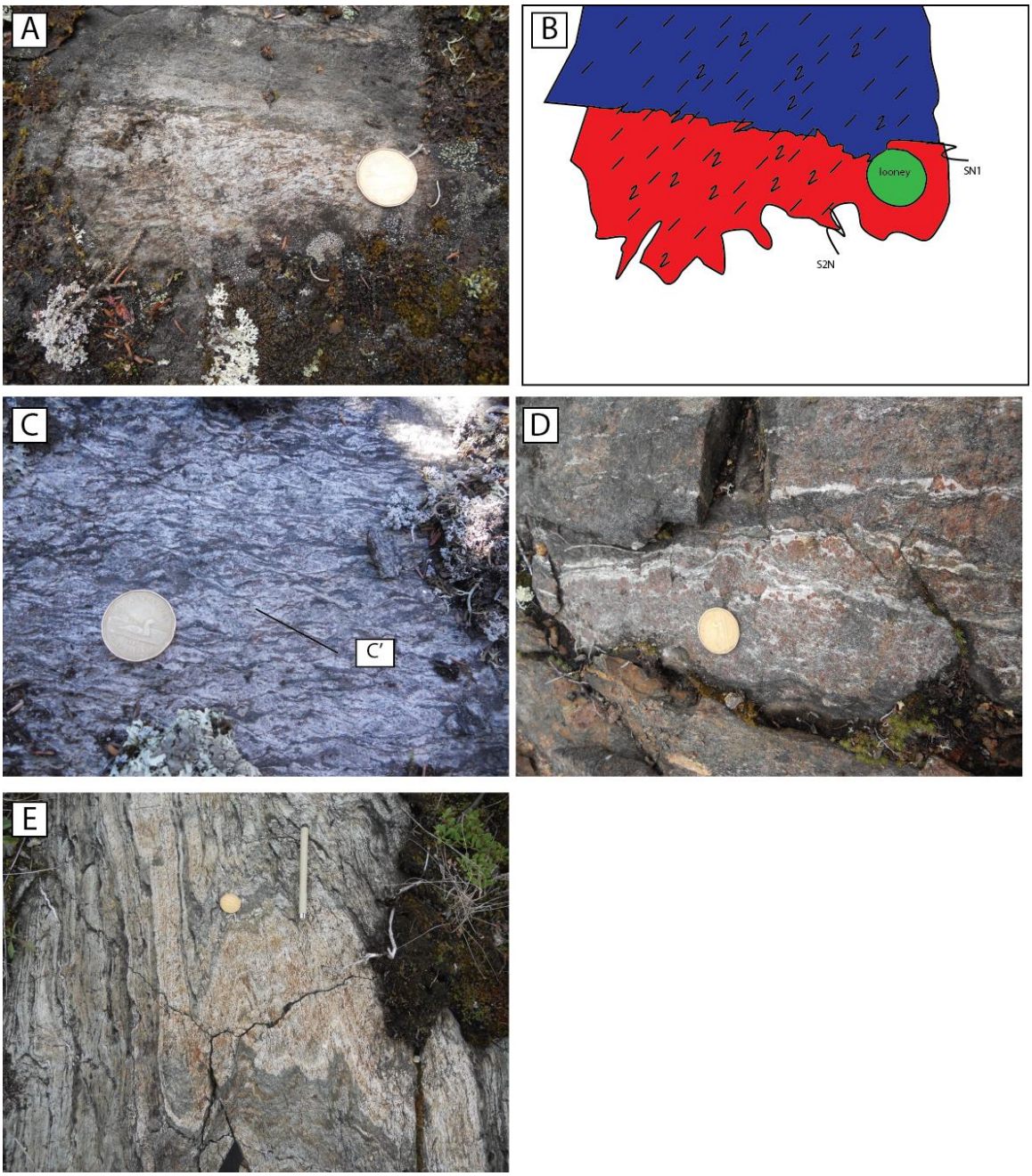

Figure 7: Schematic sketch displaying an idealized transect from the central CLsz (outlined in Fig. 2). Zones are outlined with a qualitative description of intensity represented by form lines. Blue represents portion of the CLsz interpreted to represent reworked footwall, and red representing reworked hangingwall. See text for zone descriptions.

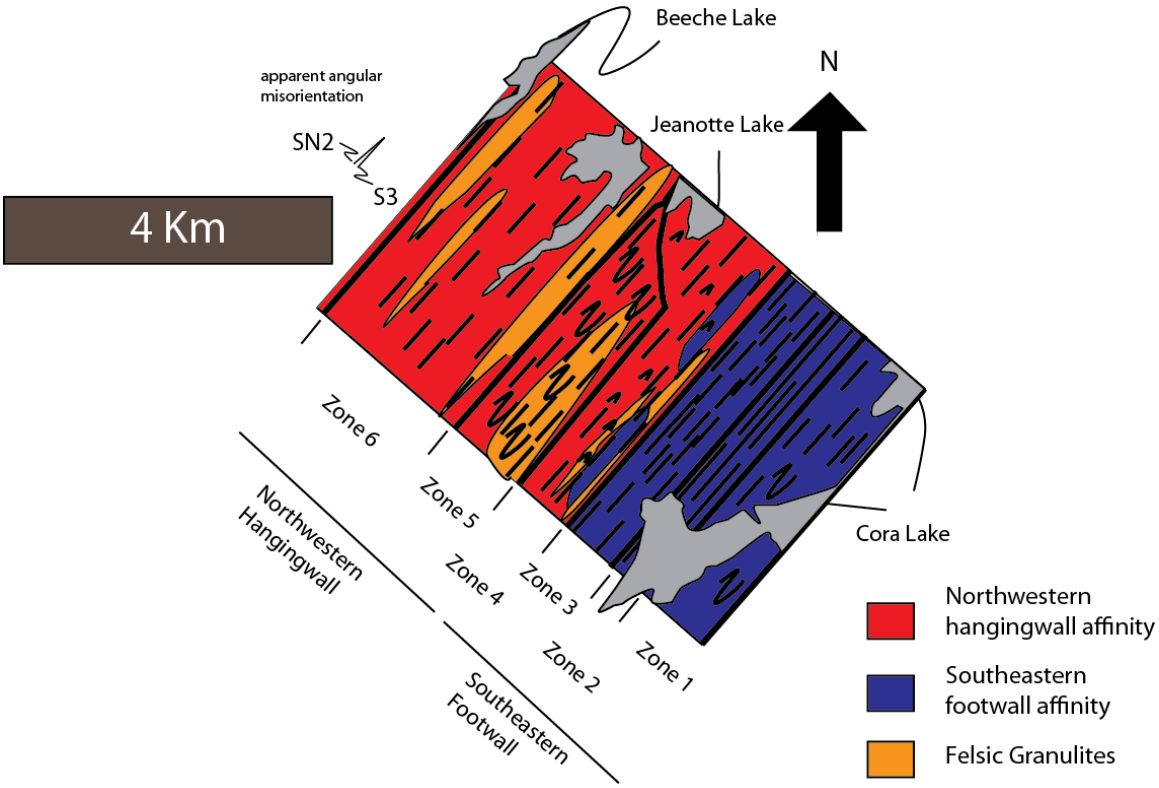

Figure 8: Schematic sketch displaying an idealized transect from the central CLsz (outlined in Fig. 2). Zones are outlined with a qualitative description of intensity represented by form lines. Blue represents portion of the CLsz interpreted to represent reworked footwall, and red representing reworked hangingwall. See text for zone descriptions.

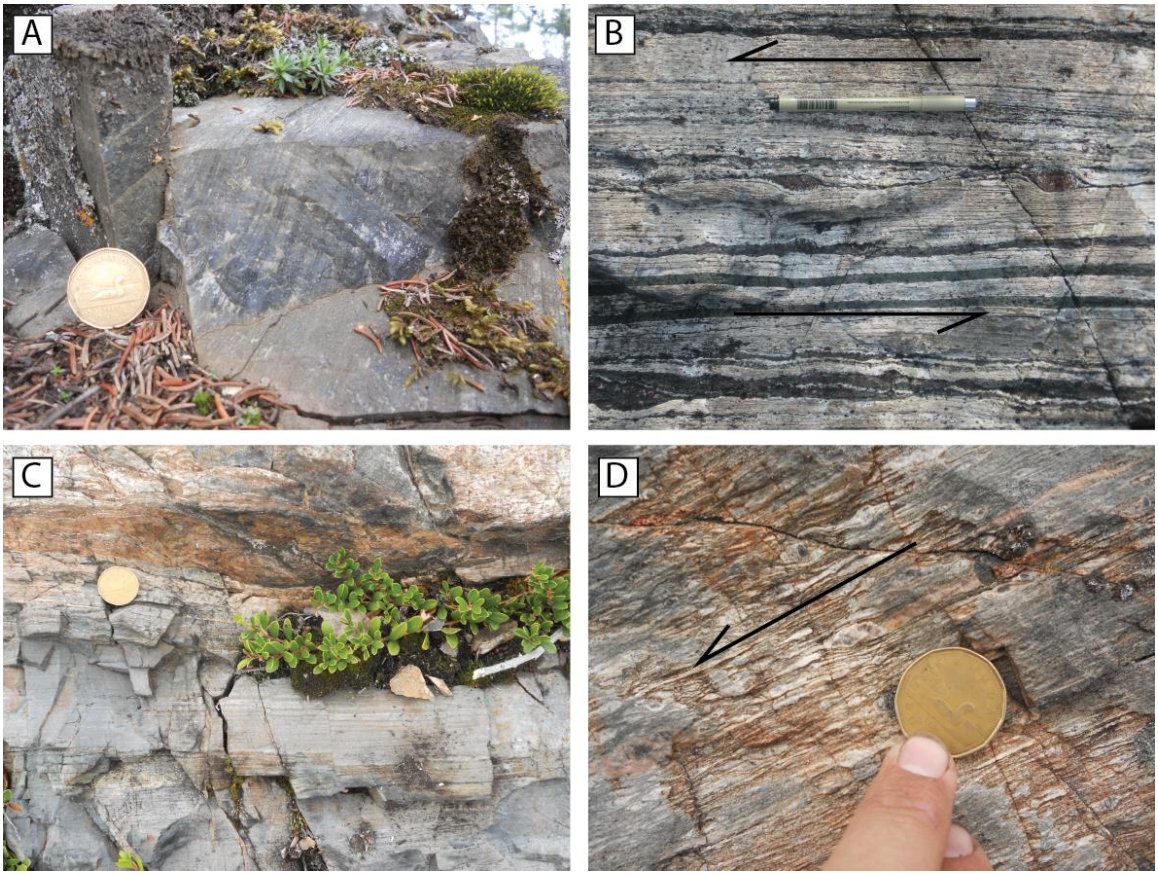

Figure 9: Photographs from the Cora Lake shear zone: (A) glassy anorthosite from Zone 2 displaying spectacular ultramylonitic textures with grain sizes approaching a micron, Canadian dollar for scale; (B) sinistral σ-clast developed around coarse garnet porphyroblasts within zone 3 chipman tonalite mylonite, pen for scale; (C) strain gradient within zone 3 with higher strained mafic granulite on the bottom of photograph, and coarser (still mylonitic) felsic granulite, Canadian dollar for scale; (D) Zone 5 porphyroclastic granitoid (Mary granodiorite?) with core-mantle structures developed within feldspar porphyroclasts displaying sinistral σ-clast asymmetry, Canadian dollar for scale.

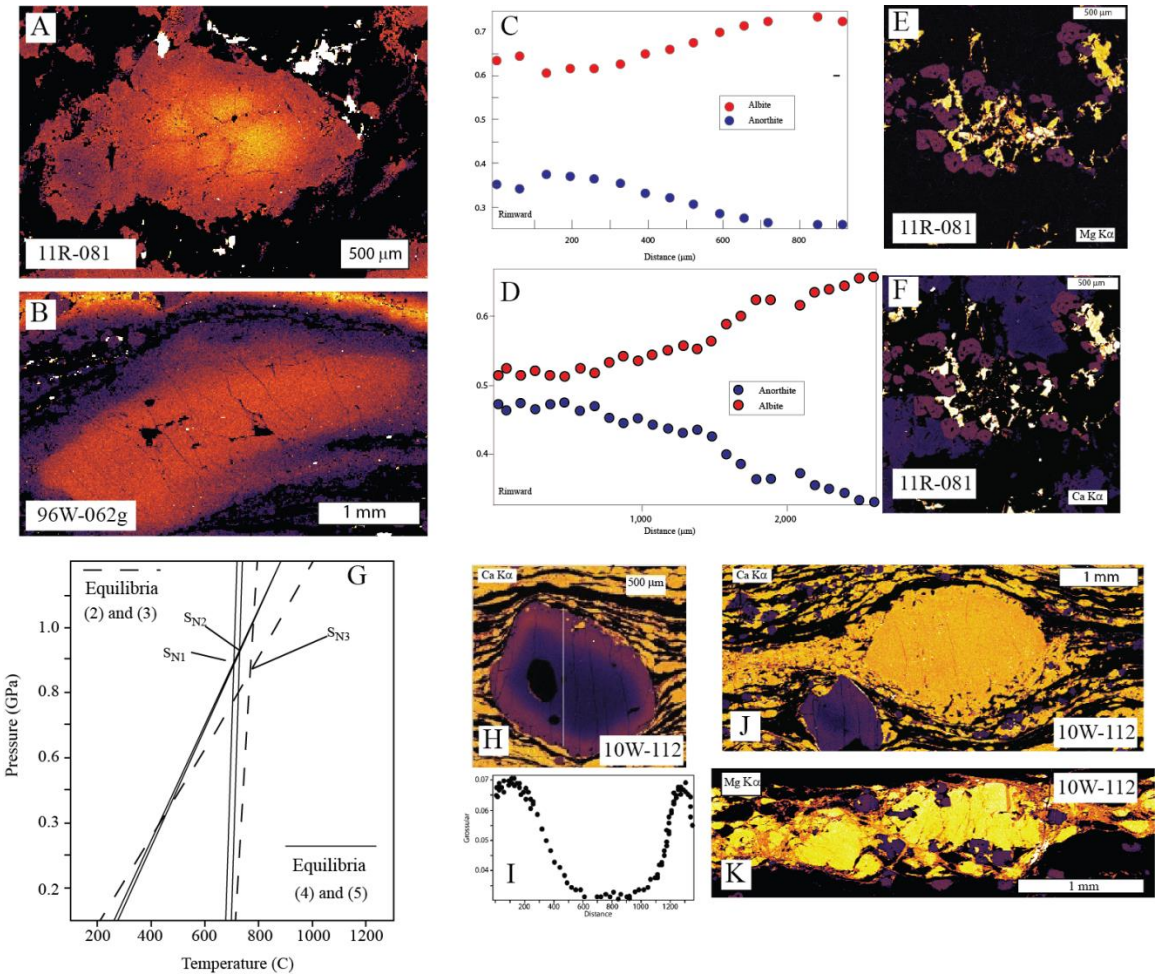

Figure 10: Electron microprobe results for Northwestern hangingwall rocks (11R-081 and 96W-62g), and hangingwall affinity sample within the CLsz (10W-112). Brighter colors indicate a higher concentration of the labeled element. (A) Ca Kα WDS map of a plagioclase porphyroclast along S_{N1}. (B) Ca Kα WDS map of plagioclase porphyroclast along S_{N2}. (C) and (D) WDS quantitative results of plagioclase from (A) and (B), respectively. (E) and (F) Mg Kα and Ca Kα WDS maps (respectively) of coronitic texture along S_{N1} of clinopyroxene and garnet around primary orthopyroxene intergrown with ilmenite. (G) TWQ results from all samples in northwestern hangingwall using equilibria (2), (3), (4), and (5) (see text for description). (H) Ca Kα WDS map of a garnet porphyroblast from hangingwall affinity mylonite within the CLsz, notice the grossular zonation. (I) WDS quantitative results for garnet in (H). (I) Ca Kα WDS map of a plagioclase porphyroclast from sample 10W-112. Notice the lack of compositional zonation that is pervasive outside of the shear zone. (J) Mg Kα WDS map of orthopyroxene from sample 10W-112.

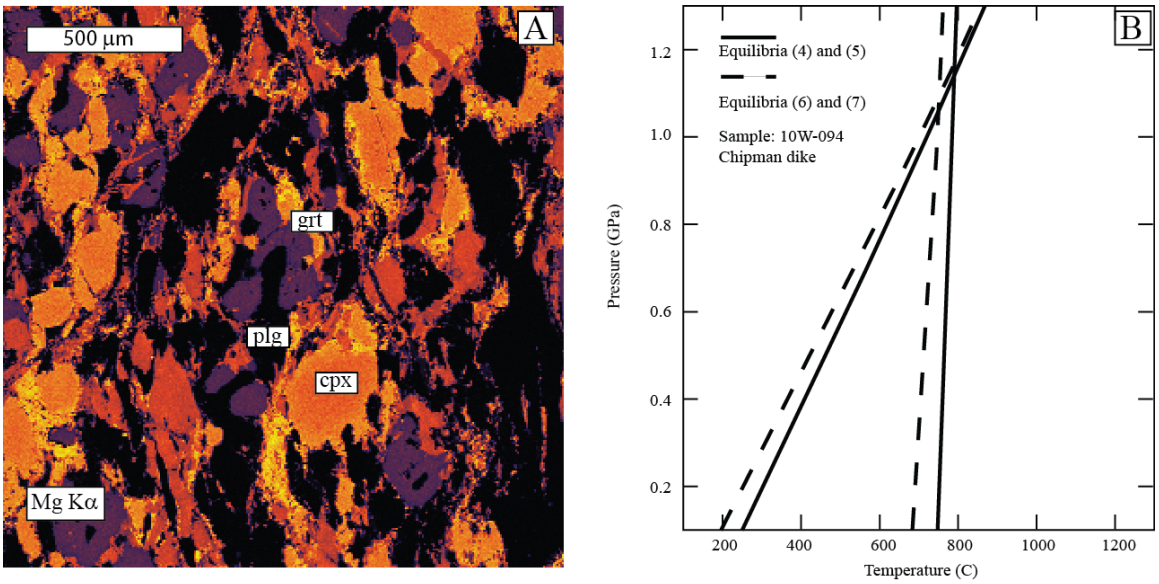

Figure 11: (A) Mg Kα map of a Chipmandike (10W-094a) with a peak metamorphic assemblage (M2C) including clinopyroxene (cpx) and garnet (grt), with minor retrogression back to a hornblende and plagioclase (plg) assemblage. (B) TWQ output calculated for the peak and retrograde (dashed lines) equilibrium compositions.

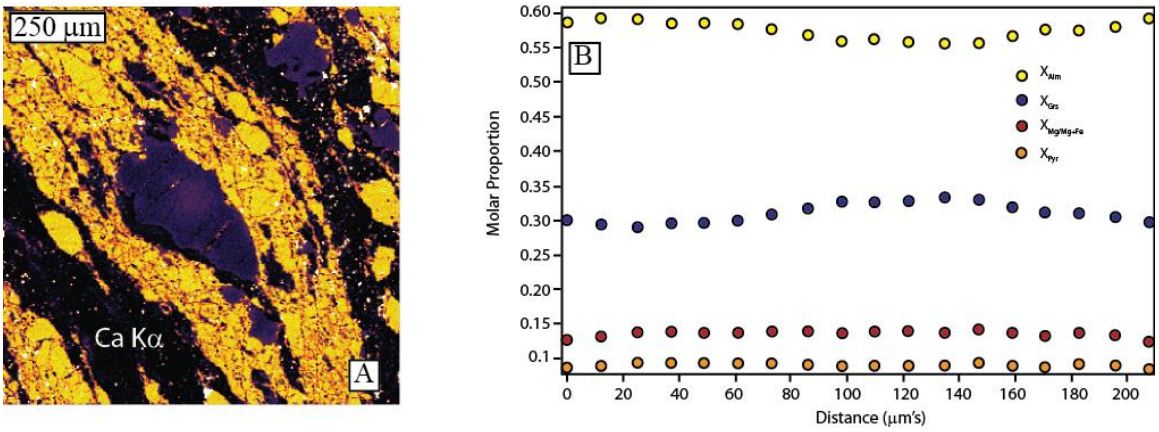

Figure 12: Compositional analysis of 10W-100 (Zone 3, low strain): (A) Ca Kα compositional map of matrix garnet, and surrounding clinopyroxene and hornblende; (B) WDS quantitative results from a garnet transect from (A).

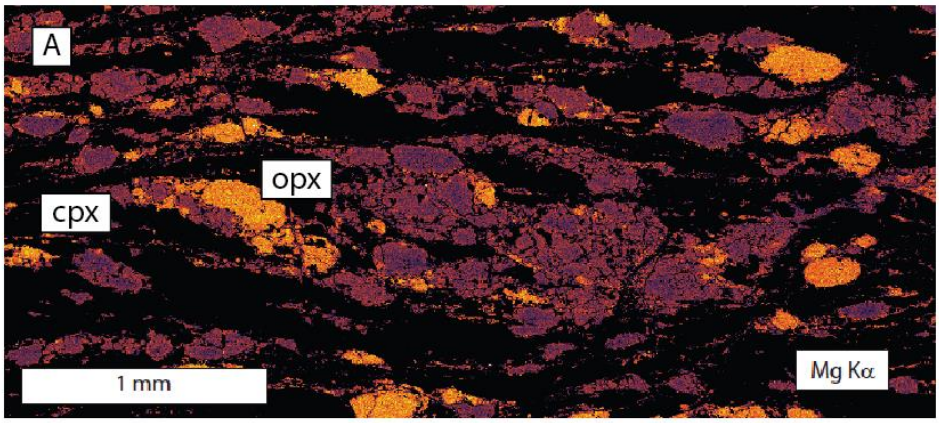
A
opx
cpx
1 mm
Mg Kα

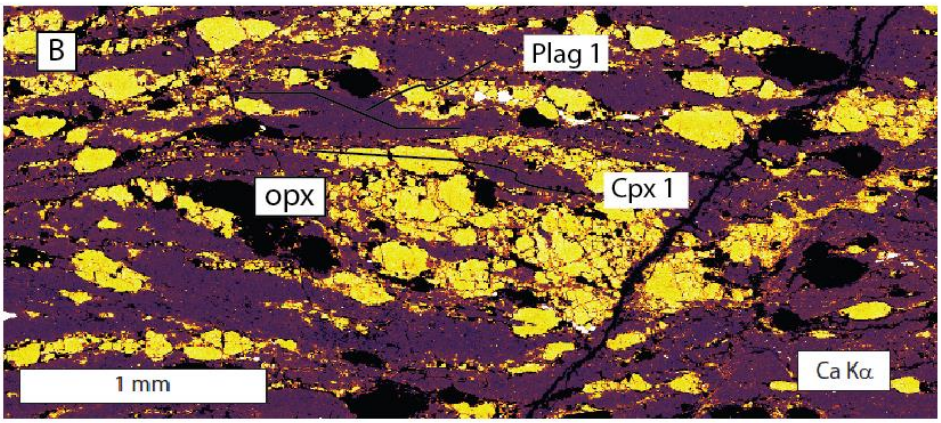
B
Plag 1
opx
Cpx 1
1 mm
Ca Kα

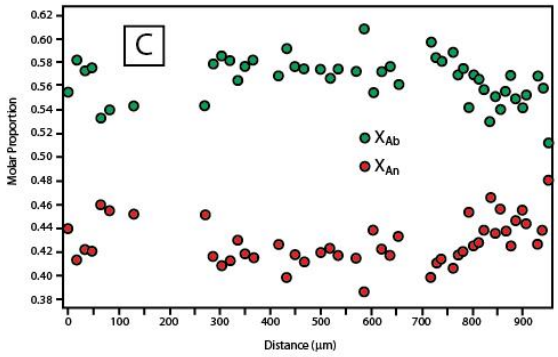
C
Molar Proportion
X_{Ab}
X_{An}
Distance (μm)

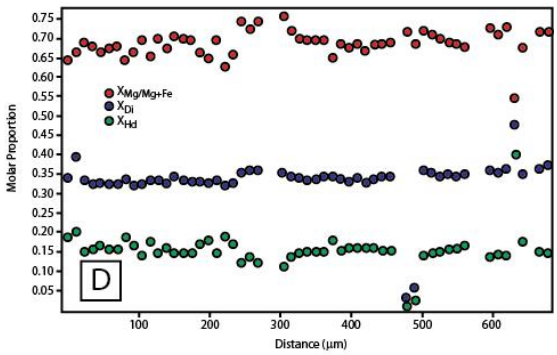
D
Molar Proportion
$X_{Mg/Mg+Fe}$
X_{Di}
X_{Hd}
Distance (μm)

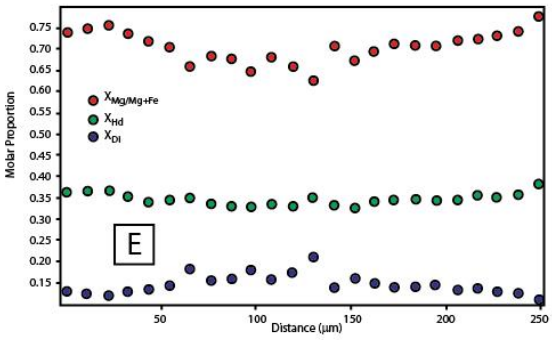
E
Molar Proportion
$X_{Mg/Mg+Fe}$
X_{Hd}
X_{Di}
Distance (μm)

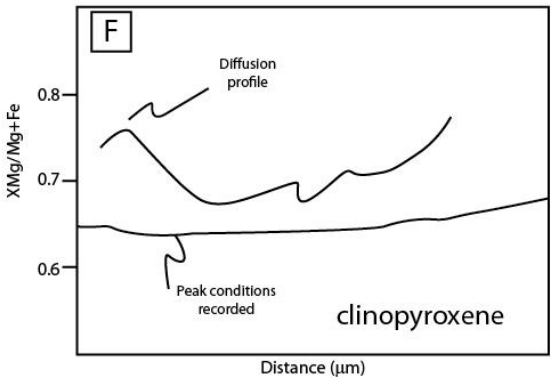
F
Diffusion profile
Peak conditions recorded
clinopyroxene
XMg/Mg+Fe
Distance (μm)

Figure 13: Compositional analysis of 10W-099 (Zone-3, high strain): (A) Mg Kα compositional map from a representative portion of the thin section displaying sinistral S-C-C' asymmetry; (B) Ca Kα compositional map from same area as (A); (C) XAn and XAb components from rim to rim analysis of plagioclase feldspar labels in (B); (D) Clinopyroxene compositional transect from a crystal away from garnet; (E) Clinopyroxene compositional transect from a crystal adjacent to garnet; (F) A comparison of the XMg/Mg+Fe ratio of the two clinopyroxene crystals analyzed.

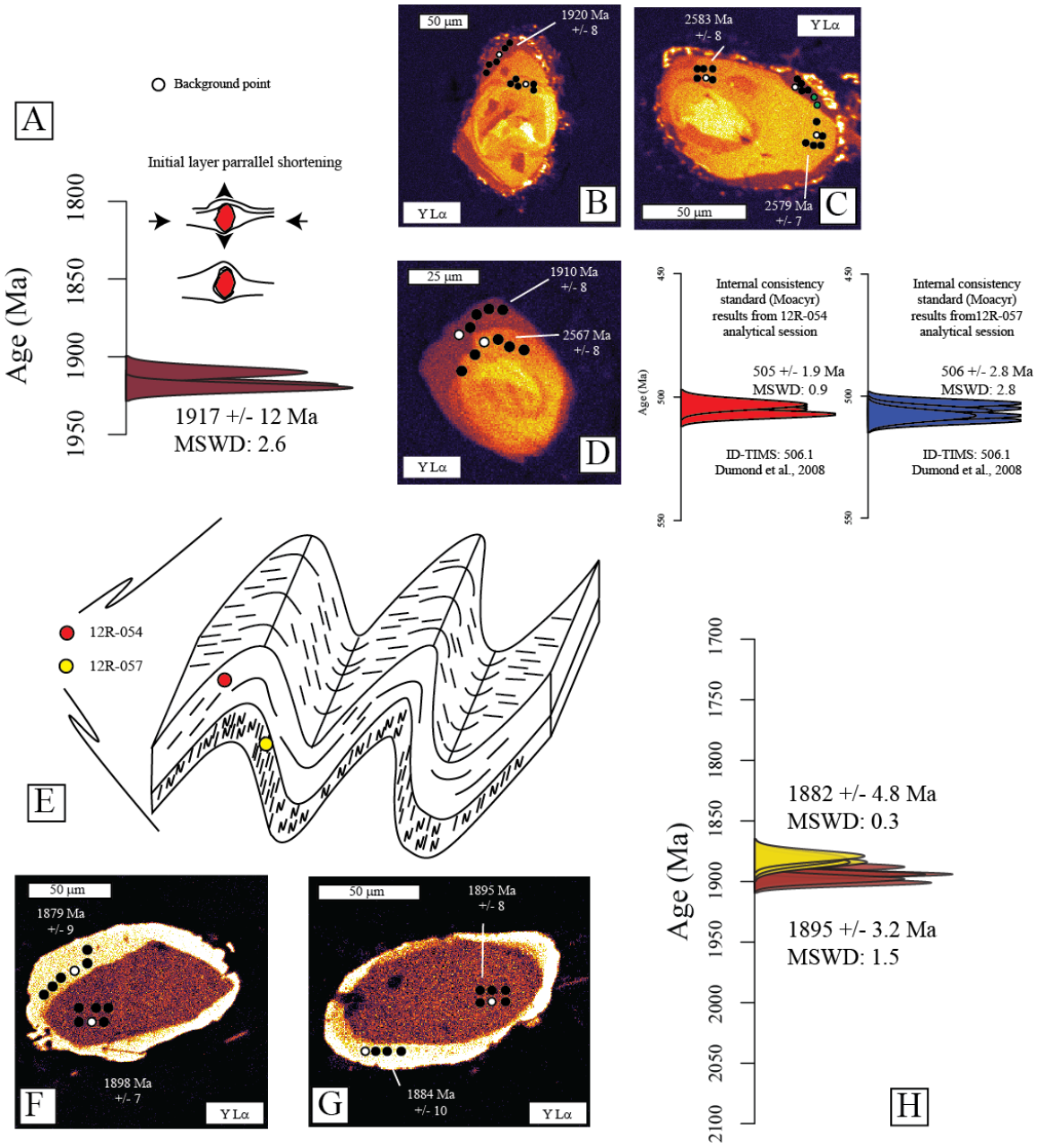

Figure 14: Geochronological results from the Beed Lake region. Gaussian histograms depict a series of analyses within distinct compositional domains, that are combined to produce a single age based on a weighted mean. Top: results from the Beed granite that contains no S2N. Bottom: results from 12R-057c that contains S2N as the only tectonic fabric. Consistency standard results from the separate analytical sessions mid-right.

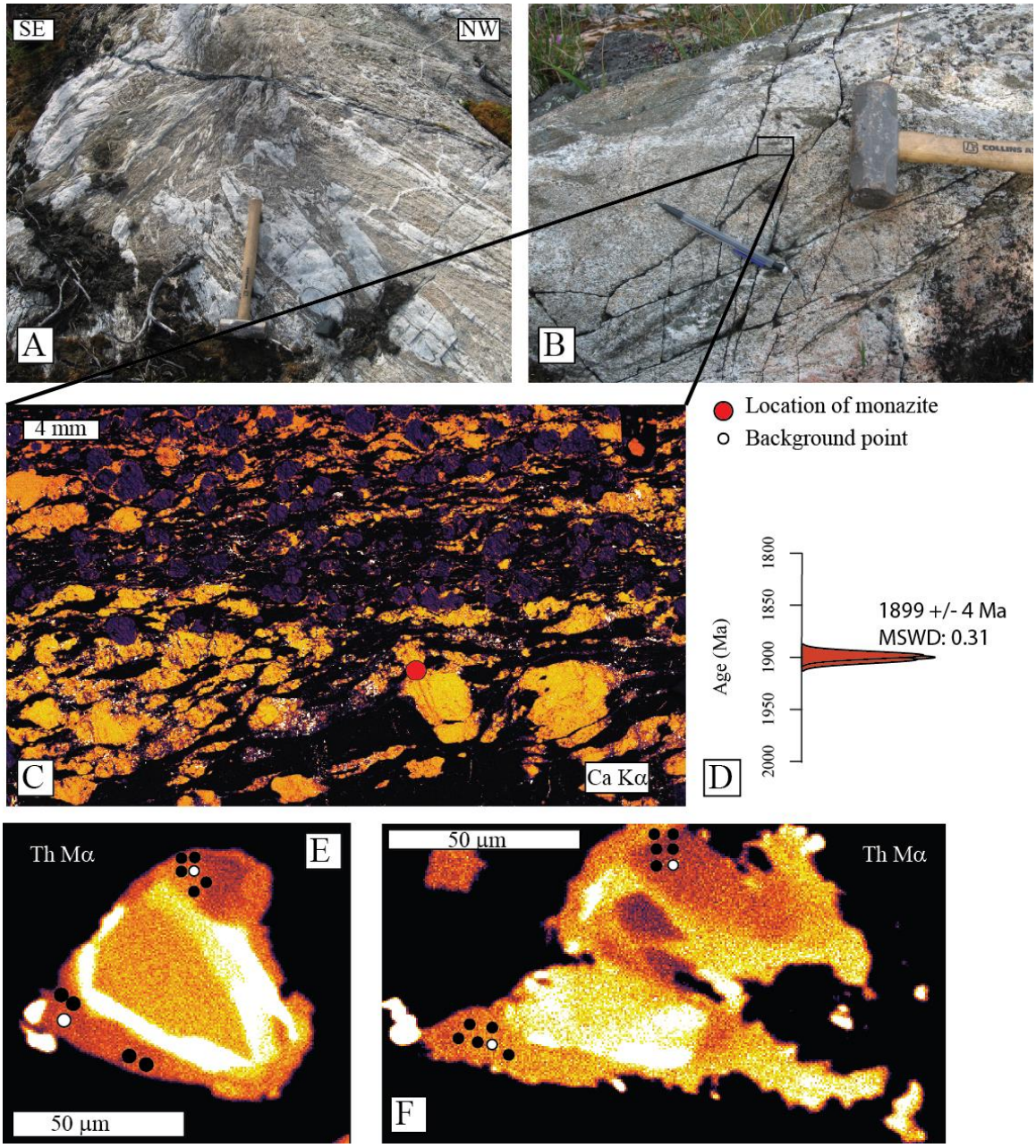

Figure 15: Geochronological results from the southeastern footwall (sample: 10W-094g). (A) Outcrop photo of meter-scaled folds with axial planar (S2C). (B) Close up photograph of (A), where compositional layering is oblique to a strong S2C mineral alignment (Pencil). (C) Ca K WDS compositional map of a full thin section. The red dot represents the location of the two monazite grains in (E) and (F). (D) Gaussian histogram displaying the results from three sets of rim analyses. (F) and (G) Th M WDS compositional map of monazite grains that contain rims elongated into the axial planar fabric (S2C). Analytical spots are labeled.

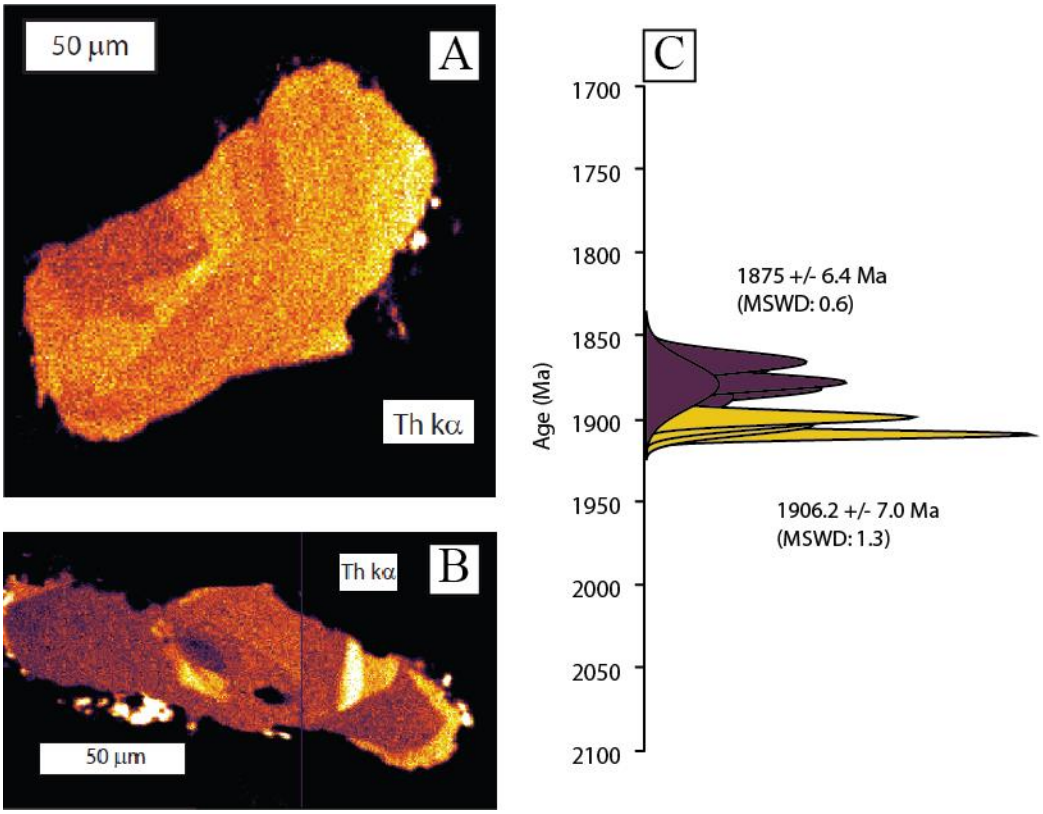

Figure 16: Summary of monazite results from 11R-028b: (A) Th Mα compositional map of m1 showing characteristic oscillatory Th zonation in the core; (B) Th Mα compositional map of m8 with oscillatory zoned core with elongated tail interpreted to represent CLsz deformation; (C) (Age histogram from all analyses performed on 11R-028b, yellow histograms are cores, and purple are rims.

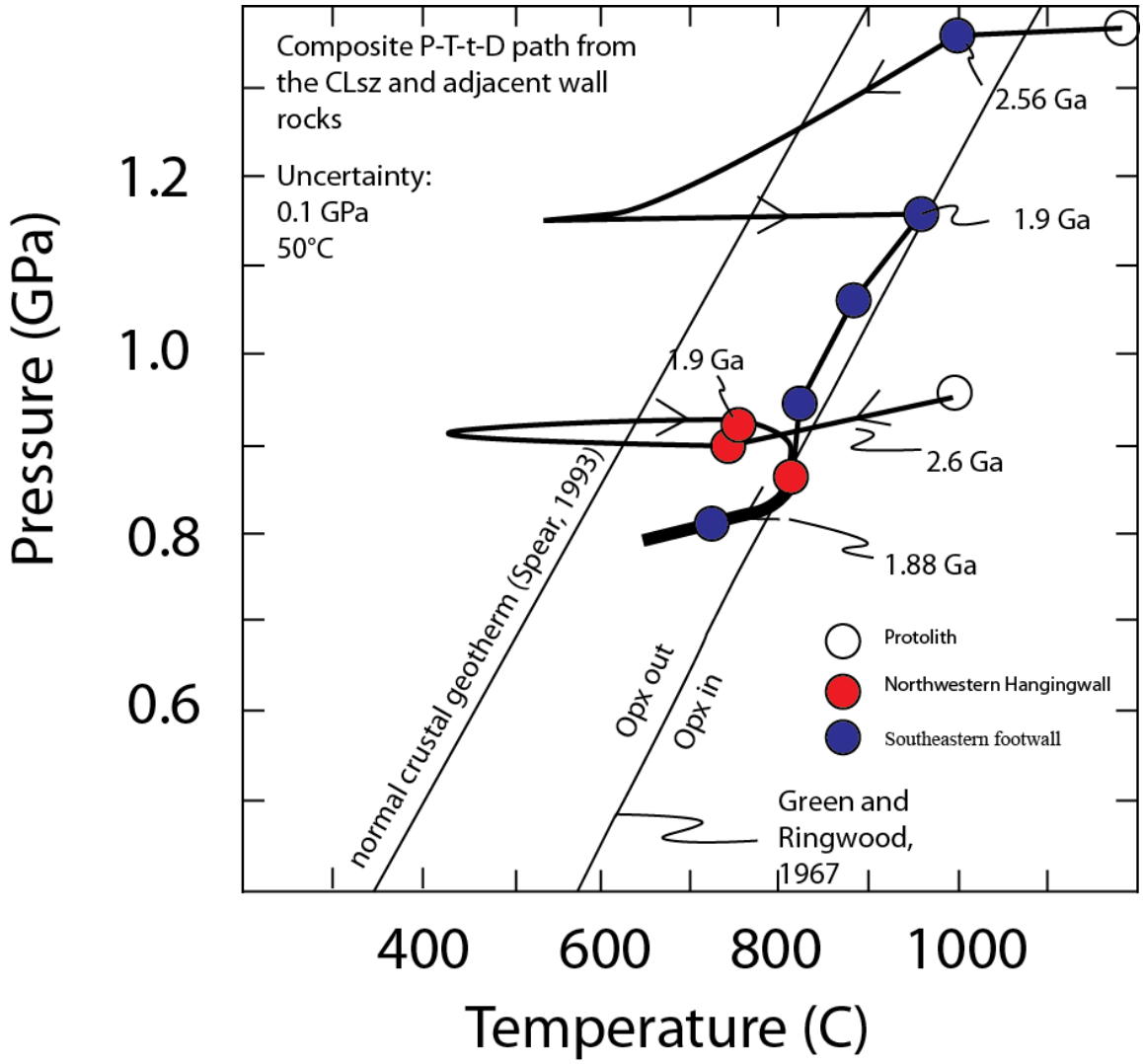

Figure 17: A composite P-T-t-D path of wall rocks and CLsz. Notice:the CLsz records where the P-T paths of wall rock converge.

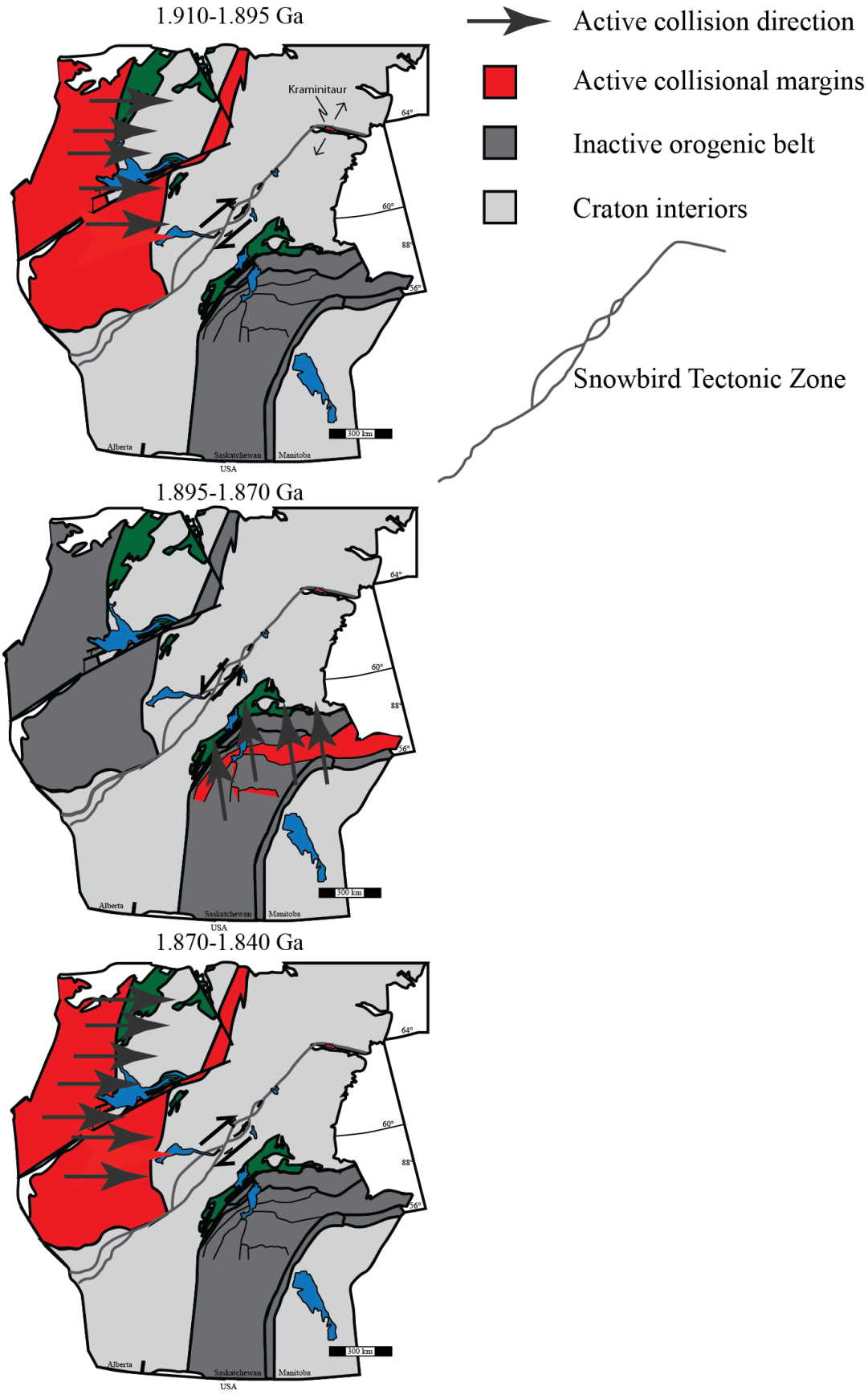
1.910-1.895 Ga
Kraminitaur
64°
60°
88°
56°
300 km
Alberta
Saskatchewan
Manitoba
USA
1.895-1.870 Ga
64°
60°
88°
56°
300 km
Alberta
Saskatchewan
Manitoba
USA
1.870-1.840 Ga
64°
60°
88°
56°
300 km
Alberta
Saskatchewan
Manitoba
USA
Active collision direction
Active collisional margins
Inactive orogenic belt
Craton interiors
Snowbird Tectonic Zone

Figure 18: Tectonic interpretation regarding anomalous kinematics within the CLsz at ca. 1.875 Ga. (A) Folding, dextral shearing, and peak metamorphic conditions coincide with the end phase of Taltson-Thelon orogenisis and initial indentation of the Slave Craton into the Rae domain of the western Churchill Province. (B) Sinistral deformation within the CLsz coincides with the docking of the Lynn-Lake and La Ronge arcs along the southern flank of the Churchill Province at ca. 1.875 Ga. (C) Rejuvenated convergence along the western margin of the contiguous Slave/Churchill Province and the reactivated Great Slave Lake shear zone coincides with renewed dextral shearing associated within the Legs Lake shear zone.

Table 1: Structural nomenclature for the CLsz and surrounding wall rock

Structural Generation	Domain	Orientation	Sense of Shear	P-T	Age	Refs
$S_{1N}/M_{1C}/D_{1C}$	Northwestern hangingwall	Subhorizontal	Top to the ESE	0.90 GPa; 750°C	2577 Ma	(1); this study
$S_{1C}/M_{1C}/D_{1C}$	Southeastern footwall	Subhorizontal	n/a	1.35 GPa; 850°C	2557 Ma	(2)
$S_{2N}/M_{2N}/D_{2N}$	Northwestern hangingwall	Steeply dipping to the NW	Dextral on shallowly plunging lineation	0.90 GPa; 750°C	1900 Ma	(1)(3); this study
$S_{2C}/M_{2C}/D_{2C}$	Southeastern footwall	Steeply dipping to the NW	Dextral, with increasing sinistral component towards CLsz	1.17 GPa; 800°C	1900 Ma	(4)(5); this study
$S_3/M_3/D_3$	Both (localized)	Moderately to steeply dipping to the NW	Sinistral on a moderate to shallowly plunging lineation	1.06-0.82 GPa; 800-700°C	1880-1870 Ma	This study

(1) Dumond et al. (2010); (2) Mahan et al. (2008); (3) Williams et al. (2000); (4) Williams et al. (1995); (5) Flowers et al. (2006a)

Table 2: Electron microprobe results from sample 11R-081

	11R-081					
	Cpx 1	Cpx 2	Cpx 3	Grt 1	Pla 1	Pla 2
FeO	17.46	17.2	17.48	31.51	0.06	0.06
MgO	8.04	8.34	8.31	2.15		
MnO	0.16	0.14	0.17	0.87		
CaO	20.71	20.4	20.55	7	5.51	5.23
Na2O	0.5	0.54	0.49	0.02	8.26	8.21
K2O	0.01	0	0.01		0.18	0.18
TiO2	0.15	0.14	0.14	0.04	0	0
Al2O3	1.59	1.65	1.67	20.72	24.06	23.78
SiO2	49.5	49.97	49.87	37.22	61.22	61.2
Total	98.11	98.38	98.68	99.53	99.3	98.66
Mg/Mg+Fe	0.451	0.464	0.459	0.109		
X_{di}	0.236	0.244	0.242			
X_{Hd}	0.288	0.282	0.286			
Alm				0.697		
Pyr				0.085		
Sps				0.019		
Grs				0.198		
An					0.267	0.257
Ab					0.723	0.732

Table 3: Electron microprobe results for sample 96W-062g.

96W-062g			
	Cpx 1*	Grt 1*	Pla 1*
FeO	12.12	29.83	0.05
MgO	12.19	4.5	
MnO	0.09	0.57	
CaO	21.41	6.74	6.98
Na2O	0.53	0.02	7.55
K2O	0.01		0.22
TiO2	0.13	0.06	0.02
Al2O3	1.73	21.32	25.86
SiO2	50.98	36.38	59.7
Total	99.19	99.42	100.38
Mg/Mg+Fe	0.642	0.212	
Diop	0.343		
Hd	0.191		
Alm		0.634	
Pyr		0.171	
Sps		0.012	
Grs		0.183	
An			0.334
Ab			0.653

Table 4: Electron microprobe results for sample 10W-094a

	10W-094a				
	Cpx 1*	Grt 1*	Pla 1*	Amph 1*	Pla 2*
FeO	14.12	29.12	0.28	18.83	0.34
MgO	9.85	4.06		8.35	
MnO	0.21	1.04		0.11	
CaO	19.84	6.49	5.38	11.53	5.81
Na2O	0.96		8.59	1.44	8.35
K2O	0		0.19	1.53	0.14
TiO2	0.4	0.05	0	2.2	0
Al2O3	4.57	20.67	24.65	12.38	24.94
SiO2	48.26	37.89	60.91	40.96	60.66
Total	98.19	99.32	100	97.33	100.23
Mg/Mg+Fe	0.554	0.199		0.442	
Diop	0.282				
Hd	0.227				
Alm		0.637			
Pyr		0.158			
Sps		0.023			
Grs		0.182			
An			0.254		0.276
Ab			0.735		0.717
XFe				0.557	
XMg				0.44	
XMn				0.003	

Table 5: Electron microprobe results for sample 10W-112b

	10W-112b								
	Opx 1 *	Opx 2	Opx 3	Grt 1	Grt 2	Grt 3	Grt 4*	Pla 1*	Pla 2
FeO	23.74	22.68	20.26	26.53	28.15	27.33	26.39	0.01	0
MgO	22.15	23.31	19.11	9.39	8.27	10.07	9.74	0	0
MnO	0.15	0.13	0.11	0.63	0.78	0.68	0.68		
CaO	0.16	0.11	0.57	2.57	2.38	1.19	2.41	7.06	6.89
Na2O	0	0.01	0.1					7.48	7.24
K2O	0.01	0	1.89					0.16	0.38
TiO2	0.1	0.01	1.81	0.05	0.04	0.04	0.03	0.04	0.01
Al2O3	2.88	2.1	6.75	22.42	22.23	22.28	22.16	25.36	25.28
SiO2	52.08	52.92	40.46	39.35	38.66	39.27	39.28	60.82	61.25
Total	101.27	101.27	91.07	100.94	100.5	100.86	100.7	100.93	101.04
Mg/Mg+Fe	0.624	0.647	0.627	0.387	0.344	0.396	0.397		
En	0.623	0.645	0.626						
Fs	0.375	0.352	0.372						
Alm				0.562	0.602	0.575	0.555		
Pyr				0.355	0.315	0.378	0.365		
Sps				0.014	0.017	0.014	0.015		
Grs				0.07	0.065	0.032	0.065		
An								0.34	0.337
Ab								0.651	0.641

Table 6: Electron microprobe results for sample 10W-100a.

	10W-100a			
	Cpx 1*	Grt 1*	Grt 2	Pla 1*
FeO	14.94	27.44	26.6	0.25
MgO	9.30	2.38	2.28	
MnO	0.17	1.20	1.18	
CaO	22.20	10.47	11.36	9.76
Na2O	0.46	0	0.01	5.99
K2O	0.01			0.09
TiO2	0.19	0.18	0.15	0.01
Al2O3	1.58	20.65	20.86	28.04
SiO2	51.68	37.43	37.68	56.52
Total	100.53	99.70	100.12	100.67
Mg/Mg+Fe	0.526	0.134	0.133	
Diop	0.265			
Hd	0.239			
Alm		0.593	0.573	
Pyr		0.092	0.088	
Sps		0.026	0.026	
Grs		0.290	0.314	
An				0.471
Ab				0.524

Table 7: Electron microprobe results for sample 10W-099.

	10W-099					
	Cpx 1*	Cpx 2	Grt 1*	Grt 2	Pla 1*	Pla 2
FeO	8.7	9.05	29.34	27.46	0.18	0.12
MgO	12.96	12.89	3.17	4.78		
MnO	0.24	0.25	2.23	1.79		
CaO	22.7	22.56	6.77	6.98	8.98	8.8
Na2O	0.35	0.33	0.02	0.01	6.64	6.5
K2O	0.01	0.01			0.09	0.09
TiO2	0.14	0.04	0.14	0.07	0.02	0.03
Fe2O3	0.83	1.34	0.51	0.81		
Al2O3	1.6	0.74	20.89	21.35	27.16	26.98
SiO2	52.37	52.45	36.87	38.37	56.84	57.11
Total	99.89	99.67	99.95	101.62	99.92	99.63
MgRat	0.726	0.717	0.162	0.237		
Diop	0.362	0.362				
Hd	0.137	0.143				
Alm			0.639	0.587		
Pyr			0.123	0.182		
Sps			0.049	0.039		
Grs			0.189	0.191		
An					0.425	0.426
Ab					0.57	0.569

Table 8: EPMA monazite results

Sample	domain	UO2	K2O	ThO2	CaO	SO3	P2O5	Y2O3	SrO	SiO2	PbO
12R-054	m13_rim1	0.405682	0.021084	6.900454	1.139003	0.048666	28.59802	0.537754	0.010854	0.644561	0.618838
12R-054	m15_rim1	0.409087	0.050451	6.959125	1.300073	0.017848	29.3841	0.486967	0.007351	0.515854	0.71542
12R-054	m1_outerrim1	0.475185	0.038248	7.055884	1.31757	0.035195	29.6151	0.762528	0.002433	0.528614	0.747413
10W-094g_2	m2_rim1	0.301355	0.037192	5.853527	0.96283	0.030537	29.4513	0.186708	0.017065	0.596422	0.583883
10W-094g_2	m2_core1	0.133433	0.015275	7.999402	1.137632	0.032174	29.09235	0.053856	0	0.769227	0.88306
10W-094g_2	m3_outerrim	0.328959	0.022045	7.576222	1.283676	0.037858	29.40464	0.064365	0.010072	0.667441	0.977785
10W-094g_2	m3_outerrim2	0.293824	0.057262	4.784502	0.924681	0.020924	29.8605	0.188356	0.00976	0.348088	0.492746
10W-094g_2	m3_outerrim3	0.269722	0.056725	6.160433	1.275493	0.033763	30.23392	0.167247	0.015809	0.272085	0.5905
10W-094g_2	m9_outerrim1	0.178823	8.64E-05	10.86748	1.412108	0.027468	28.00168	0.035392	0.016812	1.367724	1.32834
10W-094g_2	m2_rim2	0.250719	0.043751	6.594348	1.032365	0.024395	29.2384	0.164099	0.00109	0.627595	0.629355
10W-094g_2	m2_innerrim1	0.427238	0.013453	16.06368	1.382454	0.021132	26.01604	0.132578	0.005633	2.524874	1.476184
12R-057c.1	m2outercore1	0.162316	0.020248	7.508792	0.721616	0.015006	28.1332	0.029432	0.012042	1.202886	0.685859
12R-057c.1	m2outercore2	0.12585	0.008436	6.028996	0.624202	0.019638	28.66076	0.032999	0	0.899113	0.547022
12R-057c.1	m1innercore1	0.368344	0	12.76237	0.44468	0.019708	25.36245	0.096774	0	2.733137	1.189558
12R-057c.1	m1innercore2	0.259893	0	8.62689	0.435555	0.024863	27.00115	0.083553	0	1.704868	0.806019
12R-057c.1	m1innerrim1	0.315237	0	10.24646	0.45176	0.019251	26.35487	0.083509	0	2.088293	0.962417
12R-057c_1	m2_innercore1	0.616192	0.00482	4.424125	0.82369	0.019158	29.31438	0.532598	0.004211	0.402439	0.562897
12R-057c.1	m2outercore3	0.143884	0	6.838206	0.636824	0.018908	28.44788	0.03499	0.001594	1.103195	0.612926
12R-057c.1	m2outerrim1	0.59038	0.004048	4.040665	0.780245	0.016659	28.7639	0.806907	0.001563	0.417132	0.533601
12R-057c.1	m16innercore1	0.148768	0.016752	6.686682	0.749807	0.020823	28.59018	0.075633	0.004494	0.932617	0.60418
12R-057c.1	m16rimright1	0.705995	0.023049	3.903813	0.650131	0.007565	29.10843	0.218726	0	0.556715	0.544879
12R-057c.1	m16outerrim1	0.601747	0.01159	3.848253	0.747098	0.007248	29.5018	0.578217	0	0.486724	0.505134
12R-057c.1	m16outercore1	0.256728	0	8.469182	0.444679	0.022997	27.2462	0.05948	0.00065	1.64366	0.786315

12R-057c.2	m4_outerrim1	0.534136	0.009604	5.06928	0.653615	0.015566	28.81891	0.43366	0	0.784042	0.588408
	m4core1	0.148958	0	5.319532		0.020429	28.98175	0.075595	0	0.760619	0.490283
12R-057c.1	m4_coreright1	0.829898	0.028359	5.431033	0.747629	0.014895	28.94328	0.258038	0.009661	0.845488	0.71118
12R-057c.1	m4_coreleft1	0.807063	0.009903	5.503027	0.745669	0.017379	28.76057	0.282898	0.000791	0.852954	0.713056
12R-057c.1	m7_outercore1	0.237364	0.005884	4.586986	0.530909	0.011508	28.94488	0.051968	0.001725	0.651046	0.452995
12R-057c.1	m7_outerrim1	0.322438	0.032532	2.777258	0.53137	0.013694	29.66948	0.459811	0.001927	0.271288	0.329427
12R-057c.2	m3_coreleft1	0.479976	0.01397	4.781186	0.633266	0.015578	29.01981	0.260328	0.001681	0.694239	0.547558
12R-057c.2	m3_outerrim1	0.285687	0.005028	4.225262	0.621327	0.01133	29.40224	0.760222	0	0.505585	0.437583
12R-057c.1	m6_rim1	0.637331	0.051544	5.155655	1.026498	0.039261	29.65492	1.814238	0.0115	0.432949	0.634251
12R-057c.1	m6_core1	0.392559	0.021792	4.305269	0.668674	0.018274	29.33827	0.669314	0.00325	0.511022	0.480363
11R-028b	m8 rim right	0.114308	0	2.449268	0.512048	0.025893	29.93914	0.032611	0.010618	0.188209	0.236313
11R-028b	m8 up core	0.138139	0.001712	2.964958	0.601876	0.009127	29.86174	0.144772	0	0.200357	0.292768
11R-028b	m8 rim left	0.11729	0.000301	2.662588	0.55991	0.020543	29.86887	0.03054	0	0.182764	0.256938
11R-028b	m8 high Th slice	0.085068	0	4.580038	0.834009	0.014766	29.47928	0.029902	0.01212	0.34342	0.406823
11R-028b	m4rim bot	0.065333	0	3.490828	0.694445	0.012617	29.5572	0.061198	0.011156	0.254811	0.307474
11R-028b	m4 innercore	0.074464	0	2.701746	0.545081	0.014711	30.06988	0.065444	0	0.179502	0.249968
11R-028b	m4 outercore	0.079926	0.001289	3.156003	0.662026	0.010505	30.4382	0.065861	0.00903	0.206714	0.285556
11R-028b	m1 innercore	0.048808	0	3.34628	0.618628	0.017423	29.98414	0.035758	0.010386	0.249523	0.295534
11R-028b	m1 outerrim	0.064647	0	4.198064	0.707429	0.024015	29.84328	0.046549	0.005849	0.309482	0.364591
11R-028b	m1innerrim1	0.072321	0	3.800378	0.711555	0.026619	29.88076	0.024011	0.005707	0.266714	0.33925
11R-028b	m2 outercore	0.071499	0	3.41469	0.612249	0.020381	29.98008	0.052866	0.002881	0.243234	0.304573
10W-110a_a	m2 outerrim left	0.134036	0	4.25612	0.523223	0.016611	29.56366	0.133832	0.005794	0.549502	0.394487
10W-110a_a	m9 outerrimleft	0.116725	0	3.077358	0.529193	0.020587	29.7523	0.063253	0.002242	0.423923	0.29464
10W-110a_a	m2 innercore1	0.178718	0	3.93414	0.43699	0.023565	29.41512	0.847566	0	0.648511	0.549213
10W-110a_a	m2 outercore	0.132649	0	3.561157	0.608075	0.014645	30.06548	0.789759	0	0.307621	0.479695
10W-110a_a	m2 rim1 interior	0.066585	0	4.88815	0.794268	0.019186	29.58088	0.42064	0	0.405778	0.599718
10W-110a_a	m2 rim1 left	0.038339	0	5.076913	0.849813	0.015705	29.66598	0.39345	0	0.379017	0.612305
10W-110a_a	m2 rim 2 low	0.164799	0.005488	2.908268	0.368985	0.019625	29.80188	0.859667	0.000856	0.402492	0.411961

10W-110a_a	m9 innercore	0.286641	0	1.97958	0.336133	0.033905	29.82568	0.837196	0	0.270961	0.352983
10W-110a_a	m9 outercorelow	0.070296	0	5.140566	0.808133	0.027416	29.4054	0.423525	0.013931	0.450087	0.626509
Sample	domain	UO2	K2O	ThO2	CaO	SO3	P2O5	Y2O3	SrO	SiO2	PbO
10W-110a_a	m9 rim right	0.132385	0.015635	3.642685	0.417506	0.039032	29.2902	0.041358	0	0.565314	0.34687

Sample	domain	La2O3	Ce2O3	Nd2O3	Pr2O3	Eu2O3	Sm2O3	Tb2O3	Dy2O3	Er2O3	Gd2O3
12R-054	m13_rim1	UO2	K2O	ThO2	CaO	SO3	P2O5	Y2O3	SrO	SiO2	PbO
12R-054	m15_rim1	0.405682	0.021084	6.900454	1.139003	0.048666	28.59802	0.537754	0.010854	0.644561	0.618838
12R-054	m1_outerrim1	0.562919	0.004613	6.696695	1.521753	0.028107	29.8183	1.60549	0.003765	0.262125	1.038743
10W-094g_2	m2_rim1	0.594523	0.030763	6.300905	1.419155	0.020117	30.30373	1.780353	0.001784	0.261107	1.001867
10W-094g_2	m2_core1	0.301355	0.037192	5.853527	0.96283	0.030537	29.4513	0.186708	0.017065	0.596422	0.583883
10W-094g_2	m3_outerrim	0.133433	0.015275	7.999402	1.137632	0.032174	29.09235	0.053856	0	0.769227	0.88306
10W-094g_2	m3_outerrim2	0.328959	0.022045	7.576222	1.283676	0.037858	29.40464	0.064365	0.010072	0.667441	0.977785
10W-094g_2	m3_outerrim3	0.293824	0.057262	4.784502	0.924681	0.020924	29.8605	0.188356	0.00976	0.348088	0.492746
10W-094g_2	m9_outerrim1	0.269722	0.056725	6.160433	1.275493	0.033763	30.23392	0.167247	0.015809	0.272085	0.5905
10W-094g_2	m2_rim2	0.178823	8.64E-05	10.86748	1.412108	0.027468	28.00168	0.035392	0.016812	1.367724	1.32834
10W-094g_2	m2_innerrim1	0.250719	0.043751	6.594348	1.032365	0.024395	29.2384	0.164099	0.00109	0.627595	0.629355
12R-057c.1	m2outercore1	0.427238	0.013453	16.06368	1.382454	0.021132	26.01604	0.132578	0.005633	2.524874	1.476184
12R-057c.1	m2outercore2	0.162316	0.020248	7.508792	0.721616	0.015006	28.1332	0.029432	0.012042	1.202886	0.685859
12R-057c.1	m1innercore1	0.12585	0.008436	6.028996	0.624202	0.019638	28.66076	0.032999	0	0.899113	0.547022
12R-057c.1	m1innercore2	0.368344	0	12.76237	0.44468	0.019708	25.36245	0.096774	0	2.733137	1.189558
12R-057c.1	m1innerrim1	0.259893	0	8.62689	0.435555	0.024863	27.00115	0.083553	0	1.704868	0.806019
12R-057c_1	m2_innercore1	0.315237	0	10.24646	0.45176	0.019251	26.35487	0.083509	0	2.088293	0.962417
12R-057c.1	m2outercore3	0.616192	0.00482	4.424125	0.82369	0.019158	29.31438	0.532598	0.004211	0.402439	0.562897
12R-057c.1	m2outerrim1	0.143884	0	6.838206	0.636824	0.018908	28.44788	0.03499	0.001594	1.103195	0.612926
12R-057c.1	m16innercore1	0.59038	0.004048	4.040665	0.780245	0.016659	28.7639	0.806907	0.001563	0.417132	0.533601
12R-057c.1	m16rimright1	0.148768	0.016752	6.686682	0.749807	0.020823	28.59018	0.075633	0.004494	0.932617	0.60418
12R-057c.1	m16outerrim1	0.705995	0.023049	3.903813	0.650131	0.007565	29.10843	0.218726	0	0.556715	0.544879
12R-057c.1	m16outercore1	0.601747	0.01159	3.848253	0.747098	0.007248	29.5018	0.578217	0	0.486724	0.505134
12R-057c.2	outerrim2	0.256728	0	8.469182	0.444679	0.022997	27.2462	0.05948	0.00065	1.64366	0.786315
12R-057c.2	m4_outerrim1	0.572076	0.00633	4.055875	0.772553	0.024456	29.41923	0.878218	0.005636	0.449068	0.517305
12R-057c.2	m4core1	0.534136	0.009604	5.06928	0.653615	0.015566	28.81891	0.43366	0	0.784042	0.588408
12R-057c.1	m4_coreright1	0.148958	0	5.319532	0.590404	0.020429	28.98175	0.075595	0	0.760619	0.490283

12R-057c.1	m4_coreleft1	0.829898	0.028359	5.431033	0.747629	0.014895	28.94328	0.258038	0.009661	0.845488	0.71118
12R-057c.1	m7_outercore1	0.807063	0.009903	5.503027	0.745669	0.017379	28.76057	0.282898	0.000791	0.852954	0.713056
12R-057c.1	m7_outerrim1	0.237364	0.005884	4.586986	0.530909	0.011508	28.94488	0.051968	0.001725	0.651046	0.452995
12R-057c.2	m3_coreleft1	0.322438	0.032532	2.777258	0.53137	0.013694	29.66948	0.459811	0.001927	0.271288	0.329427
12R-057c.2	m3_outerrim1	0.479976	0.01397	4.781186	0.633266	0.015578	29.01981	0.260328	0.001681	0.694239	0.547558
12R-057c.1	m6_rim1	0.285687	0.005028	4.225262	0.621327	0.01133	29.40224	0.760222	0	0.505585	0.437583
12R-057c.1	m6_core1	0.637331	0.051544	5.155655	1.026498	0.039261	29.65492	1.814238	0.0115	0.432949	0.634251
11R-028b	m8 rim right	0.392559	0.021792	4.305269	0.668674	0.018274	29.33827	0.669314	0.00325	0.511022	0.480363
11R-028b	m8 up core	0.114308	0	2.449268	0.512048	0.025893	29.93914	0.032611	0.010618	0.188209	0.236313
11R-028b	m8 rim left	0.138139	0.001712	2.964958	0.601876	0.009127	29.86174	0.144772	0	0.200357	0.292768
11R-028b	m8 high Th slice	0.11729	0.000301	2.662588	0.55991	0.020543	29.86887	0.03054	0	0.182764	0.256938
11R-028b	m4rim bot	0.085068	0	4.580038	0.834009	0.014766	29.47928	0.029902	0.01212	0.34342	0.406823
11R-028b	m4 innercore	0.065333	0	3.490828	0.694445	0.012617	29.5572	0.061198	0.011156	0.254811	0.307474
11R-028b	m4 outercore	0.074464	0	2.701746	0.545081	0.014711	30.06988	0.065444	0	0.179502	0.249968
11R-028b	m1 innercore	0.079926	0.001289	3.156003	0.662026	0.010505	30.4382	0.065861	0.00903	0.206714	0.285556
11R-028b	m1 outerrim	0.048808	0	3.34628	0.618628	0.017423	29.98414	0.035758	0.010386	0.249523	0.295534
11R-028b	m1innerrim1	0.064647	0	4.198064	0.707429	0.024015	29.84328	0.046549	0.005849	0.309482	0.364591
11R-028b	m2 outercore	0.072321	0	3.800378	0.711555	0.026619	29.88076	0.024011	0.005707	0.266714	0.33925
10W-110a_a	m2 outerrim left	0.071499	0	3.41469	0.612249	0.020381	29.98008	0.052866	0.002881	0.243234	0.304573
10W-110a_a	m9 outerrimleft	0.134036	0	4.25612	0.523223	0.016611	29.56366	0.133832	0.005794	0.549502	0.394487
10W-110a_a	m2 innercore1	0.116725	0	3.077358	0.529193	0.020587	29.7523	0.063253	0.002242	0.423923	0.29464
10W-110a_a	m2 outercore	0.178718	0	3.93414	0.43699	0.023565	29.41512	0.847566	0	0.648511	0.549213
10W-110a_a	m2 rim1 interior	0.132649	0	3.561157	0.608075	0.014645	30.06548	0.789759	0	0.307621	0.479695
10W-110a_a	m2 rim1 left	0.066585	0	4.88815	0.794268	0.019186	29.58088	0.42064	0	0.405778	0.599718
10W-110a_a	m2 rim 2 low	0.038339	0	5.076913	0.849813	0.015705	29.66598	0.39345	0	0.379017	0.612305
10W-110a_a	m9 innercore	0.164799	0.005488	2.908268	0.368985	0.019625	29.80188	0.859667	0.000856	0.402492	0.411961
10W-110a_a	m9 outercorelow	0.286641	0	1.97958	0.336133	0.033905	29.82568	0.837196	0	0.270961	0.352983
10W-110a_a	m9 rim right	0.070296	0	5.140566	0.808133	0.027416	29.4054	0.423525	0.013931	0.450087	0.626509

CHAPTER 3

RECOGNITION OF A CA. 2.1 Ga DIKE SWARM ALONG THE CENTRAL SNOWBIRD TECTONIC ZONE: IMPLICATIONS FOR STRUCTURAL INHERITANCE DURING PALEOPROTEROZOIC TRANSPRESSION

Assembly of the Western Churchill Province and Significance of the Snowbird Tectonic Zone

The western Churchill Province is one of four major Archean cratons, which are linked by thick Paleoproterozoic orogenic belts that compose the western Canadian Shield (Hoffman, 1988). The Churchill Province has been subdivided into the northwestern Rae and southeastern Hearne subprovinces along the Snowbird Tectonic Zone (STZ; Hoffman, 1988). The significance of the STZ, originally delineated in the horizontal gravity gradient map of the western Canadian Shield, has been widely debated. Interpretations include: 1) a Paleoproterozoic suture between Rae and Hearne subprovinces, which collided at ca. 1.91 Ga (Hoffman, 1988; Berman et al., 2007; Martel et al., 2008; Rainbird et al., 2010), 2) an intracontinental strike-slip system active during the Archean (Hanmer et al., 1994); 3) an anastomosing tapestry of strike-slip shear zones and reverse-slip shear zones (Mahan and Williams, 2005; Dumond et al., 2013; Regan et al., 2014); and 4) a reactivated Archean boundary (Aspler and Chiarenzelli, 1996). The Paleoproterozoic was a time of widespread deformation and metamorphism along the STZ (Flowers et al., 2006a,b), which, in the central segment, involved dextral transpression (Dumond et al., 2013; Regan et al., 2014).

Geochronology of the Chipman Dike Swarm

The Chipman Dike swarm is located within the Chipman subdomain and Chipman panel (Fig. 1) exposed along the eastern portion of the Rae subprovince. The dike swarm is hosted by dominatly ca. 3.4 – 3.2 Ga Chipman tonalite (Williams et al., 1995; Hanmer, 1997; Martel et al.,

2008), and minor ca. 2.6 Ga megacrystic granite (Fehr granite; Mahan et al., 2003; Koteas et al., 2010). The Chipman subdomain within the study region is bound by the 1.88 Ga Cora Lake shear zone (Regan et al., 2014) on its northwestern margin, and by the 1.86 – 1.84 Ga Legs Lake shear zone along the southeastern margin (Mahan et al., 2003; 2006a). Dikes range in size and degree of deformation, but commonly cross cut host rock gneissosity, and contain chill margins. Most dikes have a penetrative foliation and lineation (D_2 of Regan et al., 2014) and contain evidence for granulite grade metamorphism and upright folding with pressure and temperature exceeding >1.0 GPa and 825°C, respectively, during 1.9 Ga tectonism in the Chipman subdomain (Williams et al., 1995; Mahan and Williams, 2005; Martel et al., 2008; Regan et al., 2014). The dike swarm continues into the Legs Lake shear zone (Fig. 1; Mahan et al., 2003), but is absent within greenstone in the immediately adjacent Hearne subprovince, likely due to levels of exposure (granulite in Rae and mid greenschist in Hearne; Mahan et al., 2003).

The entire region underwent large amplitude folding and dextral strike-slip shear at ca. 1.9 Ga (F_2 of Regan et al., 2014) and the Chipman dikes have long since been considered to be syn-kinematic with this event (Williams et al., 1995; Flowers et al., 2006a). Flowers et al. (2006a) performed ID-TIMS geochronology on zircon grains found within leucosome within the Chipman dikes, which yielded a precise age of 1.8962 +/-0.0003 Ga (2 σ). Based on the syn-kinematic relationships described in Williams et al. (1995), the zircon data was also interpreted to approximate the emplacement age of the dikes.

Targeted sampling was performed in the summer of 2013 with the aim of finding igneous zircon crystals to establish a crystallization age for the Chipman dike swarm. Samples of coarse dike centers, pegmatitic dike regions, and relatively undeformed dikes were collected throughout the exposure of the Cds, but focused sampling was carried out within the Legs Lake shear zone, where grades of metamorphism are interpreted to be lowest (Mahan et al., 2003). Electron microprobe microanalysis was performed at the University of Massachusetts, Amherst. Thin

sections were mapped with the Cameca SX-50 electron microprobe with one spectrometer set to Zr, to identify all zircon grains within the slide. Individual grains were characterized for morphology and BSE and CL zonation. Grains were then mapped by WDS (Y, Hf, U, Th, Yb) at high resolution (submicron; for exact analytical conditions see supplement). Selected grains were then analyzed with the SX-100 ultrachron electron microprobe at the University of Massachusetts. Both major and trace elements were analyzed on compositional domains identified by WDS mapping.

At the University of California, Los Angeles, samples were drilled out of the thin section with a 3 mm drill bit. Individual round thin section pieces were mounted with a zircon standard (Duluth gabbro), and coated with gold. Zircon grains were then analyzed with the Cameca 1270 ionization mass spectrometer. The field aperture within the transfer case of the mass spectrometer was limited to approximately 8 - 10 microns, to avoid surrounding phases (methods after Chamberlain et al., 2010). Measurements were taken on an electron multiplier with thirty cycles per analysis. Due to the low impact of the ion beam on the sample (pit depths less than 1μm), several analyses were taken from individual grains.

Four dike samples contained micro-zircon, too small to effectively separate by standard procedures. Most grains were compositionally zoned (also apparent in BSE, and CL signal) and contain cores and rims. Cores typically have higher HREEs concentrations and a darker BSE and CL signal than corresponding rims. Cores are interpreted as igneous in origin based on the high HREE content consistent with growth pre-garnet growth, while rims developed during granulite facies metamorphism and garnet growth. Analyses were reproducible both within a 30 cycle analysis, and between multiple analyses. No evidence of common Pb was detected during any analysis. $^{207}Pb/^{206}Pb$ ages are reported herein. In-SIMS analysis (Chamberlain et al., 2010) of all grains yielded $^{207}Pb/^{206}Pb$ ages ranging from 1.9 to 2.1 Ga; zircon are slightly discordant and

show evidence of recent disturbance, but all intersect concordia. Negative lower intercepts were set to zero.

One sample, a coarse grained dike from Legs Lake, contained a subhedral zircon approximately 15 to 20 µms wide and 45 µm long crystal with faint zoning (13R-099a_2_z1). Compositionally it contained higher Y (1.43 weight %), Er_2O_3 (0.25 weight %), and Yb_2O_3 (0.33 weight %) than other grains analyzed within this study. A very small (<5 µm) rim that corresponds with a sharp decrease in Y (0.13 weight %), Er_2O_3 (0.03 weight %), and Yb_2O_3 (0.06 weight %), among other HREEs, is interpreted to be metamorphic in origin (Figure 20). The size of this grain, volume of core material, and <5 micron-thick rim allowed for repeat analysis of homogenous core material. Four spot analyses along the length of this grain yields a weighted mean of 2.117 +/- 14 Ga (MSWD: 0.66; pof: 0.61). A relatively coarse grained porphyroclastic dike from Lytle Lake also contained zircon grains with relatively coarse cores, and four analyses yielded a weighted mean of 2.070 +/- 14 Ga (MSWD: 2.0; pof: 0.62). Two analyses of the core region yielded $^{207}Pb/^{206}Pb$ dates of 2087 +/-29 Ma and 2099 +/- 18 Ma, within error of the subhedral grain described above. Although dominated by core material, the outer edges of these grains have been partially recrystallized (Flowers et al., 2008) and thus likely yield a close minimum age for igneous crystallization. Other zircon grains yielded ages between ca. 1.9 Ga and 2.1 Ga, however, the size and quality of the grains is subordinate to those discussed above. Therefore, we interpret 2.117 +/- 14 Ga as the best constrained crystallization age for the Chipman dike swarm.

Incipient Extension and Regional Correlation

Integrating the field, electron microprobe, and ion microprobe data via in-situ analysis of primary zircon grains has yielded a date of 2.117 +/- 14 Ga, interpreted as the time of crystallization of the Cds. A younger suite of dikes (~ 1.9 Ga) may also be present based on syn-kinematic relationships given in Koteas et al. (2010) and Williams et al. (1995). The analysis of

samples from distal parts of the dike swarm will confirm the geographic extent of this event, however, at least one component of mafic magmatism and dike emplacement occurred at 2.1 Ga in the central Snowbird Tectonic Zone and provides constrains on its tectonic history. This result also confirms that the Cds was emplaced during deposition of the neighboring Murmac Bay Group with a max deposition age of 2.17 Ga (Ashton et al., 2013), and perhaps other proximal infolded Paleoproterozoic supracrustal rocks near Snowbird Lake (Martel et al., 2008)

Flowers et al. (2006a) also presented detailed geochemical and isotopic data constraining the igneous petrogenesis of the Cds. They contain a muted incompatible element signal when normalized to primitive mantle (Sun and McDonough, 1989), with a small negative Nb anomoly. They contain fairly flat, transitional, REE element trends when normalized to chondrites (Sun and McDonough, 1989). Sm - Nd isotopic compositions reported in Flowers et al. (2006a) have a wide range in ε_{Nd} values, and corresponding decrease in $\varepsilon_{Nd(Tc)}$ (t_c = 1.9 Ga) values with increasing SiO_2 suggesting contamination of the Cds by preexisting lithosphere. At 1.9 Ga, ε_{Nd} values plot just below CHUR, and extend down 8 epsilon units. Taken together, these results were interpreted as being indicative of asthenospherically derived magmas that were contaminated by older, predominately Mesoarchean lithosphere (Flowers et al., 2006a; Martel et al., 2008).

Whole rock geochemistry and the wide range in epsilon Nd values of the Cds suggest an asthenospheric source modified by contamination with older lithosphere (Flowers et al., 2006a). Crustal contamination in tandem with flat incompatible element signatures is consistent with an extensional setting and assimilation of country rocks. Therefore, the Cds delineates an extensional event (Flowers et al., 2006a; Williams and Flowers, 2008) marked by modification of the pre-existing topography and the creation of sedimentary basins (Martel et al., 2008; Ashton et al., 2013). However, the lack of preserved oceanic crust, unconformable deposition on top of

older basement gneisses, and lack of proximal foredeep sedimentation suggests that incipient extension and rifting may have been short lived or aborted.

The Chipman dike swarm share a similar age to the recently analyzed Clearwater complex south of the Athabasca Basin, also along the Snowbird tectonic zone (Card et al., 2014). Although the geochronology presented in Card et al. (2014) yielded complex results, the authors interpreted a ca. 2.11 Ga age for the large anorthosite batholith exposed west of the Virgin River shear zone (Bickford et al., 1992; Card et al., 2014). The Clearwater batholith is exposed along Paleoproterozoic strike (S_2 of Regan et al., 2014), but based on the new geochronology, both the Cds and Clearwater appear to predate ca. 1.9 Ga regional deformation, and collectively make up a large igneous province (LIP) that extends for distances greater than 800 km in length (referred to as STZ LIP; Flowers et al., 2006a; Williams and Flowers, 2008; Martel et al., 2008; Card et al., 2014)

The Griffin Gabbro sills exposed within the Hurwitz basin in the central Hearne subprovince have also been dated at ca. 2.11 Ga (Patterson and Heaman, 1991; Heaman and La Cheminant, 1993; Aspler et al., 2002) and are exposed as laterally extensive sill networks exposed throughout the lower Hurwitz basin (Aspler et al., 2003) in the Henik and Kaminak segments. They and their extrusive equivalents, the pillowed Happotiyik Member of the Ameto Formation (Sandeman et al., 2003), are believed to represent distal mafic magmatism associated with the opening of the Maniwekan Ocean between the Hearne and Superior Provinces (Aspler et al., 2003). At Angikuni Lake, further north along strike, a mafic dike swarm cross-cuts Archean lithologies within domains bounded by anastomosing branches of Paleoproterozoic shear zones and faults (Aspler et al., 1999). Although currently undated, their concentration along the STZ suggests they may be temporal equivalents to the Chipman dike swarm and Griffin gabbors and have a similar major and trace element geochemistry to the Chipman dike swarm (Cousens et al., 1998).

Although recent interpretations regarding the central STZ involve a ca. 1.9 Ga collisional event between Rae and Hearne subprovinces (Berman et al., 2007), recent work by Regan et al. (2014) favors an intracontinental setting during ca. 1.9 Ga tectonism. Therefore, comparison with the proximal Griffin Gabbros is warranted. The Griffin gabbros have a restricted SiO_2 content (< 55 wt %), flat incompatible element trends when normalized to primitive mantle, and plot between CHUR and contemporaneous depleted mantle at time of crystallization. Major and trace element chemistry are nearly identical to the Cds. Furthermore, when Nd isotopic data from Flowers et al. (2006) is corrected to 2.11 Ga, the two plot in identical locations, with the Cds containing a spread to lower ε_{Nd} values, likely the result of contamination (Flowers et al., 2006a). Therefore, the Griffin gabbros and Cds may have formed in relatively close proximity in both space and time as the result of intracontinental extension, but the Cds underwent a greater amount of lithospheric contamination (Aspler et al., 2002; Aspler et al., 2003; Flowers et al., 2006) consistent with more evolved lithosphere underlying the northwestern Hearne and Rae subprovinces (Petts et al., 2014).

Implications for Paleoproterozoic Evolution of the Snowbird Tectonic Zone

The central STZ persists as a major source of uncertainty regarding the growth and evolution of the western Churchill Province. New age constraints on the Cds provide additional insight into this enigmatic boundary. The similarity in age, geochemistry, and isotopic composition, the Griffin gabbro sills in the central Hearne subprovince and Cds suggests the two may be part of a coeval extensional event that crosscuts the STZ (Aspler et al., 1998). If so, the entire Rae and Hearne subprovinces were assembled prior to ca. 2.11 Ga, consistent with a number of other observations. This contradicts models invoking a ca. 1.9 Ga accretionary origin for the STZ and is consistent with the lack of associated arc magmatism, foredeep sedimentation, and the relatively short-lived Paleoproterozoic thermal peak (Flowers et al., 2006a,b; Regan et al., 2014).

The central STZ has been widely recognized as a major transpressional zone at ca. 1.9 Ga (Regan et al., 2014). A 2.1 Ga emplacement age and extensional origin for the Chipman dike swarm revises later syntectonic emplacement in structurally unfavorable locations during a granulite-facies transpression. It also makes the correspondence of the Chipman dike swarm and transpressional deformation along strike for at least 400 km a geospatial, rather than temporal, problem.

The distribution of the Chipman dike swarm and the Clearwater anorthosite west of the Virgin River shear zone (Card et al., 2014) correspond spatially to upright folding, dextral shear, and the geophysical trace of the STZ. However, the Chipman dike swarm are ca. 200 my older than granulite-facies Paleoproterozoic transpression. This relationship is best explained by ca. 1.9 Ga use of a preexisting weakness that is defined by the Chipman dike swarm and related magmatism (thinned lithosphere?), perhaps during indentation of the Slave into the western margin of the Rae craton (Hanmer et al., 1992; Regan et al., 2014). Similarly to the Griffin gabbros in the central Hearne subprovince (Aspler et al., 2002), the Chipman dike warm was emplaced during incipient extension of the western Churchill Province at ca. 2.1 Ga. This event likely provided the basins and topography where infolded Paleoproterozoic metasediments were deposited. Subsequent dextral transpression was focused along the trace of this extensional feature, which behaved as a long-lived weak zone during the protracted growth of the Laurentian craton (Hoffman, 1988; Corrigan et al., 2011; Regan et al., 2014).

Comparison with the Lip Record of the Western Canadian Shield and Implications for Introverted Supercontinent Cycles

Figure 21 presents a compilation of all large igneous provinces (LIPs) of the major cratons that compose the western Canadian Shield. With the recognition of a 2.1 Ga age for the Chipman dike swarm, all cratons of the western Canadain Shield contain LIPs of this age (Ernst and Bleeker, 2010; and references therein). The Sask craton, considered exotic, is the only

cratonic block without recognized ca. 2.1 Ga magmatism. However, undated, abundant, and highly deformed and dismembered, dikes cut ca. 2.5 Ga basement gneisses in enveloping shear zones but do not cross cut structurally overlaying 1.88-1.84 Ga gneisses (Chiarenzelli et al., 1998) and are prime candidates for future geochronologic work.

A detailed summary by Aspler and Chiarenzelli (1998) suggested an internal orogen scenario (Collins et al., 2011) for the assembly of the Nuna supercontinent at ca. 1.82 Ga based on the early Paleoproterozoic sedimentologic record of the region, specifically the distribution of passive vs intracratonic successions. Aspler et al. (2002) presented geochemical data that the Griffin Gabbro sills, and their extrusive equivalents (Sandeman et al., 2003) suggesting that they were emplaced during opening of the Manikewan Ocean between Hearne and Superior cratons. However, recent work presented in Bleeker and Ernst (2005) and Pehrsson et al. (2013) reinterpret this configuration for two main reasons: 1) LIP configurations, and specifically ca. 2.1 Ga magmatism that is not recognized in 'Rae-like' cratons; and 2) the recognition of an accretionary origin for the Rae-Hearne boundary at ca. 1.91 Ga (Berman et al., 2007; Rainbird et al., 2010).

The two assumptions listed above deserve reevaluation based on data presented above, and elsewhere (Regan et al., 2014; Chapter1, 3, 4). We have demonstrated that ca. 2.1 Ga magmatism affected the eastern Rae subprovince, and work presented in Regan et al. (in prep) suggests that incipient rifting may have utilized a Neoarchean hinterland. Therefore, the entire western Canadian Shield underwent incipient extension and mantle upwelling at ca. 2.1 Ga in locations of Neoarchean tectonism. The southern Hearne, Sask, and Superior cratons likely proceeded to a mature ocean basin suggested by the development of passive margin strata preserved along the southern periphery of the Hearne subprovince (Wollaston Group; Aspler et al., 1998; 2001), and northern margin of the Superior (Huronian).

No passive margin sequence has been observed within the vicinity of the Rae-Hearne subprovince boundary. Therefore, extension related with the STZ LIP was likely localized, relatively short lived, and never progressed to a full ocean basin. This is confirmed by the linearity and narrowness of the Cds and the corresponding discrete nature of the gravity anomaly, which originally delineated the STZ (Ross, 1992). Furthermore, these results suggest that the STZ was one of several extensional zones active throughout the western Canadian Shield at 2.1 Ga. Therefore, extension and corresponding mafic magmatism along the STZ at 2.1 Ga is part of the previously recognized protracted breakup of a preexisting Neoarchean supercontinent (Aspler et al., 2001, Flowers et al., 2006a)). Based on the lateral and temporal variation of basins throughout the western Canadian Shield originally presented in Aspler and Chiarenzelli (1998) and the failure of the two assumptions above, the role of an internal orogeny (Collins et al., 2011) needs to be revisited for the assembly of the Nuna supercontinent.

Conclusions

New IN-SIMS micro zircon geochronology yielded a ca. 2.117 +/- 0.014 Ga emplacement age for the Chipman dike swarm. 2.11 Ga magmatism is present across the Rae and Hearne subprovince boundary of the western Churchill Province, and thus demands the two together prior to 2.11 Ga. The Griffin Gabbro sills in the central Hearne subprovince, exposed within the lower Hurwitz basin are interpreted to be distal correlatives to the Chipman dike swarm (Aspler et al., 2003).

References

Ashton, K.E., Hartlaub, R.P., Bethune, K.M., Heaman, L.M., and Niebergail, G., 2013, New depositional age constraints for the Murmac Bay group of the southern Rae Province, Canada: Precambrian Research, v. 232, p. 70-88.

Aspler, L.B., Cousens, B.L., and Chiarenzelli, J.R., 2002, Long-distance intracratonic transport of mafic magmas during opening of the Manikewan ocean (Trans-Hudson orogen): Griffin gabbro sills (2.11 Ga), Hurwitz Basin, Nunavut, Canada: Precambrian Research, v. 117, p. 269-294.

Aspler, LB., Chiarenzelli, J.R., Cousens, B.L., McNicoll, V.J., and Davis, W.J., 2001, Paleoproterozoic intracratonic basin processes, from breakup of Kenorland to assembly of Laurentia: Hurwitz Basin, Nunavut, Canada: Sedimentary Geology, v. 141-142, p. 287-318.

Aspler, L.B., anc Chiarenzelli, J.R., 1998, Two Neoarchean supercontinents? Evidence from the Paleoproterozoic: Sedimentary Geology, v. 120, p. 75-104

Berman, R.G., Davis, W.J., and Pehrsson, S., 2007, Collisional Snowbird tectonic zone resurrected: Growth of Laurentia during the 1.9 Ga accretionary phase of the Hudsonian orogeny: Geology, v. 35, n. 10, p. 911-914, doi:10.1130/G23771A.1.

Bethune, K.M., Berman, R.G., Rayner, N., and Ashton, K.E., 2013, Structural, petrological and U-Pb SHRIMP geochronological study of the western Beaverlodge domain: Implications for crustal architecture, multi-stage orogenesis and the extent of the Taltson orogen in the SW Rae craton, Canadian Shield: Precambrian Research, v. 232, p. 89-118.

Bleeker, W., 2005 North America: Precambrian continental nucleus: *In* Encyclopedia of geology w Ed(s) R.C. Selley, L.R.M. Cocks and I.R., Plimer, Elsevier, Oxford, UK, pp. 8-21.

Bleeker, W., and Ernst, R., 2006, Short-lived mantle generated magmatic events and their dyke swarms: The key unlocking Earth's paleogeographic record back to 2.6 Ga: *In* Dyke swarms – time marker of crustal evolution w Ed(s) E. Hanski, S. Mertanen, T. Ramo, and J. Vuollo, Taylor and Francis/Balkema, London, UK, pp. 3-26.

Card, C.D., Bethune, K.M., Davis, W.J., Rayner, N., and Ashton, K.E., 2014, The case for a distinct Taltson orogeny: Evidence form Northwest Saskatchewan, Canada: Precambrian Research, v. 255, p. 245 – 265.

Chamberlain, K.R., Schmitt, A.K., Swapp, S.M., Harrison, M., Swoboda-Colberg, N., Bleeker, W., Peterson, T.D., Jefferson, C.W., and Khuduley, A.K., 2010, In situe U-Pb SIMS (IN-SIMS) micro-baddeleyite dating of mafic rocks: Method with examples: Precambrian Research, v. 183, p. 379-387.

Corrigan, D., Pehrsson, S., Wodicka, and de Kemp, E., 2009, The Paleoproterozoic Trans-Hudson Orogen: a prototype of modern accretionary processes: in Ancient Orogens and Modern Analogues, Ed(s)
Murphy et al., Geological Society of London, Special Publications, v. 327, p. 457-479, doi:10.1144/SP327.19.

Cousens, B.L., Aspler, L.B., Chiarenzelli, J.R., Donaldson, J.A., Sandeman, H., Peterson, R.D., LeCheminant, A.N., 2001, Enriched Archean lithospheric mantle beneath western Churchill Province tapped during Paleoproterozoic orogenesis: Geology, v. 29, n. 9, p. 827-830.

Dumond, G., McLean, N., Williams, M.L., Jercinovic, M.J., and Bowring, S.A., 2008, High resolution dating of granite petrogeneisis and deformation in a lower crustal shear zone: Athabasca granulite terrane, western Canadian Shield: Chemical Geology, v. 16, n. 4, p. 175-196, doi:10.1016/j.chemgeo.2008.04.014.

Dumond, G., Goncalves, P., Williams, M.L., and Jercinovic, M.J., 2010, Subhorizontal fabric in exhumed continental lower crust and implication for lower crustal flow: Athabasca granulite terrane, Western Canadian Shield: Tectonics, v. 29, TC2006, doi:10.1029/2009TC002514.

Dumond, G., Mahan, K.H., Williams, M.L., and Jercinovic, M.J., 2013, Transpressive uplift and exhumation of continental lower crust revealed by synkinematic monazite reactions: Lithosphere, v. 5, n. 5, p. 507-512, doi: 10.1130/L292.1

Ernst, R., and Bleeker, W., 2010, Large igneous provinces (LIPs), giant dyke swarms, and mantle plumes: significance for breakup events within Canada and adjacent regions from 2.5 Ga to the present: Canadian Journal of Earth Sciences, v. 47, p. 695-739.

Flowers, R., Bowring, S.A., Mahan, K.H., and Williams, M.L., 2006a, Timescales and significance of high pressure, high-temperature metamorphism and mafic dike anatexis, Snowbird tectonic zone, Canada: Contribution to Mineralogy and Petrology, v. 151, n. 5, p. 558-581, doi:10.1007/s00410-006-0066-7.

Flowers, R.M., Mahan, K.H., Bowring, S.A., Williams, M.L., Pringle, M.S., and Hodges, K.V., 2006b,Multistage exhumation and juxtaposition of lower continental crust in the western

Canadian Shield: linking high resolution U-Pb and $^{40}Ar/^{39}Ar$ thermochronometry with pressure-temperature-deformation paths: Tectonics, v. 25, TC4003, doi:10.1029/2005TC001912.

Flowers, R.M., Bowring, S.A., Mahan, K.H., Williams, M.L., and Williams, I.S., 2008, Stabilization and reactivation of cratonic lithosphere from the lower crustal record in the western Canadian shield: Contributions to Mineralogy and Petrology, v. 156, n. 4, p. 529-549, doi:10.1007/s00410-008-0301-5.

Gilboy, C.F., 1980, Bedrock compilation geology: Stony Rapids area (NTS 74p)-Prelimanary geological map, scale 1:250,000, Sask. Geol. Surv., Sask. Energy and mines, Regina.

Hanmer, S., 1994, Geology, East Athabasca mylonite triange, Saskatchewan, Map 1859A, scale 1:100,000, Geol. Surv. Of Can., Ottawa.

Hanmer, S., 1997, Geology of the Striding-Athabasca mylonite zone, northern Saskatchewan and southeastern District of Mackenzie, Northwest Territories: Pap. Geol. Surv., of Can., Ottawa.

Hanmer, S., Parrish, R., Williams, M., and Kopf, C., 1994, Striding-Athabasca Mylonite: Complex Archean deep crustal deformation in the East Athabasca mylonite triangle, N. Saskatchewan: Canadian Journal of Earth Sciences, v. 31, p. 1287-1300, doi:10.1139/e94-111.

Hoffman, P.F., 1988, United Plates of America, the birth of a craton: Early Proterozoic assembly and growth of Laurentia: Annual Review of Earth and Planetary Sciences, v. 16, p. 543-603, doi:10.1146/annurev.ca.16.050188.002551.

Koteas, G.C., Williams, M.L., Seaman, S.J., and Dumond, G., 2010, Granite genesis and mafic-felsic magma interaction in the lower crust: Geology, v. 38, p. 1067-1070, doi:10.1130/G31017.1.

Lewry, J.F., and Sibbald, T.I.I., 1980, Thermotectonic evolution of the Churchill Province in northern Saskatchewan: Tectonophysics, v. 68, p. 45-82.

Mahan, K.H., Williams, M.L., and Baldwin, J.A., 2003, Contractional uplift of deep crustal rocks along the Legs Lake shear zone, western Churchill Province, Canadian Shield: Canadian Journal of Earth Sciences, v. 40, n. 8, p. 1085-1110, doi:10.1139/e03-039.

Mahan, K.H., and Williams, M.L., 2005, Reconstruction of a large deep-crustal terrane: Implication for the Snowbird tectonic zone and early growth of Laurentia: Geology, v. 33, n. 5, p. 385-388, doi:10.1130/G21273.1.

Mahan, K.H., Goncalves, P., Williams, M.L., and Jercinovic, M.J., 2006a, Dating metamorphic reactions and fluid flow: Application to exhumation of high-P granulites in a crustal-scale shear zone, western Canadian Shield: Journal of Metamorphic Geology, v. 24, n. 3, p. 193-217, doi:10.1111/j.1525-1314.2006.00633.x.

Mahan, K.H., Williams, M.L., Flowers, R.M., Jercinovic, M.J., Baldwin, J.A., and Bowring, S.A., 2006b, Geochronological constraints on the Legs Lake shear zone with implications for regional exhumation of lower continental crust, western Churchill Province, Canadian Shield: Contributions to Mineralogy and Petrology, V. 152, n. 2, p. 223-242, doi:10.1007/s00410-006-0106-3.

Mahan, K.H., Goncalves, P., Flowers, R., Williams, M.L., and Hoffman-Setka, D., 2008, The role of heterogeneous strain in the development and preservation of a polymetamorphic record in high-P granulites, western Canadian Shield: Journal of metamorphic geology, v. 26, n. 6, p. 669-694, doi:10:111/j.1525-1314.2008.00783.x.

Martel, E., van Breeman, O., Berman, R.G., and Pehrsson, S., 2008, Geochronology and tectonometamorphic history of the Snowbird Lake area, Northwest Territories, Canada: New insights into the architecture and significance of the Snowbird tectonic zone: Precambrian Research, v. 161, n. 3-4, p. 201-230, doi:10.1016/j.precamres.2007.07.007.

Pehrsson, S.J., Berman, R.G., Elington, B., and Rainbird, R., 2013, Two Neoarchean supercontinents revisited: The case for a Rae family of cratons: Precambrian Research, v. 232, p. 27-43.

Petts, D.C., Davis, W.J., Moser, D.E., and Longstaffe, F.J., 2014, Age and evolution of the lower crust beneath the western Churchill Province: u-Pb zircon geochronology of kimberlite-hosted granulite xenoliths, Nunavut, Canada: Precambrian Research, v. 241, p. 129-145.

Rainbird, R.H., Davis, W.J., Pehrsson, S.J., Wodicka, N., Rayner, N., and Skulski, T., 2010, Early Paleoproterozoic supracrustal assemblages of the Rae domain, Nunavut, Canada: intracratonic basin development during supercontinent break-up and assembly: Precambrian Research, v. 181, p. 166-186.

Regan, S.P., Williams, M.L., Leslie, S.R., Mahan, K.H., Jercinovic, M.J., and Holland, M.E., 2014, The Cora Lake shear zone, Athabasca granulite terrane (Snowbird Tectonic Zone), an

intraplate response to far-field orogenic processes during the amalgamation of Laurentia: Canadian Journal of Earth Sciences

Ross, G.M., Broome, J., and Miles, W., 1994, Potential fields and basement structure – western Canada sedimentary basin: *in* Geological Atlas of the Western Canada Sedimentary Basin, G.D. Mossop and I. Shetsen (comp.), Canadian Society of Petroleum Geologists and Alberta Research Council, URL <http://www.ags.gov.ab.ca/publications/wcsb_atlas/atlas.html>, [Date last accessed online].

Ross, G.M., Eaton, D.W., Boerner, D.E., and Miles, W., 2000, Tectonic entrapment and its role in the evolution of continental sphere: an example from the Precambrian of western Canada: Tectonics, v. 19, p. 116-134.

Sandeman, H.A., Cousens, B.L., and Hemmingway, C.J., 2003, Continental Tholeiitic mafic rocks of the Paleoproterozoic Hurwitz Group, Central Hearne sub-domain, Nunavut: insight into the evolution of the Hearne sub-continental lithosphere: Canadian Journal of Earth Sciences, v. 40, p. 1219-1237.

Williams, M.L., Hanmer, S., Kopf, C., and Darrach, M., 1995, Syntectonic generation and segregation of tonalitic melts from amphibolite dikes in the lower crust, Striding-Athabasca mylonite zone, northern Saskatchewan: Journal of Geophysical Research, V. 100, n. B8, p. 15,717-15,734, doi:10.1029/95JB00760.

Williams, M.L., Melis, E.A., Kopf, C.F., and Hanmer, S., 2000, Microstructural tectonometamorphic processes and the development of gneissic layering: A mechanism for

metamorphic segregation: Journal of Metamorphic Geology, v. 18, p. 41-57, doi:10.1046/j.1525-1314.2000.00235.x.

Williams, M.L., and Flowers, R.M., 2008, The Chipman dyke swarm, Saskatchewan, Canada: Component of the 1.9 Ga Snowbird large igneous province in the western Canadian Shield: LIP of the Month, January, 2008: http://www.largeigneousprovinces.org/08jan

Williams, M.L., Karlstrom, K.E., Dumond, G., and Mahan, K.H., 2009, Perspectives on the architecture of continental crust from integrated field studies of exposed isobaric sections: in Miller, R.B., and Snoke, A.W., eds., Crustal Cross Sections from the Western North American Cordillera and Elsewhere: Implication for Tectonic and Petrologic Processes: GSA Special Paper 465, p. 219-241, doi:10.1130/2009.2456(08).

Williams, M.L., Mahan, K.H., Dumond, G., Jercinovic, M.J., Regan, S.P., and Leslie, S., 2011, Linking metamorphism and deformation using in-situ monazite geochronology: interpretation of multistage tectonic histories: GSA annual meeting, Minneapolis, MN.

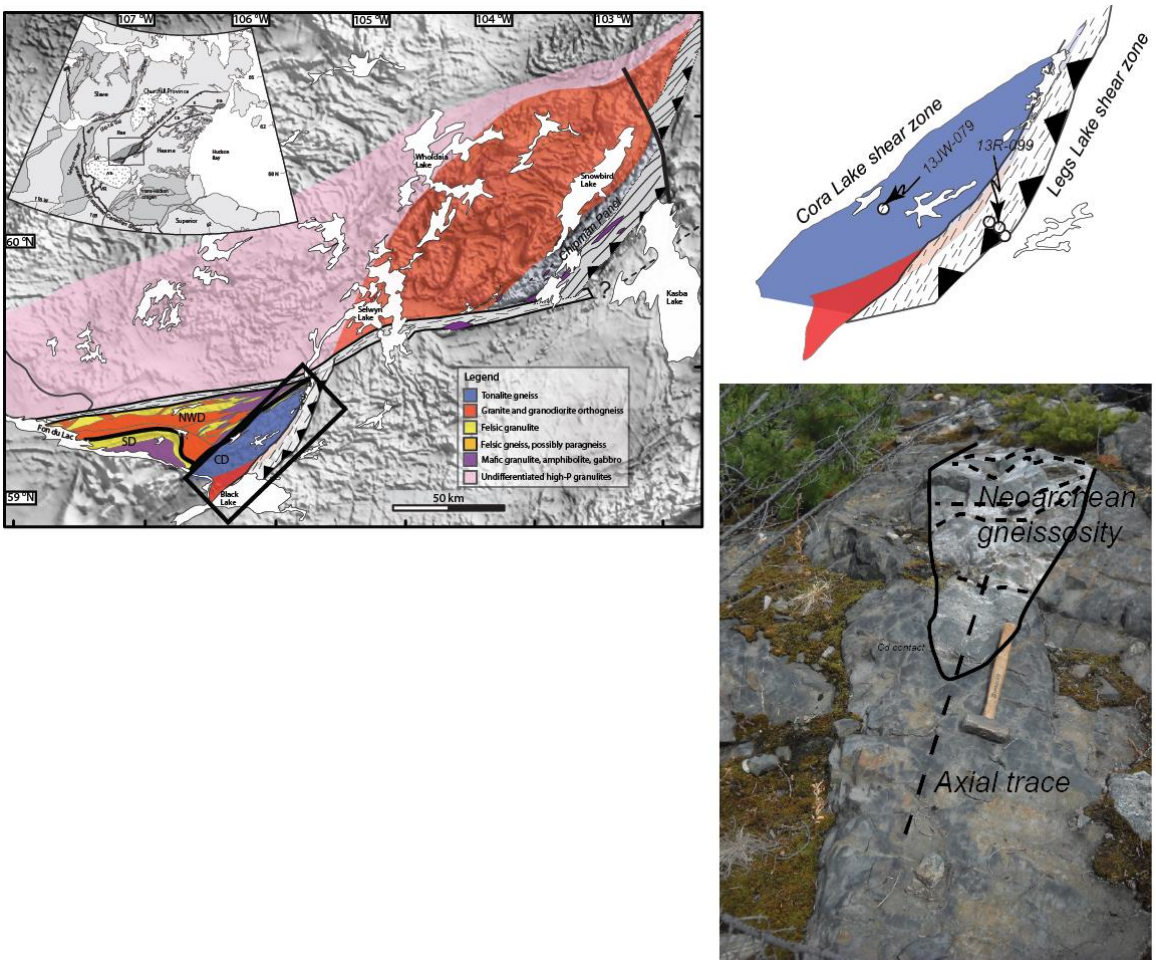

Figure 19: A) Map of the eastern Rae subprovince within the vicinity of the central Snowbird Tectonic zone. Chipman dikes occur within the Chipman panel in blue; inset: map of the western Canadian Shield showing location of Fig. 1a. B) Sample locations within the Chipman subdomain of the Cds. C) A field photograph of a folded Chipman dike that is crosscutting Neoarchean gneissic layering in ca. 3.2 Ga tonalitic gneiss.

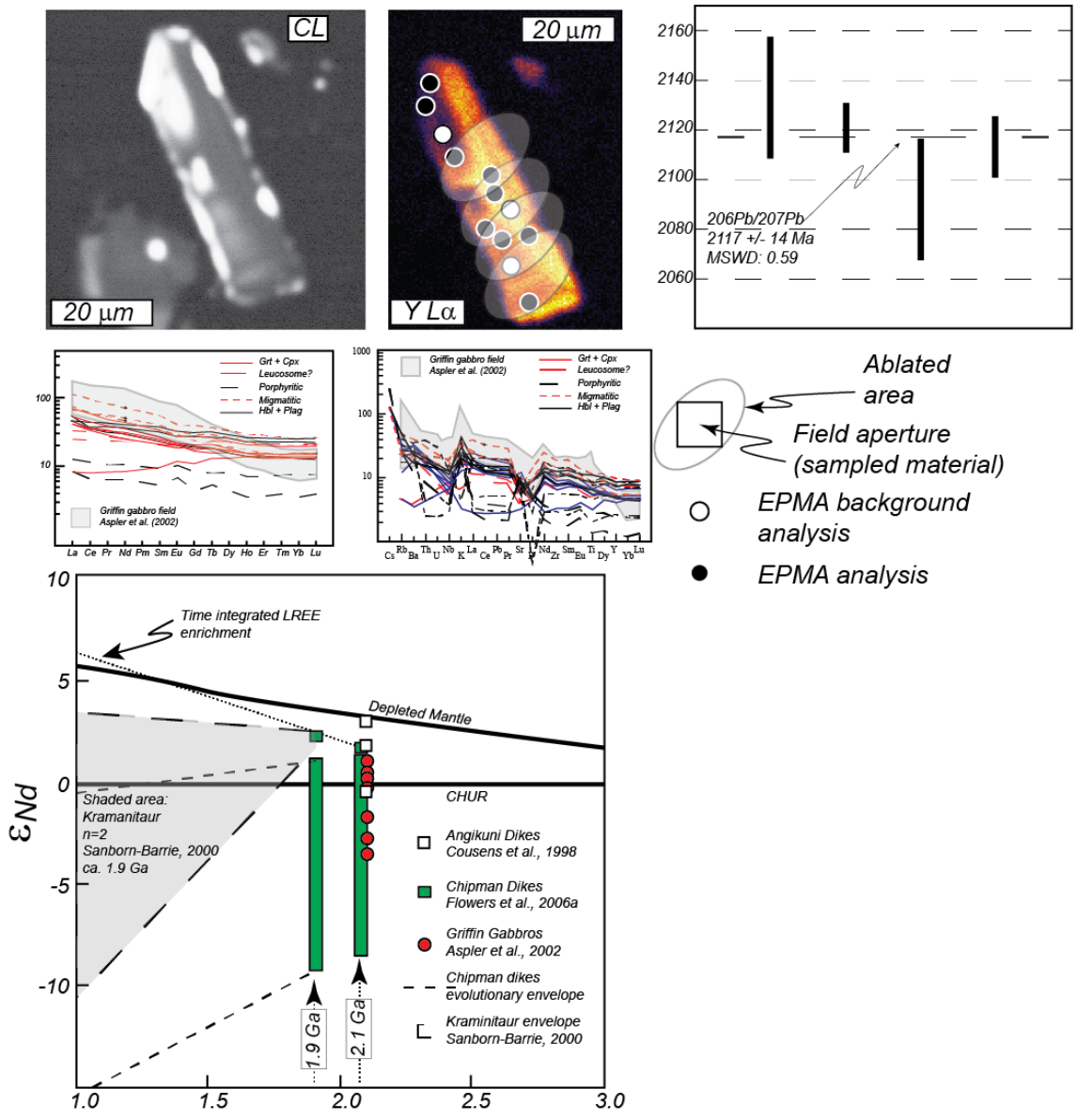

Figure 20: A) CL and B) Yt Lα map of 13R-099a_2_z1 grain found in-situ. Location of EPMA and IN-SIMS analyses labeled on B. C) IN-SIMS results for zircon in Fig. 2a,b ($^{207}Pb/^{206}Pb$). D) REE and E) incompatible element diagram comparing the Cds (data from Flowers et al. (2006) and Griffin Gabbro sills (data from Aspler et al., 2003). F) Nd evolutionary diagram for the Cds, compared with Griffin gabbros, ca. 1.9 Ga Kraminitaur Complex, and dikes from the northern segment of the STZ (Angikuni Lake. The Cds are plotted at both 1.9 Ga and 2.1 Ga.

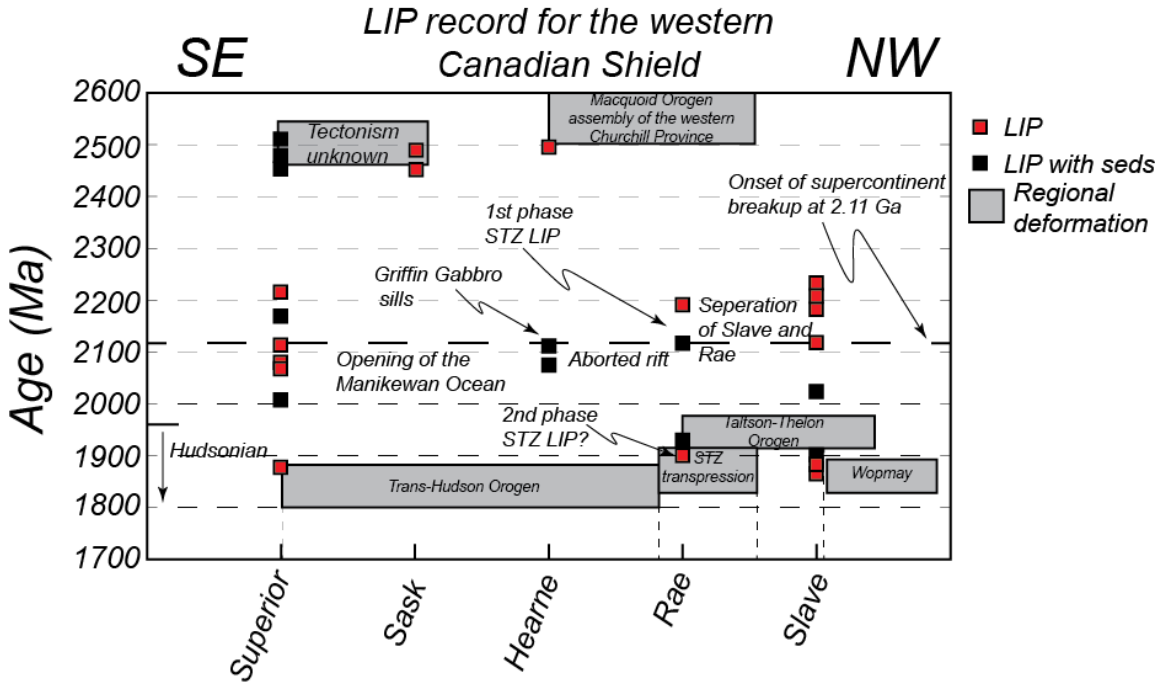

Figure 21: LIP record of the western Canadian Shield with phases of regional deformation labeled.

Table 9: IN-SIMS results

	Isotope ratios						Age (Ma)					
	$^{207*}Pb/^{206*}Pb$	2σ	$^{207*}Pb/^{235}U$	2σ	$^{206*}Pb/^{238}U$	2σ	$^{207*}Pb/^{206*}Pb$	2σ	$^{206*}Pb/^{238}U$	2σ	$^{207*}Pb/^{235}U$	2σ
13JW-079a_z2@1	0.1267	0.0007	6.36	0.54	0.3638	0.0307	2053	10	2000	145	2027	74
13JW-079a_z2@2	0.1286	0.0010	6.45	0.52	0.3638	0.0289	2079	14	2000	137	2039	70
13JW-079a_zr2@3	0.1301	0.0013	6.73	0.77	0.3752	0.0427	2099	18	2054	200	2077	101
13JW-079a_z2@4	0.1292	0.0021	6.13	0.42	0.3443	0.0238	2087	29	1907	114	1995	60
13R-099a2_zr1@1	0.1327	0.0019	4.67	0.59	0.2553	0.0322	2133	25	1466	166	1762	106
13R-099a2_z1@4	0.1317	0.0008	7.42	2.04	0.4085	0.1120	2121	10	2208	513	2163	246
13R-099a2_z1@5	0.1326	0.0043	-2.17	0.35	-0.1186	0.0187	2132	56	-814	137	n/A	n/A
13R-099a2_z1@6	0.1292	0.0021	5.71	0.98	0.3207	0.0552	2087	29	1793	269	1933	149
13R-099a2_z1@7	0.1311	0.0009	4.45	0.38	0.2461	0.0207	2113	12	1418	107	1721	70
13R-099a2_z3	0.1223	0.0010	2.75	0.25	0.1630	0.0143	1990	15	974	79	1342	66
13R-099a2_z3@2	0.1228	0.0013	4.08	0.63	0.2407	0.0371	1998	19	1390	193	1650	126
13R-099a2_z3@3	0.1252	0.0009	4.83	0.83	0.2794	0.0480	2032	12	1588	242	1789	145
13R-099a2_z3@4	0.1224	0.0018	2.71	0.36	0.1603	0.0209	1991	26	958	116	1330	98
13R-099a2_z2@1	0.1125	0.0005	2.38	0.31	0.1535	0.0197	1840	8	920	110	1237	92
13R-099a2_z2@2	0.1114	0.0008	3.44	0.69	0.2241	0.0447	1822	13	1304	235	1514	158
13R-099a1_z2@1	0.1279	0.0012	9.72	2.14	0.5513	0.1210	2069	17	2830	502	2409	202

Notes: 207/206 ages used for weighted means

Table 10: EPMA results for zircon

Sample	13R-099a_2_zr1_core1	13R-099a_2_zr1_rim1	13R-099a_2_zr1_rim2	13R-099a_2_zr2_core1	13JW-079a_zr6_core1	13JW-079a_zr5_rim1	13JW-079a_zr1_core1	13JW-079a_zr1_rim1	13JW-079a_zr2_rim1	13JW-079a_zr2_core1	13JW-079a_zr2_rim2	13JW-079a_zr4_core1	13R-099a_1_zr4_core1	13R-099a_1_zr4_rim1	13R-099a_1_zr5_core1	13R-099a_1_zr5_rim1	13R-099a_1_zr2_core1
UO2	0.06	0.04	0.03	0.14	0.04	0.06	0.04	0.04	0.05	0.03	0.06	0.03	0.02	0.02	0.09	0.04	0.09
K2O	0.00	0.00	0.00	0.00	0.00	0.00	0.00	0.01	0.00	0.00	0.00	0.00	0.00	0.00	0.01	0.00	0.00
ThO2	0.04	0.01	0.01	0.06	0.00	0.02	0.00	0.01	0.01	0.00	0.01	0.00	0.00	0.00	0.30	0.01	0.11
CaO	0.05	0.07	0.05	0.94	0.06	0.11	0.05	0.06	0.08	0.05	0.10	0.08	0.05	0.06	0.08	0.10	0.18
SO3	0.00	0.00	0.00	0.00	0.00	0.00	0.00	0.00	0.00	0.00	0.00	0.00	0.00	0.00	0.00	0.00	0.00
P2O5	0.27	0.06	0.13	0.09	0.00	0.00	0.01	0.00	0.02	0.02	0.02	0.02	0.00	0.00	0.05	0.03	0.06
Y2O3	1.81	0.18	0.82	0.27	0.01	0.02	0.10	0.00	0.05	0.06	0.08	0.06	0.08	0.10	0.31	0.23	0.52
SrO	0.05	0.05	0.03	0.07	0.06	0.06	0.07	0.06	0.06	0.07	0.06	0.06	0.06	0.06	0.07	0.05	0.08
SiO2	30.77	32.01	31.26	31.29	31.27	31.22	31.62	32.29	32.67	31.39	30.84	31.37	29.77	30.53	31.80	31.78	30.72
PbO	0.02	0.02	0.02	0.05	0.02	0.02	0.02	0.02	0.02	0.01	0.02	0.02	0.01	0.01	0.07	0.01	0.04
Ho2O3	0.00	0.00	0.00	0.00	0.00	0.00	0.00	0.00	0.00	0.00	0.00	0.00	0.00	0.00	0.08	0.00	0.00
Yb2O3	0.33	0.06	0.15	0.13	0.00	0.00	0.06	0.00	0.03	0.03	0.03	0.02	0.05	0.03	0.13	0.07	0.15
Tm2O3	0.04	0.01	0.00	0.03	0.00	0.02	0.00	0.01	0.01	0.00	0.00	0.01	0.01	0.00	0.03	0.02	0.01
Gd2O3	0.00	0.01	0.00	0.00	0.00	0.00	0.00	0.00	0.02	0.00	0.00	0.00	0.00	0.00	0.11	0.00	0.00
Er2O3	0.25	0.03	0.12	0.05	0.00	0.00	0.02	0.01	0.03	0.03	0.02	0.01	0.01	0.02	0.09	0.04	0.06
Dy2O3	0.17	0.02	0.08	0.03	0.00	0.00	0.00	0.00	0.02	0.00	0.00	0.00	0.00	0.00	0.05	0.01	0.01
Tb2O3	0.00	0.00	0.00	0.00	0.00	0.00	0.00	0.00	0.00	0.00	0.00	0.00	0.00	0.00	0.02	0.00	0.00
Sm2O3	0.00	0.00	0.00	0.00	0.00	0.00	0.00	0.00	0.01	0.00	0.00	0.00	0.00	0.00	0.02	0.00	0.00
Eu2O3	0.00	0.00	0.00	0.00	0.00	0.00	0.00	0.00	0.00	0.00	0.00	0.00	0.00	0.00	0.01	0.00	0.00
Pr2O3	0.00	0.01	0.00	0.02	0.00	0.02	0.04	0.00	0.01	0.01	0.00	0.00	0.00	0.00	0.05	0.01	0.00
Nd2O3	0.00	0.02	0.01	0.02	0.00	0.00	0.01	0.00	0.00	0.00	0.00	0.00	0.00	0.00	0.03	0.03	0.00
Ce2O3	0.00	0.01	0.00	0.02	0.00	0.01	0.01	0.01	0.00	0.00	0.00	0.01	0.01	0.01	0.23	0.02	0.00
La2O3	0.01	0.00	0.01	0.01	0.01	0.00	0.00	0.00	0.00	0.00	0.00	0.00	0.00	0.01	0.03	0.00	0.01
As2O5	0.13	0.23	0.14	0.23	0.12	0.16	0.24	0.14	0.22	0.15	0.15	0.14	0.12	0.14	0.25	0.12	0.15
V2O5	0.00	0.00	0.00	0.01	0.00	0.00	0.02	0.01	0.01	0.00	0.00	0.00	0.00	0.00	0.00	0.00	0.00
ZrO2	64.42	67.57	66.94	67.44	67.97	67.99	67.31	67.89	67.47	67.21	66.37	66.28	64.14	64.63	66.74	65.44	65.65
Ta2O5	0.01	0.00	0.00	0.00	0.01	0.00	0.02	0.00	0.02	0.00	0.00	0.00	0.00	0.01	0.06	0.02	0.00
HfO2	1.04	1.16	1.11	1.25	1.21	1.35	1.73	1.39	1.55	1.33	1.52	1.32	1.08	1.12	1.44	1.02	1.35
Nb2O5	0.28	0.30	0.30	0.30	0.31	0.31	0.28	0.29	0.34	0.31	0.28	0.30	0.32	0.32	0.34	0.29	0.32
total	99.58	101.75	100.95	102.18	100.84	101.04	101.35	102.03	102.64	100.52	99.29	99.47	95.50	96.93	102.43	99.17	99.12

CHAPTER 4

NEOARCHEAN ARC MAGMATISM AND SUBSEQUENT COLLISIONAL OROGENISIS ALONG THE EASTERN RAE DOMAIN, WESTERN CHURCHILL PROVINCE: IMPLICATIONS FOR THE EARLY GROWTH OF LAURENTIA

Introduction

The Canadian Shield is one of the Earth's major cratons with crustal material dating back as old as 3.9 Ga (Bowring et al., 1989). It consists of a number of Archean provinces separated by Paleoproterozoic orogenic belts (Hoffman, 1988). The region offers a superb opportunity to investigate the growth and evolution of the North American continent, and to evaluate the degree with which modern tectonic processes were active during the growth and ultimate stabilization of the Archean lithosphere. Many of the stitching Paleoproterozoic orogenic belts (Hoffman, 1988), perhaps none quite as well characterized as the Trans-Hudson Orogen (Chiarenzelli et al., 1998; Corrigan et al., 2005; 2009; Maxeiner and Rayner., 2010), are routinely and justifiably interpreted in terms of modern plate-tectonic processes given the similar size, geometry, and composition to modern orogens (Corrigan et al., 2009). The nature of Archean boundaries in the Canadian Shield, and of Archean tectonic processes in general, is much less well known.

The timing and character of Archean tectonics have been particularly unclear in the Churchill Province of the Canadian Shield, partly because of the vast size and remoteness of the region and partly because of the complex overprinting and interleaving of Proterozoic and Archean components (Mahan et al., 2006a; Williams et al., 2009; Dumond et al., 2010; Bethune et al., 2013). The Churchill Province has typically been subdivided into two large subprovinces, Rae and Hearne domains, separated by the geophysically defined Snowbird Tectonic Zone (STZ; Hoffman, 1988). Debate persists regarding the history of this enigmatic boundary (even whether it is fundamentally an Archean or Proterozoic feature - Hoffman, 1987; Hanmer et al., 1994; Cousens et al., 2001; Berman et al., 2007), and consequently, the fundamental relationship

between the Rae and Hearne subprovinces remains uncertain (Aspler et al., 1999; Berman et al., 2007).

The Athabasca granulite terrane (AGT) is a broad region (>20,000 km^2) of high pressure granulite exposed along the eastern margin of the Rae domain. It preserves a well exposed transect across the Snowbird Tectonic zone and into the Hearne Domain (Williams and Hanmer, 2006; Williams et al., 2009; Dumond et al., 2014). One important component of the AGT is a large suite of ca. 2.6 Ga meta-plutonic rocks that vary in composition from mafic to felsic. The location of this suite, along the present-day boundary between the Rae and Hearne domains, suggest that it may help to illuminate the Archean history of the boundary. This contribution presents new structural, petrologic, geochemical, and geochronologic data in order to constrain the tectonic setting and evolution of the 2.6 Ga igneous suite within the AGT. The data suggest that the rocks formed part of a large Archean arc batholith and that soon after assembly, the margin underwent significant thickening, high-grade metamorphism, and high-T lateral flow, all consistent with continental collision along the boundary of the Rae Province. The new data suggest that although the Snowbird tectonic zone is currently dominated by Proterozoic structures elements, it may have originated as an Archean suture.

Regional Background

Western Churchill Province

The 2800 km long, geophysically defined, Snowbird Tectonic Zone (STZ) was interpreted as the boundary between the Rae and Hearne domains of the western Churchill Province (Gilboy, 1980; Ross, 1994). The lineament is defined by a positive anomaly in the horizontal gravity gradient map and also consists of an anastomosing tapestry of aeromagnetic patterns. This dramatic feature has been recognized from the subsurface of Alberta to northwestern Hudson Bay (Hoffman, 1988; Ross et al., 1994). The origin and geological significance of the lineament has been considered enigmatic, and it even has been called into question whether portions of the STZ correspond to a Rae-Hearne boundary (Berman et al.,

2007). The focus herein will be on the eastern Rae domain, including rocks and structures that correspond to the STZ.

The Rae domain, at least near the STZ, is characterized by relatively high grade metamorphic assemblages (amphibolite and granulite facies), which contain evidence for multiple phases of deformation within both Neoarchean basement rocks, and infolded Paleoproterozoic cover sequences (Ashton et al., 2013; Berman et al., 2013; Bethune et al., 2013; Martel et al., 2008). Basement rocks include a wide variety of rock types but 2.67-2.30 Ga granitoids are particularly common (Hanmer et al., 1994; Martel et al., 2008; Hartlaub et al., 2007; Sanborn-Barrie et al., 2014a). There are rare and isolated regions of >3.0 Ga basement (Hanmer et al., 1994; Henderson and Theriault, 1994; Martel et al., 2008; Sanborn-Barrie et al., 2014a), and dominant Neoarchean supracrustal belts that contain distinctive Komatiite successions, some associated with fuschite-bearing quartzites (Machattie, 2008; Corrigan et al., 2013; Pehrsson et al., 2013; Sanborn-Barrie et al., 2014b). Cover sequences include the Paleoproterozoic Murmac Bay and Amer-Chantry groups, and large tracts of undifferentiated, infolded, paragneiss (Aspler and Chiarenzelli, 1998; Aspler et al., 2001; Martel et al., 2008; Rainbird et al., 2010; Ashton et al., 2009;2013).

The Rae domain contains abundant evidence for reworking during the 1980-1930 Ma Taltson-Thelon Orogen, focused along the western margin of the domain (Hanmer et al., 1992; Bethune et al., 2013; Ashton et al., 2009; 2013; Hildebrand et al., 2010; Card et al., 2014b). Structural evidence of this event decreases from west to east, towards the central STZ. In contrast, the metamorphic grade of cover sequence rocks increases from west to east. This metamorphism is generally interpreted to postdate the Taltson-Thelon tectonism, and is generally attributed to the 1.9 Ga Snowbird event (Berman et al., 2007; Ashton et al., 2009; Bethune et al., 2013). In the easternmost portions of the Rae domain, closest to the STZ, metamorphic grades in

the cover rocks are similar to those in the Archean basement (high P-T granulite), making it difficult to distinguish Archean and Proterozoic rocks and events.

The Hearne Domain, southeast of the STZ, is predominately characterized by Paleoproterozoic sedimentary sequences (Hurwitz Group), Neoarchean basement exposures within antiformal windows (Aspler et al., 2002a), and one of the largest autochthonous greenstone belts in North America, the 2.7 Ga Ennadai -Rankin- greenstone belt (Aspler and Chiarenzelli, 1996). Metamorphic grades are generally in the greenschist or amphibolite facies (Hanmer et al., 2004; Davis et al., 2004; Mahan et al., 2003; Cousens et al., 2004). Archean basement of the Hearne domain differs from that of the Rae domain, in that it contains a greater amount of Archean supracrustal rocks. The Hearne domain also contains, on average, slightly older Neoarchean basement (2.73 – 2.68 Ga; Cousens et al., 2004). Aspler and Chiarenzelli (1996) presented detailed stratigraphy and petrology on the Ennadai-Rankin belt (Henik segment) and inferred a Neoarchean history for the Ennadai-Rankin greenstone belt. They suggested that its development was far removed from a continental influence (at ca. 2.70 Ga). Geochemical, isotopic, and geochronological analyses suggest that bimodal volcanism was caused by partial melting of a depleted mantle source (Cousens et al., 2004), and ryholitic flows were derived from melting of older basaltic crust (Cousens et al., 2004; Davis et al., 2004). These authors interpreted an infant arc setting for the central Hearne domain during the Archean, akin to the modern day western Pacific Ocean (Cousens et al., 2004; Hanmer et al., 2004).

The Athabasca Granulite Terrane

The Athabasca granulite terrane exposes >20,000 km^2 of granulite facies rocks, and has been interpreted as an isobarically-cooled terrane (Mezger, 1992) and a representative view of lower continental crust (Mahan and Williams, 2005; Williams and Hanmer, 2006; Williams et al., 2009). The eastern margin of the Rae domain and the STZ are particularly well exposed in the eastern part of the Athabasca granulite terrane (Dumond et al., 2008). The East Athabasca

mylonite triangle (Tantato domain of Gilboy, 1980) is a high grade region of nested shear zones exposed along the easternmost margin of the Rae, and is particularly well characterized (Hanmer et al., 1994; Williams et al., 2009).

One major characteristic of the eastern Athabasca granulite terrane is a block style architecture, with disparate lithotectonic subdomains divided by thick ductile shear zones (*briefly discussed below;* Flowers et al., 2006b). Detailed work has demonstrated that the steeply to moderately dipping shear zones that divide domains are Paleoproterozoic in age (Williams et al., 2009; Mahan et al., 2006a; Dumond et al., 2014; Regan et al. 2014). The major focus of this contribution will be on older tectonic events, evidence for which is heterogeneously preserved internal to each lithotectonic block or subdomain (Mahan et al., 2008).

Subdomains

The Chipman subdomain is primarily underlain by the heterogeneous ca. 3.2 – 3.4 Ga Chipman tonalite (Chipman panel of Martel et al., (2008))(Hanmer, 1995). Despite the rarity of similar exposures throughout the mapped Rae domain, Mesoarchean crust and lithosphere has been interpreted to underlay much of the Rae domain (Petts et al., 2014). Along the western flank of the Chipman subdomain, there are meter to decimeter scale lozenges of Archean mafic granulite and associated felsic granulite (Mahan et al., 2008; Flowers et al., 2008), which record evidence of polymetamorphism interpreted to have both Archean and Paleoproterozoic components (*for further discussion see Mahan et al., 2008*). The ca. 1.9 Ga Chipman mafic dike swarm cross-cuts gneissosity and typically has a strong tectonic fabric defined by a granulite facies metamorphic assemblage (hornblende – plagioclase – garnet – clinopyroxene (Williams et al., 1995; Mahan and Williams 2005; Flowers et al., 2006a; Mahan et al., 2008; Regan et al., 2014).

The Northwestern subdomain is characterized by Neoarchean plutonic rocks with subordinate felsic granulite screens. The subdomain is bounded by the Cora Lake and Grease

River shear zones. Plutonic rocks of the Northwestern subdomain range in composition from felsic to intermediate, with subordinate mafic lithologies (*see below).* The largest, and best studied component is the Mary granodiorite (Hanmer, 1994; 1995; Williams et al., 2000; 2014; Dumond et al., 2010). Felsic granulite (classically the "Reeve diatexite" after Hanmer, 1994) commonly forms concordant, semi-continuous screens completely engulfed by the meta-plutonic rocks. Detailed structural work has focused within charnockitic (opx-bearing granitoid; terminology after Frost and Frost, 2008b) lithologies, which preserve evidence for both Neoarchean and Paleoproterozoic deformational phases (Dumond et al, 2010; Regan et al., 2014). Early, subhorizontal gneissosity (S_1) has been interpreted to represent Neoarchean crustal flow(Dumond et al., 2010), while subsequent folding and the development of a heterogeneously developed axial planar (S_2) fabric developed throughout the region is interpreted to represent Paleoproterozoic (ca. 1.9 Ga) deformation (Regan et al., 2014).

The upper deck (also referred to as the southern domain (Baldwin et al. 2004; Flowers et al., 2006b)) consists of abundant migmatitic paragneiss, mafic granulite, and minor eclogite (Snoeyboss et al., 1997; Baldwin et al., 2003, 2004). The dominant rock type is a garnetiferous quartzofeldspathic gneiss, interpreted to represent a deformed migmatite that has had variable amounts of melt loss. It is referred to as the "white gneiss" (Snoeyenboes et al., 1995; Baldwin et al., 2006; Dumond et al., 2015). The white gneiss contains an assemblage of ternary feldspar, quartz, kyanite, garnet, and rutile +/- sillimanite (Snoeyenboes et al., 1995). Although production of eclgite assemblages was initially interpreted to be Paleoproterozoic and approximately 700 my after migmatization (Baldwin et al., 2006), recent work by Dumond et al., (2015) suggests that eclogitization was synchronous with anatexis during the Neoarchean.

Shear zones delineate the major lithotectonic blocks (subdomains) of the Athabasca granulite terrane. The Cora Lake shear zone seperates the Northwestern subdomain from the Chipman subdomain and is thought to have been active at the waning phases of Paleoproterozoic

granulite facies deformation (ca. 1.89-1.87 Ga; Regan et al., 2014). The Legs Lake shear zone represents the southeastern margin of the Athabasca granulite terrane, containing evidence for ca. 20 km of vertical throw of high P granulites of the Chipman subdomain above mid-crustal Hearne domain rocks (Mahan et al., 2003). The Legs Lake shear zone is thought to have been active from ca. 1.86 – 1.84 (Mahan et al., 2006a.b). The Grease River shear zone marks the northern margin of the Northwestern subdomain, and accommodated ca. 110 km of right-lateral slip at ca. 1.80 Ga (Mahan and Williams, 2005). Recent work by Dumond et al. (2008; 2014) suggests that the Grease River shear zone may also have an older history as well (ca. 1.9 Ga), but the relative importance and magnitude remains unclear. Based on the kinematics and timing of each shear zone, Regan et al. (2014) interpreted them as having formed during and as a result of orogenisis along the western and southern margins of the western Churchill Province.

Analytical Methods

Geochemistry

Major and trace element compositional analyses were carried out by ACME analytical laboratories in Vancouver, British Columbia by inductively-coupled plasma mass spectrometry (ICP-MS). Samples were cut into slabs, and weathered edges were trimmed. Samples were crushed into powders at ACME analytical facilities. Samples were analyzed by x-ray fluorescence (major elements) and inductively coupled plasma - mass spectrometry (trace and rare earth elements).

Bulk compositional analyses for isochemical pseudosection modeling were performed by x-ray fluorescence (XRF) at the University of Massachusetts, Amherst. Samples were crushed in a tungsten carbide shatter box. One sample analyzed in this study is a compositionally layered migmatite (*see below*), which contains two relatively isolated, and distinct compositions. Three samples were cut from the rock, the first consists of half garnetite and half leaucosome, the second contains only leucosome, and the third consists of only garnetite. XRF analytical methods are described in detail in Rhodes (1996).

Isochemical thermodynamic modeling

Phase compositions and zoning were evaluated on a Cameca SX-50 electron microprobe at the University of Massahcusetts, Amherst, using 5 wavelength dispersive spectrometers (WDS). High resolution compositional mapping of individual phases or small areas was performed using a 100nA current, a 100ms dwell time, and a step of 2 to 10 μm set equal to the beam size. WDS maps were used to guide electron microprobe analysis. Analyses of all phases were performed at 20nA current, and 15 KeV. A 4 μm beam diameter was used for biotite analyses, a 3 μm beam for feldspar, and a focused beam for garnet. Calibration was performed on standards similar to the phase of interest. Matrix corrections were carried out using a PAP model (Pouchou and Pichoir, 1984).

Theriak-Domino (de Capitani and Petrakakis, 2010) was used to construct isochemical phase diagrams (pseudosections) and model the composition of individual phases in order to investigate the petrogenetic evolution of felsic granulite sample (10W-094g) and meta-plutonic rock (12R-054). The database of Holland and Powell (tcdb55c2d) was used due to the capability of modeling anatexis (Holland and Powell, 1998).

In-situ monazite U-Th-total Pb geochronology

All monazite grains were identified from full thin section WDS maps, made on a Cameca SX-50 electron microprobe, using a 300 nA current at 15 KeV. The step size was 35μm, with a defocused beam approximately 30 μm in diameter. Grains were found with a spectrometer set on the Ce Mα x-ray line, along with a minimum of two other maps (base maps) of common elements (typically Mg Kα and Ca Kα). Grains were subsequently mapped at high resolution with a focused 200 nA beam, using beam rastering technique with a fixed stage. This provides submicron compositional resolution (see Williams et al., 2006).

In-situ U-Th-total Pb monazite geochronology was performed at the University of Massachusetts, Amherst, on the Cameca SX-100 “ultrachron” electron microprobe (for analytical

procedures see Williams et al., 2006; Dumond, 2008). Five spectrometers measured U, Th, Pb, S, Ca, K,Sr, Si, Y, and P, and the full suite of REEs. Each reported date consists of one background analysis and four to eight peak analyses all made within a single compositionally homogeneous domain, thus a single date is the result of 4 – 8 analyses. Background for U, Th, and Pb were acquired using a multipoint method, where 8-10 measurements were taken in positions of no known spectral interference (Allaz et al., 2013). An exponential fit was used to regress background through the peak position to evaluate the background curvature. Lead was measured by integrating counts from two VLPET crystals.

Standardization was done using both natural and synthetic standards. Calibration was performed on pyromorphite ($PbPO_4$), Barbanite ($ThPO_4$), and UO_2 for Pb Mα, Th Mα, and U Mβ, respectively. Peak positions were routinely updated on synthetic phosphates for P, Ce, La, and Nd prior to each analytical session. Prior to, and after each analytical session, as well as several times within a session, an in-house consistency standard, Moacyr (506 +/- 1Ma; Dumond et al., 2008), was analyzed using the same analytical procedure to evaluate the consistency of analyses.

Results

Constraints on the emplacement age and geometry of Northwestern subdomain plutonic rocks

Table 1 displays existing U-Th-Pb geochronologic data from the east Athabasca mylonite triangle that pertain to emplacement ages of metaigneous rocks. The majority of constraints are presented in Hanmer et al. (1997), and were performed via multi-grain TIMS analysis (Parrish, unpublished data) Although the majority of felsic igneous rocks appear slightly older than the analyzed mafic rocks, given the multi-grain TIMS method employed, we can not account for metamorphic grains developed within mafic endmembers, potentially lowering the aggregate age slightly. Collectively, plutonic rocks of the Northwestern subdomain can be thought of as a ca. 2.6 Ga composite batholith.

The northwestern subdomain is dominated by ca. 2.6 Ga plutonic rocks that contain evidence for at least two periods of penetrative deformation (Dumond et al., 2010; Regan et al., 2014). The earliest tectonic fabric contains a subhorizontal enveloping surfrace throughout the entire northwestern subdomain (Dumond et al., 2010; Regan et al., 2014). This strong tectonic fabric parallels compositional variability present within the composite batholith. This major structural fabric, however, has been modified by subsequent, ca. 1.9 Ga open, upright folds that plunge shallowly to the southwest (Dumond et al., 2010; Regan et al., 2014). Unfolding of F_2 results in a southwest dipping S_1 (~ 12°). We assume that this dip, at least to some degree, represents the post S_1 configuration (ie. Dipping slightly to the south). Therefore, the early compositional layering is currently tilted, and thus the Northwestern subdomain may represent an oblique section of the ca. 2.63-2.60 Ga composite batholith.

The northeastern part of the plutonic belt is dominated by intermediate and subordinate mafic units of the bohica suite. These units grade into granodioritic to granitic units to the southeast, which are largely textural vairants of the Mary batholith (Hanmer, 1994). Therefore, the Neoarchean composite batholith grades from more mafic endmembers at structurally lower ends to an increasing felsic component with increasing structural hieght. The lack of discrete mylonite zones at compositional boundaries, and the pervasive high strain internal to S_1 compositional layering suggests that compositional endmembers were not tectonically juxtaposed, but were emplaced and deformed together as one coherent composite batholith.

Petrology of Neoarchean plutonic rocks

Rocks of the Neoarchean plutonic suite have a broad compositional range, but contain similar textural characeristics. A vast majority of the rocks contain plagioclase porphyroclasts, with variable amounts of orthopyroxene, hornblende, clinopyroxene, garnet, +/-kspar +/- quartz. Accessory phases include apatite, ilmenite, and zircon. However, equigranular, pyroxene-absent, granites are also common (ie. Beed granite and correlatives, see below).

Intermediate to mafic endmembers

The intermediate to mafic rocks (ca. 2.6 Ga; Bohica complex of Hanmer, 1994, 1997) is located within the eastern portions of the Northwestern subdomain (Hanmer, 1994). This suite ranges from dioritic to leauconoritic with subordinate gabbroic compositions (Hanmer, 1997). Throughout the compositional array the Bohica intermediate to mafic complex is predominately porphyroclastic, with plagioclase as the major coarse phase, along with subordinate orthopyroxene. Both ortho and clinopyroxene crystals are commonly fine grained and intergrown with ilmenite. Plagioclase porphyroclasts form ribbons while some preserve core-mantle structures with decreasing X_{An} content from core to rim. This zoning is similar to that in the more felsic compositions where it has been attributed to garnet growth during D_1 (*see Williams et al., 2014*). Evidence for this early granulite facies metamorphic event is well preserved within crenulated domains, where X_{An} zoning can be observed around crenulation hinges, and is thus older than F_2 folds.

Felsic to intermediate endmembers

Granitoid compositions are dominant in the southwestern portions of the east Athabasca mylonite triangle, and becomes less abundant to the northeast (Hanmer, 1994). The suite consists of variably deformed, porphyroclastic granitoids, that typically contain primary orthopyroxene (charnockitic), and range from granitic to granodioritic (Frost and Frost, 2008). However, a vast majority of the rocks contain a strong tectonic fabric and a metamorphic assemblage of Na - plagioclase, clinopyroxene, garnet, ilmenite, quartz and K-feldspar, informally referred to as the 'Mary Reaction' (Williams et al., 2000; Dumond et al., 2010; Williams et al., 2014; Regan et al., 2014). Hornblende and biotite are common where S_2 is particularly well developed. S_2 appears to be focused along the limb regions of large amplitude, upright folds (F_2; Regan et al., 2014). Deformed quartz veins are common in samples that show evidence for protomylonitic to mylonitic strain (Williams et al., 2000).

Felsic granulite

The Northwestern subdomain also contains subordinate garnetiferous felsic granulite screens (referred to as Reeve diatexite; Hanmer, 1994). These are interpreted to have formed via large degrees of partial melting (Snoeyenboss et al., 1995; Baldwin et al., 2004; Mahan et al., 2006b; Dumond et al., 2015). The bulk assemblage varies little, and is commonly composed of plagioclase, garnet, quartz, biotite, sillimanite, K-feldspar, and rare orthopyroxene (Hanmer, 1997; Dumond et al., 2010). They usually occur as semiconcordant lenses parallel with S_1. This unit commonly has abundant accessory monazite, making it an ideal target for geochronology (*see below;* Mahan et al., 2006a).

Geochemistry

A sampling of nine ca. 2.63 – 2.60 Ga plutonic rocks along a northeast to southwest transect, oblique to S_1 strike have been used to characterize the Neoarchean plutonic complex owing to the parallelism of S_1 and compositional layering (Figure 5). SiO_2 contents range from 58.01 – 73.71 weight percent. Plots of major oxides (Harker diagrams) plotted against SiO_2 display tight, linear trends. With increasing SiO_2, all samples decrease with CaO, Fe_2O_3, TiO_2, P_2O_5, and MnO, but MgO displays no variation.

Rocks range from ferroan to magnesian with respect to the Fe index ($Fe_2O_3/MgO+Fe_2O_3$) of Frost and Frost (2008). Samples define a linear trend with a shallow slope on modified alkali lime index (Na_2O+K_2O – CaO against SiO_2) diagrams and plot as calc-alkalic to alkalic-calcic. All samples plot within the volcanic arc field in all four of the tectonic discrimination diagrams based on Y, Yb, Rb, Nb, and Ta (Pearce et al., 1984). Some of the higher SiO_2 samples (Beed Granite), plot near the boundary of rift-related granite fields.

All samples are LREE enriched, and HREE depleted, and show a strong, concave up, negative slope when normalized to chondrites (Figure 6a; Sun and Mcdonough, 1989). That is, samples are characterized by a LREE negative slope, and a fairly flat and depleted HREE slope.

La_N/Sm_N (chondrite normalization of McDonough and Sun, 1995) ranges from 4.31 – 12.10. Incompatible element trends display strong depletions in high field strength elements, and enrichments in large ion lithophile elements and Pb when normalized to primitive mantle (Sun and McDonough, 1989). These trends are most commonly associated with derivation from a metasomatized lithospheric source (Cousens et al., 2001; Chiarenzelli et al., 2010).

Published Nd isotopic analyses from the northwestern subdomain show remarkable similarity (Hanmer et al., 1994). Samples range from -1.84 to 1.55 $\varepsilon_{Nd(t)}$, and are slightly below contemporaneous depleted mantle (Hanmer, 1997). Model ages (T_{DM}) range from 2686 to 3019 Ma, and are thus likely derived from both juvenile and older crustal sources. On Nd evolutionary diagrams, all samples share similar slopes and a relatively small ε_{Nd} range. Differences may reflect varying LREE concentrations due to fractionation (Figure 7). When compared with the whole rock geochemistry presented above, it seems likely that the entire northwestern subdomain consists of a large and petrogenetically linked, Neoarchean composite arc batholith, that was built in ca. 30 my, or less.

Comparison with other 2.6 Ga plutonic rocks

The majority of the Rae domain of the western Churchill Province is underlain by Meso to Neoarchean plutonic rocks (Hoffman, 1988). However, geochemical data for Neoarchean rocks in the Rae domain are sparse. Two major suites of granite are exposed along the southeastern margin of the Chipman subdomain, and into the Legs Lake shear zone: The Fehr and Stevenson granites (Mahan et al., 2003). Data from the Fehr Granite plot collinearly on Harker diagrams with the rocks from the northwestern subdomain. The Fehr granite also plots in the volcanic arc granite field on tectonic discrimination diagrams, and identical trace element patterns. These data suggest a potential petrogenetic relationship between the Fehr granite and plutonic rocks exposed within the Northwestern subdomain (ca. 2.6 Ga; Hanmer, 1997; Koteas et al., 2010; *supplement*). These data suggest that the Fehr granite may be a member of the

Neoarchean plutonic complex exposed in the Chipman subdomain. There is no existing whole-rock geochemistry or zircon geochronology available on the Stevenson granite, but the age and geochemical analyses are currently being performed.

Unpublished data from Angikuni Lake, 450 km NE along the Rae-Chesterfield-Hearne boundary (Aspler et al., 1999; Berman et al, 2007) within the vicinity of the geophysically defined Snowbird Tectonic zone provide an additional spatial comparison to test if the Neoarchean plutonic complex exposed in the east Athabasca mylonite triangle continues along the margin of the Rae domain. Little geochronologic data exist for metaigneous rocks at Angikuni Lake, but preliminary data suggest ages ranging from 2.7 – 2.6 Ga (Aspler et al., 1999; Aspler, personal communication). The older populations are likely related to the initial growth of the Ennaidai – Rankin greenstone belt, however, ca. 2.6 Ga plutonic rocks that straddle the geophysically defined STZ (zone 1, 2, 6, and 7; Aspler et al., 1999). On Frost diagrams (Frost et al., 2001; Frost and Frost 2008), the rocks plot as largely ferroan to magnesian, and form linear trends on the modified alkali-lime index, plotting from alkali-calcic to calc alkalic. Similar to the Neoarchean plutonic rocks in the AGT, they plot in the volcanic arc granite fields on all Pearce diagrams (Pearce et al., 1984), and contain enrichments in their LILE and depletions in HFSE. Sm-Nd isotopic systematics are also quite similar to published data from Hanmer et al. (1994), with rocks of the east Athabasca mylonite triangle having very similar, time integrated, ε_{Nd} values. In all respects, the ca. 2.6 Ga plutonic rocks are similar to the AGT and suggest that the easatern Rae domain may be more broadly characterized by Noearchean arc magmatism.

Pressure-Temperature analysis

There has been two decades of thermobarometric analysis performed on rocks exposed within the Athabasca granulite terrane (Williams et al., 1995; 2000; 2014; Krikorian, 2002; Mahan et al., 2003; 2006a; 2008; Mahan and Williams, 2005; Dumond et al., 2010; 2015; Regan et al., 2014; *among others*). One of the biggest challenges is developing direct links to mineral

reactions, thermobarometric analysis via simultaneous equilibria, forward-modelling, and absolute time. Generally rocks with a detailed monazite record contain non-ideal phases for thermobarometric analysis, and structural linkages have provided the foundation for interpreting pressure-temperature-time (P-T-t) linkages. The goal in this section is to highlight two samples, one from the Northwestern and Chipman subdomain, that contain abundant monazite, but were chosen for forward modelling to provide direct links to existing thermobarometry and time from a single bulk composition and thin section. This analysis was chosen to augment similar work performed in the Upper deck by Dumond et al. (2015).

Despite substantial work, little is known regarding the temporal evolution of the entire Chipman subdomain, likely due to the tonalites long and enigmatic history. However, recent mapping and structural analysis within the region suggests that it contains two main fabric generations (S_1 and S_2)(Mahan et al., 2003, 2008; Regan et al., 2014). An early granulite grade fabric, present within mafic granulites and diatextic screens (Figure 4b,d) within the western portions of the subdomain is thought to have formed at ca. 1.35 GPa and 850°C (Mahan et al., 2008). This tectonic fabric (S_1) is folded into open to tight, upright folds, which range from well preserved to completely overprinted by S_2, and define the axial plane of F_2 folds (Figure 3a, 3c). Chipman dikes are typically seen cross cutting S_1, but are also folded. Others, however, appear to be crosscutting S_2, but the possibility remains that these examples are S_1 fabrics that have been rotated into S_2 parrallelism. S_1 in the Chipman tonalite varies from nearly igneous compositional layering, to a weak tectonic fabric. Although deciphering kinematics has been troublesome for the early tectonic fabric (S_1), S_2 shows evidence for dextral sense of shear on a shallow to the southwest lineation (Figure 3e; 09 to 236; n= 30). Based on metamorphic zircon geochronology presented in Flowers et al. (2008), Mahan et al. (2008) tentatively interpreted S_1 to be Neoarchean, and folding during retrogression. A subset of analyses yielded ca. 1.9 Ga ages and

evidence for a second granulite-facies event led to the interpretation of minor reactivation of S_2 at that time ($S_{3a,b}$ of Mahan et al., 2008; Flowers et al., 2008).

The structural evolution of the northwestern subdomain is better constrained than the others due to the detailed work done along its southwestern margin (Dumond et al., 2010). Similarly to the Chipman subdomain, there are two main structural fabrics internal to it, an early subhorizontal gneissic layering (S_1), and subsequent upright folding and dextral shearing fabric defining the axial plane (S_2)(Figure 3b,d,f)(Dumond et al., 2010; Regan et al., 2014). S_2 contains abundant dextral S-C-C' and both σ and δ asymmetries suggesting that dextral shear was the pervasive kinematic component during regional deformation. Regan et al. (2014) suggested that the majority of steep fabrics within the subdomain contain dextral kinematics, and define the axial plane to large amplitude, open, folds (S_2: 237, 81; n=99; L_2: 15 to 240; n=47). Folds are open, and generally plunge shallowly to the southwest (Dumond et al., 2010; Regan et al., in review). Based on in-situ monazite U-Th-total Pb geochronology presented in Dumond et al. (2010) and Regan et al. (2014), S_1 is suggested to have developed at approximately 2570 Ma, 50-30 my subsequent to the emplacement of the composite batholith. Kinematics along S_1 are consistently top to the east throughout the northwestern subdomain. Folding has been constrained to have initiated by approximately 1915 Ma, and the development of S_2 occurred at ca. 1.9 Ga (Regan et al., in review). Both fabrics have been interpreted to develop under nearly identical metamorphic conditions (0.9 GPa and 750°C)(Williams et al., 2000; Dumond et al., 2010; Regan et al., in 2014).

Pressure-Temperature analysis of 10W-094g

Sample 10W-094g, from the southwestern shore of Cora Lake, is a felsic granlite migmatite interleaved with mafic granulite and tonalitic gneiss. Individual pieces of leaucosome and garnetite (restite) were modeled separately and as a single homogenized sample (*see analytical methods*). This sample was targeted for detailed petrologic analysis and forward

modeling due to minimal overprinting of D_1 by D_2 and abundant monazite, to better constrain a P-T-t-D path. The structural preservation is critical for understanding how the metamorphic assemblage within the sample has changed during strain, and monazite is critical to directly link these variations to time.

Sample 10W-094g contains an assemblage of plagioclase, quartz, kspar, garnet, and biotite with accessory ilmenite, rutile, sillimanite, monazite and zircon. The migmatitic layering (S_1) is folded about upright folds with an axial plane coincident with the regional S_2. It contains pods, lenses, and continuous layers of garnetite with interstitial K-feldspar, plagioclase, quartz and biotite. Within the garnetite, S_2 is not well developed and biotite forms mats adjacent to garnet porphyroblasts that are commonly restricted to garnet fractures and along the quadrants of the garnet crystal coincident with the S_2 plane. Biotite mats on garnet exteriors are commonly aligned with basal cleavage oriented perpendicular to the S_2 defined in the leaucosome, suggesting growth in the S_2 extensional direction, with basal cleavage oriented perpendicular to S_2. Networks of veins and layers of leaucosome consists of plagioclase and subordinate garnet porphyroblasts (xenocrysts?) in a quartz rich matrix with kspar and biotite. Garnet is interpreted as a peritectic phase that grew during anatexis. Fractures within garnet are oriented perpendicular to the S_2 plane and are interpreted to represent syn-D_2 garnet cataclasis. The S_2 fabric within the leaucosome is defined by biotite and dynamically recrystallized feldspar. .

Mineral zoning and composition

Sample 10W-094g consists of plagioclase, garnet, kspar, biotite, and quartz. Plagioclase is both porphyroclastic and porphyroblastic (up to 2 cm) within the leaucosome due to growth during D_1 and subsequent strain along S_2. Plagioclase porphyroblasts were not identified within the garnetite. Also, porphyroblastic plagioclase has dynamically recrystallized tails oriented along the trace of the S_2 folia. Cores contain a substantial X_{Or} component, which decreases rimward (Figure 8), contain little to no zoning with respect to Anorthite component (X_{An} (0.31)),

but have a slight increase in X_{Ab} from core to rim (0.66 to 0.70) with a corresponding decrease of X_{Or}. Finer grained, recrystallized, plagioclase contains negligable K_2O, and exhibits flat compositional profiles with a composition of X_{An} 0.28 and X_{Ab} 0.72. There is a slight increase of X_{An} to 0.32 within dynamically recrystallized tails. Garnet crystals (up to 3 cm) contain fairly flat compositional profiles (X_{Alm} = 0.45 and X_{Pyr} = 0.50). X_{Gr} is increases slightly, from 0.035 to 0.05 within the outer 10-50 μm of the crystal. This increase corresponds to a drop in X_{Pyr} and an increase in X_{Alm}, interpreted to be related to $FeMg_{-1}$ exchange (Figure 9) occurring during D_2 plagioclase recrystallization, and caused changes in corresponding X_{Gr} composition in garnet outerrims.

Compositions of silicate phases in the garnetite are similar to those in leucosome. e is anhedral, surrounds garnet, and typically contains a shape-preferred orientation parallel to the gneissic layering (S_1). Plagioclase grains are unzoned (X_{An} = 0.29) except for a sharp increase in X_{An} (to 0.36) along the outerrim not adjacent to garnet. Garnet is also unzoned (0.45 X_{Alm}, 0.50 X_{Pyr}, and 0.03 X_{Grs}). X_{Grs} increases to 0.05 along the rim of garnet crystals, and along fracture margins is an increase in the (Figure 10). This compositional trend is in contrast to garnet within the leucosome, suggesting syn or post garnet fracturing diffusional exchange.

Biotite in both the leaucosome and garnetite occurs primarily adjacent to garnet. Within the leaucosome, biotite commonly defines the S_2 fabric, and is symmetrically developed about garnet porphyroclasts as rims. Within the garnetite, biotite forms mats along garnet margins with c-axes oriented parallel to the S_2 orientation (basal cleavage perpendicular to S_2), and is exclusively developed on the extensional quadrants of garnet crystals with respect to S_2. However, given the restricted textural setting of biotite, and the lack of evidence for it during S_1, we interpret biotite growth to reflect a syn-S_2 reaction, which produced biotite at the expense of garnet, and diffusion out of the plagioclase porphyroblasts. Biotite is TiO_2 rich, ranging from 4.0-6.0 weight %, suggesting growth at relatively high temperature.

Isochemical modeling results

Bulk compositions were attained for three compositional domains. 10W-094g-a is the garnetite domain, b is the leaucosome, and c is a homogenized sample including both domain types. 10W-094g-a was not modeled to evaluate D_2 conditions due to its abundant inherited garnet produced during M_1, which likely acted as a reservoir for Fe, Mg, and Ca, which were not capable of participating in requilibration of the rock. In short, the abundance of early – garnet that likely removed substantial Ca, Mg, Fe, and Al from reequilibration, in different proportions due to vulnerability for thermal exchange.

The calculated phase diagram for the bulk rock 10W-094g_c is characterized by broad divariant fields with varying amounts of biotite, orthopyroxene, garnet, and melt (Figure 12a). However, there is no evidence for early (S_1) orthopyroxene or biotite (as inclusions or pseudomorphs), and abundant evidence for the production of abundant modal garnet within the sample (20 vol %) within the rock itself. Quartz, plagioclase, and kspar are stable throughout the modeled P-T space. Figure 12a highlights one region on the pseudosection, with an assemblage of garnet+plagioclase+quartz+kspar+melt and no orthopyroxene or biotite. This small field becomes larger with with increasing pressure. If this field represents the migmatitic assemblage, then it formed at a minimum of 1.33 GPa, and approximately 850°C. Forward modeling of garnet mode (vol%) was also performed to predict garnet mode in the P-T range of interest. Garnet is abundant throughout the majority of the pseudosection, but reaches 20 modal % within the P-T region listed above. The steep isopleths of increasing garnet, increasing melt, and decreasing biotite modes are the result of biotite dehydration melting. These results corroborate the initial work of Mahan et al. (2008), who suggested an early high P tectonometamorphic event of nearly identical metamorphic conditions, 1.35 GPa and 850°C. Using the same bulk composition, we modeled the X_{Or} in plagioclase feldspar within a limited P-T region. Results yielded isopleths that are nearly pressure independent. The plagioclase porphyroblasts display zoning indicative of cooling from higher X_{Or} contents in their core to negligible values in their

rim. We interpret the decreasing X_{Or} contents in plagioclase porphyroblasts to represent diffusion during cooling after the peak metamorphic conditions along a similar P-T-t trajectory proposed by Mahan et al. (2008).

The calculated phase diagram for the leaucosome composition has a similar topology (Figure 12b). However, slightly less H_2O was input into this model due to large degrees of dehydration melting thought to have occurred during migmatization. The model, in turn, produced a heightened solidus (ca. 825°C) compared to the homogenous sample. Garnet modes (vol%) are significantly smaller than for the bulk rock composition. Regions of orthopyroxene and biotite stability are mutually exclusive (do not occur together) aside from a narrow P-T range at lower Pressure (ca.1.0 GPa, and 800°C). No orthopryoxene was observed within the rock, but there is minor biotite within both the leaucosome and garnetite, suggesting that the stability was outside the orthopyroxene field, and within the biotite field. Also, because no additional leaucosome seems to be associated with the development of S_2, the P-T conditions of the rock did not likely exceed the solidus. A broad region on the pseudosection matches the observed assemblage below 810°C and above 0.95 GPa. Due to the correspondence of X_{Gr} zoning with $FeMg_{-1}$ exchange on the margin of garnet crystals and how this signal is occasionally present along fractures, X_{Gr} isopleths were modelled throughout the entire P-T region to further constrain D_2 metamorphic conditions. The diffusional signal along garnet rims with respect to their X_{Alm} and X_{Pyr}, which corresponds to an increase X_{Gr} suggests minor amounts of garnet growth during plagioclase recrystalliztion, followed by or synchronous with diffusional reequilibration owing to the lack of other Ca-bearing phases. This additional constraint significantly reduced the P-T range of interest within the forward models. Figure 36 outlines the region of interest for D_2 metamorphic conditions, just under 1.2 GPa, and just below 800°C. These results are compatible and consistent with thermobarometric data presented from a Chipman dike less than 20 meters away from the sample discussed here (1.17 GPa and 825°C; Regan et al., 2014).

Pressure-Temperature analysis of 12R-054

The Beed granite forms a 50 meter thick concordant lozenge within the eastern part of the 2.6 Ga (Table 1; geochron below) plutonic complex in the eastern northwestern subdomain. It is megacrystic with K-feldspar crystals greater than 10 cms in length in a matrix of plagioclase, quartz, biotite, with very minor muscovite and hornblende and rare garnet, largely replaced by biotite (<1% modal). The sample was taken from the hinge region of a large amplitude F_2 fold. The specimen contains no S_2 fabric, but a very strong S_1 fabric. The sample was chosen to constrain P-T conditions of D_1 within the structurally lower portion of the Northwestern subdomain.

Mineral zoning and compositions

Plagioclase occurs in two size populations: relatively coarse porphyroclasts and fine grained, anhedral matrix population. Porphyroclasts are variably zoned compositionally, most with only very slight changes from core to rim from core (X_{An} = 0.33) to rims (X_{An} = 0.28). Rare plagioclase porphyroclasts display high X_{An} cores (0.46), with euhedral compositional zoning outlined in WDS maps, interpreted to be magmatic (Fig.16). However, within the dynamically recrystallized tails adjacent to the high X_{An} plagioclase, the composition of the grains abruptly changes to the more typical matrix value of 0.28. Biotite has variable TiO_2 content, with a maximum of just under 3.0 weight %.

Isochemical modeling results

The calculated phase diagram is characterized by broad regions in P-T space. Garnet mode (vol %) and plagioclase composition were both modeled in hopes to reduce range of P-T conditions indicated. Given the lack of garnet (only one grain was observed in thin section, but additional garnet was seen at outcrop), modal garnet is interpreted to be between 0 and 1 mode (vol %). 5 modal % is expected at approximately 1.2 GPa. Plagioclase compositions from dynamically recrystallized rims have a composition of X_{An} 0.28. These two constraints constrain the Pressure to > 1.0 GPa, but Temperature remains largely unconstrained (< 750°C). Applying

an average of the temperatures calculated from other studies in the Northwestern subdomain (Williams et al., 2000; Dumond et al., 2010; Regan et al., 2014; Williams et al., 2014) suggests peak metamorphic conditions to be near 1.1 GPa and 725°C. These results are consistent with the TiO_2 concentrations in biotite. Furthermore, these data suggest a pressure increase from previously studied rocks from the southwest to the northeast, approximately 0.2 GPa presented here. These are consistent with the structural data suggesting increasing structural height to the southwest.

In-situ monazite U-Th-total Pb geochronology

Three geochronology samples were chosen to constrain the timing of igneous (arc magmatism) event and to further constrain the timing of peak phases of deformation/anatexis. Samples containing monazite were modelled above in an attempt to better link metamorphic conditions to the regionally developed structure, particularly the development of S_1.

Sample S823b

Sample S823b is located at East Hawkes Lake. It is a very low strain and equigranular sample of the Mary Granite, with little to no penetrative tectonic fabric, and an assemblage of plagioclase, K-feldspar, quartz, minor orthopryoxene and accessory zircon, monazite, ilmenite, and apatite. Four monazite grains were mapped, and three grains analyzed. The grains are generally unzoned with minimal compositional variation, with a very outerrim of m1 having slightly lower Y_2O_3, (0.77 weight percent) compared to the remainder of the grains containing greater than 0.83 weight percent (a range of 0.83 to 0.95).

Six sets of analyses were performed on the monazite crystals. Five core and outercore analyses yielded an age of 2612 Ma interpreted to reflect the crystallization age. One analysis of the outerrim yielded an age of 2574 Ma, interpreted to represent metamorphic monazite growth.

Sample 10W-094g

Sample 10W-094g is from the southwestern shore of Cora Lake, along the southern flank of the Cora Lake shear zone (preliminary results presented in Regan et al., 2014). The sample is a garnet-rich migmatite adjacent to a mafic granulite boudin and a cross cutting Chipman dike (*for petrologic description, see above*). The outcrop contains well preserved S_1 folded by upright F_2 folds and contains an axial planar mineral alignment (S_2) oblique to migmatitic layering (S_1). The sample was cut to provide a fold profile view. It is characterized by layers of garnetite interlayered with pods and layers of granitoid leaucosome. Thirty monazite domains were analyzed and dated from both the garnetite and leaucosome, which will be described separately. A total of 20 monazite grains were mapped.

The garnetite contains several complexly zoned grains. They typically have high Y_2O_3 and low ThO_2 cores, interpreted to have grown before anatexis, surrounded by a higher ThO_2 and lower Y_2O_3 rims, interpreted to have grown during melting. The leucosome contains monazite with three domains and several grains that have rims aligned parallel to S_2 (Regan et al., 2014). Commonly, monazite cores in the leucosome are high Y_2O_3, and low ThO_2, interpreted to have grown during prograde metamorphism. There are typically high ThO_2 innerrims, that have low Y_2O_3 contents and vary in morphology interpreted as syn-melt (see Dumond et al., 2015). Surrounding these domains are outer rims that are both low Y_2O_3 and ThO_2, which are consistently developed along S_2 fabric (syn-S_2), suggesting an elongation direction parallel to both the thin section and regional, S_2 discussed in Regan et al. (2014).

Twenty-eight sets of analyses from the garnetite yield three distinguishable populations. Cores yield a poorly constrained age of 3138 +/- 40 Ma. Two other sets of core analyses that are similar in composition, with slightly higher ThO_2 yielded ages of 2962 +/- 9 Ma and 2996 +/- 57 Ma. On average, rim analyses are higher ThO_2 and lower Y_2O_3, and yielded a wide spread of ages from 2580 Ma to 2525 Ma, and are interpreted to have grown during partial melting and

tectonism. The leaucosome contains a bimodal age distribution. Both cores and inner rims yield indistguidable ages of ca. 2565 Ma. Rims yield a weighted average of 1900 +/- 3 Ma based on eight sets of analyses (Regan et al., 2014).

These data suggest that migmatization occurred during the Neoarchean. The drastic increase in ThO_2 and drop in Y_2O_3 is interpreted to reflect garnet growth during biotite dehydration melting similar to migmatites analyzed by Dumond et al. (2015) in the neighboring Upper Deck subdomain. This interpretation is also consistent with the lack of S_2 within the garnetite, and the corresponding lack of Paleoproterozoic ages. Analyses from the leaucosome confirm that S_2 developed at 1.9 Ga, as previously constrained in the Northwestern subdomain (Dumond et al., 2008, 2010; Regan et al. 2014). The two Mesoarchean populations remain enigmatic. A ca. 3.2 Ga age coincides with some of the igneous grains from the Chipman tonalite (Hanmer et al., 1994; Martel et al., 2008). However, the 2.9 Ga ages do not correspond to any known igneous intrusive suite, or recognized widespread-metamorphic event within the immediate vicinity (Mahan et al., 2006a). Therefore, we attribute these ages to either the initial juxtaposition of these rocks adjacent to Mesoarchean tonalite, related to the intrusion of mafic granulite bodies that remain unconstrained in age but have ca. 2.8-3.1 Ga depleted mantle model ages (Flowers et al., 2008), or are detrital in origin.

Sample 12R-054

Sample 12R-054 is a sample of Beed granite (*also used for isochemical modeling above*), which is a megacrystic biotite granite with coarse K-feldspar and plagioclase porphyroclasts, but contains little to no garnet (1 pseudomorphed garnet) 24 monazite grains were mapped. 10 sets of analyses were attained on all monazite domains, three of which were presented in a separate contribution (Regan et al., 2014).

Four distinctive morphological populations are apparent: 1) Innercores (low ThO_2, high Y_2O_3) are surrounded by 2) outercores that are low Y_2O_3, 3) high ThO2 outercores, and 4)

innterrims containing moderate Y_2O_3 and high ThO_2. Cores yielded a single population of 2608 +/- 8.4 (MSWD: 2.5). Outercores and innerrims yielded a separate, and slightly younger date, which yielded an average of 2577+/- 22 Ma (MSWD: 6.8), and likely represent more than one statistical population. These results are interpreted to represent the igneous crystallization and subsequent lateral flow of the Beed granite associated with a small amount of garnet growth. Lastly, a population of 1917 Ma is represented as very fine (< 5μm) rims that are interpreted and discussed in detail in Regan et al. (2014).

Discussion

A Neoarchean arc plutonic complex

The Athabasca granulite terrane is underlain by Meso to Neoarchean plutonic rocks (Hanmer, 1994). The Neoarchean granitoids that dominate the entire northwestern subdomain, and varying amounts of adjacent Chipman and Upper deck subdomains, are broadly coeval (ca. 2.63 – 2.60 Ga)(Hanmer, 1997), and contain Nd isotopic systematics compatible with being derived from a similar, metasomatized lithospheric source (Hanmer et al., 1994). The suite of rocks has a wide range of SiO_2 contents (> 15 wt %) and modal mineralogy, and grade from more mafic rocks in the northeast, to relatively more felsic endmembers in the southwest. Composite compositional/S_1 layering was tilted to the SW prior to or during to F_2 folding as suggested by Pressure gradients preserved on S_1 (Dumond et al., 2010; Regan et al., 2014), and thus, grades from mafic to more felsic lithologies with increasing structural height.

Circa 2.6 Ga plutonic rocks within the AGT show marked similarity to modern arc plutons. They span a wide compositional range, form shallow calc-alkaline trends with respect to the modified alkali lime index (Frost and Frost, 2008) and plot in the volcanic arc granite field on tectonic discrimination diagrams (Pearce et al., 1984). Trace element signatures display systematic enrichments in LILE and Pb, and corresponding depletions of HFSE when normalized to primitive mantle (Sun and Mcdonough, 1989), which is characteristic of high T metasomatism similar to that thought to occur in the overriding mantle wedge (Sun and Mcdonough, 1989;

Chiarenzelli et al., 2010). These attributes are also seen in similar aged rocks in adjacent subdomains (Kopf, 1995; Koteas et al., 2010). Given the range in composition and the ubiquitous major and trace element chemistry indicative of arc processes, we interpret that the ca. 2.6 Ga plutonic rocks to have formed above an active subduction zone, and that rocks represent a large, intact arc plutonic complex.

Structural measurements combined with new and published thermobaromtric calculations provide insight into the original geometry of the composite batholith. S_1 is defined by both a strong planar fabric, and compositional layering. Only rare fold closures have been observed, but do not involve large recumbent folding. Furthermore, there is no increase in strain across discrete compositional changes, or layers, suggesting that compositional heterogeneity was, at least in part, close in orientation to S_1 (Dumond et al, 2010; Regan et al., 2014). Layering currently dips shallowly to the southwest, parallel to the F2 hinges, modified by a variably developed axial planar fabric (S_2; Dumond et al., 2010; Regan et al., 2014). Thermobarometry from the southwestern edge (more felsic) of the Northwestern subdomain yield estimates of 0.9 GPa and 750° C (Dumond et al., 2010). Calculations from the central Northwestern subdomain are nearly identical (East Hawkes Lake; Williams et al., 2000; Regan et al., 2014). No quantitative thermobarometry exists for rocks in the northeastern (lower) portion of the subdomain, mainly due to the altered and retrogressed assemblage. However, forward petrologic modelling presented above suggests that the Beed granite was deformed at higher pressures than those observed to the west. These data indicate that compositional layering was tilted after the formation of a strong S_1, which suggests that the Northwestern subdomain is a tilted section (~12 ° plunge) of an Archean arc batholith.

Timing of events: implications for fingerprinting tectonic processes

The eastern Rae domain within the study region displays a three step evolution involving: 1) arc plutonism, 2) high grade metamorphism, and 3) crustal flow (Dumond et al., 2010; 2015).

Arc construction took place from ca. 2.63 – 2.60 Ga (Hanmer, 1997), and may extend to the Northeast along the Rae margin. Below we discuss the timing and conditions of deformation within both the Northwestern and Chipman subdomains.

Timing and conditions of deformation within the Northwestern subdomain

Paired forward petrologic modelling and in-situ geochronology of the Beed granite were undertaken to augment existing data from the southwestern portion of the Northwestern subdomain. Monazite geochronology from the Beed granite suggests that it crystallized (ca. 2.61 Ga) and was deformed at approximately the same time as the rest of the plutonic rocks of the Northwestern subdomain (ca. 2.57 Ga)(Dumond et al., 2010). Circa 2.57 Ga corresponds to the development of a penetrative fabric, with top to the east kinematics, but forward modelling suggests that it formed at slightly higher pressures (ca. 1 GPa) than the felsic plutonic rocks to the southwest (Williams et al., 2000, 2014; Dumond et al., 2010)..

Dumond et al. (2010) showed that rocks exposed along the western margin of the Northwestern subdomain contained kinematic evidence for subhorizontal top to the east flow. This was interpreted to represent gravity-driven flow, as an analogue for crustal flow in modern orogens (Beaumont et al., 2006). Kinematics are identical within the Beed Lake region (top to the east) within the northeastern segment of the Northwestern subdomain. Our new geochronologic results suggest that the development of S_1 was synchronous throughout the Northwestern subdomain. We suggest that the whole Northwestern subdomain may represent a very thick zone of crustal detachment and flow that developed shortly after the plutonic rocks were emplaced. Based on a geobaric gradient of 1 GPa equal to 37 km, based on a ca. 0.2 GPa difference observed within the Northwestern subdomain, the suggested vertical thickness may have been on the order of ca. 7.5 km. The kinematics are consistently top to the ESE throughout the exposure suggesting that subhorizontal flow was focused within a zone of greater than 7 km thickness, with consistent kinematics.

Timing and conditions of deformation within the Chipman subdomain

Migmatites are common within the ca. 3.2 Ga Chipman batholith (Mahan et al., 2008), particularly in the western segment where they are typically associated with mafic granulite (Mahan et al., 2008; Flowers et al., 2008). Evidence for polymetamorphic mineral growth associated with deformation is well preserved within this suite of rocks (Mahan et al., 2008; Flowers et al., 2008). Mahan et al. (2008) determined that early, subhorizontal gneissic layering corresponds with the development of a clinopyroxene + plagioclase assemblage (M_1) that likely formed at ca. 1.35 GPa and temperatures in excess of 850 ° C. This event was followed by a med-P event that involved the partitioned development of folds and an axial planar fabric ($M_{3a,b}$ of Mahan et al., 2008). Single grain TIMS and SHRIMP geochronology on the same suite (Flowers et al., 2008) yielded ca. 2.56 Ga metamorphic zircon that formed a discordant array with a lower intercept at ca. 1.9 Ga. These ages were interpreted to correspond to the two phases of deformation, respectively.

Sample 10W-094G, presented here, contains two primary compositional components that define the migmatitic layering. Partial melting, and the growth of abundant garnet, occurred at P-T conditions greater than 1.3 GPa and temperatures exceeding 835 °C. Monazite composition shows a drastic decrease in Y_2O_3 and increase in ThO_2 between 2.59 and 2.57 Ga. These are interpreted to have grown during partial melting and development of the S_1 migmatitic layering. Although, folding was previously interpreted as being Archean (Mahan et al., 2008), new monazite evidence presented in Regan et al. (2014) suggest that upright folding took place at ca. 1.9 Ga. The whole subdomain underwent metamorphism at pressures of ca. 1.15 GPa at 1.9 Ga, approximately 0.2 GPa difference between the two phases of tectonism. We interpret that decompression of the Chipman subdomain relative to the neighboring Northwestern subdomain to have occurred between D_1 and D_2, as suggested by the P-T path presented in Mahan et al. (2008).

Crustal Flow

Neoarchean deformation in the Athabasca granulite terrane was widespread, and involved extensive partial melting. Furthermore, monazite geochronology suggests that anataexis and penetrative deformation postdated the igneous crystallization of the Neoarchean plutonic complex (ca. 2.59 – 2.54 Ga). Therefore, subsequent to voluminous plutonism, the region underwent increasing pressures and temperatures, which resulted in subhorizontal flow (Dumond et al., 2010). Neoarchean sedimens are exposed within the region, and thus suggests that some components of the region were at the surface prior to D_1 (Dumond et al., 2015; Regan, unpublished data). Flow occurred throughout the 2.6 Ga plutonic rocks at conditions ranging from 0.9 GPa to 1.05 GPa and 700 to 775°C, based on new and existing P-T data. Interpreted by Dumond et al. (2010) to have accommodated lateral flow due to pressure gradients similar to the Himalaya, the possibility exists that lateral flow was accommodating further crustal thickening of the Rae towards the Hearne subprovince.

Accretionary Model

The eastern Rae domain preserves evidence of a three step evolution. First, voluminous arc magmas were emplaced into Meso to Neoarchean basement. This was followed by a phase of deformation and high grade metamorphism at lower crustal depths showing evidence of increasing pressure through time (Dumond et al., 2015), interpreted to reflect thrusting and shortnening of the arc (Baldwin et al., 2004; Mahan et al., 2008; Dumond et al., 2010; Regan et al., 2014; Williams et al., 2014; *new data*). Granulite facies metamorphism likely postdated magmatism. Lastly, the juvenile lithologies of the Neoarchean arc plutonic complex accommodated subhorizontal lateral flow throughout the entire Northwestern subdomain, interpreted to have formed via gravitational processes similar to the Himalaya (Dumond et al., 2010).

The sequence of events recorded by rocks in the eastern Rae domain is most aptly categorized as having formed within an environment similar to a modern active margin. Arc

construction was followed by crustal thickening, high grade metamorphism, crustal flow, and anatexis. The cessation of arc magmatism is interpreted as representing the onset of collisional orogenisis. Abundant migmatite formed during the Neoarchean (10W-094g; Baldwin et al., 2004; Mahan et al., 2006a; Dumond et al., 2010, 2015; Regan et al., 2014). The migmatites found throughout the region formed during collision, and thus may represent the source of such aluminous and alkalic magmas indicative of lower crustal generation (Frost et al., 2001; Peck et al., 2013). The region provides a tangible exposure of the transition of mantle-driven arc magmatism to a lower crust derived, syn-collisional type magmatism (Pearce et al., 1984).

Regional correlations and arc geometry

Arc rocks typically define linear arrays of plutonic or volcanic rocks and structures that delineate the general trend of a subduction zone. Identifying these trends in the Archean may be difficult due to probable modification during subsequent Proterozoic and/or Phanerozoic tectonism (Hoffman, 1988). The western Churchill Province is underlain by several Neoarchean plutonic complexes, but there are significant regions containing little to no geochronology or field data to interpret, making these correlations difficult and preliminary. Circa 2.6 Ga granitoids exist in the Snowbird Lake region to the Northeast along the geophysical lineament of the STZ (Martel et al., 2008), but there is no available whole-rock geochemical data to assess whether they too contain an arc signature. There are several ca. 2.60 Ga plutonic rocks to the northwest, but no available geocmemical data is available to constrain tectonic heritage (Bethune et al., 2013) Circa 2.5 – 2.3 Ga plutonic rocks dominate in the Zemlack and Beaverlodge subdomains (Hartlaub et al., 2003; Bethune et al., 2013; Ashton et al., 2013), where the southeast (Hearne domain), contains both Archean and Proterozoic supracrustal rocks, with little intrusive events at ca. 2.6 Ga (Aspler et al., 2002a; eastern SK). Unpublished data from zone 7 of the Angikuni Lake region (Aspler et al., 1999) contain many of the geochemical trends indicative of an arc setting, and are chemically similar to those discussed above. We tentatively suggest that a belt of arc-related plutonic rocks may continue along the eastern margin of the Rae domain to the

Northeast, perhaps as far as Angikuni Lake, and that this plutonism was followed by a collisional event.

The Macquoid orogeny has been recognized throughout the northern Rae and Chesterfield blocks of the western Churchill Province (Berman et al., 2007; Pehrsson et al., 2013). It is thought to represent the collision between Rae and Chesterfield (formerly NW Hearne domain; Berman et al., 2007) following a protracted phase of crustal-scale deformation and magmatism from ca. 2.55-2.50 Ga (Davis et al., 2006). The Athabasca granulite terrane is ca. 475 km to the southwest of the Chesterfield block, but contains evidence of a similar age and scale event within the eastern Rae domain, that is preceeded by arc magmatism. However, the Macquoid Orogeny, as defined, extends from ca. 2.55 – 2.50 Ga, in contrast to the eastern Rae domain further to the south where penetrative deformation appears to have occurred just prior. Whether these two events represent a single progressive mountain building event, or two distinct and isolated events, remains unknown.

Finding a suture

The STZ has recently been interpreted to correspond with a major Paleoproterozoic suture (ca. 1.90 Ga; Berman et al., 2007), between the Rae and Hearne domains (Martel et al., 2010; Pehrsson et al, 2012). As has been described in many contributions, the eastern Rae domain and STZ corresponds to a large region of Paleoproterozoic nested shear zones (Mahan and Williams, 2005; Dumond et al., 2014; Regan et al., 2014). Many of these shear zones contain thick zones of mylonite, and accommodated major differential motion between major lithotectonic subdomains (Mahan and Williams, 2005; Flowers et al., 2006a; Regan et al., 2014). However, none appear to correspond with a significant change in rock type, geochemistry, or geologic history. Ca. 2.6 Ga plutonism occurs both sides of each shear zone (Hanmer, 1994). 2.6 Ga granitoids have been recognized east of the Legs Lake shear zone, suggesting that if a suture

is exposed on the ground, it is existed prior to 2.60 Ga (Regan, unpublished data). If a younger suture is present, it is east of Charlebois Lake in the western Hearne domain (northern SK).

Taken together, all these observations collectively suggest that the Rae and Hearne, or something outboard of the Hearne, collided during the Neoarchean, during a phase of collisional orogensis at ca. 2.60 Ga – 2.55 Ga. Furthermore, the change from infant arc processes in the central Hearne at ca. 2.7 Ga, to a fully developed continental arc by ca. 2.65 Ga along the eastern Rae is consistent with a western Pacific modern analogue originally proposed by Cousens et al. (2004) and Davis et al. (2004). The growth of many volcanic edifices (Aspler and Chiarenzelli, 1996) as a result of foundering oceanic lithosphere (Cousens et al., 2004), progressed to more evolved subduction beneath the more evolved Rae domain by 2.63 Ga (Hanmer, 1997). This model would collectively account for the differences between the Northwestern and central Hearne domains as well as the temporal variations in magmatism and tectonism.

Recognition of Arc Processes in a tectonic cycle

Many workers primarily rely on geochemistry to constrain the tectonic context and place regions into a tectonic framework. Three major tectonic stages are inherent to the eastern margin of the Rae domain including: 1) arc magmatism, 2) deformation-metamorphism associated with crustal thickening (Dumond et al., 2015), and 3) flow of the lower crust (Dumond et al., 2010). First, ca. 2.63 – 2.60 Ga magmatism contains the petrology and geochemical signature for being arc related. Second, subsequent to intrusion of the voluminous plutonic rocks of the northwestern subdomain, the entire region underwent crustal thickening and high grade metamorphism/migmatization after arc magmatism had ceased. Lastly, lateral flow of the lower continental crust during granulite grade metamorphism with kinematics consistent large region encompassing both a large area and structural depth (throughout the Northwestern subdomain, > 0.1 GPa difference) suggesting top to the east flow (Dumond et al., 2010; Regan et al., 2014).

We suggest that these data are consistent with an active margin setting, and rocks of the eastern Rae domain preserve the attributes of an arc-collision history.

The three processes discussed above, in the respective order described, greatly strengthens the case for continental accretions by horizontal plate tectonics. The Neoarchean history of the eastern Athabasca granulite terrane contains a series of events that are entirely consistent with modern-style plate-tectonics. We have demonstrated arc magmatism, crustal thickening, and extensive migmatization of the lower continental crust during a period of 100 my. Identifying and interpreting active margin processes should involve the identification of not one, but all of these three processes in the respective order presented above.

References

Allaz, J., Selleck, B., Williams, M.L., and Jercinovic, M.J., 2013, Microprobe analysis and dating of monazite from the Potsdam Formation, New York: A progressive record of chemical reaction and fluid interaction: American Mineralogist, ed(s) Gregory Dumond and Callum Hetherington: versatile monazite: Resolving geological ecords and solving challenges in materials science, v. 98, p. 1106 – 1119.

Ashton, K.E., Hartlaub, R.P., Heaman, L.M., Morelli, R.M., Card, C.D., Bethune, K., and Hunter, R.C., 2009, Post-Taltson sedimentary and intrusive history of the southern Rae Province along the northern margin of the Athabasca Basin, Western Canadian Shield: Precambrian Research, v. 175, p. 16-34.

Ashton, K.E., Hartlaub, R.P., Bethune, K.M., Heaman, L.M., and Niebergail, G., 2013, New depositional age constraints for the Murmac Bay group of the southern Rae Province, Canada: Precambrian Research, v. 232, p. 70-88.

Aspler, L.B., and Chiarenzelli, J.R., 2002, Mixed siliciclastic-carbonate ramp sedimentation in a rejuvenated Paleoproterozoic intracratonic basin: upper Hurwitz Group, Nunavut, Canada: In: Altermann, W., Corcoran, P., (Eds.), Precambrian Sedimentary Environments: a Modern Approach to Ancient Depositional Systems, International Association of Sedimentology Special Publication, v. 33, p. 293-321.

Aspler, L.B., Chiarenzelli, J.R., and McNicoll, V.J., 2002a, Paleoproterozoic basement-cover infolding and thick-skinned thrusting in Hearne domain, Nunavut, Canada: intracratonic response to Trans-Hudson orogen: Precambrian Research, v. 116, p. 331-354

Aspler, L.B., Cousens, B.L., and Chiarenzelli, J.R., 2002b, Long-distance intracratonic transport of mafic magmas during opening of the Manikewan ocean (Trans-Hudson orogen): Griffin gabbro sills (2.11 Ga), Hurwitz Basin, Nunavut, Canada: Precambrian Research, v. 117, p. 269-294.

Aspler, L.B., and Chiarenzelli, J.R., 1996, Stratigraphy, sedimentology and physical volcanology of the Henik Group, central Ennadai-Rankin greenstone belt, Northwest Territories, Canada: late Archean paleogeography of the Hearne Province and tectonic implications: Precambrian Research, v. 77, p. 59-89.

Aspler, L.B., anc Chiarenzelli, J.R., 1998, Two Neoarchean supercontinents? Evidence from the Paleoproterozoic: Sedimentary Geology, v. 120, p. 75-104.

Aspler, LB., Chiarenzelli, J.R., Cousens, B.L., McNicoll, V.J., and Davis, W.J., 2001, Paleoproterozoic intracratonic basin processes, from breakup of Kenorland to assembly of Laurentia: Hurwitz Basin, Nunavut, Canada: Sedimentary Geology, v. 141-142, p. 287-318.

Aspler, L.B., Chiarenzelli, J.R., Cousens, B.L., and Valentino, D., 1999, Precambrian geology, northern Angikuni Lake, and a transect across the Snowbird tectonic zone, western Angikuni Lake, Northwest Territories (Nunavut): Geological Survey of Canada open file report, p. 107-118.

Baldwin, J.A., Bowring, S.A., Williams, M.L., and Williams, I.S., 2004, Eclogites of the Snowbird tectonic zone: Petrologic and U-Pb geochronological evidence for Paleoproterozoic

high-pressure metamorphism in the western Canadian Shield: Contributions to Mineralogy and Petrology, v. 147, n. 5, p. 528-548, doi: 10.10007/s00410-004-0572-4.

Berman, R.G., Davis, W.J., Aspler, L.B., and Chiarenzelli, J.R., 2002, SHRIMP U-Pb ages of multiple metamorphic events in the Angikuni Lake area, western Churchill Province, Nunavut: Radiogenic Age and Isotopic Studies: Report 15; Geological Survey of Canada current research, 2002-F3, p. 1-9.

Berman, R.G., Davis, W.J., and Pehrsson, S., 2007, Collisional Snowbird tectonic zone resurrected: Growth of Laurentia during the 1.9 Ga accretionary phase of the Hudsonian orogeny: Geology, v. 35, n. 10, p. 911-914, doi:10.1130/G23771A.1.

Berman, R.G., Pehrosson, S.L., Davis, W.L., Ryan, J.J., Qui, H., Ashton, K., 2013, The Arrowsmith orogeny: geochronological and termobarometric constraints on its extent and tectonic setting in the Rae craton, with implications for pre-Nuna supercontinent reconstruction: Precambrian Research, v. 232, p. 44-68.

Bethune, K.M., Berman, R.G., Rayner, N., and Ashton, K.E., 2013, Structural, petrological and U-Pb SHRIMP geochronological study of the western Beaverlodge domain: Implications for crustal architecture, multi-stage orogenesis and the extent of the Taltson orogen in the SW Rae craton, Canadian Shield: Precambrian Research, v. 232, p. 89-118.

Bickford, M.E., Collerson, K.D., and Lewry, J.F., 1994, Crustal history of the rae and Hearne provinces, southwestern Canadian Shield, Saskatchewan: constraints from geochronologic and isotopic data: Precambrian Research, v. 68, p. 1-21.

Bowring, S.A., Williams, I.S., and Compston, W., 1989, 3.96 Ga gneisses from the Slave province, Northwest Territories, Canada: Geology v. 17, p. 871-975.

Brown, L.L., Webber, J., Williams, M.L., Regan, S., Seaman, S., *in review*, Magnetism of the Lower Crust: observations from the Chipman Domain, Athabasca Granulite Terrain, northern Canada: Tectonophysics

Bryant, J.A., Yogodzinski, G.M., Hall, M.L., Lewicki, J.L., and Bailey, D.G., 2006, Geochemical constraints on the origin of volcanic rocks from the Andean northern volcanic zone, Ecuador: Journal of Petrology, V. 47, N. 6, p. 1147-1175, doi: 10.1093/petrology/eg1006

Card, C.D., 2002, New investigations of basement to the western Athabasca basin: Saskatchewan Geological Survey Summary of Investigations 2002, v. 2, p. 1-17.

Card, C.D., Bethune, K.M., Davis, W.J., Rayner, N., and Ashton, K.E., 2014, The case for a distinct Taltson orogeny: Evidence form Northwest Saskatchewan, Canada: Precambrian Research, v. 255, p. 245 – 265.

Chiarenzelli, J.R., Lupulescu, M., Cousens, B., Thern, E., Coffin, L., and Regan, S., 2010, Enriched Grenbillian lithospheric mantle as a consequence of long-lived subduction beneath Laurentia: Geology, v. 38, p. 151-154

Corrigan, D., Hajnal, Z., Nemeth, B., and Lucas, S.B., 2005, Tectonic framework of a Paleoproterozoic arc-continent to continent-continent collisional zone, Trans-Hudson Orogen, from geological and seismic reflection studies: Canadian Journal of Earth Sciences, v. 42, p. 421-434, doi: 10.1139/05-025.

Corrigan, D., Pehrsson, S., Wodicka, and de Kemp, E., 2009, The Paleoproterozoic Trans-Hudson Orogen: a prototype of modern accretionary processes: in Ancient Orogens and Modern Analogues, Ed(s)
Murphy et al., Geological Society of London, Special Publications, v. 327, p. 457-479, doi:10.1144/SP327.19.

Corrigan, D., Scott, D.J., and St-Onge, M.R., 2001, Geology of the northern margin of the Trans-Hudson Orogen (Foxe-Fold Belt), central Baffin Island, Nunavut: Geological Survey of Canada Current research 2001-C23, p.1-11.

Corrigan, D., Nadeau, L., Brouillette, P., Wodika, N., Houle, M.G. Tremblay, T., Machado, G., and Keating, P., 2013, Overview of GEM Multiple Metals-Melville Peninsula project, central Melville Peninsula, Nunavut: Geological Survey of Canada, Current Research, 2013-19, p. 1 – 17.

Cousens, B.L., Aspler, L.B., Chiarenzelli, J.R., Donaldson, J.A., Sandeman, H., Peterson, R.D., LeCheminant, A.N., 2001, Enriched Archean lithospheric mantle beneath western Churchill Province tapped during Paleoproterozoic orogenesis: Geology, v. 29, n. 9, p. 827-830.

Cousens, B.L., Aspler, L.B., and Chiarenzelli, J.R., 2004, Dual sources of ensimatic magmas, Hearne domain, western Churchill Province, Nunavut, Canada: Neoarchean “infant arc” processes?: Precambrian Research, v. 134, p. 169-188.

Cutts, K.A., Stevens, G., Hoffmann, E., Buick, I.S., Frei, D., and Munker, C., 2014, Paleo- to Mesoarchean polymetamorphism in the Barberton Granite-Greenstone Belt, South Africa:

Constraints from U-Pb monazite and Lu-Hf garnet geochronology on the tectonic processes that shaped the belt: Geological Society of America Bulletin, v. 126, n. ¾, p. 251-270.

Davis, W.J., Hanmer, S., and Sandeman, H.A., 2004, Temporal evolution of the Neoarchean central Hearne supracrustal belt: rapid generation of juvenile crust in a suprasubduction zone setting: Precambrian Research, v. 134, p. 85-112.

deCapitani, C. and K. Petrakakis, 2010, The computation of equilibrium assemblage diagrams with Theriak/Domino software: American Mineralogist,v. 95, n. 7, p. 1006-1016.

Dumond, G., McLean, N., Williams, M.L., Jercinovic, M.J., and Bowring, S.A., 2008, High resolution dating of granite petrogeneisis and deformation in a lower crustal shear zone: Athabasca granulite terrane, western Canadian Shield: Chemical Geology, v. 16, n. 4, p. 175-196, doi:10.1016/j.chemgeo.2008.04.014.

Dumond, G., Goncalves, P., Williams, M.L., and JHercinovic, M.J., 2010, Subhorizontal fabric in exhumed continental lower crust and implication for lower crustal flow: Athabasca granulite terrane, Western Canadian Shield: Tectonics, v. 29, TC2006, doi:10.1029/2009TC002514.

Dumond, G., Mahan, K.H., Williams, M.L., and Jercinovic, M.J., 2013, Transpressive uplift and exhumation of continental lower crust revealed by synkinematic monazite reactions: Lithosphere, v. 5, n. 5, p. 507-512, doi: 10.1130/L292.1

Dumond, G., Goncalves, P, Williams, M.L., and Jercinovic, M.J., 2013, UHT-HP Metamorphism in an exhumed lower crustal hot zone: GSA abstracts and Programs.

Chamberlain, K.R., Schmitt, A.K., Swapp, S.M., Harrison, M., Swoboda-Colberg, N., Bleeker, W., Peterson, T.D., Jefferson, C.W., and Khuduley, A.K., 2010, In situe U-Pb SIMS (IN-SIMS) micro-baddeleyite dating of mafic rocks: Method with examples: Precambrian Research, v. 183, p. 379-387.

Flowers, R., Bowring, S.A., Mahan, K.H., and Williams, M.L., 2006a, Timescales and significance of high pressure, high-temperature metamorphism and mafic dike anatexis, Snowbird tectonic zone, Canada: Contribution to Mineralogy and Petrology, v. 151, n. 5, p. 558-581, doi:10.1007/s00410-006-0066-7.

Flowers, R.M., Mahan, K.H., Bowring, S.A., Williams, M.L., Pringle, M.S., and Hodges, K.V., 2006b,Multistage exhumation and juxtaposition of lower continental crust in the western Canadian Shield: linking high resolution U-Pb and $^{40}Ar/^{39}Ar$ thermochronometry with pressure-temperature-deformation paths: Tectonics, v. 25, TC4003, doi:10.1029/2005TC001912.

Flowers, R.M., Bowring, S.A., Mahan, K.H., Williams, M.L., and Williams, I.S., 2008, Stabilization and reactivation of cratonic lithosphere from the lower crustal record in the western Canadian shield: Contributions to Mineralogy and Petrology, v. 156, n. 4, p. 529-549, doi:10.1007/s00410-008-0301-5.

Frost, B.R., Barnes, C.O., Collins, W.J., Arculus, R.J., Ellis, D.J., and Frost, C.D., 2001, A geochemical classification for granitic rocks: Journal of Petrology, v. 42, p. 2033 – 2048.

Frost, B.R., and Frost, C.D., 2008a, A geochemical classification for feldspathic igneous rocks: Jounral of petrology, v. 49, n. 11, p. 1955 - 1969

Frost, B.R., and Frost, C.D., 2008b, On charnockites: Gondwana Research, v. 13, p. 30-44.

Gerbi, C., Culshaw, N., and Marsh, J., 2010, Magnitude of weakening during crustal-scale shear zone development: Journal of Structural Geology, v. 32, p. 107-117.

Gilboy, C.F., 1980, Bedrock compilation geology: Stony Rapids area (NTS 74p)-Prelimanary geological map, scale 1:250,000, Sask. Geol. Surv., Sask. Energy and mines, Regina.

Hamilton, W.B., 2011, Plate tectonics began in Neoproterozoic time, and plumes from deep mantle have never operated: Lithos, v. 123, p. 1-20.

Hanmer, S., Bowring, S.A., Van Breeman, O., and Parrish, R.R., 1992, Great Slave Lake shear zone, northwest Canada: mylonitic record of Early Proterozoic convergence, collision, and indentation: Journal of Structural Geology, v. 14, p. 757-773.

Hanmer, S., 1994, Geology, East Athabasca mylonite triange, Saskatchewan, Map 1859A, scale 1:100,000, Geol. Surv. Of Can., Ottawa.

Hanmer, S., 1997, Geology of the Striding-Athabasca mylonite zone, northern Saskatchewan and southeastern District of Mackenzie, Northwest Territories: Pap. Geol. Surv., of Can., Ottawa.

Hanmer, S., Parrish, R., Williams, M., and Kopf, C., 1994, Striding-Athabasca Mylonite: Complex Archean deep crustal deformation in the East Athabasca mylonite triangle, N. Saskatchewan: Canadian Journal of Earth Sciences, v. 31, p. 1287-1300, doi:10.1139/e94-111.

Hanmer, S., Williams, M., and Kopf, C., 1995, Modest movements, spectacular fabrics in an intracontinental deep-crustal strike-slip fault: Striding-Athabasca mylonite zone, NW Canadian Shield: Journal of Structural Geology, v. 17, n. 4, p. 493-507, doi:10.1016/0191-8141(94)00070-G.

Hanmer, S., and Williams, M.L., 2001, Targeted fieldwork in the Daly Bay Complex, Hudson Bay, Nunavut: Geological Survey of Canada Current Research 2001-C15, p. 1-26.

Hanmer, S., Sandeman, H.A., Davis, W.J., Aspler, L.B., Rainbird, R.H., Ryan. J.J., Relt, C., Roest, W.R., Peterson, T.D., 2004, Neoarchean tectonic setting of the Central Hearne supracrustal belt, western Churchill Province, Nunavut, Canada: Precambrian Research, v. 134, p. 63-83.

Herzberg, C., and Rudnick, R., 2012, Formation of cratonic lithosphere: an integrated thermal and petrological model: Lithos, v. 149, p. 4-15.

Hildebrand, R.S., Hoffman, P.F., and Bowring, S.A., 2010, the Calderian orogeny in Wopmay orogen (1.9 Ga), northwestern Canadian Shield: Geological Society of America Bulletin, v. 122, p. 794-814, doi: 10.1130/B26521.1

Hoffman, P.F., 1988, United Plates of America, the birth of a craton: Early Proterozoic assembly and growth of Laurentia: Annual Review of Earth and Planetary Sciences, v. 16, p. 543-603, doi:10.1146/annurev.ca.16.050188.002551.

Holland, T., and Powell, R., 1998, An internally consistent thermodynamic dataset for phases of petrological interest: Journal of Metamorphic Geology, v. 16, p. 309-343.

Holland, M.E., Williams, M.L., and Regan, S.P., 2012, The mary reaction: timing deep crustal deformation and metamorphism with implications for strengthening and stabilization of flowing lower crust: NEGSA 47th abstracts with programs.

Hynes, A., 2014, How feasible was subduction in the Archean?: Canadian Journal of Earth Sciences, v. 51, n. 3, p. 286-296.

Kinny, P.D., and Maas, R.2003, Lu-Hf and Sm-Nd isotope systems in zircon: in Zircon, Hanchar, J.M., and Hoskin, P.W.O. ed(s), Zircon: Reviews of Mineralogy and Geochemistry, v. 53, p. 327-341.

Kopera, J.P., Davis, P., and Williams, M.L., 2003, Peering through the ~1400 Ma overprint: Recent insights into the tectonic evolution of the Tusas Mountains, northern New Mexico: 55th annual Rocky Mountain GSA abstracts with programs.

Koteas, G.C., Williams, M.L., Seaman, S.J., and Dumond, G., 2010, Granite genesis and mafic-felsic magma interaction in the lower crust: Geology, v. 38, p. 1067-1070, doi:10.1130/G31017.1.

Krikorian, L., 2002, Geology of the Wholdaia Lake Segment of the Snowbird Tectonic Zone, Northwest Territories (Nunavut): A view of the deep crust during the assembly and stabilization of the Laurentian craton: MSc Thesis, Advisor: Michael L. Williams, University of Massachusetts, Amherst.

Leslie, S.R., Mahan, K.H., Regan, S., Williams, M.L., and Dumond, G., *in review*, Contrasts in sillimanite deformation in felsic tectonites from anhydrous granulite- and anhydrous amphibolite-facies shear zones, western Canadian Shield: submitted to Journal of Structural Geology.

Leslie, S., 2012, Contrasts in sillimanite deformation in felsic tectonites from anhydrous granulite- and hydrous amphibolite-facies shear zones, western Canadian Shield [M.S.: University of Colorado, 69 p.

Leslie, S., Mahan, K., Regan, S., and Willaims, M. L., 2011a, The role of temperature and fluid content in sillimanite deformation and recrystallization mechanisms in felsic granulites, Athabasca granulite terrane, western Canadian Shield: Annual Meeting of Geological Association of Canada.

Leslie, S., Mahan, K., Regan, S., and Willaims, M. L., 2011b, Heterogeneity within a deep crustal strike-slip shear zone with implications for lower crustal flow, Athabasca granulite terrane, western Canadian Sheild: American Geophysical Union, Fall Meeting 2011, abstract #T23B-2392.

Lewry, J.F., and Sibbald, T.I.I., 1980, Thermotectonic evolution of the Churchill Province in northern Saskatchewan: Tectonophysics, v. 68, p. 45-82.

Macdonald, R., 1980, New edition of the geological map of Saskatchewan, Precambrian Shield area, in Summary of Investigations, Misc. Rep. 01-4.2, p. 19-21, Sask. Geol. Surv., Sask. Ind. And Resour, Regina.

MacHattie, T.G., Geochemistry and geochronology of the late Archean Prince Albert group (PAg), Nunavut, Canada: Ph.D. thesis, University of Alberta, p. 1 - 340

MacLachlan, K., Davis, W., and Relt, C., 2005, U/Pb geochronological constraints on Neoarchean tectonism: Multiple compressional events in the Northwestern Hearne domain, western Churchill Province, Canada: Canadian Journal of Earth Sciences, v. 42, p. 85-109.

MacRae, N.D., Armitage, A.E., Miller, A.R., Roddick, J.C., Jones, A.L., and Mudry, M.P., 1996, The diamondiferous Akluilak lampophyre dyke, Gibson Lake area, NWT: Geological Survey of Canada Open File, v. 3228, p. 101-107.

Mahan, K.H., Williams, M.L., and Baldwin, J.A., 2003, Contractional uplift of deep crustal rocks along the Legs Lake shear zone, western Churchill Province, Canadian Shield: Canadian Journal of Earth Sciences, v. 40, n. 8, p. 1085-1110, doi:10.1139/e03-039.

Mahan, K.H., and Williams, M.L., 2005, Reconstruction of a large deep-crustal terrane: Implication for the Snowbird tectonic zone and early growth of Laurentia: Geology, v. 33, n. 5, p. 385-388, doi:10.1130/G21273.1.

Mahan, K.H., Goncalves, P., Williams, M.L., and Jercinovic, M.J., 2006a, Dating metamorphic reactions and fluid flow: Application to exhumation of high-P granulites in a crustal-scale shear zone, western Canadian Shield: Journal of Metamorphic Geology, v. 24, n. 3, p. 193-217, doi:10.1111/j.1525-1314.2006.00633.x.

Mahan, K.H., Williams, M.L., Flowers, R.M., Jercinovic, M.J., Baldwin, J.A., and Bowring, S.A., 2006b, Geochronological constraints on the Legs Lake shear zone with implications for regional exhumation of lower continental crust, western Churchill Province, Canadian Shield: Contributions to Mineralogy and Petrology, V. 152, n. 2, p. 223-242, doi:10.1007/s00410-006-0106-3.

Mahan, K.H., Goncalves, P., Flowers, R., Williams, M.L., and Hoffman-Setka, D., 2008, The role of heterogeneous strain in the development and preservation of a polymetamorphic record in high-P granulites, western Canadian Shield: Journal of metamorphic geology, v. 26, n. 6, p. 669-694, doi:10:111/j.1525-1314.2008.00783.x.

Mahan, K.H., Smit, C.A., Williams, M.L., Dumond, G., and Van Reenan, D.D., 2011a, Heterogeneous strain and polymetamorphism in high-grade terranes: Insight into crustal processes from the Athabasca Granulite Terrane, western Canada, and the Limpopo Complex, southern Africa: in van Reenen, D.D., Kramers, J.D., McCourt, S., and Perchuk, L.L., eds., Origin and evolution of Precambrain High-Grade Gneiss terranes, with Special Emphasis on the Limpopo Complex of Southern Africa: GSA Memoir, V. 207, p. 269-287, doi:10.1130/2011.1207(14).

Martel, E., van Breeman, O., Berman, R.G., and Pehrsson, S., 2008, Geochronology and tectonometamorphic history of the Snowbird Lake area, Northwest Territories, Canada: New insights into the architecture and significance of the Snowbird tectonic zone: Precambrian Research, v. 161, n. 3-4, p. 201-230, doi:10.1016/j.precamres.2007.07.007.

Maxeiner, R.O., and Rayner, N., 2010, continental arc magmatism along the southeast Hearne Craton margin in Saskatchewan, Canada: Comparison of the 1.92 – 1.91 Ga Porter Bay Complex and the 1.86 – 1.85 Ga Wathaman batholith: Precambrian Research, v. 184, p. 93 – 120.

Mezger, K., 1992, Temporal evolution of regional granulite terranes: Implication for the formation of lowermost continental crust: Continental Lower Crust, Ed(s): R.M. Fountain et al., p. 447-472.

Pehrsson, S.J., Berman, R.G., Elington, B., and Rainbird, R., 2013, Two Neoarchean supercontinents revisited: The case for a Rae family of cratons: Precambrian Research, v. 232, p. 27-43.

Pehrsson, S.,J., Jenner, G., and Kjarsgaard, B.A., 2002, The Ketyet River Group: correlation with Paleoproterozoic supracrustal sequences of northeastern Rae and implications for Proterozoic orogenesis in the western Churchill Province: Geological Association of Canada Annual Meeting, p. 90

Petts, D.C., Davis, W.J., Moser, D.E., and Longstaffe, F.J., 2014, Age and evolution of the lower crust beneath the western Churchill Province: u-Pb zircon geochronology of kimberlite-hosted granulite xenoliths, Nunavut, Canada: Precambrian Research, v. 241, p. 129-145.

Pouchou, J.L., and Pichoir, F., 1984, Possibilités d'analyse en profondeur à la microsonde électronique: *Recherche Aérospatiale, v. 5, p. 349-351.*

Rainbird, R.H., Davis, W.J., Pehrsson, S.J., Wodicka, N., Rayner, N., and Skulski, T., 2010, Early Paleoproterozoic supracrustal assemblages of the Rae domain, Nunavut, Canada: intracratonic basin development during supercontinent break-up and assembly: Precambrian Research, v. 181, p. 166-186.

Regan, S.P., Williams, M.L., Leslie, S.R., Mahan, K.H., Jercinovic, M.J., and Holland, M.E., 2014, The Cora Lake shear zone, Athabasca granulite terrane (Snowbird Tectonic Zone), an intraplate response to far-field orogenic processes during the amalgamation of Laurentia: Canadian Journal of Earth Sciences

Relf, C., and Hanmer, S., 2000, A speculative and critical summary of the current state of knowledge of the western Churchill province: A NATMAP perspective: Geological Association of Canada-Mineralogical Association of Canada Abstracts, v. 25, p. 857.

Rhodes, J.M., 1996, Geochemical stratigraphy of lava flows sampled by the Hawaii Scientific Drilling Project: Journal of Geophysical Research, v. 101, n. B5, p. 11,729-11,746.

Ross, G.M., Broome, J., and Miles, W., 1994, Potential fields and basement structure – western Canada sedimentary basin: *in* Geological Atlas of the Western Canada Sedimentary Basin, G.D. Mossop and I. Shetsen (comp.), Canadian Society of Petroleum Geologists and Alberta Research Council, URL <http://www.ags.gov.ab.ca/publications/wcsb_atlas/atlas.html>, [Date last accessed online].

Ross, G.M., Eaton, D.W., Boerner, D.E., and Miles, W., 2000, Tectonic entrapment and its role in the evolution of continental sphere: an example from the Precambrian of western Canada: Tectonics, v. 19, p. 116-134.

Sanborn-Barrie, M., Carr, S.D., and Theriault, R., 2001, Geochronological constraints on metamorphism, magmatism, and exhumation of deep-crustal rocks of the Kramanitaur Complex with implications for the Paleoproterozoic evolution of the Archean western Churchill Province, Canada: Contributions to Mineralogy and Petrology, v. 141, p. 592-612.

Sanborn-Barrie, M., Chakungal, J., James, D., Rayner, N., and Whalen, J., 2014a, Precambrian bedrock geology, Southampton Island, Nunavut: Geological Survey of Canada Canadian Geoscience Map 132, 1:100,000

Sanborn-Barrie, M., Davis, W.J., Berman, R.G., Rayner, N., Skulski, T., and Sandeman, H., 2014b, Neoarchean-continental crust formation and Paleoproterozoic deformation of the central rae craton, Committee Bay belt, Nunavut: Canadian Journal of Earth Sciences, v. 51, p. 635 – 667.

Sandeman, H.A., Schultz, M., and Rubingh, K., 2005, Results of bedrock mapping of the Darby Lake-Arrowsmith River north map areas, central Rae Domain, Nunavut: Geological Survey of Canada, Current Research 2005-C2, p. 1-11.

Sandeman, H.A., Cousens, B.L., and Hemmingway, C.J., 2003, Continental Tholeiitic mafic rocks of the Paleoproterozoic Hurwitz Group, Central Hearne sub-domain, Nunavut: insight into the evolution of the Hearne sub-continental lithosphere: Canadian Journal of Earth Sciences, v. 40, p. 1219-1237.

Shirey, S.B., Kamber, B.S., Whitehouse, M.J., Mueller, P.A., and Basu, A.R., 2008, A review of the isotopic and trace element evidence for mantle and crustal processes in the Hadean and Achean: implications for the onset of plate tectonic subduction, *in* Condie, K.C. and Pease, V., *eds.*,When did Plate Tectonics Begin on Planet Earth?: Geological Society of America Special Paper 440, p. 1-29, doi: 10.1130/2008.2440(01).

Slimmon, W.L., 1989, Bedrock compilation geology: Fond du Lac (NTS 74-O): Saskatchewan Geological Survey, Saskatchewan Energy and Mines, Map 247A, scale 1:250,000.

Van Kranendonk, 2010, Two types of Archean continentral crust: plume and plate tectonics on early earth: American Journal of Science, v. 310, p. 1187-1209.

Ward, D., 2010, The relative influence of quartz and mica on crustal seismic anisotropy [M.S.: University of Colorado, 89 p.

Williams, M.L., and Hanmer, S., 2006, Structural and metamorphic processes in the lower crust: Evidence from a deep-crustal isobarically cooled terrane, Canada: Evolution and Differentiation of the Continental Crust, ed(s) M. Brown and T. Rushmer, p. 231-267, Cambridge University Press, Cambridge.

Williams, M.L., Hanmer, S., Kopf, C., and Darrach, M., 1995, Syntectonic generation and segregation of tonalitic melts from amphibolite dikes in the lower crust, Striding-Athabasca mylonite zone, northern Saskatchewan: Journal of Geophysical Research, V. 100, n. B8, p. 15,717-15,734, doi:10.1029/95JB00760.

Williams, M.L., Melis, E.A., Kopf, C.F., and Hanmer, S., 2000, Microstructural tectonometamorphic processes and the development of gneissic layering: A mechanism for metamorphic segregation: Journal of Metamorphic Geology, v. 18, p. 41-57, doi:10.1046/j.1525-1314.2000.00235.x.

Williams, M.L., and Flowers, R.M., 2008, The Chipman dyke swarm, Saskatchewan, Canada: Component of the 1.9 Ga Snowbird large igneous province in the western Canadian Shield: LIP of the Month, January, 2008: http://www.largeigneousprovinces.org/08jan

Williams, M.L., Karlstrom, K.E., Dumond, G., and Mahan, K.H., 2009, Perspectives on the architecture of continental crust from integrated field studies of exposed isobaric sections: in Miller, R.B., and Snoke, A.W., eds., Crustal Cross Sections from the Western North American

Cordillera and Elsewhere: Implication for Tectonic and Petrologic Processes: GSA Special Paper 465, p. 219-241, doi:10.1130/2009.2456(08).

Williams, M.L., Mahan, K.H., Dumond, G., Jercinovic, M.J., Regan, S.P., and Leslie, S., 2011, Linking metamorphism and deformation using in-situ monazite geochronology: interpretation of multistage tectonic histories: GSA annual meeting, Minneapolis, MN.

Williams, M.L., and Jercinovic, M.J., 2012, Tectonic interpretation of metamorphic tectonites: integrating compositional mapping, microstructructural analysis and in situ monazite dating: Journal of Metamorphic Petrology, v. 30, p. 739-752

Williams, M.L., Mahan, K., Dumond, G., Regan, S., and Holland, M., in prep, Garnet-forming reactions in felsic orthogneiss: implications for strengthening and densification of the lower continental crust: to be submitted to the Journal of Metamorphic Petrology

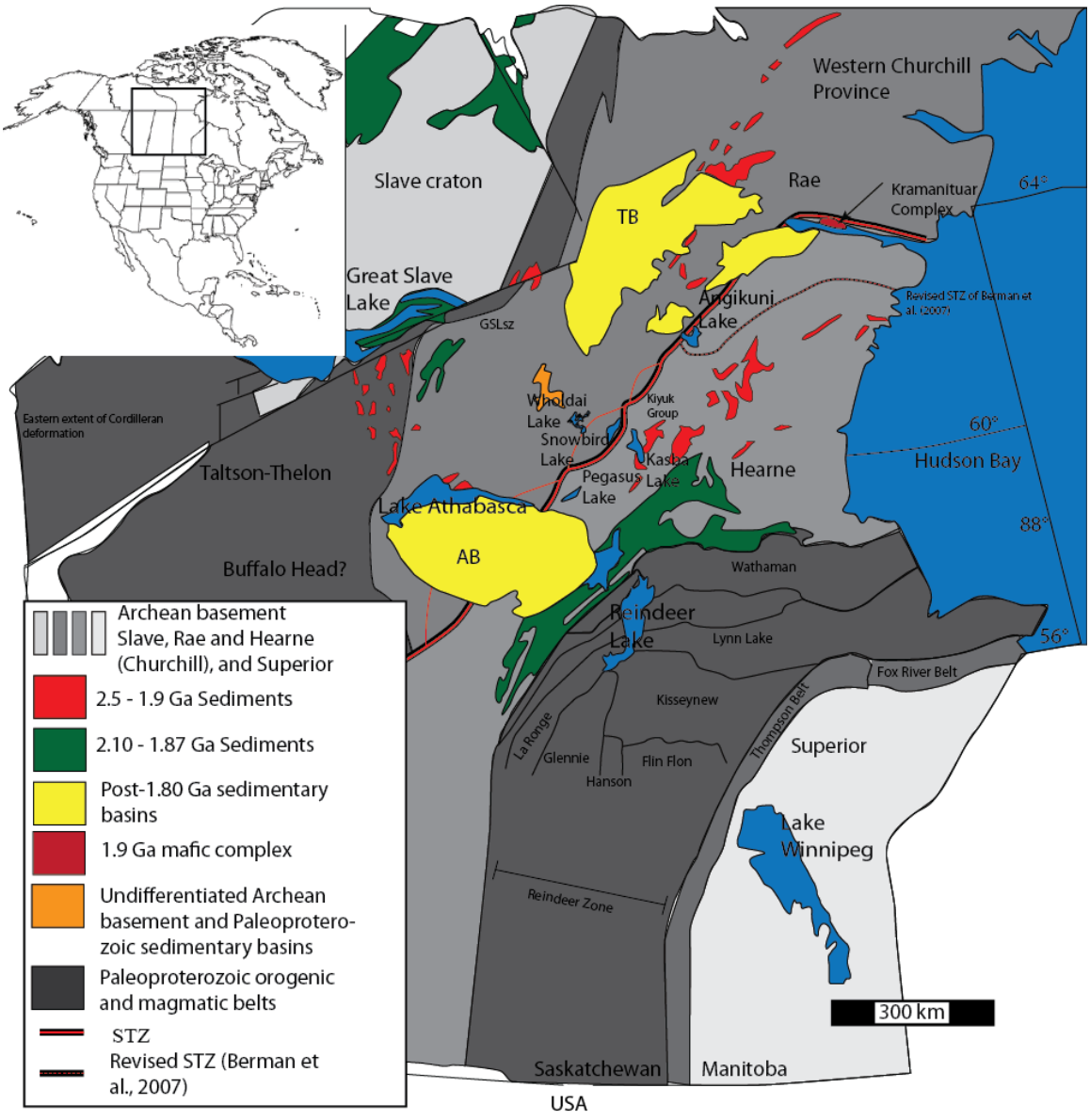

Figure 22: Lithotectonic map of the western Canadian Shield (modified from Aspler et al., 2002b). The Snowbird Tectonic Zone defines the enigmatic boundary between Rae and Hearne domains of the western Churchill Province. Box outlines triangular region (east Athabasca mylonite triangle) depicted in figure 2. Angikuni Lake, 450 km to the northeast of the study region is outlined with a white box.

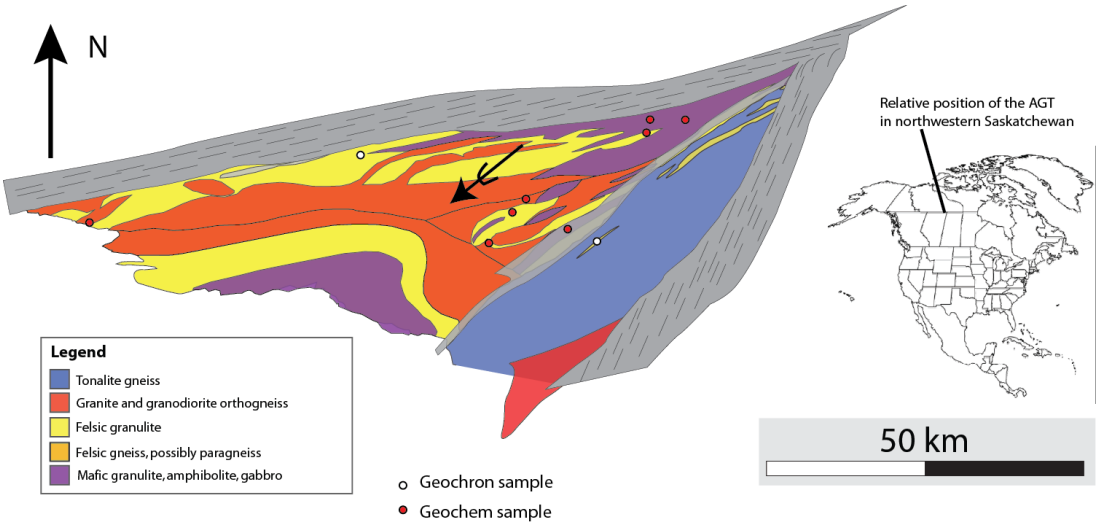

Figure 23: Geologic map of the east Athabasca mylonite triangle (Gilboy, 1981; Hanmer, 1994) also displaying sample localities for this study. The region can be split into three distinctive lithotectonic domains that are divided by thick ductile shear zones.

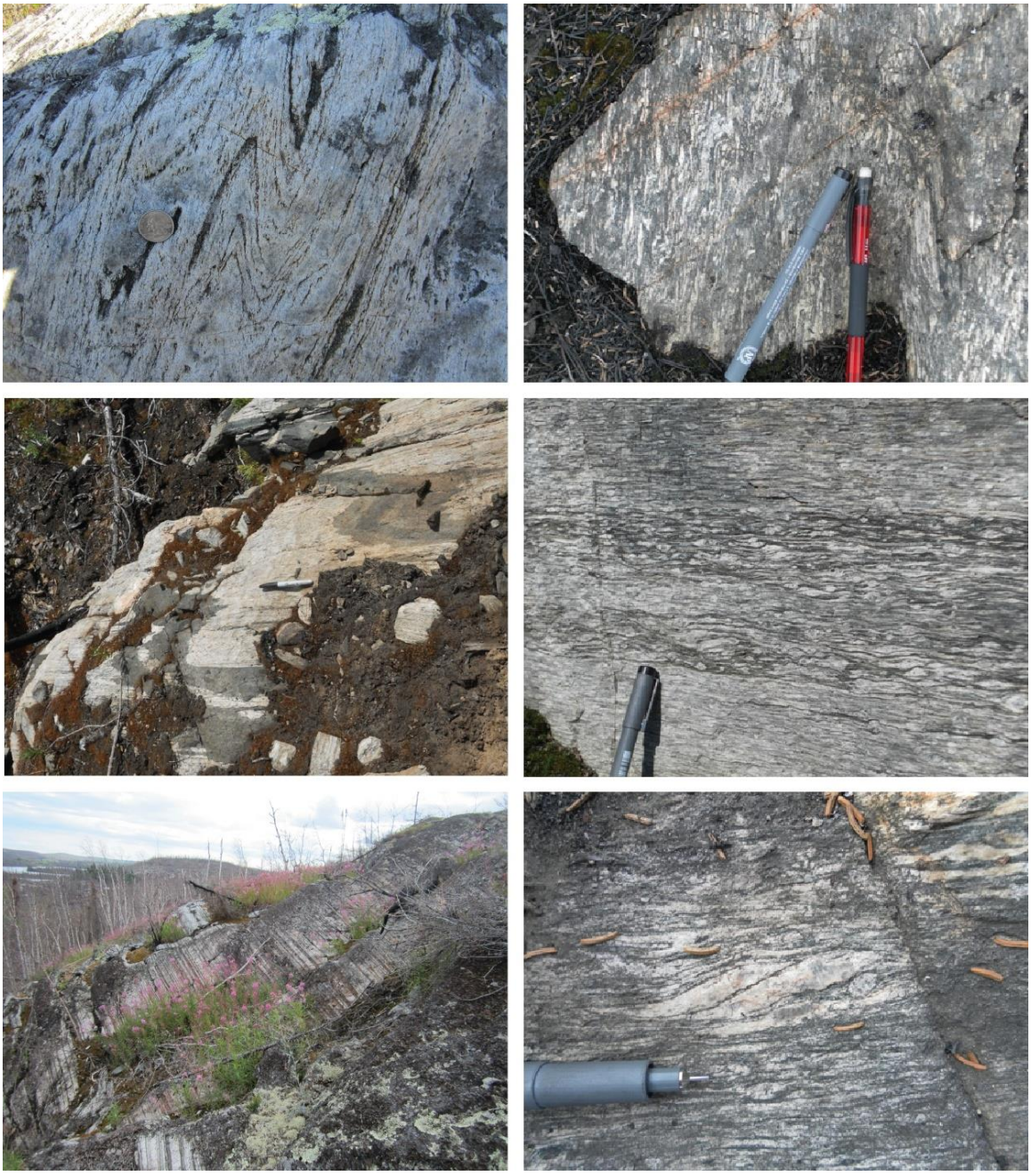

Figure 24: Photographs of S_1 and S_2 relationships from the Chipman and northwestern subdomains. A) Crenulated Chipman tonalite (ca. 3.2 Ga), where the early tectonic fabric (S_1) is overprinted by an axial planar fabric (S_2); B) Crenulated Bohica intermediate gneiss from the northwestern subdomain (ca. 2.6 Ga), where feldspar porphyroclasts form ribbons along the early, subhorizontal S_1, and are folded and variably aligned with S_2 (Pen oriented along the S_1 enveloping surface and the pencil is aligned with S_2); C) Meter-scaled fold of a Chipman dike that is cross cutting S_1, but is folded about an F_2 fold axis; D) Early tectonic layering in the Bohica intermediate gneiss with little to no S_2 development showing abundant asymmetric porphyroclasts and S-C-C' geometries indicative of top to the east shear; E) Highly transposed Chipman anorthosite with a strong S_2, with little to no evidence of earler tectonic gneissic layering; F) Dextral S-C-C' kinematic indicator in the Bohica suite developed along a strong L_2.

Figure 25: Photographs showing felsic granulite migmatites from various locations throughout the Chipman and northwestern subdomain. A) Reeve Lake diatexite (sample 11G-020) with a strong S_1 gneissic layering with little to no evidence of S_2; B) Cora Lake felsic granulite (sample 10W-094g) displaying strong evidence for anatexis along S_1, and a variably overprinting S_2 fabric that also defines the axial plane of the fold; C) Dismembered garnet porphyroblasts in felsic granulite from the Cora Lake shear zone (Jeanotte Lake); E) Brecciated garnet porphyroblast within a felsic granulite from the Cora Lake shear zone.

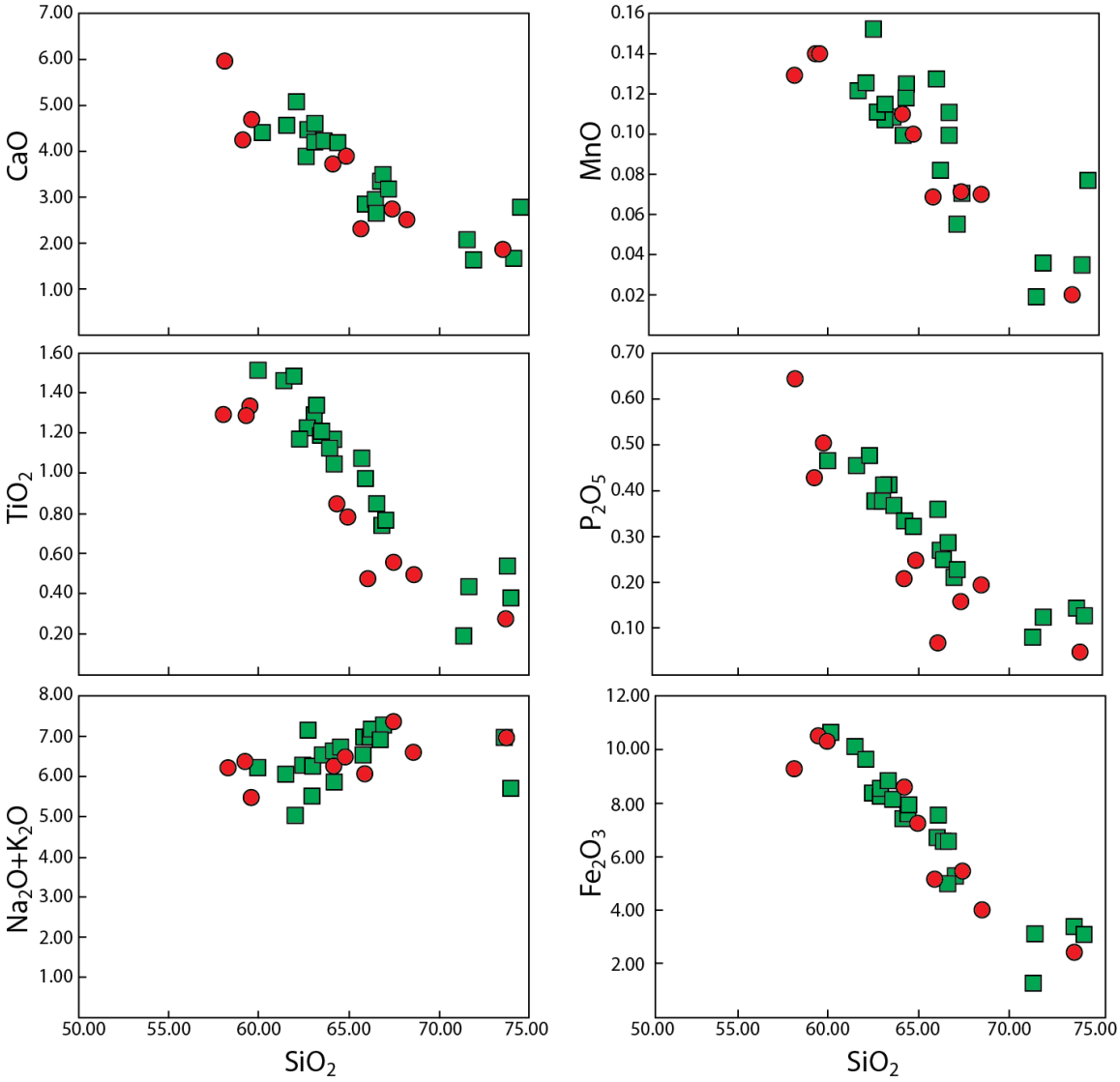

Figure 26: Harker diagram for Neoarchean plutonic rocks from the east Athabasca mylonite triangle. Green squares are the Fehr granite in the Chipman subdomain (Koteas et al., 2010) and red circles are new data from the Hawkes plutonic suite.

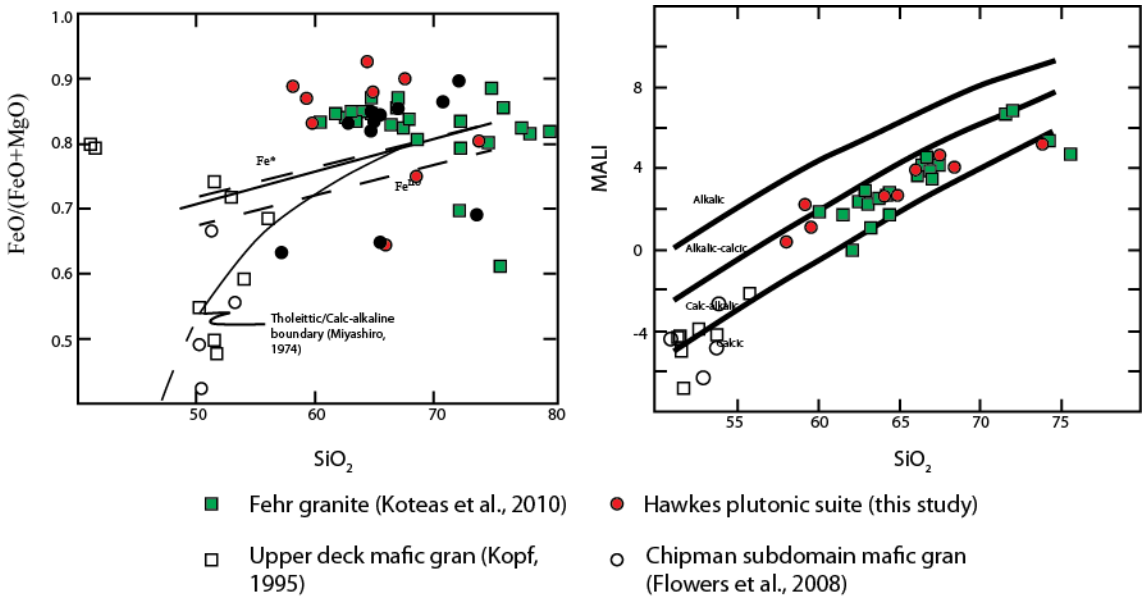

Figure 27: Frost diagrams for Neoarchean plutonic rocks from the east Athabasca mylonite triangle. Left: Modified alkali lime index projection; right: Fe-index vs SiO2.

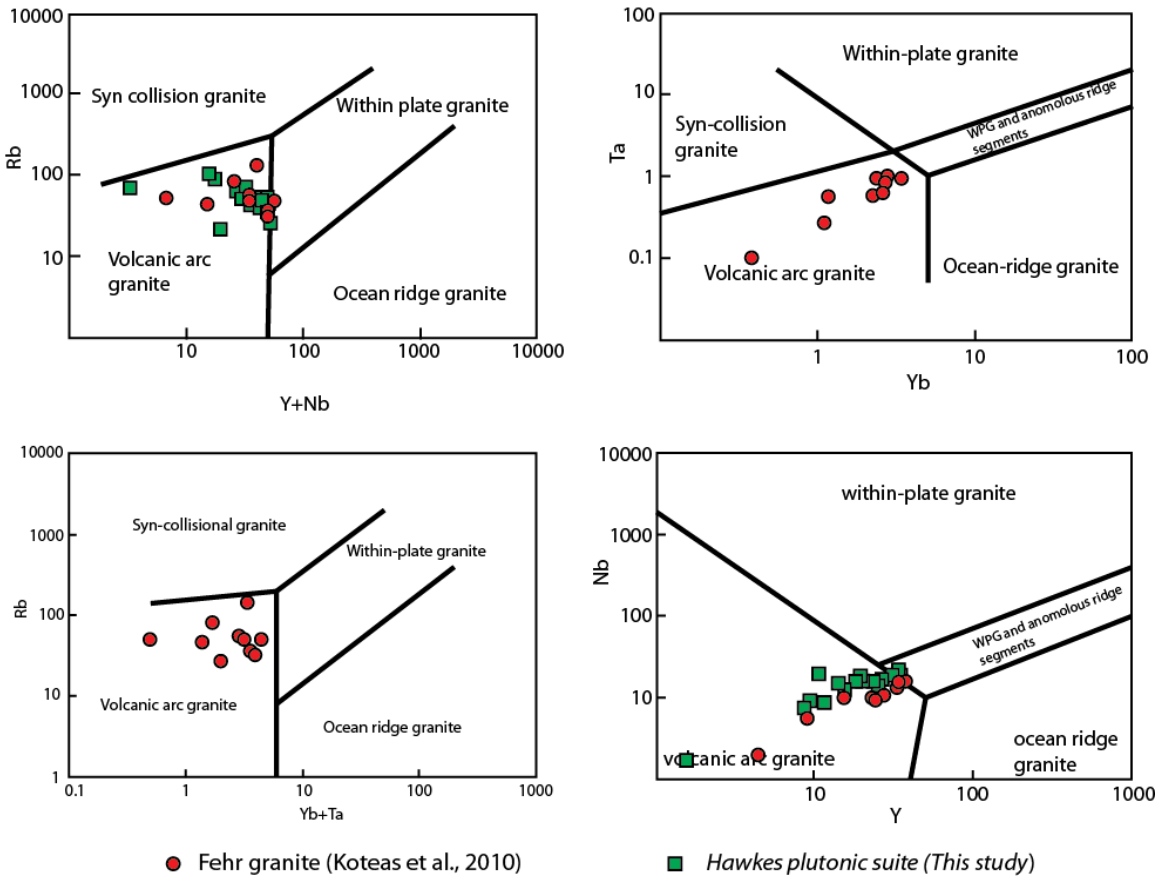

Figure 28: Tectonic discrimination for ca. 2.6 Ga plutonic rocks from the east Athabasca mylonite triangle (Pearce et al., 1984).

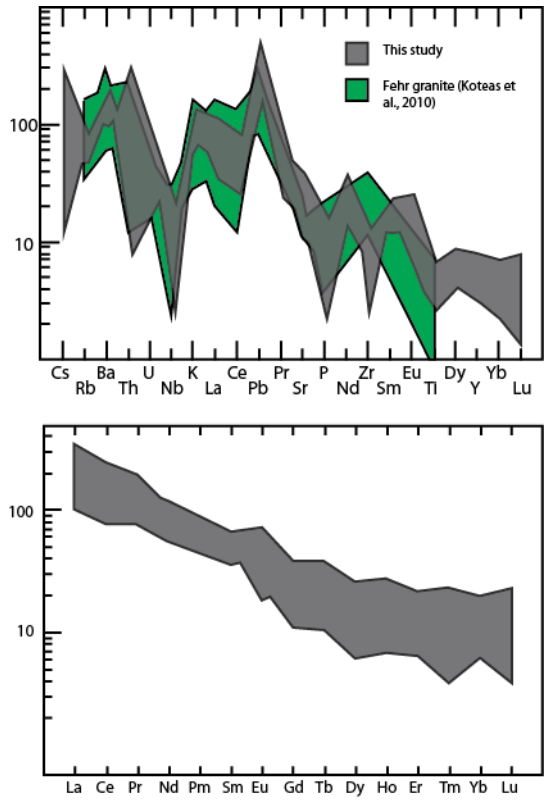

Figure 29: Spider diagrams for Neoarchean plutonic rocks. Top: incompatible element diagram normalized to primitive mantle (Sun and Mcdonough, 1989); bottom: REE plot normalized to chondrites (Sun and McDonough, 1989).

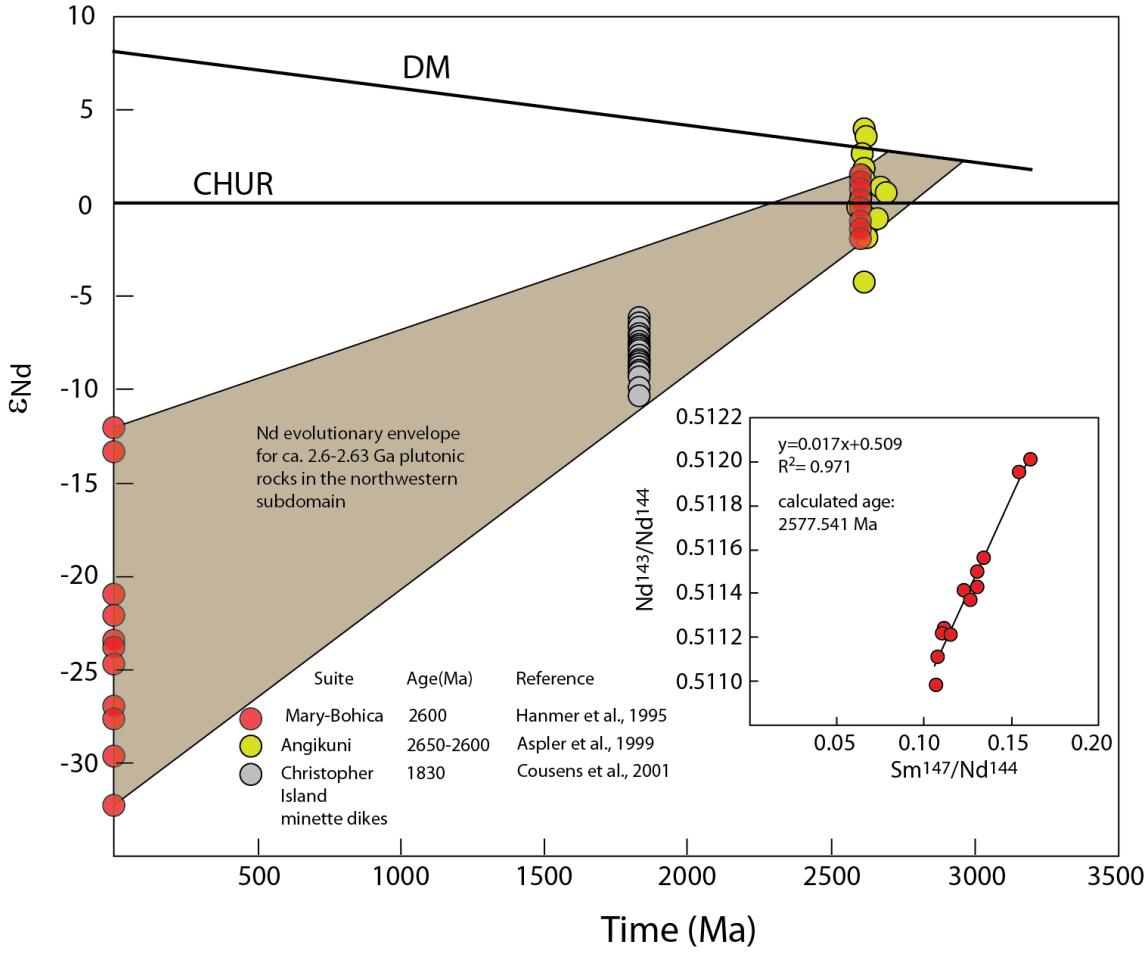

Figure 30: Neodymium evolutionary diagram for Sm-Nd isotopic results from plutonic rocks in the northwestern subdomain presented in Hanmer et al. (1994). Inset diagram is an isochron calculated from published data. No access to raw data prohibited statistical analysis, thus no error could be calculated. Also plotted on the diagram are unpublished results from Angikuni Lake, and results from Cousens et al. (2001) for ultrapotassic minette dikes within the Christopher Island Formation. Notice the minette dikes plot within the Nd evolutionary envelope of the ca. 2.6 Ga plutonic rocks.

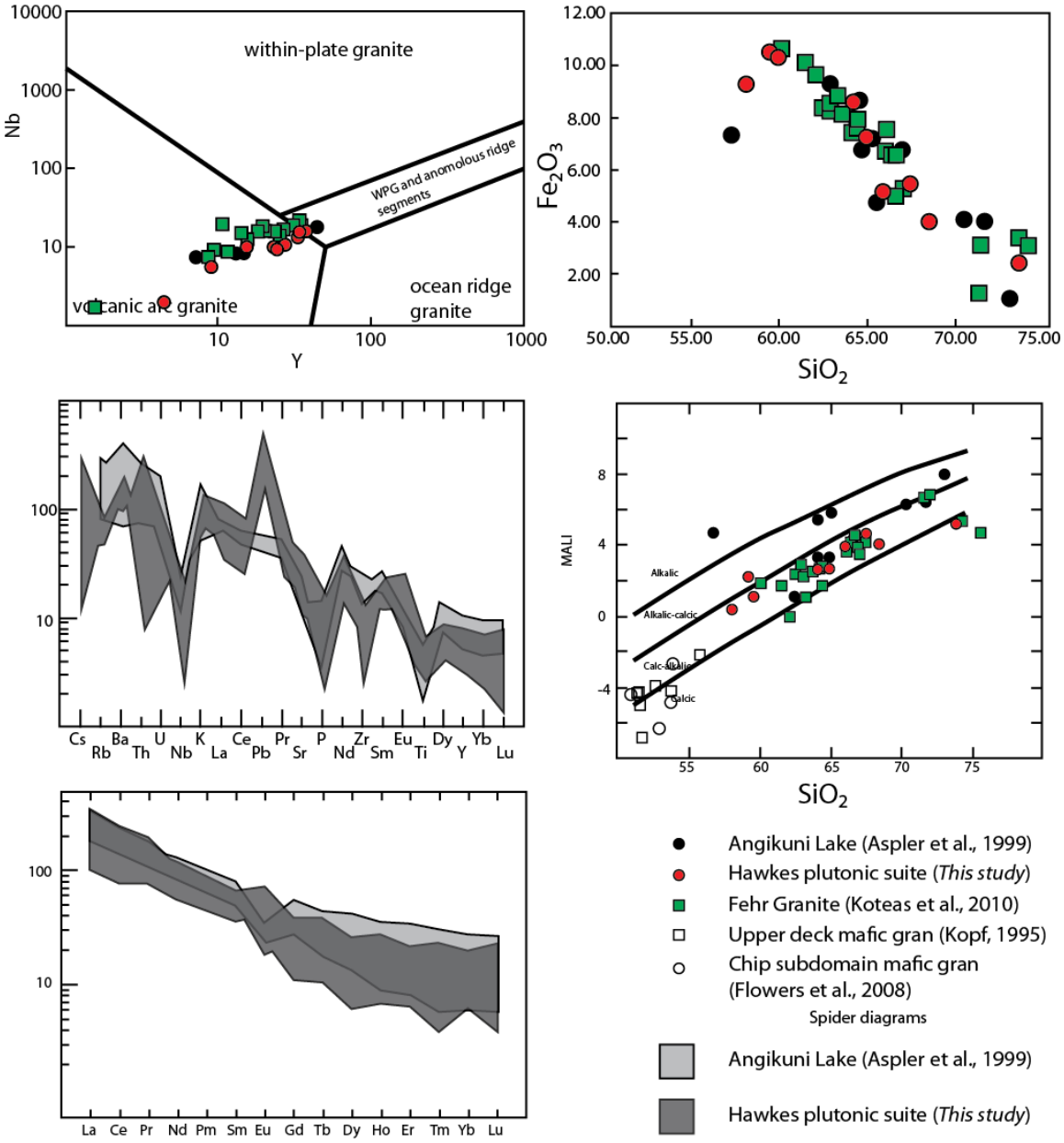

Figure 31: Geochemical comparison between Neoarchean plutonic rocks within the east Athabasca mylonite triangle and Neoarchean meta-igneous rocks from Angikuni Lake (Aspler et al., 1999).

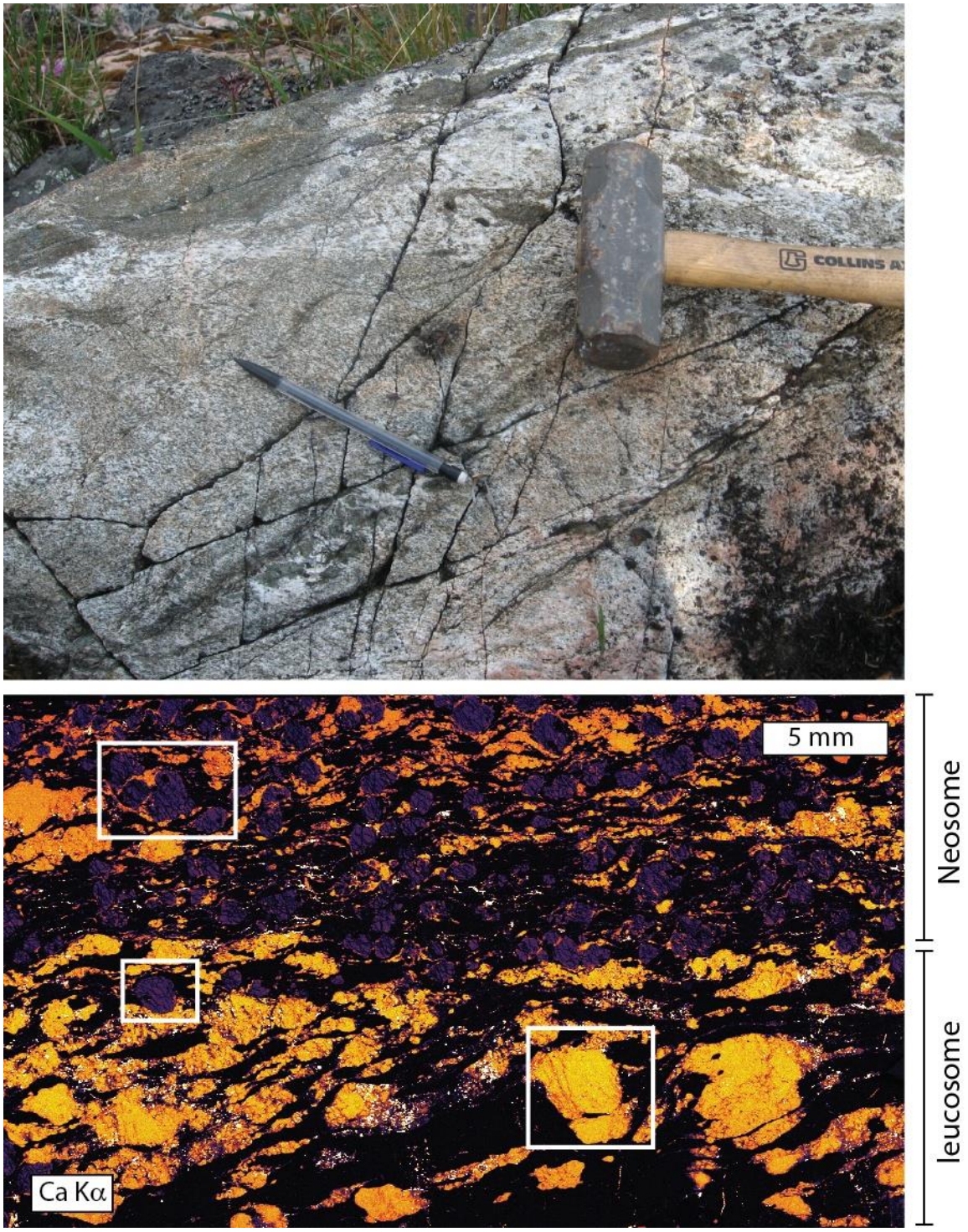

Figure 32: A) Field photograph of 10W-094g sample location (see also Regan et al., in review). Hammer is situated parallel to compositional/migmatitic layering and pencil is oriented parallel to the axial planar S2 fabric that is defined by a subtle mineral alignment in the outcrop. B) Ca Kα WDS compositional map of the entire thin section. Boxes outline regions of extensive silicate analysis presented below. Notice the thin section contains two components, a garnetite and a leaucosome, that is overprinted in the leaucosome by a well developed S2

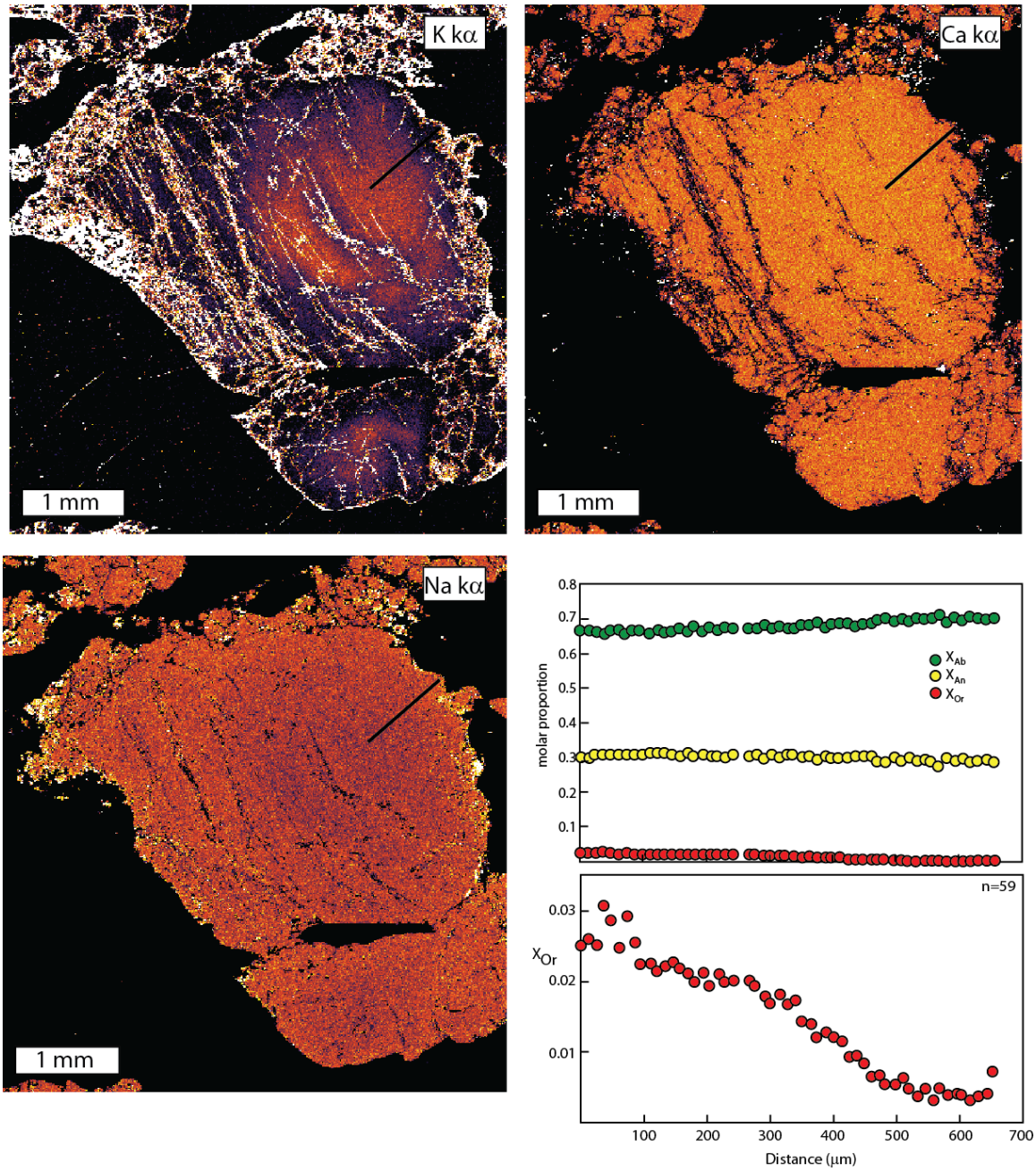

Figure 33: WDS compositional analysis of a plagioclase porphyroblast from the leaucosome of 10W-094g. Microanalysis transect is labeled with black line. A) K Kα WDS map; notice the high abundance of K in the core of the plagioclase grain, and the smooth zonation towards the rim of the crystal. B) Ca Kα WDS map showing little to no zonation. C) Na Kα WDS compositional map displaying subtle zonation corresponding to the variation in K. D) Electron microprobe results for the plagioclase grain with components plotted over distance. E) X_{Or} component plotted over distance showing the gradual decrease from core to rim.

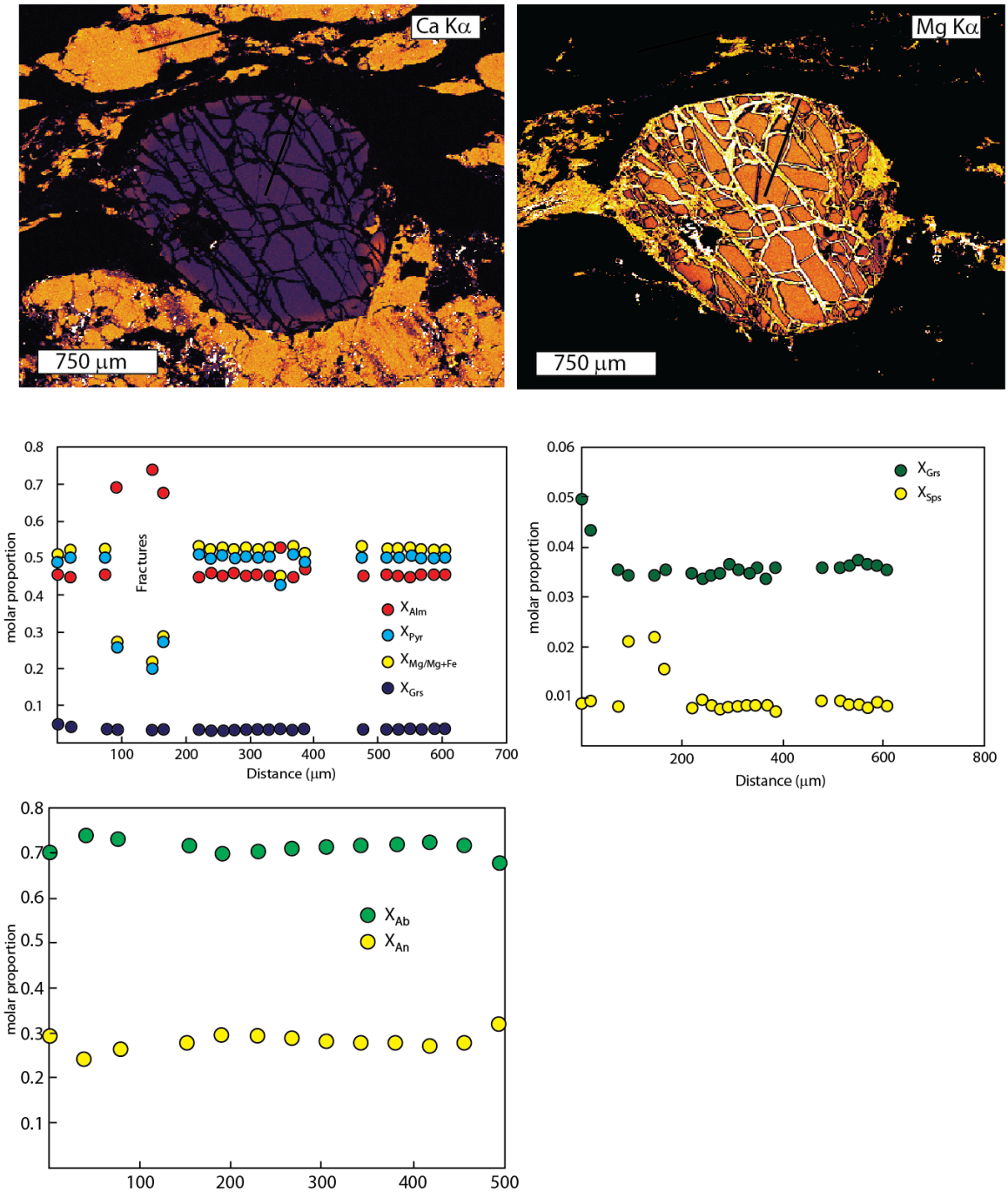

Figure 34: Electron microprobe results for region 2 outlined in Figure 8. Electron microprobe transects are labeled with a black line. A) Ca Kα map of garnet porphyroclast within the leaucosome. Notice the increase in Ca at the edge of the crystal. B) Mg Kα WDS map of garnet porphyroclast. C-D) Electron microprobe results for garnet analysis. E) Electron microprobe results for plagioclase analysis adjacent to garnet.

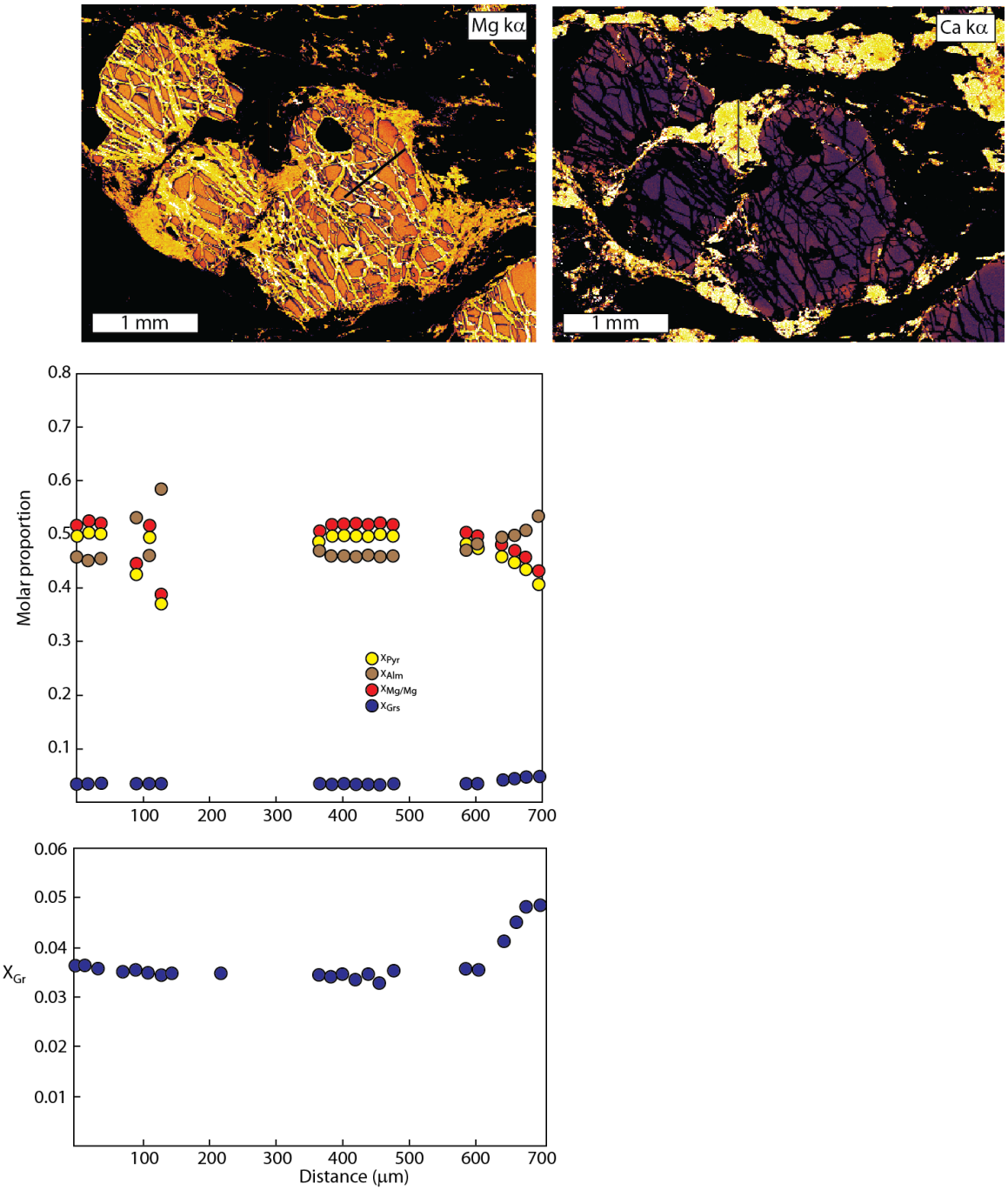

Figure 35: Electron microprobe results for region 3 outlined in Figure 29. A) Mg Kα WDS map of garnet porphyroblast. Notice the mat of biotite on its lower left margin, aligned with S2 in the rock. Also, the fractures in the garnet are oriented perpendicular to S2. B) Ca Kα WDS map of the garnet porphyroblast. Similar to Figure 10, this garnet also contains a Ca enrichment along the very outerrim. C-D) Electron microprobe analytical results for garnet analysis shown by black line in Figure 32a and b.

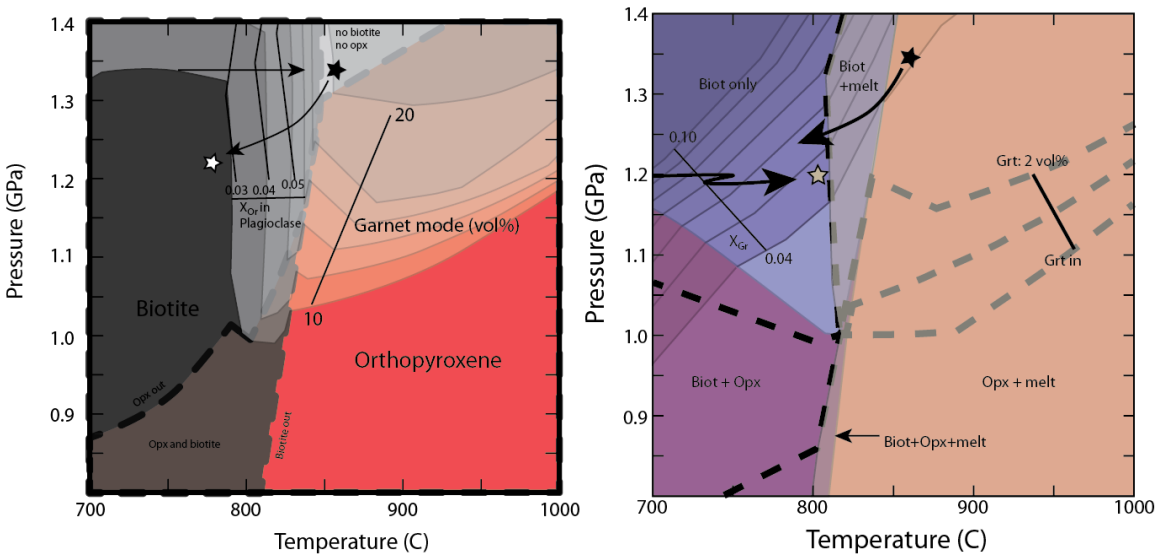

Figure 36: Isochemical pseudosection modeling results for sample 10W-094. A) Pseudosection of 10W-094g_c (bulk rock) with phases that vary over the P-T range of interest labeled. Also plotted on this pseudosection are results for garnet mode (vol %) and X_{Or} in plagioclase. Black star is the peak assemblage, and represents the likely conditions that facilitated the migmitiation during the development of S_1. B) Pseudosection of 10W-094g_b (leaucosome). Also modeled and overlain of the assemblage diagram is garnet mode (vol %; dark dashed lines) and X_{Gr} isopleths which significantly reduced the P-T range of interest. White star denotes the maximum P-T conditions for the development of S_2

S_2.

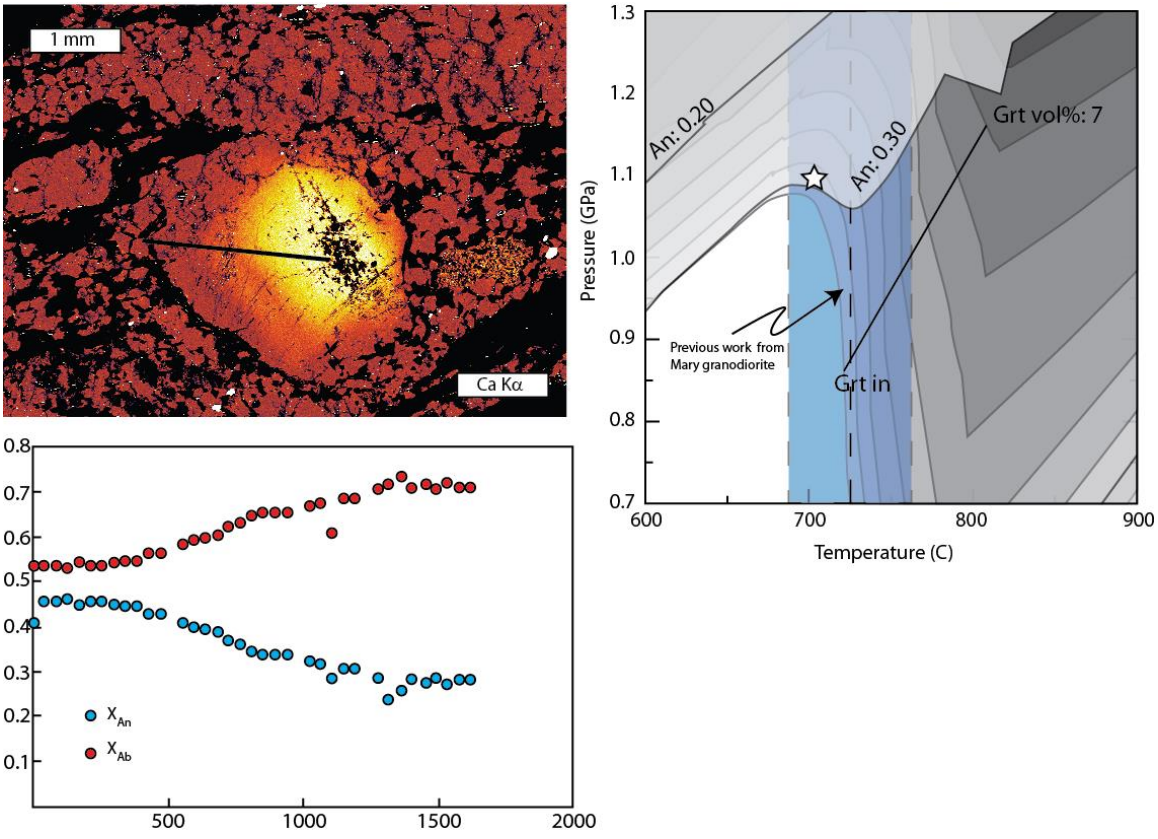

Figure 37: Electron microprobe results for sample 12R-054 (Beed granite). A: Ca K□ WDS map of a plagioclase porphyroclast with relict igneous zoning. Note that XAn decreases markedly within the dynamically recrystalled tail. B: Compositional transect across plagioclase grain from A (labeled on WDS map). C) Isochemical modeling results, star for appropriate assemblage (see text for details).

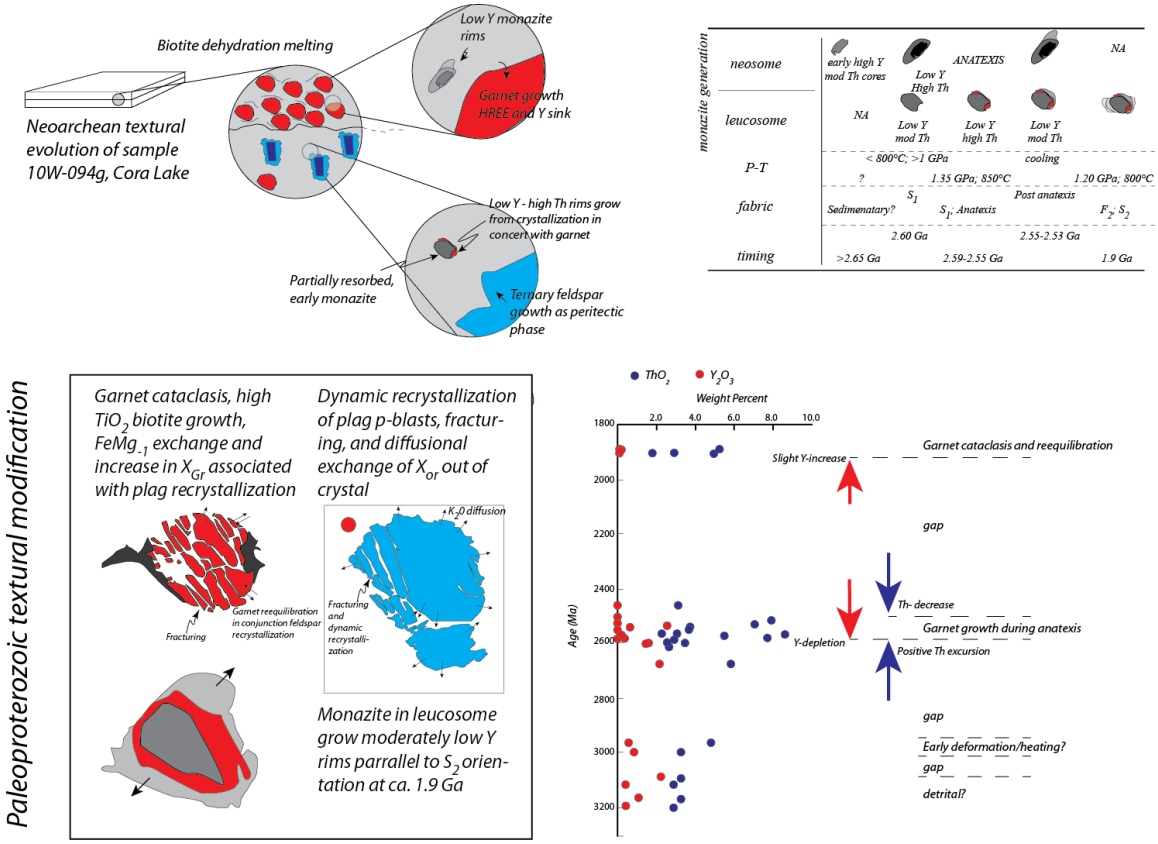

Figure 38: Textural evolution of sample 10W-094g

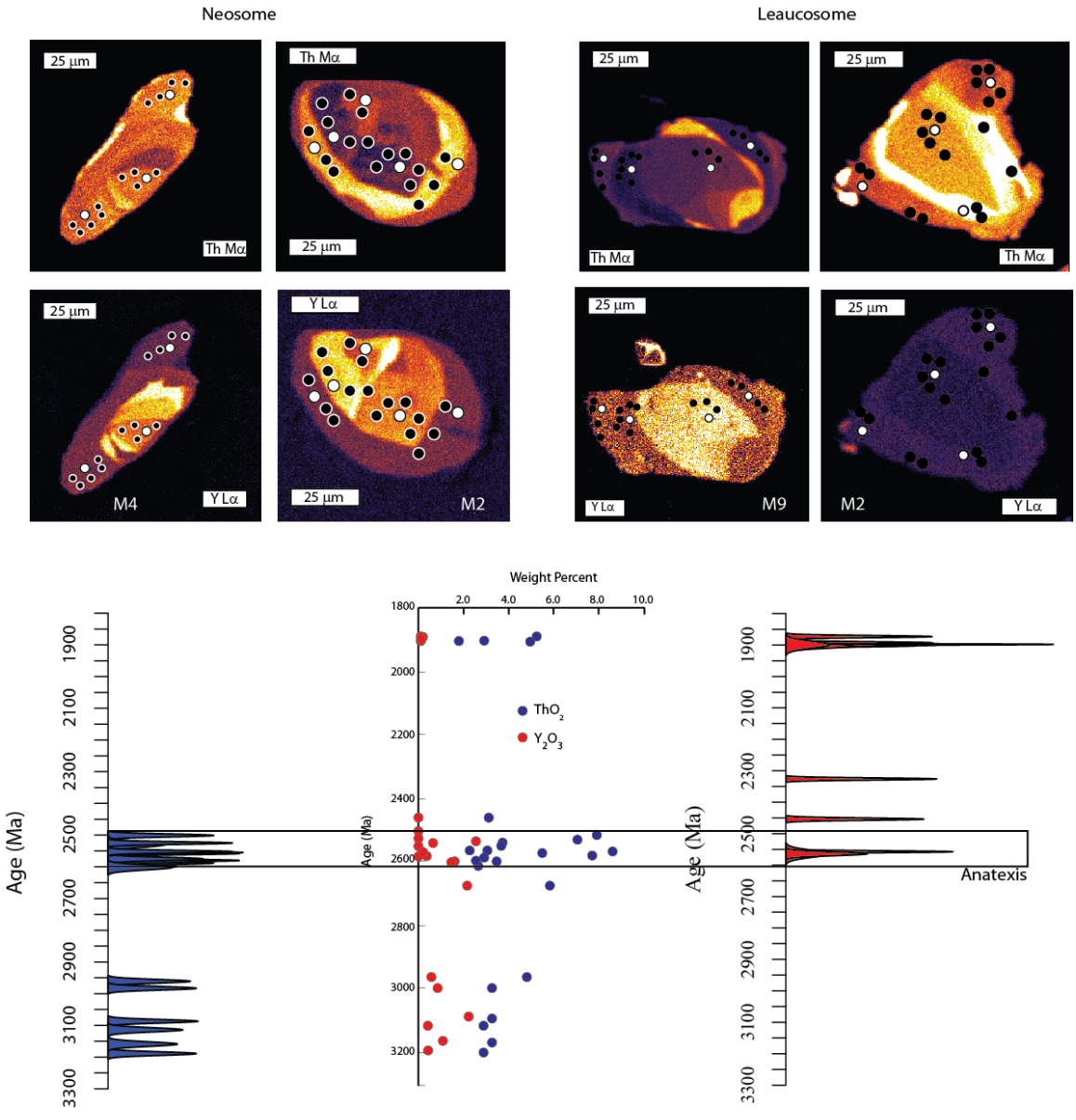

Figure 39: Geochronology results for sample 10W-094g. Notice results from the neosome are on the left, and results from the leaucosome are on the right.

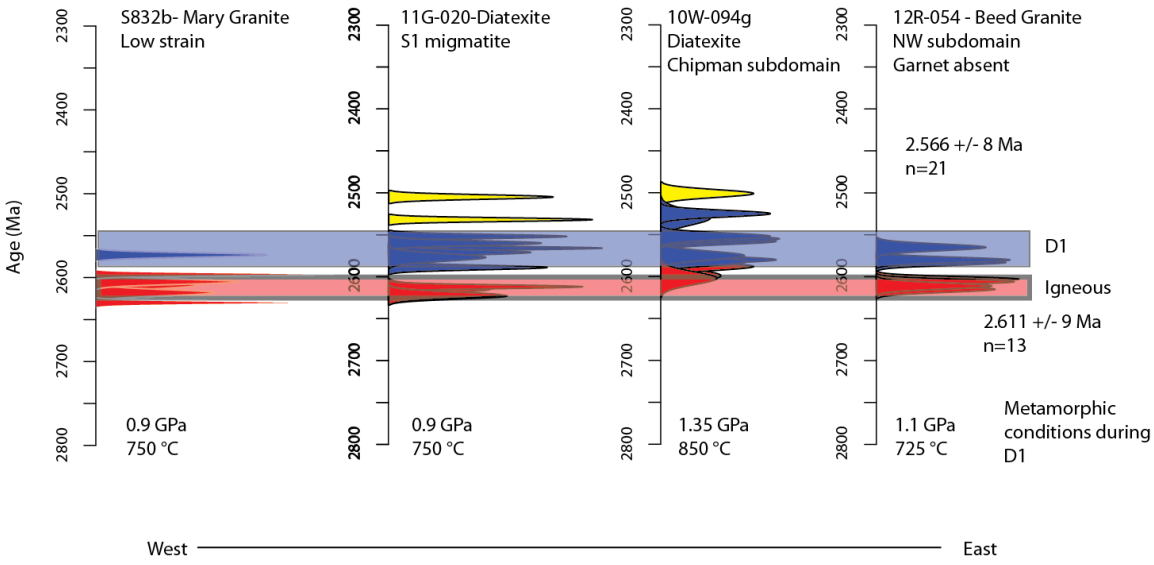

Figure 40: Monazite geochronology summary for all samples analyzed. Weighted means of ages of a certain population listed to right. Below histograms are the metamorphic conditions calculated for individual samples corresponding to the development of a strong S1 fabric. It is important to note that igneous activity is quickly followed by crustal thickening and pervasive deformation/migmatization.

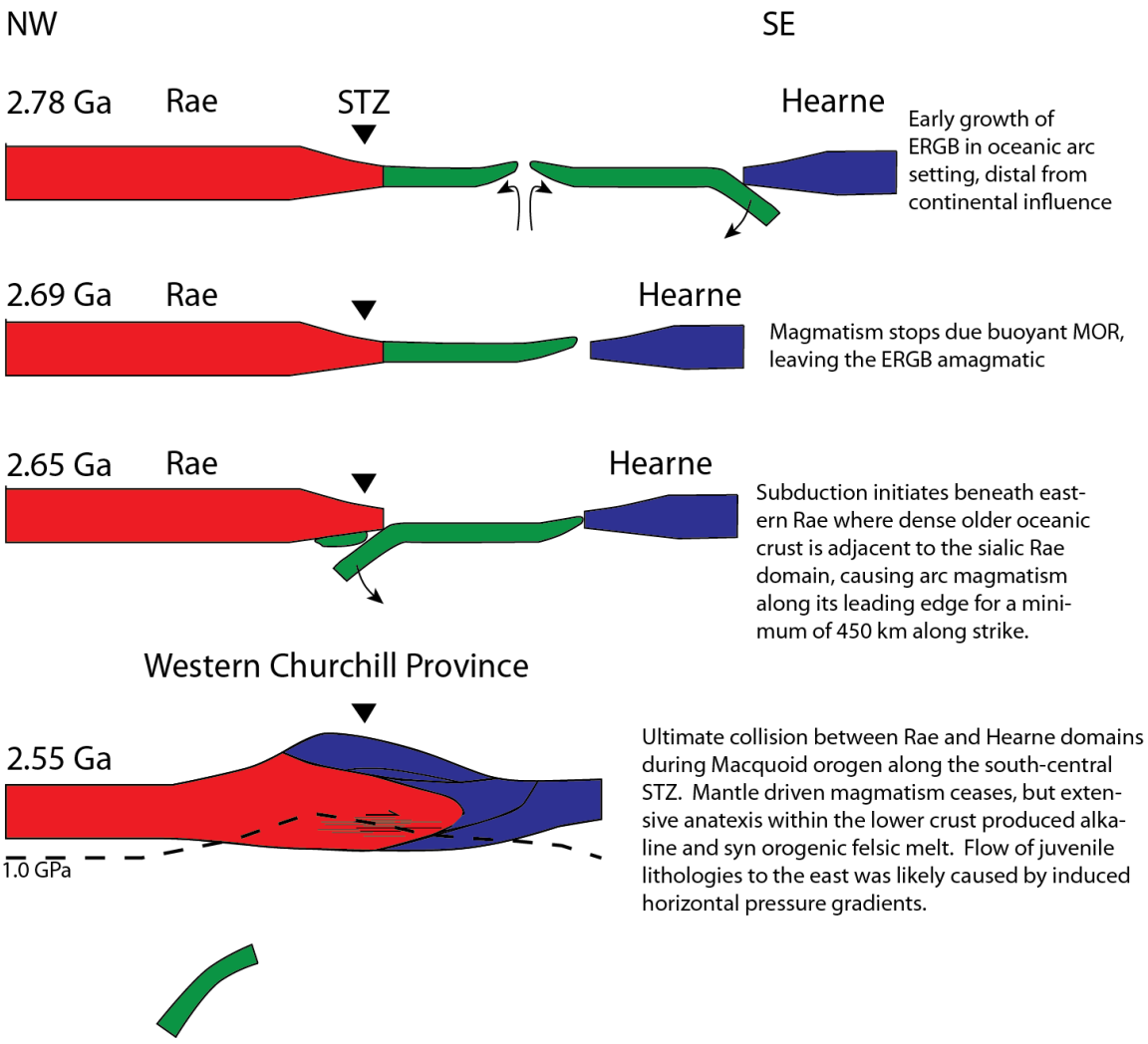

Figure 41: Serial tectonic model regarding the Neoarchean history of the western Churchill Province.

Table 11: Summary of existing geochronology pertaining to igneous crystallization

Suite	Subdomain	Member	Age (Ma)	Reference	Method	Phase
Mary-Bohica	Northwestern	Mary Granite	2606+13/-11	Hanmer et al., 1997	Multi grain TIMS	Zircon
Mary-Bohica	Northwestern	Godrey Granite	2618+/-4	Hanmer et al., 1997	Multi grain TIMS	Zircon
Mary-Bohica	Northwestern	Brykea Granite	2601+/-4	Hanmer et al., 1997	Multi grain TIMS	Zircon
Mary-Bohica	Northwestern	Bradley Granite	2584+40/-15	Hanmer et al., 1997	Multi grain TIMS	Zircon
Mary-Bohica	Northwestern	Rea Granite	2604+/-1	Hanmer et al., 1997	Multi grain TIMS	Zircon
Mary-Bohica	Northwestern	Hawkes Granite	2610+/-1	Hanmer et al., 1997	Multi grain TIMS	Zircon
Mary-Bohica	Northwestern	Bohica mafic complex	2596+/-12 2620+34/-21	Hanmer et al., 1997	Multi grain TIMS	Zircon
Mary-Bohica	Nothwestern	Felsic Lake leaucogranite	2629+26/-20	Hanmer et al., 1997	Multi grain TIMS	Zircon
McGillivray	Chipman	McGillivray	2621 +/-3	Hanmer et al., 1997	Multi grain TIMS	Zircon
Fehr	Chipman	Fehr Granite	2598+/-3	Hanmer et al., 1997	Multi grain TIMS	Zircon
Fehr	Chipman	Bompass Granite	Ca. 2600	Hanmer et al., 1997	Multi grain TIMS	Zircon
Chipman batholith	Chipman	Anorthosite	3149+/-100	Hanmer et al., 1997	Multi grain TIMS	Zircon
Axis Gabbronorite	Upper deck	Mafic Granulite	Ca. 2600	Hanmer et al., 1997	Multi grain TIMS	Zircon
Clut granite	Upper deck	Clut granite	2614 +9/-7	Hanmer et al., 1997	Multi grain TIMS	Zircon
Clut granite	Upper deck	Melby-Turnbull granites	2610+/-2	Hanmer et al., 1997	Multi grain TIMS	Zircon
Mafic Granulite	Chipman	Mafic Granulite	2554.5+/-4.3*	Flowers et al., 2008	Single grain TIMS/SHRIMP	Zircon
Chipman Dikes-Leucosome	Chipman	Migmatitic Dike	1896.2+/-0.3 *	Flowers et al., 2006a	Single grain TIMS	Zircon
Axis Gabbronorite	Upper deck	Mafic granulite	2550-2520	Baldwin et al., 2004	Single grain TIMS	Zircon
Mary	Upper deck	Godfrey Granite	2610	Baldwin et al., 2003	Single grain TIMS	Zircon
Mary-Bohica	Northwestern	Beed Granite	2608+/- 9	This study	EPMA: in-situ	Monazite
Mary-Bohica	Northwestern	Mary Granite	2612	This study	EPMA: in-situ	Monazite

Table 12: Major and trace element geochemical results

Sample	10w-110a	11R-077	06G-017	12R-031	12R-054	11R-112	12R-032 b	12R-068	11R-081	12R-072a	10W-094gb	10W-094gc
SiO2	73.71	67.39	65.81	59.25	68.35	58.01	59.59	64.24	64.85	45.85	84.08	72.12
Al2O3	13.20	14.59	15.42	14.97	15.24	16.58	14.34	15.12	14.79	15.14	9.09	13.06
Fe2O3	2.46	5.71	5.21	10.56	4.15	9.42	10.45	8.73	7.49	12.31	1.14	4.76
MgO	0.60	0.63	2.92	1.64	1.39	1.25	2.13	0.72	1.04	9.01	0.97	3.34
CaO	1.86	2.69	2.31	4.25	2.51	5.92	4.64	3.73	3.84	10.94	1.30	1.74
Na2O	2.73	2.73	2.87	3.28	3.21	3.55	3.14	3.29	3.08	2.05	1.98	2.20
K2O	4.31	4.58	3.27	3.10	3.40	2.68	2.34	2.98	3.41	1.70	1.05	1.65
TiO2	0.28	0.55	0.48	1.28	0.50	1.30	1.34	0.84	0.80	0.94	0.19	0.53
P2O5	0.05	0.16	0.07	0.43	0.19	0.64	0.50	0.21	0.25	0.33	0.02	0.03
MnO	0.02	0.07	0.07	0.14	0.07	0.13	0.14	0.11	0.10	0.18	0.03	0.08
Cr2O3	0.002	0.003	0.020	0.003	0.005	0.002	0.005	0.002	0.003	0.026		
Total	99.22	99.10	98.45	98.90	99.02	99.48	98.62	99.97	99.65	98.48	99.85	99.51
Cs	0.1	0.9	2.5	0.9	0.3	0.9	0.4	0.2	0.2	0.6		
Rb	53.7	138.6	46.9	51.2	83.9	36.0	32.2	47.9	58.0	27.0		
Sr	312	238	351	353	295	585	353	375	324	870		
Ba	1149	1203	947	1383	731	1380	1184	1547	1442	401		
Ta	0.1	0.9	0.3	0.9	0.5	0.9	1.0	0.6	0.6	0.9		
Nb	1.95	11.33	5.85	16.07	10.45	15.12	15.80	9.97	10.23	40.17		
Pb	22.12	37.28	17.89	19.82	28.16	19.38	17.93	18.91	19.90	12.59		
Hf	2.63	8.27	1.99	7.88	4.18	2.16	2.83	4.43	3.77	0.80		
Zr	96.8	323.0	72.8	321.7	146.5	72.0	123.4	203.7	160.8	29.7		
Y	4.6	27.5	9.3	38.3	15.0	34.3	33.6	23.9	23.6	15.4		
Sc	3.1	11.5	11.0	19.0	9.1	17.9	21.6	17.6	14.6	21.4		
Ni	4.9	6.3	63.6	9.3	14.2	4.2	15.9	4.9	5.6	42.4		
Zn	32.2	80.2	80.7	134.7	46.5	150.3	126.0	125.4	89.8	174.0		
V	52	26	96	73	54	46	95	23	57	212		
Cu	4.17	12.40	30.54	12.77	8.38	8.15	20.93	8.24	11.42	40.55		
Th	22.3	7.8	5.1	3.2	28.6	3.4	1.2	0.7	0.8	1.9		
U	1.0	1.5	0.5	1.2	2.2	1.1	0.5	0.4	0.4	0.4		
Ga	15.04	20.78	18.55	22.48	16.93	25.40	20.47	23.24	20.88	16.37		
La	154.58	84.43	51.77	98.31	118.74	104.35	79.63	48.17	58.16	91.72		
Ce	19.4	10.2	6.7	14.0	16.0	15.9	12.1	7.4	8.2	16.0		
Pr	55.4	34.6	21.0	47.7	49.3	53.8	42.4	27.0	29.5	57.0		
Nd	7.1	6.4	3.6	9.7	9.1	10.7	8.3	5.8	5.7	10.3		
Sm	1.5	2.1	0.9	2.9	1.1	4.3	3.0	3.3	2.4	3.0		
Eu	2.3	5.6	2.1	7.6	5.0	8.3	7.7	5.1	4.9	5.9		
Gd	0.4	0.9	0.4	1.5	0.9	1.4	1.3	0.8	0.9	0.8		
Tb	1.0	4.7	1.6	6.7	3.3	6.6	6.5	3.9	4.1	3.1		
Dy	0.2	1.1	0.4	1.6	0.6	1.5	1.4	1.0	1.1	0.6		
Ho	0.3	2.9	1.1	3.7	1.3	3.5	3.3	2.7	2.3	1.3		
Er	<0.1	0.5	0.1	0.6	0.2	0.6	0.5	0.4	0.4	0.2		
Tm	0.4	2.5	1.1	3.5	1.2	2.8	2.9	2.6	2.3	1.1		
Yb	<0.1	0.4	0.1	0.6	0.2	0.6	0.5	0.4	0.4	0.2		
Lu	154.58	84.43	51.77	98.31	118.74	104.35	79.63	48.17	58.16	91.72		

Table 13: Summary of existing P-T constraints from Chipman and Northwestern subdomains

Subdomain	Pressure (GPa)	Temperature (°C)	Proposed timing (Ga)	Rock Type	Reference
Chipman	1.17	850	1.9	Chipman dike	Williams et al., 1995
Chipman	1.17	850	1.9	Chipman dike	Mahan and Williams, 2005
Chipman	1.06	800	<1.9	2.6 Ga Mafic Granulite	Mahan et al., 2008
Chipman	1.35	850	2.56	2.6 Ga Mafic Granulite	Mahan et al., 2008
Chipman	1.17	850	1.9	Chipman dike	Regan et al., 2014
Chipman	1.17	850	1.9	Chipman dike	Martel et al., 2008
Chipman (CLsz)	1.06	800	1.89	Mafic granulite	Regan et al., 2014
Chipman (CLsz)	0.9	775	1.88	3.2 Ga Anorthosite	Regan et al., 2014
Chipman (CLsz)	0.8	750	1.88	Mafic Granulite	Regan et al., 2014
Northwestern (CLsz)	0.8	775	1.88	Felsic Granulite	Regan et al., 2014
Northwestern	0.9	750	1.9	Mary Granodiorite	Regan et al., 2014
Northwestern	0.9	750	2.56	Mary Granodiorite	Regan et al., 2014
Northwestern	0.9	750	2.56	Mary Granite	Dumond et al., 2010
Northwestern	0.9	750	1.9	Mary granodiorite	Williams et al., 2000
Northwestern	1.0	750	1.9	Mary Granodiorite	Williams et al., 2000
Northwestern	1.05	725	2.56	Beed Granite	*This study*
Chipman	1.35	850	2.56	Felsic Granulite	*This study*
Chipman	1.17	815	1.9	Felsic Granulite	*This study*

Table 14: Electron microprobe results for sample 10W-094g

	10W-094g						
	biot*	Grt 1	Grt1*	Grt2	Grt2*	Plag1	Plag1*
FeO	12.54	28.11	24.58	22.58	22.72	0.00	0.00
MgO	14.59	10.02	11.79	13.95	13.57	0.00	0.00
MnO	0.01	0.45	0.47	0.38	0.42	0.00	0.00
CaO	0.00	1.29	1.82	1.42	1.92	6.56	6.37
Na2O	0.13	0.00	0.00	0.00	0.00	7.73	8.17
K2O	8.58	0.00	0.00	0.00	0.00	0.52	0.07
TiO2	6.25	0.02	0.00	0.00	0.00	0.00	0.00
Al2O3	17.76	22.84	22.84	23.12	22.77	24.83	24.47
SiO2	35.36	38.06	38.99	39.50	38.24	59.93	60.85
Total	94.34	100.8	100.48	100.06	99.66	99.57	99.93
Mg/Mg+Fe	0.6903	0.3886	0.461	0.524	0.516		
Alm		0.5846	0.508	0.455	0.456		
Pyr		0.372	0.434	0.501	0.486		
Sps		0.009	0.010	0.008	0.009		
Grs		0.034	0.048	0.008	0.049		
An						0.310	0.300
Ab						0.661	0.696
Or						0.029	0.004
XFe	0.2283						
XMg	0.5655						
XMn							

Table 15: Electron microprobe results for sample 12R-054

12R-054			
	biot*	Plag1	Plag1*
FeO	19.84	0.02	0.05
MgO	8.83	0.00	0.00
MnO	0.15	0.00	0.00
CaO	0.00	9.36	5.87
Na2O	0.07	6.13	8.14
K2O	9.36	0.09	0.14
TiO2	2.92	0.00	0.00
Al2O3	18.69	28.12	24.99
SiO2	35.27	55.95	60.94
Total	95.26	99.67	100.13
Mg/Mg+Fe	0.442		
Alm			
Pyr			
Sps			
Grs			
An		0.455	0.283
Ab		0.540	0.709
Or		0.005	0.008
XFe	0.403		
XMg	0.357		
XMn			

Table 16: EPMA monazite geochronology results

Sample	domain	UO2	K2O	ThO2	CaO	SO3	P2O5	Y2O3	SrO	SiO2	PbO
12R-054	m13_outercore1	0.547581	-0.01167	6.41353	1.27987	0.021327	29.67768	1.97982	-0.0025	0.404157	1.000564
12R-054	m12_innercore1	0.612756	0.006874	4.797385	1.190083	0.014745	30.17553	2.077418	0.003954	0.158628	0.85679
12R-054	m12_outercore1	0.584783	0.003482	7.014313	1.610588	0.019481	29.84515	1.299607	-0.00269	0.240102	1.09768
12R-054	m12_innerrim1	0.55805	0.020476	6.592563	1.539185	0.021241	29.64473	1.574027	0.006089	0.235433	1.037067
12R-054	m13_innerrim1	0.562919	0.004613	6.696695	1.521753	0.028107	29.8183	1.60549	0.003765	0.262125	1.038743
12R-054	m1_outercore1	0.206373	0.012945	6.621407	0.839065	0.033765	28.80868	1.492458	0.006619	0.870019	0.874166
12R-054	m15_outercore1	0.594523	0.030763	6.300905	1.419155	0.020117	30.30373	1.780353	0.001784	0.261107	1.001867
10W-094g_1	m1core1	0.134081	0.005649	7.658608	1.165067	0.016957	29.74308	0.045535	-0.00435	0.845461	0.94851
10W-094g_1	m2outerrim1	0.094723	0.047222	3.726248	0.762986	0.026432	31.07804	0.043733	0.008202	0.301838	0.388272
10W-094g_1	m2_outercore1	0.435077	0.022087	2.587753	0.665859	0.011185	30.96018	1.563933	0.00491	0.140128	0.508728
10W-094g_1	m2_innercore1	0.373545	0.014773	4.806685	1.17362	0.024574	30.7907	0.597151	-0.01142	0.147552	0.860286
10W-094g_1	m2_innerrim1	0.288526	0.005723	7.93177	1.20468	0.018629	30.12584	0.035685	-0.00663	0.961841	1.042439
10W-094g_1	m3outercore1	0.50075	0.012168	2.909715	0.797825	0.014791	31.08667	0.459473	0.001388	0.140914	0.749698
10W-094g_1	m3innercore1	0.457113	0.003545	3.25613	0.865644	0.024015	30.63233	2.274542	0.002832	0.125786	0.739238
10W-094g_1	m4_upperrim1	0.639305	0.033454	3.523196	1.025977	0.016525	30.69696	0.329312	3.18E-05	0.096847	0.71081
10W-094g_1	m4_innercore1	0.408152	0.03073	3.192088	0.793082	0.016382	30.26618	1.097682	0.015925	0.186186	0.721024
10W-094g_1	m4_innercore1	0.408152	0.03073	3.192088	0.793082	0.016382	30.26618	1.097682	0.015925	0.186186	0.721024
10W-094g_1	m4lowerrim1	0.55809	0.023931	2.939597	0.833398	0.026662	30.44608	0.420638	-0.00564	0.095094	0.603028
10W-094g_1	m2coreright1	0.545806	0.014316	3.732083	0.979084	0.023805	30.3653	0.615028	0.009281	0.11762	0.676583
10W-094g_1	m1rimlower1	0.176183	0.027033	5.481374	0.9383	0.014798	29.40696	0.04891	0.012297	0.509413	0.715086
10W-094g_1	m1rcore2	0.099	-0.01712	8.587853	1.186718	0.009506	28.43983	0.029289	0.00261	1.043552	1.028765
10W-094g_1	m2innerrim2	0.308284	0.01147	7.91644	1.20702	0.016628	29.6507	0.046561	0.006666	0.97593	1.024695
10W-094g_1	m6outerrim2	0.121935	0.066217	3.139412	0.611526	0.010838	30.66504	0.076871	0.016202	0.253973	0.399367
10W-094g_1	m3outercore2	0.509332	0.0384	2.964578	0.823992	0.019727	30.92963	0.437214	0.00788	0.132564	0.739236
1.119098	m2innerrim3	0.286151	0.029965	7.05663		0.013378	29.81694	0.038573	-0.00066	0.812095	0.928382
10W-094g_1	m7uppercore1	0.863397	0.00843	3.692984	0.983073	0.016603	30.97354	2.601848	0.005547	0.168465	0.82129

10W-094g_1	m3_innerrim1	0.285916	0.019087	2.795598	0.673709	0.011912	30.968	1.503593	0.005653	0.134233	0.462452
10W-094g_1	m2coreright2	0.664399	0.02361	3.296285	0.934656	0.014501	30.49918	0.82367	0.020754	0.17605	0.835789
10W-094g_1	m7_upperrim1	0.435778	0.032853	5.878366	1.069742	0.019481	30.08038	0.487898	-0.00606	0.581824	0.795293
10W-094g_1	m7_lowerrim1	0.293911	-0.00165	7.006493	1.51854	0.02103	30.37513	0.212263	0.012718	0.354624	0.832356
Sample	domain	UO2	K2O	ThO2	CaO	SO3	P2O5	Y2O3	SrO	SiO2	PbO
10W-04g_1	m7mid1	0.259868	0.00268	5.83513	0.972094	0.02239	30.3849	2.167565	0.008115	0.577234	0.830864
10W-094g_1	m7lowercore1	0.563031	0.004019	3.5916	0.922786	0.023501	31.0988	2.158273	-0.00512	0.179049	0.598124
10W-094g_2	m9innerrim2	0.097437	0.013636	2.31658	0.476759	0.009326	30.5217	0.041853	-0.016	0.205318	0.311621
10W-094g_2	m9_innercore1	0.566435	0.00146	3.053693	0.892768	0.020351	30.44255	0.305176	-0.0031	0.081714	0.615337
S823b	m2outercoreleft	0.406629	0.024945	5.885394	0.174794	0.010788	27.9505	0.866943	0.005505	1.549864	0.882983
S823b	m3_core1	0.238565	0.059028	9.883168	0.449991	0.017675	26.55878	0.968649	0.000147	2.163833	1.275293
S823b	m1_core1	0.754087	0.010899	16.67246	0.184669	0.025365	22.60608	0.824671	0.00128	4.41261	2.334636
S823b	m1_rim1	0.602138	0.002565	11.21105	0.236883	0.022871	25.66428	0.86355	0	2.910123	1.596798
S823b	m1_core2	0.816215	0.00047	18.44202	0.186796	0.022849	22.05058	0.92011	0	4.97252	2.533614
S823b	m1_outerrim1	0.598904	0.005304	14.0583	0.578352	0.019197	23.92173	0.777936	0	3.587325	1.901863

CHAPTER 5

PRELIMINARY DATA FROM ANGIKUNI LAKE, NUNAVUT

Introduction

The growth, modification, and ultimate stabilization of cratonic lithosphere is a fundamental process governing the preservation of large continents. Large Paleoproterozoic belts that stitch individual Archean cratonic blocks are thought to have formed due to collional orogenisis, and given their similar size and geometry to modern orogens, have been interpreted in terms of modern plate tectonic processes (Hoffman, 1988; Corrigan et a., 2009). However, the geometries, timing, and juxtaposition of disparate Archean blocks internal to large cratonic regions persists as one of the major challenges discerning a robust tectonic framework for the formation of these regions.

The western Canadian Shield is one of Earth's major cratons and is composed of at least 4 major cratonic blocks: Slave, western Churchill, Sask, and Superior cratons. These major blocks were juxtaposed during the Paleoproterozoic assembly of the supercontinent, Nuna, approximately 1.82 Ga (Corrigan et al., 2009). The degree with which these individual cratons represent coherent continents prior to the amalgamation of Nuna remain largely enigmatic. This is particularly true within the western Churchill Province, and specifically the nature and significance of the Rae and Hearne subprovinces, which have traditionally been subdivided by the geophysically defined Snowbird Tectonic Zone (STZ)(Hoffman, 1988). The lineament has been interpreted as 1) a Paleoproterozoic suture between Rae and Hearne subprovinces (Hoffman, 1988; Berman et al., 2007), 2) an Archean intracontinental strike-slip shear system (Hanmer et al., 1994), 3) a Neoarchean suture between Rae and Hearne subprovinces (Aspler and Chiarenzelli, 1996), and 4) an anastomosing tapestry of intracontinental strike-slip and dip-slip shear zones that were active during the Paleoproterozoic (Mahan and Williams, 2005; Dumond et

al., 2013; Regan et al., 2014). However, debate persists and two emerging models are specifically debated (1 and 4).

There has been substantial work by several research groups along the south-central segment of the STZ. Little work has been reported from the northern portions of the central segment (Hanmer et al., 1994). This contribution summarizes structural data, new U-Pb zircon isotopic data, and geochemistry from Angikuni Lake, Nunavut, along the geophysical trace of the STZ to test the continuity across and along the lineament. These data are then analyzed within the context of larger datasets presented elsewhere, and varying tectonic models synthesized and tested within the context of the western Churchill Province.

Regional Background

The western Churchill Province of the western Canadian Shield represents a large tract of Archean rocks that extend from the west bounding Taltson-Thelon orogen to the southeast bounding Trans-Hudson Orogen (Hoffman, 1988). Originally delineated into the northwestern Rae and southeastern Hearne subprovinces, the two were separated by a geophysical lineament defined on the horizontal gravity map (Ross, 1992). The boundary was initially, and tentatively, interpreted as an early Paleoproterozoic suture between the Rae and Hearne at approximately 1.9 Ga (Hoffman, 1988). However, subsequent work presented in Cousens et al. (2000), showed that ca. 1.83 Ga Minette dikes (ultrapotassic) that cross cut the linemant were derived from an identical lithospheric mantle source that experienced Neoarchean metasomatism. These results were interpreted to suggest that the STZ, at the latitude of Angikuni Lake (Fig. 1) did not represent a Paleoproterozoic suture.

The STZ was considered an intracontinental feature until Berman et al. (2007) presented a regional summary and new geochronologic and thermobarometric data that supported two main changes: 1) a shift of the Paleoproterozoic boundary to the south of Angikuni Lake, with a redesignation of the Northwestern portion of the Hearne into a separate block (Chesterfield), and

2) that the boundary between Rae/Chesterfield and Hearne subprovinces represented a zone of crustal thickening and deformation interpreted to represent collisional orogenisis at ca. 1.9 Ga. Subsequent stratigraphic and detrtital zircon analysis of Paleoproterozoic basins from throughout the Canadian Shield showed similar detrital age spectra post 1.91 Ga, suggesting that the Churchill Province was coherent by then (Rainbird et al., 2010).

Rae Subprovince

The Rae subprovince is considered to contain Mesoarchean crust and lithosphere, unlike much of the neighboring Hearne subprovince (Davis and Zaleski, 1998; Zaleski et al., 1999; van Breemen et al., 2005; Martel et al., 2008), which is variably exposed in blocks throughout the region. Neoarchean (2.75 – 2.65 Ga) supracrustal belts with variable amounts of plutonic rocks are common within the mapped Rae and commonly contain distinctive Komatiite successions associated with fuschite-bearing quartzites (Machattie, 2008; Corrigan et al., 2013; Pehrsson et al., 2013; Sanborn-Barrie et al., 2014b). Neoarchean plutonic rocks ranging from 2.60 – 2.65 Ga are common within the Rae, and are predominately granitoids (Martel et al., 2008; Hanmer et al., 1992; Henderson and Loveridge, 1990), but mafic varieties also occur (Baldwin et al., 2003; Mahan et al., 2008; Flowers et al., 2008; Regan et al., in review; Chapter 4).

The Athabasca granulite terrane corresponds to a swath of highly deformed granulites that extend for a region > 20,000 km^2 exposed along the eastern margin of the Rae subprovince. The region has been used as an exposure to study lower crustal properties, interpreted as representing an isobarically-cooled terrane (Mezger, 1992; Williams et al., 2009), and is considered the best studied portion of the Rae subprovince. Detailed mapping in the northern reaches of the Athabasca granulite terrane by Martel et al. (2005) have produced substantial data, and thus serve as an even greater lateral understanding of the eastern Rae subprovince. Subsequent descriptions will be focused on these data.

Plutonism

The oldest rocks within the eastern Rae subprovince are a suite of 3.4 – 3.2 Ga tonalitic gneisses (Hanmer, 1997; Martel et al., 2008). The largest exposures of these rocks represent the deepest seated portions of the exposed Rae, and outcrop along the very eastern margin of the subprovince, where this unit is truncated by the Paleoproterozoic Legs Lake shear zone (Mahan et al., 2003; 2006a,b; Martel et al., 2008). The interpretation of the Mesoarchean lithosphere underlaying varying amounts of the Rae is supported by these exposures, and from Sm-Nd isotopic work on younger plutonic and supracrustal rocks from the Rae subprovince (van Breeman et al., 2005).

Zircon analysis from tonalitic gneisses near Snowbird Lake yielded an age of 2735 +/- 6 Ma (Martel et al., 2008), which is coeval with the development of the greenstone belt exposed within the Committee Bay (Prince Albert groupi; Skulski et al., 2003) and preliminary U-Pb analysis of rocks within the Angikuni Lake region (Aspler, personal communication). Subsequent magmatism within the Snowbird Lake region consists of the Super Mario megacrystic granite (2668 +/- 6 Ma) and the Camp granodiorite (2661 +/- 12 Ma; Martel et al., 2008). Unlike the older Zebra Tonalite, the Super Mario granite and Camp granodiorite contain relatively juvenile Sm-Nd isotopic systematics, yielding Neoarchean depleted mantle model ages (T_{DM}; Martel et al., 2008).

Circa 2.63 – 2.57 Ga granitoids are best exposed within the Tantato domain (Gilboy, 1981; Hanmer, 1997), but many other granitic intrusions of this age exist throughout the Rae subprovince, including the Rambo granodiorite (2547 +/-5 Ma; Martel et al., 2008). Within the Tantato domain, a series of gabbroic to felsic plutonic rocks compose a large >1600 km^2 composite batholith bound by the Mesoarchean Chipman batholith and Cora Lake shear zone on the southeast (Regan et al., 2014), the Grease River shear zone on the north (Dumond et al., 2008). Detailed geochemical and isotopic data are summarized in chapter 4, and display clear

evidence of being derived from a juvenile metasomatically altered lithospheric mantle at ca. 2.6 Ga (Regan et al., in prep). However, 2.6 Ga granitoids exist throughout the Rae do not all contain an "arc" signature, and may be derived from partial melting of preexisting crust.

The Chipman dike swarm is exposed along the very eastern margin of the Rae subprovince. They are predominately exposed within the Chipman batholith, but also occurs in slivers of Neoarchean plutonic rocks exposed in a wedge along the southern portion of the Chipman subdomain (Williams et al., 1995; Mahan et al., 2003; Mahan and Williams, 2005; Flowers et al., 2006a; Koteas et al., 2010). Flowers et al. (2006a) analyzed zircon grains that crystallized within the leucosome of migmatized Chipman dikes at 1896.2 +/- 0.3 Ma, and based on syn-kinematic relationships outlined in Williams et al. (1995), were interpreted to approximate the igneous age of the dike swarm. However, data presented within Regan et al. (in prep; Chapter 3) suggests an earlier, ca. 2.12 Ga age for at least one component of the Chipman dike swarm. This dike swarm represents a linear array of extensional magmatism, containing isotopic evidence of substantial contamination by preexisting lithosphere (Flowers et al., 2006a) and may mark a failed rift, which accompanied Paleoproterozoic sedimentation and basement uplift in surrounding portions of the Rae subprovince (Regan et al., in prep).

Tectonism/Regional Metamorphism

The entire Rae subprovince shows evidence of multiple phases of deformation during both the Archean and Paleoproterozoic (Mahan et al., 2006a,b; 2008; Martel et al., 2008; Bethune et al., 2012; Ashton et al., 2013; Dumond et al., 2008; 2010; 2013; 2015). The most cryptic and least well understood is evidence for ca. 2.9 Ga metamorphism preserved in Mesoarchean gneisses, xenocrysts, and whole-rock isotopic analyses (Crocker et al., 1993; Mahan et al., 2006a; Regan et al., in review; Chapter 4). Martel et al. (2008) recognized a ca. 2.60 Ga metamorphic event in older plutonic rocks exposed west of Snowbird Lake. These data were interpreted as a

thermal event and are not thought to be associated with regionally significant penetrative deformation

A widespread phase of deformation/metamorphism occurred after ca. 2.6 Ga (Baldwin et al., 2003; Mahan et al., 2006a; Mahan et al., 2008) as documented throughout the Athabasca granulite terrane and elsewhere (Bethune et al., 2012; Pehrsson et al., 2012). Recognized throughout the Rae and Chesterfield block (formerly NW Hearne), it has recently been interpreted to represent the accretion of the Chesterfield to the northeast Rae from ca. 2.55 – 2.50 Ga and is referred to as the Macquoid orogen (Davis et al., 2006; Berman et al., 2007; Pehrsson et al., 2012). Although slightly older, the main phase of Archean tectonism within the Athabasca granulite terrane is of unknown tectonic significance, but involved arc plutonism (Regan et al., in review; Chapter 4), crustal thickening (Dumond et al., 2015), and lateral flow of the lower continental crust (Dumond et al., 2010; Regan et al., in review; Chapter 4) from ca. 2.60 – 2.55 Ga. Whether these two events represent two distinct and unrelated events or represent evolving tectonic geometries during a single progressive mountain building event remains unknown. Within the Athabasca granulite terrane, ca. 2.59 – 2.55 Ga tectonism involved high grade metamorphism, which varies between lithotectonic block, with metamorphic conditions ranging from 1.5 GPa and 900°C to 0.9 GPa and 750°C. Although Paleoproterozoic paragneisses are recognized north of the Grease River shear zone, partial melting of aluminous paragneisses is known to have occurred during the phase of regional tectonism (Dumond et al., 2015; Regan et al., in review; Chapter 4).

Paleoproterozoic deformation within the Rae subprovince was widespread and long-lasting and is attributed to the varying phases of orogenisis related to the construction of the supercontinent Nuna by ca. 1.82 Ga (Corrigan et al., 2005; Pehrsson et al., 2012; Regan et al., 2014). The western Rae was host to tectonism during the final collision of the Slave and Buffalo Head cratons along the western margin of the Churchill Province from ca. 1.98 – 1.93 Ga (Card et al.,

2014). The grade and degree of tectonism due to this event decreases eastward, towards the STZ, but tectonism and metamorphic grade increase due to deformation associated with the STZ at ca. 1.9 Ga (Williams et al., 1995; Mahan et al., 2008; Martel et al., 2008; Williams and Jercinovic, 2012). Following 1.9 Ga tectonism throughout the Rae, deformation was localized on thick ductile shear zones, which juxtaposed various lithotectonic subdomains of varying rock types and metamorphic grade (Flowers et al., 2006b; Dumond et al., 2013; Regan et al., 2014; Chapter 2). Regan et al. (2014) concluded that shear zone kinematics record the varying phases of accretion along the western margin (Taltson-Thelon and Wopmay orogens)(Hildebrand et al., 2010) and southern (Trans-Hudson orogen) margins (Corrigan et al., 2010).

Hearne Subprovince

The Hearne subprovince represents a large region consisting of Neoarchean mafic and felsic volcanic unites, siliclastic, chemogenic, and volcanoclastic units (Aspler and Chiarenzelli 1996). Based on 1:50,000 scale reconassaince mapping, Aspler and Chiarenzelli (1996) correlated much of Hearne subprovince as being underlain by the second largest greenstone belt in Canada: the Ennadai-Rankin Greenstone belt. However the designation of the northwestern Hearne as the Chesterfield block removes a large portion of this belt, but descriptions below are broad and apply mainly to the central Hearne (Henik, Kaminak, and Poorfish-Windy segments)(Aspler et al., 2002a; Davis et al., 2004; Cousens et al., 2004) In contrast to the shallow water and rift related greenstones in the Rae subprovince, the detailed stratigraphy and physical volcanology has shown that rocks of the central Hearne developed distal from continental influence and were largely subaqueous volcanic centers active well below storm weather wave base (Aspler and Chiarenzelli, 1996; *and references therein*).

Plutonism

Plutonic rocks of the Ennadai-Rankin greenstone belt have had relatively little work when compared to the neighboring Rae subprovince, and geochronologic descriptions below are largely derived from Davis et al. (2004) focused within Kaminak segment along the eastern

portion of the central Hearne. U-Pb zircon analysis indicate three main phases of crust formation with a well bracketed phase of deformation from 2711 to 2667 Ma (Davis et al., 2004). However, an increasing number of ca. 2.72 Ga tonalitic orthogneisses are being recognized within the central Hearne (van Breeman et al., 2007; this study). Cousens et al. (2004) performed systematic Sm-Nd and bulk rock geochemical analysis on the two main phases of plutonic and volcanogenic rocks from the Henik segment of the central Hearne subprovince. As noted by Davis et al. (2004), these authors suggested that phase 1 magmatism consisted of tholeittic trends and flat incompatible element trends indicative of a plume or incipient asthenospherically derived melt. Phase 2 magmatism contained evidence for a calc-alkaline signature and trace element patterns inidicative of a subduction-like metasomatic signature (Cousens et al., 2004; van Breeman et al., 2007). These data were interpreted as representing an infant arc setting akin to the western Pacific today, where the onset of subduction is recognized, but evidence for a fully developed arc is lacking. Evidence of older lithospheric sources is variable, and is typically restricted certain 'blocks' within the southern, and less common within the central, Hearne subprovince (van Breeman et al., 2007).

The Kaminak dike swarm form a N trending set of dikes that are exposed over a region > 10,000 km^2 (Sandeman et al., 2012). Although the southern extent of the dike swarm is not well constrained, and the presence of the Kaminak dike swarm north of the Happy Lake shear zone/Pork arch shear zone remains a debate (Berman et al., 2007), U-Pb work on a Kaminak dike yielded a precise age of 2497.1 +/- 1.1 Ma (Sandeman et al., 2012).

The Griffin Gabbro sills represent an aerially extensive suite of thick gabbroic sills present within the Paleoproterozoic Hurwitz group (Aspler et al., 2002b). U-Pb analysis yielded a ca. 2.11 Ga age for the gabbroic sills (Patterson and Heaman, 1991; Heaman and La Cheminant, 1993), and subsequent geochemical and isotopic data were carried and presented in Aspler et al. (2002b). The Griffin gabbros have flat incompatible element trends and are interpreted as being

derived from an enriched asthenospheric source (Aspler et al., 2002b). Given the lack of dikes within the surrounding Whiterock Formation of the lower Hurwitz basin, which would be obvious given the color contrast, the authors suggested that emplacement of the Griffin Gabbro sills occurred via long transport. Sm-Nd isotopic constraints are consistent with this hypothesis.

Tectonism/Regional Metamorphism

The peak metamorphic conditions reached for much of the Hearne subprovince was greenschist grade (Hanmer et al., 2004). Detailed work within the Macquoid supracrustal belt and overlaying Cross-Bay plutonic complex display strong evidence for ca. 2.55 – 2.50 Ga tectonism (Hanmer et al., 2006; Davis et al., 2006), which is one of the reasons it is now considered a separate entity (Chesterfield block; Berman et al., 2007). The remainder of the Hearne subprovince has several recognized phases of penetrative tectonism best outlined in Hanmer et al. (2004) and Davis et al. (2004). Bracketed by the two main magmatic/volcanic pulses, the first phase of deformation is interpreted as having occurred at ca. 2.69 Ga (Davis et al., 2004; Hanmer et al., 2004). The main phase of regionally extensive deformation accompanied the tail-end of the second phase of magmatism at ca. 2.68 Ga.

Paleoproterozoic deformation within the central Hearne subprovince consists of large-amplitude folding and thick-skinned thrusting (Aspler et al., 2002a). The best studied Paleoproterozoic features are exposed within the Poorfish-Windy group in the western central Hearne, east of Kasba Lake. Both Paleoproterozoic sedimentary rocks belonging to the Hurwitz group and underlying Neoarchean supracrustal rocks contain large amplitude folds with NW verging thrust faults souled in the Nearchean basement lithologies (Aspler et al., 2002a). Based on preliminary titanite ages presented in Aspler et al. (2002a), these authors suggested that this phase of deformation was due to the final collision of Superior and western Churchill Province at ca. 1.82 Ga.

Current tectonic model

There is no question that 1.9 Ga was a time of high-P, high-T, granulite facies metamorphism and deformation along and adjacent to several parts of the STZ. Metamorphic analysis combined with in-situ monazite geochronology indicates pressures on the order of 1.0 GPa and temperatures above 700 ºC (Krikorian, 2002; Mahan and Williams; 2005;Williams et al., 2009; Dumond et al., 2010;Regan et al., 2014). Deformation in many parts of the central segment involved upright folding with shallowly plunging axes, NE-striking axial planes, and a component of dextral shearing. Fold amplitudes range from meters to kilometers (Regan et al., in review; Holland et al., 2012, Martel et al., 2008). High-P-T metamorphism and deformation has also been described in the northern and southern segments of the STZ (Berman et al., 2002; Sanborn-Barrie et al., 2001; Hanmer and Williams, 2001). If inferred age constraints are correct, this metamorphism and deformation broadly accompanied emplacement of the Chipman Dike Swarm and correlatives. The 1.9 Ga granulite facies eventis, in essence, the "Snowbird event" but it is not clear if it is the cause, result, or is merely associated with the STZ. As noted above, a broad array of models have been proposed that can be divided into two distinct groups: (1) those in which the STZ represents a Proterozoic continental suture, that is, the site of an ocean basin that was closed at ca. 1.9 Ga between the Rae and Hearne continents and (2) models in which the STZ represents an Archean structure, reactivated at 1.9 Ga.

Proterozoic Collisional Model

Berman et al. (2007) suggested that the Snowbird event reflects the collision and suturing of the Rae and Hearne subprovinces at ca. 1.9 Ga, and this would certainly be considered the prevailing hypothesis among many current workers. Evidence includes the interpretation of a subduction-related delamination setting for the Chipman dike swarm, the presence of a belt of high-P assemblages (with eclogite in the East Athabasca triangle, diamond bearing lampophyre dikes interpreted to reflect subduction under the Hearne province, and general P-T-t differences across the STZ. The lack of ca. 2.60 Ga granites, which are very common throughout the Rae

and Chesterfield subprovinces, have not been identified in the Hearne (Hanmer et al., 2004; Davis et al., 2004; Pehrsson et al., 2013). A number of these pieces of evidence involve our own work in the Athabasca Granulite Terrane including the Chipman Dike Swarm, and evidence of high-P metamorphism including eclogite. Although we find alternative interpretations compelling for each piece of evidence, we admit that no data exist to unambiguously negate this interpretation..

Proterozoic Reactivation Model(s)

The alternate model, and the hypothesis of this proposed research, suggests that the Rae and Hearne domains were sutured in the Archean (ca. 2.6 Ga) and that the STZ represents a zone of Proterozoic reactivation that generally corresponds with the Rae-Hearne boundary. By this model, crustal thickening at 2.6-2.55 Ga and the resulting lower crustal flow, represent the suturing of the Rae and Hearne continental fragments (Dumond et al., 2010; Mahan et al., 2006b). The 1.9 Ga Chipman dike swarm is interpreted in terms of incipient rifting and then shearing of the already-amalgamated Churchill craton (Flowers et al., 2006a). A central aspect of our hypothesis is that deformation along the STZ, in fact the very essence of the STZ, reflects the weakening of the Churchill crust that is associated with the Chipman dike swarm. We suggest that the effects of this weakening may have persisted for as much as 50 m.y. in the deep crust until the rocks were uplifted and exhumed.

Angikuni Lake

Angikuni Lake, Nunavut, is located along the geophysically defined STZ (Aspler et al., 1999), and is the location where Cousens et al (2001) performed a systematic isotopic study of 1.83 Ga minette dikes. These results showed evidence for a common, Archean, lithospheric mantle beneath both sides of the STZ, thus confirming an intracontinental setting during the Paleoproterozoic. This prompted a movement of the Paleoproterozoic suture southward through the western side of Angikuni Lake, with everything to the east no longer considered Hearne, but belonging to a distinctive craton: the Chesterfield (Berman et al., 2007). Therefore, under the

current model, Angikuni Lake is the location where three individual Archean plates are sutured, and is thus an ideal place to test the current tectonic model.

Background and structure

Regional, 1:50,000 scale mapping was carried out within the three main map sheets that encompass the Angikuni Lake region by Aspler and Chiarenzelli in the mid 1990s. The region was subdivided into 7 main lithotectonic blocks, and detailed descriptions provided in Aspler et al. (1998, 1999) and Berman et al. (2000). We will briefly summarize the initial subdomains (domains after Aspler et al., 1998a,b; 1999).

Subdomain I

The eastern panel of the Angikuni Lake area is underlain by greenschist facies suprarustal rocks including pillow lavas, non-pillowed flows, and variably thick feeder dikes/stocks. A strong layer parallel cleavage exists in all lithologies, and warps around bioite-bearing leucogranite plutons. Top-up indicators suggest a northwest younging sequence. Underlaying the supracrustal assemblage is a thick unit of deformed psammitic gneisses that were interpreted in Aspler et al. (1998a) as immature arenites to subarkoses.

Subdomain I is bound on its western margin by a thick (ca. 0.5 km wide) north trending upper amphibolite facies shear zone. Mineral stretching lineations and intersection lineations plunge shallowly to the north (5 - 15°). σ and δ –clast asymmetry around garnet – porphyroblasts, assymetric folds, and shear bands display dextral sense of shear (Passchier and Trouw, XXXX). Supracrustal rocks of subdomain I are mylonitized within the shear zone, and is associated with the growth of fine to coarse garnet porphyroblasts.

Subdomain II:

West of subdomain I is a thick (ca. 15 km) panel dominated by variably deformed tonalitic to granitic plutonic rocks. Gneissosity developed within these orthogneiss bodies intensify near the I-II shear zone. Entrained within, and draped around, these plutonic bodies are

numerous, and sometimes spatially extensive (map-scale) and variably assimilated, supracrustal rocks that were interpreted by Aspler et al. (1998) as immature arenites or felsic tuffs. They contain multiple generations of neosome which cross cut compositional layering. A syntectonic granite from the northeastern portion of subdomain II was analyzed for U-Pb in zircon and yielded a preliminary 2.61 Ga age (Aspler, unpublished data). Most outcrops are cut by gabbroic dikes that range in orientation, with the vast majority trending NE-SW (045°) and are commonly subvertical. The dikes, which can be as large as 200 m wide, cross cut gneissosity and the cataclastic granite, commonly contain xenoliths of country rock, and exhibit chill margins. Some dikes contain a heterogeneous layering initially interpreted as a variably developed gneissosity, but evidence for subsolidus processes are lacking, and may represent igneous flow foliation.

The zone dividing subdomain II and III is a series of several hundered meter-wide fault segments that trend N, NE, and EW. Commonly these fault segments contain a distinctive granitic unit referred to as the cataclastic granite. It is similar to autobreccias studied within Nova Scotia and elsewhere (*citation*). The granite consists of a fine to medium grained matrix, with blocks of texturally distinct granite within it, all of which are cross cut by several generations of epidote + chlorite veinlets. Blocks of granite show evidence of brecciation predating surrounding granite, which are also brecciated. Therefore, we interpret the granite to have brecciated itself during emplacement, possibly during juxtaposition of subdomain II and III. In one location, a large gabbroic dike cross cuts and contains xenoliths of the cataclastic breccia, and therefore post-dates crystallization of the granite. However, these dikes do not occur in adjacent subdomains suggesting that the I-II shear zone and faulting between subdomain II and III, at least in part, occurred after dike emplacement.

Subdomain III:

Subdomain III consists of a thick greenschist facies supracrustal sequence containing two main subunits separated by an unconformity (Aspler et al., 1998). The lower unit consists of

mafic and felsic volcanic flows, pillows, and plutonic equivalents. A preliminary U-Pb zircon age presented in Loveridge et al. (1988) yielded a ca. 2.68 Ga age and contained ca. 3.0 Ga xenocrysts (Eade, 1986). Immediately overlaying the lower unit is a sequence of subarkose and quartz-pebble conglomerate forming the lower subunit to the upper sequence of subdomain III. Also paraconglomerates with a siltstone matrix are common, and contain a strong pencil lineation shallowly plunging to the north. Overlaying these sedimentary rock types is a series of felsic volcanic rocks. All rock types of subdomain III are folded by open folds with a northeast trending axial surface. The boundary between subdomain III and IV is a composite intrusive fault contact that trends to the north. Granite cataclasite is also present along this boundary.

Subdomain IV:

Granite to granodioritic rocks dominate subdomain IV, and are variably tectonized and cross cut by E-W trending fault segments. Rocks of this subdomain continue across the geophysical trace of the STZ unhindered ('Tulemalu Fault' after Eade, 1986). Rocks of this subdomain were not studied here due to accessibility and logistical limitations

Subdomain V:

The western portion of Angikuni Lake is underlain by magnetite bearing leucogranite with rare mafic supracrustal xenoliths and enclaves. There are subordinate granite gneiss, porphyroclastic granitoids, which contain a strong gneissic to mylonitic fabric. The northwestern portion of subdomain V forms a curvilinear shear zone with antiformal geometry plunging shallow to moderately to the NE. The thick heterogeneous package of subdomain VI structurally overlays rocks of Subdomain V, and represents the boundary between III/IV and V, and may itself be a thick ductile shear zone containing a mix of lithologies derived from the host wall rocks.

Subdomain VI:

Introduced in Aspler et al. (1999), rocks of subdomain VI form the structural roof to rocks of subdomain V, and is composed of transposed and intercalated metaplutonic rocks from

subdomain I, II, and V, with subordinate mafic mylonites. The dominant rock type, however, is a granodioritic gneiss. All rock types contain a strong tectonic overprint and form a curvilinear shear zone with a down dip extent of ca. 15 km. The shear zone, and whole subdomain, is assymetric and wraps around an antiformal bend to a NE trend, where rocks of subdomain VI cross the geophysical trace of the STZ. From the hinge region south, where the rocks of subdomain VI trend N-S, stretching lineations are down dip, and have consistently normal kinematics. Late, open, upright folds (lower most subdomain VI) have axes collinear with the stretching lineation and may be related to extensional deformation. Greenschist grade mylonites and cataclasite weave throughout subdomain VI, and overprint a higher grade event. Given the similarity in kinematics and orientation to higher grade (amphibolite facies) components of the shear zone, the two phases of deformation may be progressive, and due to exhumation of the higher grade footwall rocks (subdomain V) adjacent to lower grade rocks of subdomain III.

Subdomain VII:

The very northwestern portion of Angikuni Lake, approximately three km to the northwest of the geophysical trace of the STZ are rocks of subdomain VII. Strongly deformed rocks of subdomain VI are truncated by coarse-grained syenite to quartz syenite lithologies with porphyroclasts up to 10 cm. These rocks are relatively low strain, but contain abundant strain gradients cored by discrete greenschist facies, strike-lineated, ultramylonites and cataclasite.

Two sutures?

The redesignation of the NW Hearne subprovince into the Chesterfield block of Berman et al. (2007), required a suture to be drawn between the Hearne and Chesterfield at the subdomain V-VI boundary. The Rae-Chesterfield was placed within the NE trending segment of subdomain VI along the trace of the STZ. There is little evidence for contractional deformation along north trending segment of subdomain VI, which subdivides lower grade subdomain III rocks in the hangingwall from relatively higher grade rock types in the footwall (subdomain V). Kinematics suggest normal, top-down to the east, relative motion, more akin to extensional, core-complex

type, deformation (Lister and Davis, XXXX). No evidence of thrusting was observed along this boundary.

Transect across the Snowbird Tectonic Zone

The geophysical trace of the STZ at the latitude of Angikuni Lake, on the ground, is delineated by a 100m wide belt of highly brecciated and hydrothermally altered rock corresponding to a NE striking fault strand (Aspler et al., 1999). The fault zone is coring a ca. 4-5 km wide mylonite zone underlain by mylonitic orthogneisses of subdomain VI (Aspler et al., 1999). The fault zone itself consists mostly of cataclasite with chlorite and epidote mineralization. The center of the fault zone contains a ca. 1 m wide straight zone of light-colored and amorphous material with several rounded clasts. Whether this material represents a very thick zone of frictional melt (pseudotachylite) or a highly disaggregated and comminuted material remains unresolved (Pec et al., 2012). The material is evidence of major brittle motion along this fault segment in either interpretation. However, lithologic continuity across the zone suggests that it did not accommodate substantial vertical offset.

South of the breccia zone is dominated by syenitic to quartz syenitic orthogneisses containing a protomylonitic fabric that strikes NE with a subvertical dip, and a subhorizontal stretching lineation. Proximal to the fault zone, the syentic rocks contain little evidence of subsolidus deformation, and there is milky quartz in fractures, suggesting that hydrothermal alteration related to faulting may have removed the microtextural relationships preserved in rocks further away from the fault zone. Immediately to the south of the fault zone, and to the north, is mylonitized magnetite-bearing leucogranite (15R-024 below). Immediately adjacent to the fault zone, this unit loses the mylonitic fabric, and does not contain detectable magnetite, probably related to fluid flow in the adjacent fault zone. This unit continues for ca. 1.5 km across strike to the north, where it becomes interlayered on decimeter scale with biotite-garnet kspar megacrystic granite gneiss containing evidence for dextral sense of motion. There is one 5 m wide sliver of

gabbroic mylonite, which then is bound on its northern side by more ultramylonitic magnetite-bearing leucogranite. At the far northern margin of the shear zone, mylonitic felsic gneisses grade into granodioritic gneisses (sample 15R-030 below).

As noted in Aspler et al. (1999), the kinematics within the shear zone vary. The vast majority of kinematic indicators suggested dextral sense of motion, however dismembered pegmatite assymetries suggest sinistral sense of motion along the northern portion of the transect. However, dextral kinematics are the dominant sense of shear across the mylonite zone.

Analytical Methods

Geochemistry was performed at ACME labs in Vancouver for 72 elements. Pieces of fresh rock were cut and sent to be powdered in the facilities at ACME. Samples were analyzed by x-ray fluorescence (major elements) and inductively coupled plasma - mass spectrometry (trace and rare earth elements).

Zircon grains were separated from bulk sample via traditional crushing, Wilfley table, heavy liquid, and Frentz magnetic seperations at the University of Arizona, Laserchron center. Grains were mounted with three standards: R33, Sri Lanka, and FC-1. Mounts were then polished to display zircon mid-sections. All grains were imaged with both BSE and CL imaging techniques Hitachi 3400N SEM and a Gatan CL2 detector system. Grains were then analyzed by LA-ICP-MS on the Element 2. A beam size of 20μm was used. Prior to ablation, every analyzed location was cleaned with a very brief (~1 sec) laser with a 30 μm beam to ensure no surface contamination in or around the analyzed region. Analytical techniques are described in Gehrels et al. (2008) and Gehrels and Pecha, (2014).

Geochemistry

U-Pb isotopic data

Previous analytical data

The rocks at Angikuni Lake were host to a preliminary petrologic and geochronologic analysis presented in Berman et al. (2002). A paragneiss from subdomain II was selected for

detailed thermobarometry and monazite geochronology by SHRIMP (Sensitive high resolutions ion microprobe). Two generations of garnet were distinguished based on Ca content, and thought to represent metamorphic assemblages that grew at 2.55 Ga (5.4 GPa and 730 °C) and ca. 1.9 Ga (1.1 GPa and 750°C). However, more in-situ monazite geochronology is currently underway at the University of Massachusetts, Amherst. However, nearly undeformed granitic rocks yielded a U-Pb zircon age of 2.6 Ga (Aspler, unpublished data), and so more work is required to evaluate the timing of regional deformation.

15R-030

Sample 15R-030 is a granodioritic gneiss along the northern reaches of subdomain VI, north of the geophysical trace of the STZ. Backscattered electron (BSE) and cathodoluminescence (CL) imaging of zircon seperates yielded nearly identical textural relationships, and will further be subdivided on basis of BSE zonation and U/Th ratios. 35 analyses by LA-ICP-MS were performed on representative morphologies and generations defined by BSE. Six analyses were thrown out due to very low concordance likely related to corresponding high U contents.

Cores are typically dark in BSE, contain prismatic shapes and faint oscillatory zoning. Several bright irregular cores were identified in BSE, and were partially resporbed by the lower BSE, and oscillatory zoned, generation and are thus interpreted as xenocrysts. 14 analyses of igneous cores yielded a weighted mean of 2712 +/- 5.4 Ma (MSWD = 1.05; POF: 0.40). U/Th ratios of this generation display a coherent population ranging from 0.5 to 3.5. These results collectively suggest a crystallization age of the granodiorite. Bright, occasionally sector zoned, rims commonly are present as assymetric overgrowths, or contain lobate textures impinging on igneous cores. These are interpreted as metamorphic in origin, some of which, based on morphology, may be syn-kinematic with some component of deformation. U/Th ratios of this generation of zircon range from 4.0 to 12.0. Seven out of nine analyses yielded ages ranging

from 2.52 to 2.60 Ga. Two analyses, with the highest U/Th ratios, greater than 14.0, yielded ages below 2.4, and are of unknown significance.

15R-024

The magnetite-bearing leucogranite mylonite within the narrows is located along the geophysical trace of the STZ. A total of 70 analyses were performed on zircon grain separates from this sample owing to a high degree of inheritance, high U-contents, and radiation damage. 43 analyses are reported herein, and appear to be statistically robust. Grains range in size from coarse grains that vary in color and shape, and contain complex and heterogenous mixtures of both bright and dark BSE signals, and typically contain inclusions. Equant crystals range from 100 to 300 µms, with about half of the crystals containing dark cores (BSE). These cores are truncated by a generation of bright, faintly zoned rims. Bright generations of zircon also occur as full crystals without the dark cores. Therefore, the dark cores are interpreted as xenocrysts, and bright generation of zircon as igneous.

Results yielded a wide spread of ages and U/Th contents and ratios. Inherited cores yielded ages ranging from 2750 to 3100 Ma, Analyses of bright igneous cores and overgrowths on xenocrysts range from 2750 – 2650 Ma. The lowest U/Th ratios are below 10.0, and consist of six analyses that yield an average of 2671 + 35 – 21 with a 93 % confidence based on a coherent group eight from all the analyses. Younger zircon ages cluster just after crystallization and exclusively contain U/Th ratio's greater than 10.0. However, these are differentiated solely on composition without much textural evidence supporting the conclusion. This generation of zircon ages ranges down to ca. 2590 Ma. Two U/Th analyses yielded ages of 1965 and 1915 Ma, and form distinctive dark tips on an igneous core. These results are consistent with a ca. 2.67 Ga crystallization followed by both Neoarchean and Paleoproterozoic tectonism.

15R-022a

A sample of a Plagioclase + kspar megacrystic biotite granite gneiss just north of the geophysical trace of the STZ was collected for U-Pb analysis to establish a crystallization age. Zircon crystals have a wide range of morphologies, sizes, and BSE and CL signals. 35 analyses were performed to characterize each for age and U/Th ratios. Based on the wide array of BSE and CL signals, the data was differentiated based on U/Th ratios primarily, and individual zircon relationships. U/Th ratios differentiating predominantely two populations of zircon: 1) low (< 10.0) and 2) high (> 50.0).

Two xenocrystic ages were outliers within the data set, and were bright in BSE images, and form innermost cores within large zircon crystals. The remainder of low U zircon analyses range between 2689 – 2533 Ma. However, based on core – rim relationships, a weighted mean was produced on cores, which are consistently older than rim counterparts, and yielded a weighted mean of 2671 +/- 10 Ma (MSWD = 2.5), interpreted to represent the crystallization age. Rims show a minor increase in mean U/Th ratio, and range from 2626 to 2533 Ma, interpreted as metamorphic or partially recrystallized grains. The remainder of the analysis yielded Paleoproterozoic $^{206}Pb/^{207}Pb$ ages, and both form rims on Archean cores, and compose whole zircon crystals. This generation of zircon is characterized by a drastic increase in U/Th ratios, greater than 50 times that of the corresponding Neoarchean population, interpreted to reflect metamorphism/deformation within the mylonite/fault zone. The weighted mean of this generation of zircon is 1852 +/- 14 (MSWD: 8.8). The high MSWD suggest that there are several populations averaged together, and that there may be more than one generations of Paleoproterozoic metamorphic zircon.

15R-037

Two samples from the footwall of the V-III shear zone from southern Angikuni Lake were taken for zircon U-Th-Pb geochronology. The locality is composed of an equigranular, migmatized, quartz-plag-biotite-paragneiss. The outcrop contains two generations of folds, and

two generations of gneissosity. The earliest gneissosity (S_1) is defined by isoclinal folds well preserved within leucosomal lenses. This foliation is overprinted by an axial planar fabric, which is the main fabric at the outcrop (D_2) and strikes to the northwest, and dips moderately to the northeast. This foliation is effected by open moderately plunging folds that gently warp the second foliation throughout the outcrop, and plunge moderately to the Northeast. There is no axial planar fabric associated with D_3, but several thick meter thick pegmatites cross cut D_2 fabrics, but are folded by F_3. F_3 folds are interpreted to have formed during extensional deformation along the V-III shear zone (subdomain VI), consistent with parrallel stretching lineations to the axis of open folds (F_3) in the immediate footwall sampled here.

The coarse pegmatite containing F_3 folds, but cross cutting the remaining structural components was collected to place a maximum age of extensional deformation within the adjacent shear zone (15R-037a). Due to high U contents, a number of analyses were thrown out. Only analyses between 95 and 102 % concordance were kept. Analyses displayed a large degree of scatter, but based on the youngest population of zircon, which also formed the most reasonable and reproducible population, a weighted mean of 1868 +/- 13 Ma (MSWD : 3.4) is interpreted as a crystallization age. (n= 6). This places a maximum age on juxtaposition of subdomains V and III, and a minimum age for all other phases of deformation.

A sample of the migmatized host rock was collected to establish time of penetrative deformation and migmatization (15R-037b). Samples range in size and morphology from 100 to 400 μm. Analyses displayed a wide range in U-Pb ages, with a distinct spread in U/Th ratios occurring between 2.60 and 2.55 Ga, interpreted to represent metamorphic zircon growth during partial melting. A weighted mean of this zircon generation is 2575 +/- 6.2 Ma (MSWD: 0.94; n = 5). Older analyses are scattered and range from 2.65 – 2.75 Ga, and are interpreted as detrital. Several analyses yielded Paleoproterozoic ages, the most concordant being a $^{206}Pb/^{207}Pb$ age of 1902 Ma.

15R-041

Two samples from the lower subunit of the upper sequence in subdomain III were collected for detrital analysis (Aspler et al., 1998). A sample of a quartzite and paraconglomerate with siltstone matrix were acquired from a single outcrop. The quartzite did not contain abundant zircon, so results are pooled together. But analysis of the separate results yielded nearly identical results. A total of 106 analyses are reported herein.

Samples contained a youngest detrital zircon age of ca. 2685 +/- 25 Ma. The dominant detrital spectra is centered at approximately 2718 Ma, 2826 Ma, and 2978 Ma. There is a population of Mesoarchean grains as well ranging from 3100 – 3600 Ma, with the oldest grain analyzed yielding an age of 3590 +/- 11.7 Ma. These results are consistent with derivation from local sources with the predominant age populations being representative of subdomain I and III (Loveridge et al., 1988), and older generations of zircon present in the form of xenocrystic in the two igneous samples analyzed. The presence of a strong Mesoarchean signature suggests that a component of detritus was derived from exposed, and evolved, Mesoarchean crust consistent with xenocrysts analyzed from intermediate flows (Loveridge et al., 1988; Eade, 1988), and sample 15R-024 above. Therefore, the region was close to a continental influence during deposition after ca. 2.68 Ga.

Summary and interpretation of geochronology results from Angikuni Lake

Two igneous and one detrital samples above provide preliminary constraints on the growth and evolution of the Angikuni Lake region. As suggested by Aspler et al. (1999), rocks continue, unimpeded across the putative trace of the STZ, suggesting that the geophysical lineament, on the ground, does not correspond to a suture. Furthermore, sample 15R-024, the magnetite leucogranite yielded an age of 2671 Ma, and is present across the STZ, and occurs on both sides of the V-VI boundary, currently thought to represent the suture between Chesterfield

and Hearne subprovinces, suggesting the distinct blocks of western Angikuni Lake were together prior to 2671 Ma. Inheritance within this sample confirms the presence of more evolved and older lithosphere at depth, inconsistent with juvenile settings thought to compose much of the central Hearne (Cousens et al., 2004; Davis et al., 2004).

The single detrital sample taken from subdomain III yielded several populations, perhaps of biggest interest being the large Mesoarchean population. The remainder of the detrital age spectra is consistent with local derivation. The existence of Mesoarchean grains in such abundance suggest that detritus was being derived from evolved and exposed continental crust that formed during the Mesoarchean. The Rae subprovince contains abundant evidence, and exposures, of crust and lithosphere of this age (Pehrsson et al., personal communication). However, rare blocks of Mesoarchean rocks do occur in the SW Hearne as well (Aspler and Chiarenzelli, 1996).

Results suggest that granitoid rocks of the Angikuni Lake region formed during the growth of granite-greenstone belts present throughout the Rae and Hearn subprovinces (Hoffman, 1988). The detrital ages paired with the presence of xenocrystic zircon suggest a continental setting, and based on sedimentologic constrainsts outlined in Aspler et al. (1999) may have been deposited along an Archean continental margin just after ca. 2.68 Ga.

Charlebois and Balliet Lakes

Charlebois and Balliet Lakes are positioned along the very western margin of the Hearne subprovince, just south of the well studied Athabasca granulite terrane (Mahan et al., 2003). Field work done in 2015 was performed to add additional constraints on the structural evolution of the northwestern Hearne subprobince, and to collect geochronologic samples to establish a temporal framework. Charlebois was chosen due to its close proximity to the well studied Athabasca Granulite Terrane of the eastern Rae subprovince, and contained abundant structural and petrologic context provided in Mahan et al. (2003)..

Structure

Contractional deformation related to the Legs Lake shear zone (ca. 1.84 Ga; Mahan et al., 2006a) is variably present throughout the region, and is delineated by thick (ca. 300 m) zones of Northeast trending mylonite, dipping moderately to the northwest. Kinematics are consistently dextral/normal, and suggest hangingwall up, oblique-reverse slip motion consistent with mapping and structural analysis presented in Mahan et al. (2003; 2006a,b). The eastern most extent of 2.6 Ga granitoids and presence of Chipman dikes are interpreted to delineate the boundary between Rae and Hearne subprovinces on the ground. Mapping in 2015 at Balliet Lake identified this line, which is northeast trending, and cuts through the western side of Balliet Lake, and parallels the contractional Legs Lake shear zone (Mahan et al., 2003). To the east of this line is lower grade, well preserved greenstone, lower amphibolite to greenschist facies supracrustal rocks, and granite plutons.

Early structural fabrics are SE-NW, and dip shallowly to moderately to the southwest. Zones, interpreted as low strain zones, preserve this fabric and are segmented by northeast trending thrust-sense shear zones interpreted as Legs Lake –related strain. All lithologies are cut into E-W trending mylonite zones distal from any Legs Lake shear zone related strain. Similarly to rocks exposed at Angikuni Lake, there are subdomains of relatively low-grade supracrustal rocks including mafic flows and pillows, and higher grade subdomains of highly deformed gneisses.

U-Pb isotopic data

15W-042

A sample of a tonalitic to granodioritic gneiss was sampled from the structurally lowest portion of the Northwestern Hearne subprovince at Charlebois Lake. Zircon grains range in size, but are typically elongate prisms ranging from 50 to 400 µms and are dark to colorless in reflected light. Zircon grains contain multiple generations of concentric zonation in backscatter and cathodeluminescence images, and range from light to dark signals. Many grains contain rims

that range from light sector zoning to irregular embayments into darker cores. The majority of concentrically zoned cores are interpreted as igneous in origin, with those showing several generations of concentric zones representing inherited, or xenocrystic grains. A total of 33 analyses were performed to establish a crystallization age.

Nine concordant analyses of the best preserved concentrically zoned cores yield a weighted mean of 2721 +/-6.4 Ma (MSWD: 1.8), interpreted as representing a crystallization age. All Th/U ratios are below 2.0. However, cores with similar U/Th ratios range back to 2909 +/- 16 Ma, with the majority yielding ca. 2.77 Ga $^{207}Pb/^{206}Pb$ ages, and are collectively interpreted as xenocrystic. Younger rim populations gradually increase in U/Th ratios through time. Two rim analyses of a core-rim pair yielded 2522 +/- 20 and 2567 +/- 26 Ma, respectively, interpreted to be metamorphic in origin. Younger generations are scattered, consistently have very high Th/U ratios (> 20), and range from 1825 - 2350 Ma, interpreted as partially reset or metamorphic zircon crystals.

Discussion

Results presented above have bearing on current tectonic models and ongoing debate. First and perhaps foremost, is the lack of regionally extensive Paleoproterozoic deformation at the latitude of Angikuni Lake. Paleoproterozoic strain is distributed as shear zones and fault strands, all of which are cross cur by ca. 1.84 Ga Christopher Island minette dikes (Aspler et al., 1998; Cousens et al., 2000). Based on xenocrystic zircon from magnetite-bearing leucogranite and Mesoarchean xenocrystic zircon presented elsewhere (Eade, 1986), rocks at Angikuni Lake likely formed in proximity to relatively evolved continental crust. Moreover, based on geochemistry of contemporaneous supracrustal rocks (subdomain III; Cousens et al., 1998), rocks likely formed in a back arc to rift setting as discussed elsewhere (Aspler et al., 1998; 1999; Cousens et al., 1998) from ca. 2.720 to 2.660 Ga. This is in stark contrast for rocks exposed within the central Hearne, which are thought to have formed distal to any continental influence (Aspler and Chiarenzelli,

1996), but at the same time. Therefore, the timing, character, and relationships of rocks exposed at Angikuni lake are similar to those in the central Hearne, but contain more evidence of interacting with, or being derived from, more evolved continental source.

All rocks, except for those related to the deposition of the Baker Lake group (ca. 1.83 Ga), are variably deformed, with the vast majority of deformation likely having been accommodated within localized shear and fault zones that collectively form a branching structure. These discontinuities mark breaks in metamorphic grade, dominant rock types, and truncate fabrics internal to each subdomain. This illustrated well by late gabbroic dikes that cross cut the majority of granite and gneisses in subdomain II and contain little evidence of penetrative deformation. However, these dikes do not extend into neighboring subdomains, suggesting that motion along I-II shear zone, and the II-III fault zone were of a large enough magnitude to truncate the intrusive complex. U-Pb zircon analysis of these dikes is currently underway.

The largest zone of penetrativily deformed rocks at Angikuni Lake belong to subdomain VI, which can be thought of as thick ductile shear zone in of itself. The western boundary of subdomain VI currently delineates the suture between the Chesterfield and Hearne subprovinces, thought to represent a ca. 1.91 Ga suture between the two (Berman et al., 2007). However, the kinematics are predominately normal, and dips to the northeast. At its northern segment, rocks of subdomain VI swing into parallelism with the geophysical trace of the STZ and Tulemalu fault zone, into a steeply dipping, northeast trending mylonite zone. Magnetite-bearing leucogranite forms a major component of the shear zone, and also the most abundant rock type in subdomain V. Geochronology presented above suggests that this suite crystallized at ca 2690 Ma, and thus, the boundary does not likely represent a ca. 1.9 Ga suture. Based on kinematics, it is likely that rocks of subdomain VI were tectonized during the juxtaposition of the low-grade rocks in the hangingwall (subdomain III) adjacent to higher grade gneisses and leucogranites exposed in subdomain V (footwall). The shear zone ranges from amphibolite-facies, and shows evidence of

localized greenschist cataclasis and mylonitization in strands throughout. Therefore, there is evidence of progressive deformation of decreasing grade within subdomain VI, consistent with unroofing extensional collapse.

Zircon geochronology of the structurally lowest plutonic rock within the northwestern Hearne subprovince at Charlebois Lake yields insight into the differences, or lack thereof, compared to rocks currently belonging to the Chesterfield block (Berman et al., 2007). Although the absolute age alone has minimal implications owing to lack of data from other proximal rock types, they are important in that the sample contains Mesoarchean xenocrysts, similar to rocks of the 'Chesterfield block' at Angikuni Lake. One of the main reasons for justifying a Chesterfield block was the evidence of evolved continental crust (Davis et al, 2006). The presence of older xenocrysts within the sample at Charlebois Lake suggests that it too may have been close to Mesoarchean crust/lithosphere. Therefore, this attribute may not be unique to the Rae-Chesterfield subprovince, but the entire Northwestern Hearne subprovince.

Collectively, observations and new geochronology suggests that there is no exposed suture at the latitude of Angikuni Lake. And based on the proximity to evolved continental crust (Cousens et al., 1998), we interpret the tectonic setting to be a continental margin or back arc basin originally proposed in Aspler et al. (1999). This attribute may be continuous and a major feature of the Northwestern Hearne subprovince based on geochronolgy presented from sample 15W-043 presented above. Circa 2.6 Ga granitic rocks (Aspler, unpublished data) are currently being analyzed for major and trace element chemistry to see if they could be arc related correlatives to ca. 2.6 Ga plutonic rocks in the Athabasca granulite terrane 250 km to the southwest (Regan et al., in prep, Chapter 4). Furthermore, these data suggest that supracrustal rocks exposed at Angikuni lake may represent the transition of continental lithosphere prevalent throughout the Rae subprovince into more ensimatic rock types and compositions of the central Hearne subprovince (Cousens et al., 2004). Therefore, it follows that Rae and Hearne (and

formerly Chesterfield) blocks of the western Churchill Province were together prior ca. 2.6 Ga, if not before.

Conclusions

Prelimanary data presented above, within the context of the western Churchill Province, suggests that a structural suture is not present in either of the proposed locations delineated in Berman et al. (2007). Furthermore, the designation of a separate Chesterfield block may not be necessary, and some of the differences used to justify this designation may continue along the entirety of the northwestern Hearne subprovince. Strain at Angikuni lake was localized within shear zones, much like higher grade rocks of the eastern Rae subprovince to the south, which formed during Paleoproterozoic disruption of an intracontinental weak zone (Mahan and Williams, 2005; Dumond et al., 2013; Regan et al., 2014). Therefore, these data are consistent with models invoking an intracontinental setting for the STZ, and particular, those that suggest Paleoproterozoic deformation was localized along thick ductile shear zones during the amalgamation of the supercontinent Nuna.

References

Ashton, K.E., Hartlaub, R.P., Heaman, L.M., Morelli, R.M., Card, C.D., Bethune, K., and Hunter, R.C., 2009, Post-Taltson sedimentary and intrusive history of the southern Rae Province along the northern margin of the Athabasca Basin, Western Canadian Shield: Precambrian Research, v. 175, p. 16-34.

Ashton, K.E., Hartlaub, R.P., Bethune, K.M., Heaman, L.M., and Niebergail, G., 2013, New depositional age constraints for the Murmac Bay group of the southern Rae Province, Canada: Precambrian Research, v. 232, p. 70-88.

Aspler, L.B., and Chiarenzelli, J.R., 2002, Mixed siliciclastic-carbonate ramp sedimentation in a rejuvenated Paleoproterozoic intracratonic basin: upper Hurwitz Group, Nunavut, Canada: In: Altermann, W., Corcoran, P., (Eds.), Precambrian Sedimentary Environments: a Modern Approach to Ancient Depositional Systems, International Association of Sedimentology Special Publication, v. 33, p. 293-321.

Aspler, L.B., Chiarenzelli, J.R., and McNicoll, V.J., 2002a, Paleoproterozoic basement-cover infolding and thick-skinned thrusting in Hearne domain, Nunavut, Canada: intracratonic response to Trans-Hudson orogen: Precambrian Research, v. 116, p. 331-354

Aspler, L.B., Cousens, B.L., and Chiarenzelli, J.R., 2002b, Long-distance intracratonic transport of mafic magmas during opening of the Manikewan ocean (Trans-Hudson orogen): Griffin gabbro sills (2.11 Ga), Hurwitz Basin, Nunavut, Canada: Precambrian Research, v. 117, p. 269-294.

Aspler, L.B., and Chiarenzelli, J.R., 1996, Stratigraphy, sedimentology and physical volcanology of the Henik Group, central Ennadai-Rankin greenstone belt, Northwest Territories, Canada: late Archean paleogeography of the Hearne Province and tectonic implications: Precambrian Research, v. 77, p. 59-89.

Aspler, L.B., anc Chiarenzelli, J.R., 1998, Two Neoarchean supercontinents? Evidence from the Paleoproterozoic: Sedimentary Geology, v. 120, p. 75-104.

Aspler, L.B., Chiarenzelli, J.R., Powis, K., and Cousens, B.L., 1998, Progress report: Precambrian geology of the Angikuni Lake area, District of Keewatin, Northwest Territories: Geologic Survey of Canada, Current Research, v. 1998-C, p. 55-66.

Aspler, LB., Chiarenzelli, J.R., Cousens, B.L., McNicoll, V.J., and Davis, W.J., 2001, Paleoproterozoic intracratonic basin processes, from breakup of Kenorland to assembly of Laurentia: Hurwitz Basin, Nunavut, Canada: Sedimentary Geology, v. 141-142, p. 287-318.

Aspler, L.B., Chiarenzelli, J.R., Cousens, B.L., and Valentino, D., 1999, Precambrian geology, northern Angikuni Lake, and a transect across the Snowbird tectonic zone, western Angikuni Lake, Northwest Territories (Nunavut): Geological Survey of Canada open file report, p. 107-118.

Baldwin, J.A., Bowring, S.A., Williams, M.L., and Williams, I.S., 2004, Eclogites of the Snowbird tectonic zone: Petrologic and U-Pb geochronological evidence for Paleoproterozoic high-pressure metamorphism in the western Canadian Shield: Contributions to Mineralogy and Petrology, v. 147, n. 5, p. 528-548, doi: 10.10007/s00410-004-0572-4.

Berman, R.G., Davis, W.J., Aspler, L.B., and Chiarenzelli, J.R., 2002, SHRIMP U-Pb ages of multiple metamorphic events in the Angikuni Lake area, western Churchill Province, Nunavut: Radiogenic Age and Isotopic Studies: Report 15; Geological Survey of Canada current research, 2002-F3, p. 1-9.

Berman, R.G., Davis, W.J., and Pehrsson, S., 2007, Collisional Snowbird tectonic zone resurrected: Growth of Laurentia during the 1.9 Ga accretionary phase of the Hudsonian orogeny: Geology, v. 35, n. 10, p. 911-914, doi:10.1130/G23771A.1.

Berman, R.G., Pehrosson, S.L., Davis, W.L., Ryan, J.J., Qui, H., Ashton, K., 2013, The Arrowsmith orogeny: geochronological and termobarometric constraints on its extent and tectonic setting in the Rae craton, with implications for pre-Nuna supercontinent reconstruction: Precambrian Research, v. 232, p. 44-68.

Bethune, K.M., Berman, R.G., Rayner, N., and Ashton, K.E., 2013, Structural, petrological and U-Pb SHRIMP geochronological study of the western Beaverlodge domain: Implications for crustal architecture, multi-stage orogenesis and the extent of the Taltson orogen in the SW Rae craton, Canadian Shield: Precambrian Research, v. 232, p. 89-118.

Bickford, M.E., Collerson, K.D., and Lewry, J.F., 1994, Crustal history of the rae and Hearne provinces, southwestern Canadian Shield, Saskatchewan: constraints from geochronologic and isotopic data: Precambrian Research, v. 68, p. 1-21.

Bowring, S.A., Williams, I.S., and Compston, W., 1989, 3.96 Ga gneisses from the Slave province, Northwest Territories, Canada: Geology v. 17, p. 871-975.

Brown, L.L., Webber, J., Williams, M.L., Regan, S., Seaman, S., *in review*, Magnetism of the Lower Crust: observations from the Chipman Domain, Athabasca Granulite Terrain, northern Canada: Tectonophysics

Bryant, J.A., Yogodzinski, G.M., Hall, M.L., Lewicki, J.L., and Bailey, D.G., 2006, Geochemical constraints on the origin of volcanic rocks from the Andean northern volcanic zone, Ecuador: Journal of Petrology, V. 47, N. 6, p. 1147-1175, doi: 10.1093/petrology/eg1006

Card, C.D., 2002, New investigations of basement to the western Athabasca basin: Saskatchewan Geological Survey Summary of Investigations 2002, v. 2, p. 1-17.

Card, C.D., Bethune, K.M., Davis, W.J., Rayner, N., and Ashton, K.E., 2014, The case for a distinct Taltson orogeny: Evidence form Northwest Saskatchewan, Canada: Precambrian Research, v. 255, p. 245 – 265.

Chiarenzelli, J.R., Lupulescu, M., Cousens, B., Thern, E., Coffin, L., and Regan, S., 2010, Enriched Grenbillian lithospheric mantle as a consequence of long-lived subduction beneath Laurentia: Geology, v. 38, p. 151-154

Corrigan, D., Hajnal, Z., Nemeth, B., and Lucas, S.B., 2005, Tectonic framework of a Paleoproterozoic arc-continent to continent-continent collisional zone, Trans-Hudson Orogen, from geological and seismic reflection studies: Canadian Journal of Earth Sciences, v. 42, p. 421-434, doi: 10.1139/05-025.

Corrigan, D., Pehrsson, S., Wodicka, and de Kemp, E., 2009, The Paleoproterozoic Trans-Hudson Orogen: a prototype of modern accretionary processes: in Ancient Orogens and Modern Analogues, Ed(s)
Murphy et al., Geological Society of London, Special Publications, v. 327, p. 457-479, doi:10.1144/SP327.19.

Corrigan, D., Scott, D.J., and St-Onge, M.R., 2001, Geology of the northern margin of the Trans-Hudson Orogen (Foxe-Fold Belt), central Baffin Island, Nunavut: Geological Survey of Canada Current research 2001-C23, p.1-11.

Corrigan, D., Nadeau, L., Brouillette, P., Wodika, N., Houle, M.G. Tremblay, T., Machado, G., and Keating, P., 2013, Overview of GEM Multiple Metals-Melville Peninsula project, central Melville Peninsula, Nunavut: Geological Survey of Canada, Current Research, 2013-19, p. 1 – 17.

Cousens, B.L., Aspler, L.B., Chiarenzelli, J.R., Donaldson, J.A., Sandeman, H., Peterson, R.D., LeCheminant, A.N., 2001, Enriched Archean lithospheric mantle beneath western Churchill Province tapped during Paleoproterozoic orogenesis: Geology, v. 29, n. 9, p. 827-830.

Cousens, B.L., Aspler, L.B., and Chiarenzelli, J.R., 2004, Dual sources of ensimatic magmas, Hearne domain, western Churchill Province, Nunavut, Canada: Neoarchean “infant arc” processes?: Precambrian Research, v. 134, p. 169-188.

Cousens, B.L., 1998, Geochemistry and neodymium systematics of Archean and Proterozoic igneous rocks from the Angikuni and Yathkyed lakes areas, western Churchill Province,

Northwest Territories: Indian Affair and Northern Development Canada, Open File EGS 1998-6, p. 1-41

Cutts, K.A., Stevens, G., Hoffmann, E., Buick, I.S., Frei, D., and Munker, C., 2014, Paleo- to Mesoarchean polymetamorphism in the Barberton Granite-Greenstone Belt, South Africa: Constraints from U-Pb monazite and Lu-Hf garnet geochronology on the tectonic processes that shaped the belt: Geological Society of America Bulletin, v. 126, n. ¾, p. 251-270.

Davis, W.J., Hanmer, S., and Sandeman, H.A., 2004, Temporal evolution of the Neoarchean central Hearne supracrustal belt: rapid generation of juvenile crust in a suprasubduction zone setting: Precambrian Research, v. 134, p. 85-112.

Davis, W.J., Hanmer, S., Tella, S., Sandeman, H.A., and Ryan, J.J., 2006, U-Pb geochronology of the MacQuoid supracrustal belt and Cross Bay plutonic comples: Key components of the northwestern Hearne subdomain, western Churchill Province, Nunavut, Canada: Precambrian Research, v. 145, p. 53-80.

Dumond, G., McLean, N., Williams, M.L., Jercinovic, M.J., and Bowring, S.A., 2008, High resolution dating of granite petrogeneisis and deformation in a lower crustal shear zone: Athabasca granulite terrane, western Canadian Shield: Chemical Geology, v. 16, n. 4, p. 175-196, doi:10.1016/j.chemgeo.2008.04.014.

Dumond, G., Goncalves, P., Williams, M.L., and JHercinovic, M.J., 2010, Subhorizontal fabric in exhumed continental lower crust and implication for lower crustal flow: Athabasca granulite terrane, Western Canadian Shield: Tectonics, v. 29, TC2006, doi:10.1029/2009TC002514.

Dumond, G., Mahan, K.H., Williams, M.L., and Jercinovic, M.J., 2013, Transpressive uplift and exhumation of continental lower crust revealed by synkinematic monazite reactions: Lithosphere, v. 5, n. 5, p. 507-512, doi: 10.1130/L292.1

Dumond, G., Goncalves, P, Williams, M.L., and Jercinovic, M.J., 2013, UHT-HP Metamorphism in an exhumed lower crustal hot zone: GSA abstracts and Programs.

Eade, K.E., 1986, Precambrian geology of the Tulemalu Lake-Yathkyed Lake area, District of Keewatin: Geological Survey of Canada Paper, v. 84-11, p. 1-31.

Flowers, R., Bowring, S.A., Mahan, K.H., and Williams, M.L., 2006a, Timescales and significance of high pressure, high-temperature metamorphism and mafic dike anatexis, Snowbird tectonic zone, Canada: Contribution to Mineralogy and Petrology, v. 151, n. 5, p. 558-581, doi:10.1007/s00410-006-0066-7.

Flowers, R.M., Mahan, K.H., Bowring, S.A., Williams, M.L., Pringle, M.S., and Hodges, K.V., 2006b,Multistage exhumation and juxtaposition of lower continental crust in the western Canadian Shield: linking high resolution U-Pb and $^{40}Ar/^{39}Ar$ thermochronometry with pressure-temperature-deformation paths: Tectonics, v. 25, TC4003, doi:10.1029/2005TC001912.

Flowers, R.M., Bowring, S.A., Mahan, K.H., Williams, M.L., and Williams, I.S., 2008, Stabilization and reactivation of cratonic lithosphere from the lower crustal record in the western Canadian shield: Contributions to Mineralogy and Petrology, v. 156, n. 4, p. 529-549, doi:10.1007/s00410-008-0301-5.

Gilboy, C.F., 1980, Bedrock compilation geology: Stony Rapids area (NTS 74p)-Prelimanary geological map, scale 1:250,000, Sask. Geol. Surv., Sask. Energy and mines, Regina.

Gehrels, G. and Pecha, M., 2014, Detrital zircon U-Pb geochronology and Hf isotope geochemistry of Paleozoic and Triassic passive margin strata of western North America: Geosphere, v. 10 (1), p. 49-65.

Gehrels, G. and Pecha, M., 2014, Detrital zircon U-Pb geochronology and Hf isotope geochemistry of Paleozoic and Triassic passive margin strata of western North America: Geosphere, v. 10 (1), p. 49-65.)

Hamilton, W.B., 2011, Plate tectonics began in Neoproterozoic time, and plumes from deep mantle have never operated: Lithos, v. 123, p. 1-20.

Hanmer, S., Bowring, S.A., Van Breeman, O., and Parrish, R.R., 1992, Great Slave Lake shear zone, northwest Canada: mylonitic record of Early Proterozoic convergence, collision, and indentation: Journal of Structural Geology, v. 14, p. 757-773.

Hanmer, S., 1994, Geology, East Athabasca mylonite triange, Saskatchewan, Map 1859A, scale 1:100,000, Geol. Surv. Of Can., Ottawa.

Hanmer, S., 1997, Geology of the Striding-Athabasca mylonite zone, northern Saskatchewan and southeastern District of Mackenzie, Northwest Territories: Pap. Geol. Surv., of Can., Ottawa.

Hanmer, S., Parrish, R., Williams, M., and Kopf, C., 1994, Striding-Athabasca Mylonite: Complex Archean deep crustal deformation in the East Athabasca mylonite triangle, N. Saskatchewan: Canadian Journal of Earth Sciences, v. 31, p. 1287-1300, doi:10.1139/e94-111.

Hanmer, S., Williams, M., and Kopf, C., 1995, Modest movements, spectacular fabrics in an intracontinental deep-crustal strike-slip fault: Striding-Athabasca mylonite zone, NW Canadian Shield: Journal of Structural Geology, v. 17, n. 4, p. 493-507, doi:10.1016/0191-8141(94)00070-G.

Hanmer, S., and Williams, M.L., 2001, Targeted fieldwork in the Daly Bay Complex, Hudson Bay, Nunavut: Geological Survey of Canada Current Research 2001-C15, p. 1-26.

Hanmer, S., Sandeman, H.A., Davis, W.J., Aspler, L.B., Rainbird, R.H., Ryan. J.J., Relt, C., Roest, W.R., Peterson, T.D., 2004, Neoarchean tectonic setting of the Central Hearne supracrustal belt, western Churchill Province, Nunavut, Canada: Precambrian Research, v. 134, p. 63-83.

Herzberg, C., and Rudnick, R., 2012, Formation of cratonic lithosphere: an integrated thermal and petrological model: Lithos, v. 149, p. 4-15.

Hildebrand, R.S., Hoffman, P.F., and Bowring, S.A., 2010, the Calderian orogeny in Wopmay orogen (1.9 Ga), northwestern Canadian Shield: Geological Society of America Bulletin, v. 122, p. 794-814, doi: 10.1130/B26521.1

Hoffman, P.F., 1988, United Plates of America, the birth of a craton: Early Proterozoic assembly and growth of Laurentia: Annual Review of Earth and Planetary Sciences, v. 16, p. 543-603, doi:10.1146/annurev.ca.16.050188.002551.

Holland, T., and Powell, R., 1998, An internally consistent thermodynamic dataset for phases of petrological interest: Journal of Metamorphic Geology, v. 16, p. 309-343.

Hynes, A., 2014, How feasible was subduction in the Archean?: Canadian Journal of Earth Sciences, v. 51, n. 3, p. 286-296.

Koteas, G.C., Williams, M.L., Seaman, S.J., and Dumond, G., 2010, Granite genesis and mafic-felsic magma interaction in the lower crust: Geology, v. 38, p. 1067-1070, doi:10.1130/G31017.1.

Krikorian, L., 2002, Geology of the Wholdaia Lake Segment of the Snowbird Tectonic Zone, Northwest Territories (Nunavut): A view of the deep crust during the assembly and stabilization of the Laurentian craton: MSc Thesis, Advisor: Michael L. Williams, University of Massachusetts, Amherst.

Leslie, S.R., Mahan, K.H., Regan, S., Williams, M.L., and Dumond, G., *in review*, Contrasts in sillimanite deformation in felsic tectonites from anhydrous granulite- and anhydrous amphibolite-facies shear zones, western Canadian Shield: submitted to Journal of Structural Geology.

Lewry, J.F., and Sibbald, T.I.I., 1980, Thermotectonic evolution of the Churchill Province in northern Saskatchewan: Tectonophysics, v. 68, p. 45-82.

Loveridge, W.D., Eade, K.E., and Sullivan, R.W., 1988, Geochronological studies from Precambrian rocks from the southern District of Keewatin: Geological Survey of Canada Paper, v. 88-18, p. 1 – 36.

Macdonald, R., 1980, New edition of the geological map of Saskatchewan, Precambrian Shield area, in Summary of Investigations, Misc. Rep. 01-4.2, p. 19-21, Sask. Geol. Surv., Sask. Ind. And Resour, Regina.

MacHattie, T.G., 2008, Geochemistry and geochronology of the late Archean Prince Albert group (PAg), Nunavut, Canada: Ph.D. thesis, University of Alberta, p. 1 – 340.

MacLachlan, K., Davis, W., and Relt, C., 2005, U/Pb geochronological constraints on Neoarchean tectonism: Multiple compressional events in the Northwestern Hearne domain, western Churchill Province, Canada: Canadian Journal of Earth Sciences, v. 42, p. 85-109.

MacRae, N.D., Armitage, A.E., Miller, A.R., Roddick, J.C., Jones, A.L., and Mudry, M.P., 1996, The diamondiferous Akluilak lampophyre dyke, Gibson Lake area, NWT: Geological Survey of Canada Open File, v. 3228, p. 101-107.

Mahan, K.H., Williams, M.L., and Baldwin, J.A., 2003, Contractional uplift of deep crustal rocks along the Legs Lake shear zone, western Churchill Province, Canadian Shield: Canadian Journal of Earth Sciences, v. 40, n. 8, p. 1085-1110, doi:10.1139/e03-039.

Mahan, K.H., and Williams, M.L., 2005, Reconstruction of a large deep-crustal terrane: Implication for the Snowbird tectonic zone and early growth of Laurentia: Geology, v. 33, n. 5, p. 385-388, doi:10.1130/G21273.1.

Mahan, K.H., Goncalves, P., Williams, M.L., and Jercinovic, M.J., 2006a, Dating metamorphic reactions and fluid flow: Application to exhumation of high-P granulites in a crustal-scale shear zone, western Canadian Shield: Journal of Metamorphic Geology, v. 24, n. 3, p. 193-217, doi:10.1111/j.1525-1314.2006.00633.x.

Mahan, K.H., Williams, M.L., Flowers, R.M., Jercinovic, M.J., Baldwin, J.A., and Bowring, S.A., 2006b, Geochronological constraints on the Legs Lake shear zone with implications for

regional exhumation of lower continental crust, western Churchill Province, Canadian Shield: Contributions to Mineralogy and Petrology, V. 152, n. 2, p. 223-242, doi:10.1007/s00410-006-0106-3.

Mahan, K.H., Goncalves, P., Flowers, R., Williams, M.L., and Hoffman-Setka, D., 2008, The role of heterogeneous strain in the development and preservation of a polymetamorphic record in high-P granulites, western Canadian Shield: Journal of metamorphic geology, v. 26, n. 6, p. 669-694, doi:10:111/j.1525-1314.2008.00783.x.

Mahan, K.H., Smit, C.A., Williams, M.L., Dumond, G., and Van Reenan, D.D., 2011a, Heterogeneous strain and polymetamorphism in high-grade terranes: Insight into crustal processes from the Athabasca Granulite Terrane, western Canada, and the Limpopo Complex, southern Africa: in van Reenen, D.D., Kramers, J.D., McCourt, S., and Perchuk, L.L., eds., Origin and evolution of Precambrain High-Grade Gneiss terranes, with Special Emphasis on the Limpopo Complex of Southern Africa: GSA Memoir, V. 207, p. 269-287, doi:10.1130/2011.1207(14).

Martel, E., van Breeman, O., Berman, R.G., and Pehrsson, S., 2008, Geochronology and tectonometamorphic history of the Snowbird Lake area, Northwest Territories, Canada: New insights into the architecture and significance of the Snowbird tectonic zone: Precambrian Research, v. 161, n. 3-4, p. 201-230, doi:10.1016/j.precamres.2007.07.007.

Maxeiner, R.O., and Rayner, N., 2010, continental arc magmatism along the southeast Hearne Craton margin in Saskatchewan, Canada: Comparison of the 1.92 – 1.91 Ga Porter Bay Complex and the 1.86 – 1.85 Ga Wathaman batholith: Precambrian Research, v. 184, p. 93 – 120.

Mezger, K., 1992, Temporal evolution of regional granulite terranes: Implication for the formation of lowermost continental crust: Continental Lower Crust, Ed(s): R.M. Fountain et al., p. 447-472.

Pehrsson, S.J., Berman, R.G., Elington, B., and Rainbird, R., 2013, Two Neoarchean supercontinents revisited: The case for a Rae family of cratons: Precambrian Research, v. 232, p. 27-43.

Petts, D.C., Davis, W.J., Moser, D.E., and Longstaffe, F.J., 2014, Age and evolution of the lower crust beneath the western Churchill Province: u-Pb zircon geochronology of kimberlite-hosted granulite xenoliths, Nunavut, Canada: Precambrian Research, v. 241, p. 129-145.

Rainbird, R.H., Davis, W.J., Pehrsson, S.J., Wodicka, N., Rayner, N., and Skulski, T., 2010, Early Paleoproterozoic supracrustal assemblages of the Rae domain, Nunavut, Canada: intracratonic basin development during supercontinent break-up and assembly: Precambrian Research, v. 181, p. 166-186.

Regan, S.P., Williams, M.L., Leslie, S.R., Mahan, K.H., Jercinovic, M.J., and Holland, M.E., 2014, The Cora Lake shear zone, Athabasca granulite terrane (Snowbird Tectonic Zone), an intraplate response to far-field orogenic processes during the amalgamation of Laurentia: Canadian Journal of Earth Sciences

Relf, C., and Hanmer, S., 2000, A speculative and critical summary of the current state of knowledge of the western Churchill province: A NATMAP perspective: Geological Association of Canada-Mineralogical Association of Canada Abstracts, v. 25, p. 857.

Rhodes, J.M., 1996, Geochemical stratigraphy of lava flows sampled by the Hawaii Scientific Drilling Project: Journal of Geophysical Research, v. 101, n. B5, p. 11,729-11,746.

Ross, G.M., Broome, J., and Miles, W., 1994, Potential fields and basement structure – western Canada sedimentary basin: *in* Geological Atlas of the Western Canada Sedimentary Basin, G.D. Mossop and I. Shetsen (comp.), Canadian Society of Petroleum Geologists and Alberta Research Council, URL <http://www.ags.gov.ab.ca/publications/wcsb_atlas/atlas.html>, [Date last accessed online].

Ross, G.M., Eaton, D.W., Boerner, D.E., and Miles, W., 2000, Tectonic entrapment and its role in the evolution of continental sphere: an example from the Precambrian of western Canada: Tectonics, v. 19, p. 116-134.

Sanborn-Barrie, M., Carr, S.D., and Theriault, R., 2001, Geochronological constraints on metamorphism, magmatism, and exhumation of deep-crustal rocks of the Kramanitaur Complex with implications for the Paleoproterozoic evolution of the Archean western Churchill Province, Canada: Contributions to Mineralogy and Petrology, v. 141, p. 592-612.

Sanborn-Barrie, M., Chakungal, J., James, D., Rayner, N., and Whalen, J., 2014a, Precambrian bedrock geology, Southampton Island, Nunavut: Geological Survey of Canada Canadian Geoscience Map 132, 1:100,000

Sanborn-Barrie, M., Davis, W.J., Berman, R.G., Rayner, N., Skulski, T., and Sandeman, H., 2014b, Neoarchean-continental crust formation and Paleoproterozoic deformation of the central rae craton, Committee Bay belt, Nunavut: Canadian Journal of Earth Sciences, v. 51, p. 635 – 667.

Sandeman, H.A., Schultz, M., and Rubingh, K., 2005, Results of bedrock mapping of the Darby Lake-Arrowsmith River north map areas, central Rae Domain, Nunavut: Geological Survey of Canada, Current Research 2005-C2, p. 1-11.

Sandeman, H.A., Cousens, B.L., and Hemmingway, C.J., 2003, Continental Tholeiitic mafic rocks of the Paleoproterozoic Hurwitz Group, Central Hearne sub-domain, Nunavut: insight into the evolution of the Hearne sub-continental lithosphere: Canadian Journal of Earth Sciences, v. 40, p. 1219-1237.

Slimmon, W.L., 1989, Bedrock compilation geology: Fond du Lac (NTS 74-O): Saskatchewan Geological Survey, Saskatchewan Energy and Mines, Map 247A, scale 1:250,000.

Tella, S., Eade, K.E., and Sullivan, R.W., 1988, Occurene and possible tectonic significance of high-pressure granulite fragments in the Tulemalu fault zone, District of Keewatin, N.W.T., Canada: Canadian Journal of Earth Sciences, v. 23, p. 1950-1962.

Van Kranendonk, 2010, Two types of Archean continentral crust: plume and plate tectonics on early earth: American Journal of Science, v. 310, p. 1187-1209.

Ward, D., 2010, The relative influence of quartz and mica on crustal seismic anisotropy [M.S.: University of Colorado, 89 p.

Williams, M.L., and Hanmer, S., 2006, Structural and metamorphic processes in the lower crust: Evidence from a deep-crustal isobarically cooled terrane, Canada: Evolution and Differentiation

of the Continental Crust, ed(s) M. Brown and T. Rushmer, p. 231-267, Cambridge University Press, Cambridge.

Williams, M.L., Hanmer, S., Kopf, C., and Darrach, M., 1995, Syntectonic generation and segregation of tonalitic melts from amphibolite dikes in the lower crust, Striding-Athabasca mylonite zone, northern Saskatchewan: Journal of Geophysical Research, V. 100, n. B8, p. 15,717-15,734, doi:10.1029/95JB00760.

Williams, M.L., Melis, E.A., Kopf, C.F., and Hanmer, S., 2000, Microstructural tectonometamorphic processes and the development of gneissic layering: A mechanism for metamorphic segregation: Journal of Metamorphic Geology, v. 18, p. 41-57, doi:10.1046/j.1525-1314.2000.00235.x.

Williams, M.L., and Flowers, R.M., 2008, The Chipman dyke swarm, Saskatchewan, Canada: Component of the 1.9 Ga Snowbird large igneous province in the western Canadian Shield: LIP of the Month, January, 2008: http://www.largeigneousprovinces.org/08jan

Williams, M.L., Karlstrom, K.E., Dumond, G., and Mahan, K.H., 2009, Perspectives on the architecture of continental crust from integrated field studies of exposed isobaric sections: in Miller, R.B., and Snoke, A.W., eds., Crustal Cross Sections from the Western North American Cordillera and Elsewhere: Implication for Tectonic and Petrologic Processes: GSA Special Paper 465, p. 219-241, doi:10.1130/2009.2456(08).

Williams, M.L., Mahan, K.H., Dumond, G., Jercinovic, M.J., Regan, S.P., and Leslie, S., 2011, Linking metamorphism and deformation using in-situ monazite geochronology: interpretation of multistage tectonic histories: GSA annual meeting, Minneapolis, MN.

Williams, M.L., and Jercinovic, M.J., 2012, Tectonic interpretation of metamorphic tectonites: integrating compositional mapping, microstructructural analysis and in situ monazite dating: Journal of Metamorphic Petrology, v. 30, p. 739-752

Williams, M.L., Mahan, K., Dumond, G., Regan, S., and Holland, M., in prep, Garnet-forming reactions in felsic orthogneiss: implications for strengthening and densification of the lower continental crust: to be submitted to the Journal of Metamorphic Petrology

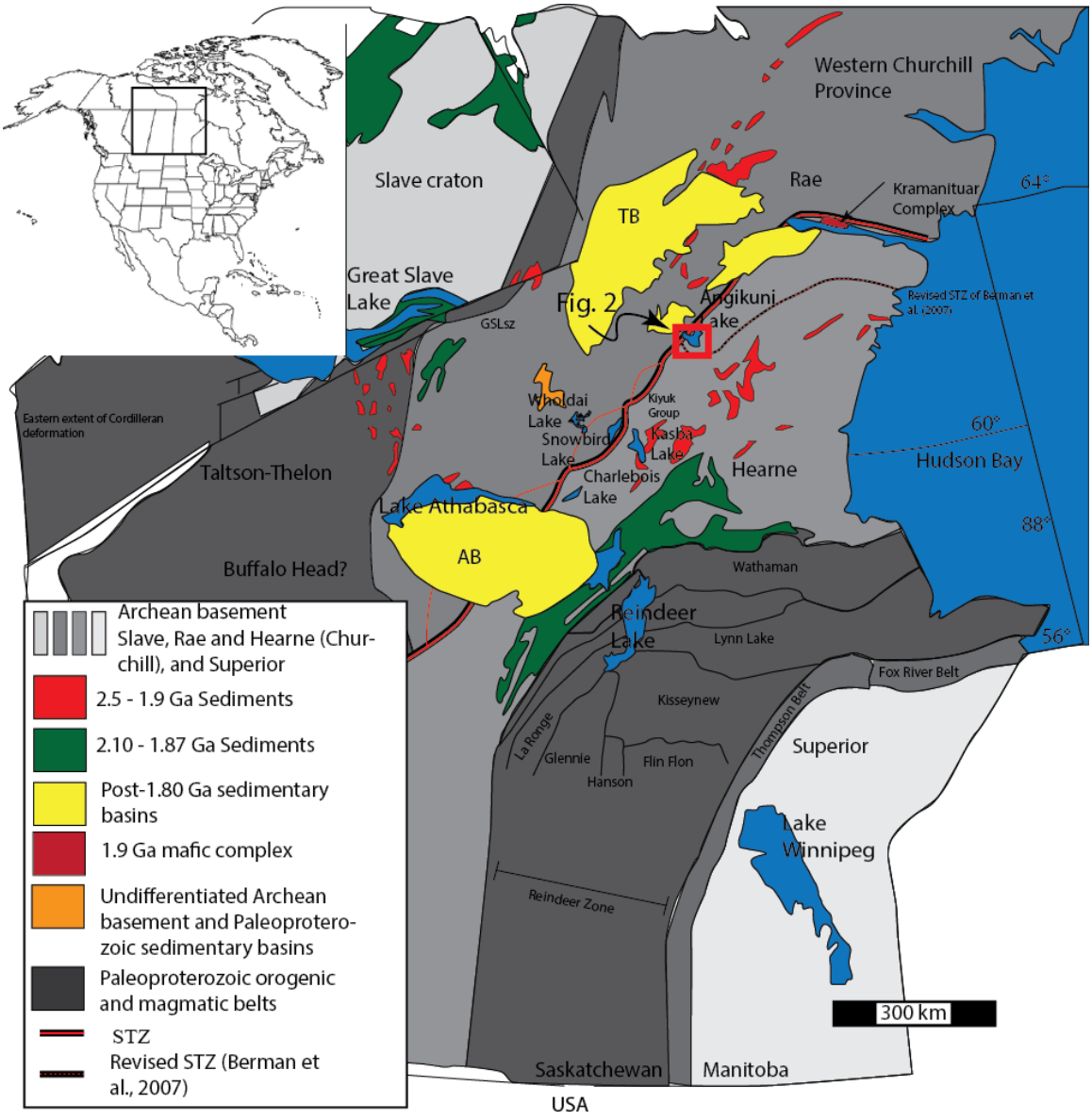

Figure 42: Lithotectonic map of the western Canadian Shield (modified from Aspler et al., 2002b). The Snowbird Tectonic Zone defines the enigmatic boundary between Rae and Hearne domains of the western Churchill Province. Box outlines triangular region (east Athabasca mylonite triangle) depicted in figure 43. Angikuni Lake, 450 km to the northeast of the study region is outlined with a white box.

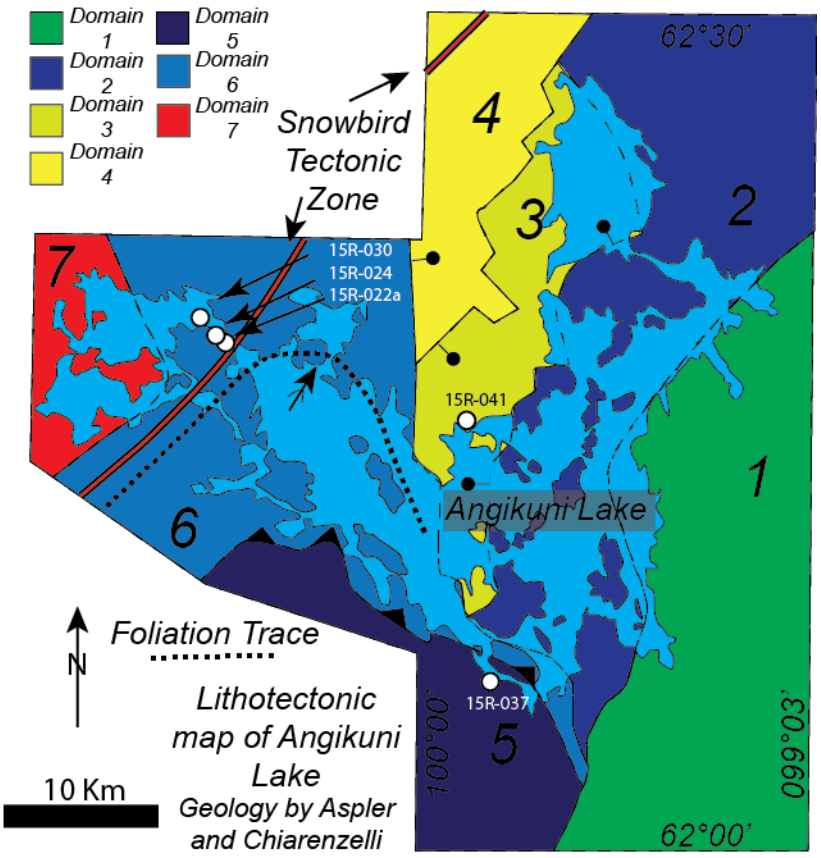

Figure 43: Lithotectonic map of the Angikuni Lake region. Mapping was performed by Aspler and Chiarenzelli.

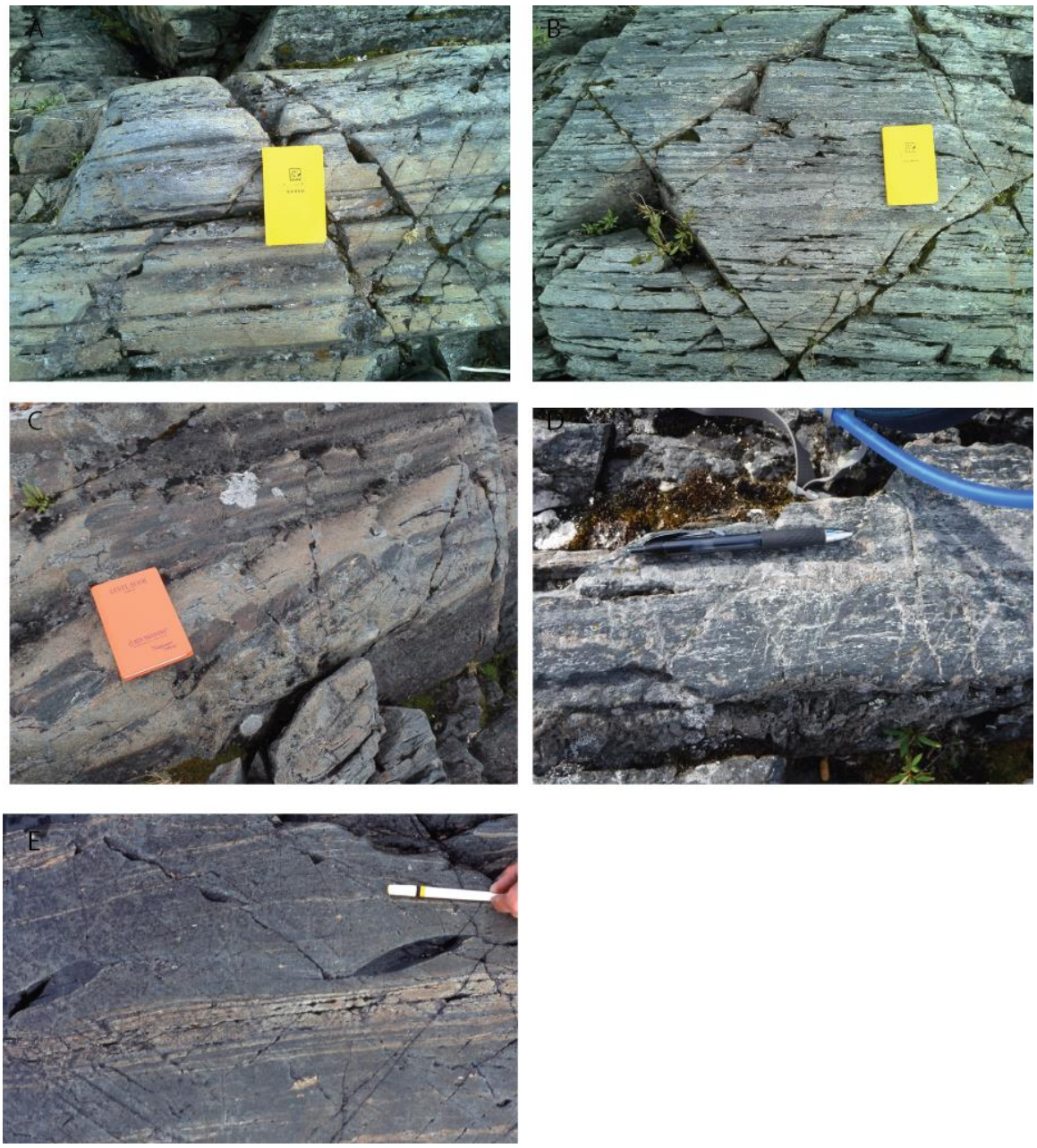

Figure 44: Field photographs of the shear zone seperating subdomains I and II.

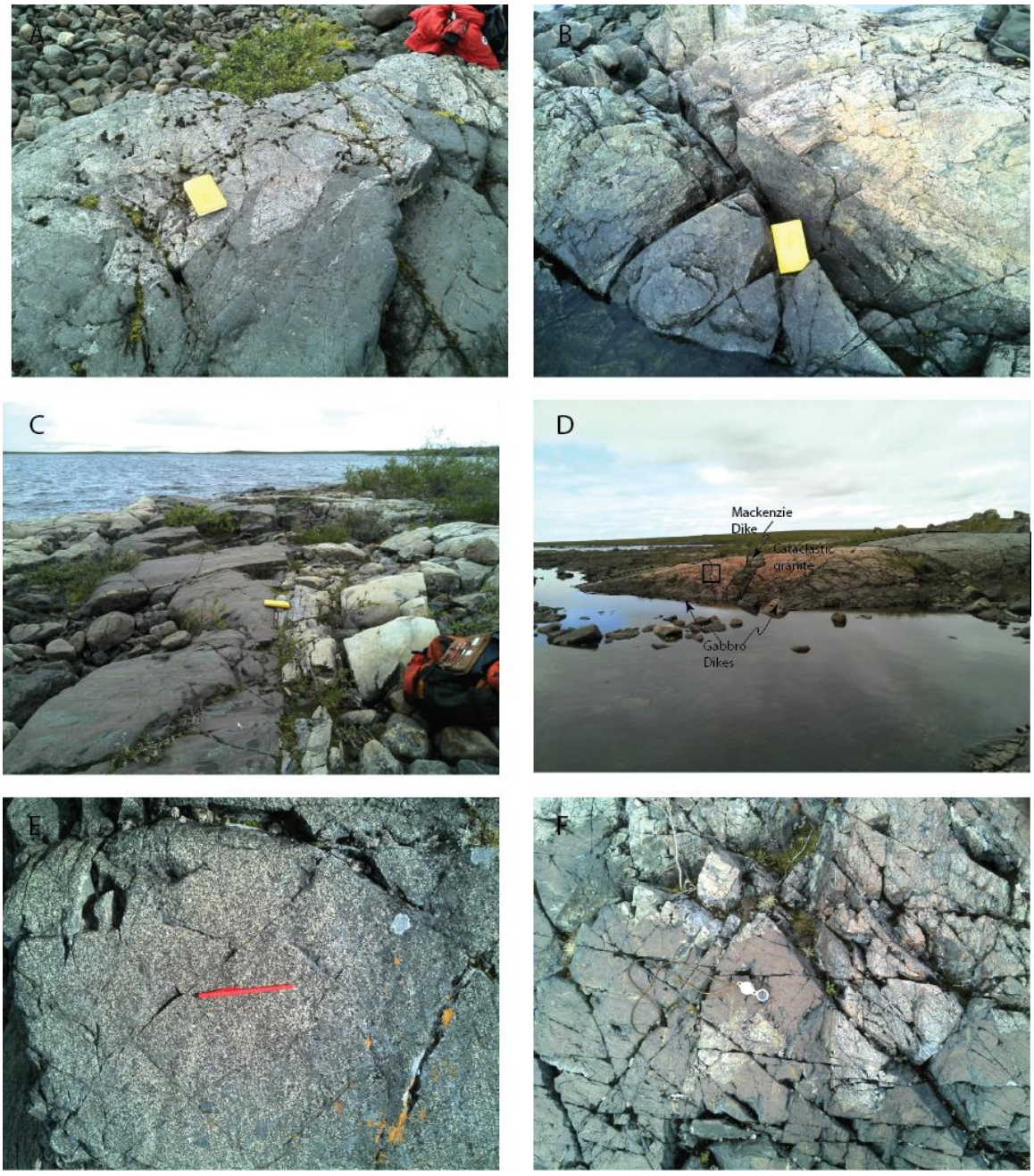

Figure 45: Field photographs of NE trending gabbroic dikes that cross cut all rock types exposed in subdomain II.

Figure 46: Representative field photographs of rock types in subdomain II.

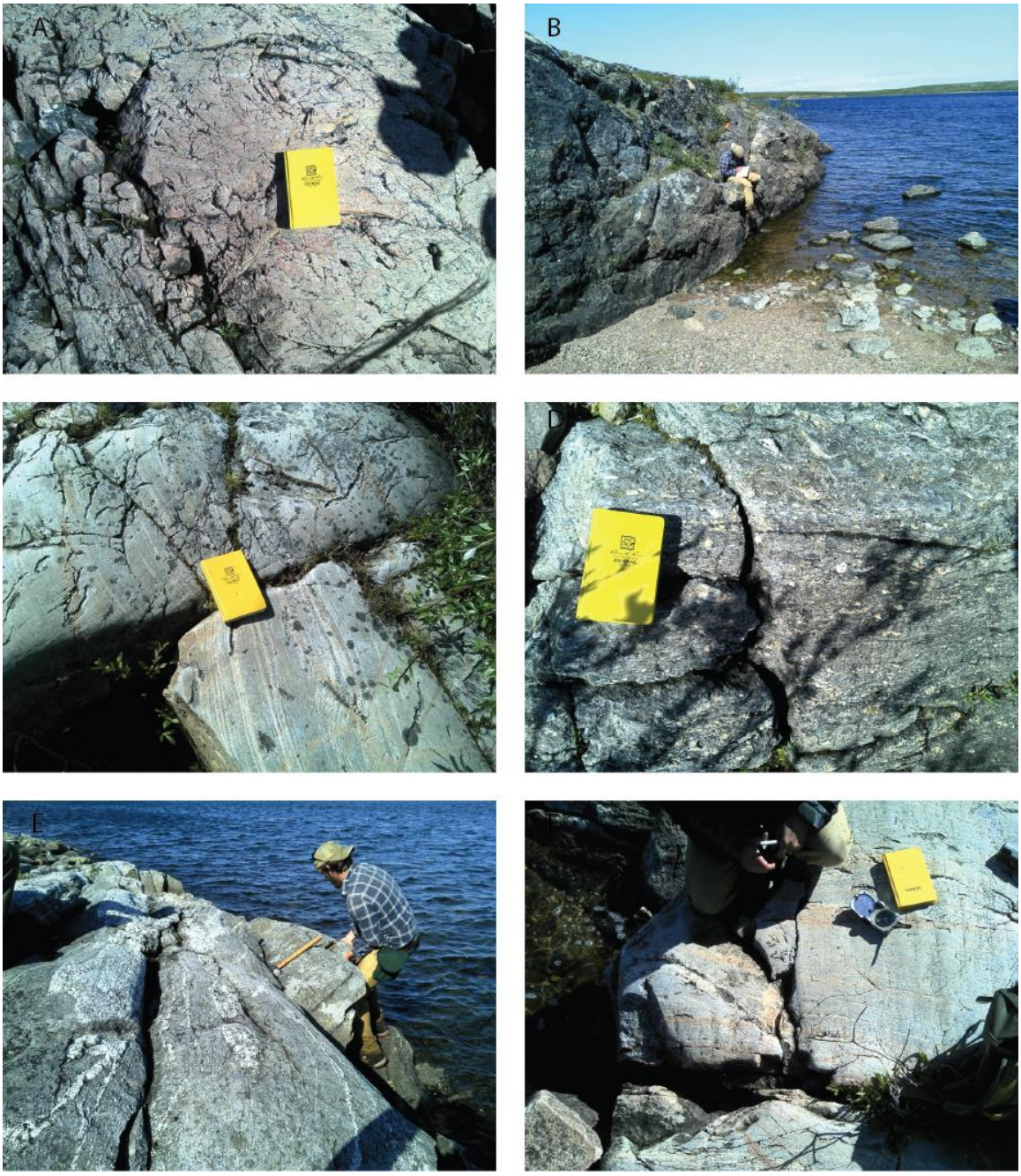

Figure 47: Field photographs from a transect across the STZ.

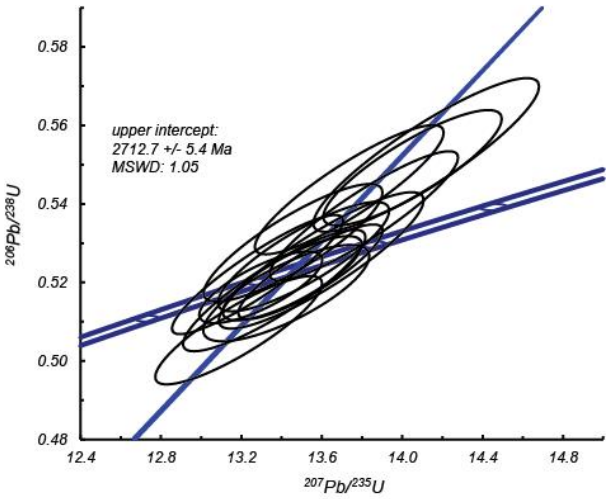
upper intercept:
2712.7 +/- 5.4 Ma
MSWD: 1.05
0.58
0.56
0.54
0.52
0.50
0.48
12.4
12.8
13.2
13.6
14.0
14.4
14.8
$^{206}Pb/^{238}U$
$^{207}Pb/^{235}U$

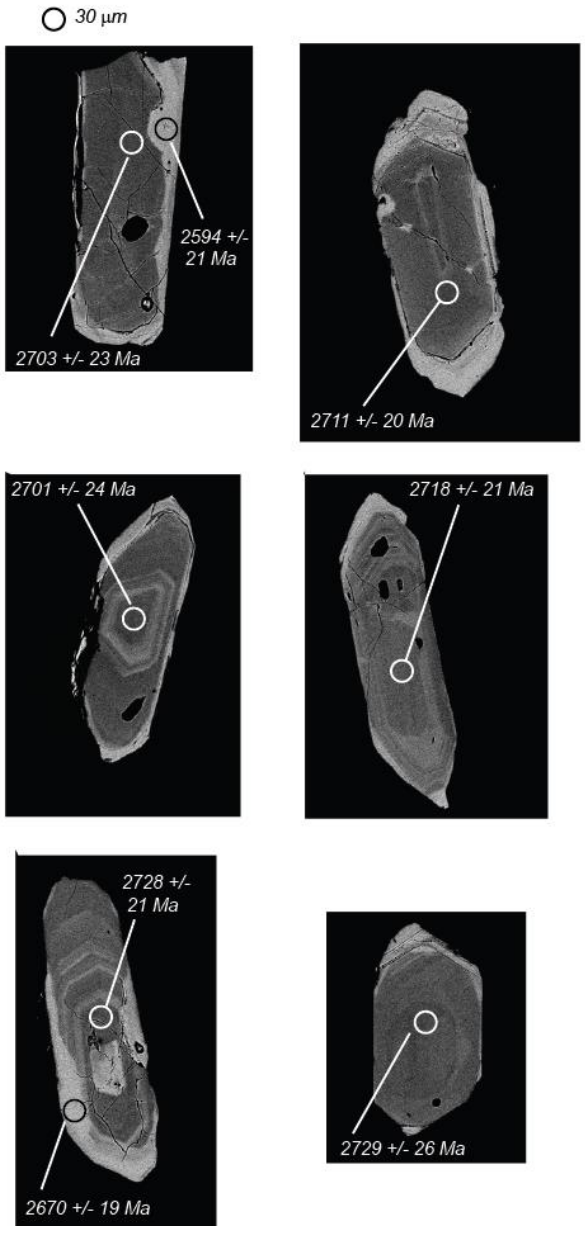
30 µm
2594 +/- 21 Ma
2703 +/- 23 Ma
2711 +/- 20 Ma
2701 +/- 24 Ma
2718 +/- 21 Ma
2728 +/- 21 Ma
2670 +/- 19 Ma
2729 +/- 26 Ma

Figure 48: Zircon U-Th-Pb results for sample 15R-030. Images are BSE

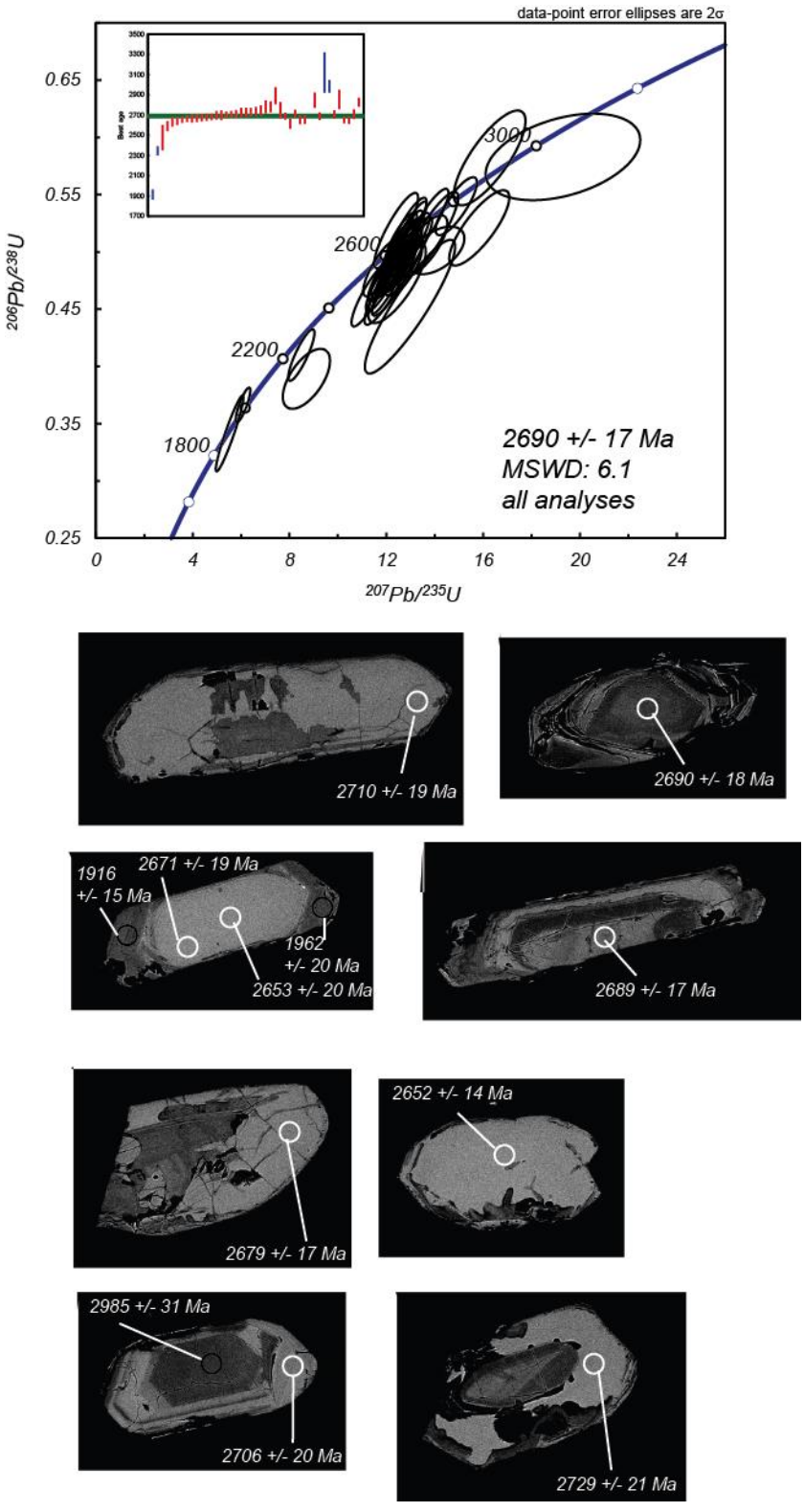

Figure 49: Zircon U-Th-Pb results for sample 15R-024. Images are BSE.

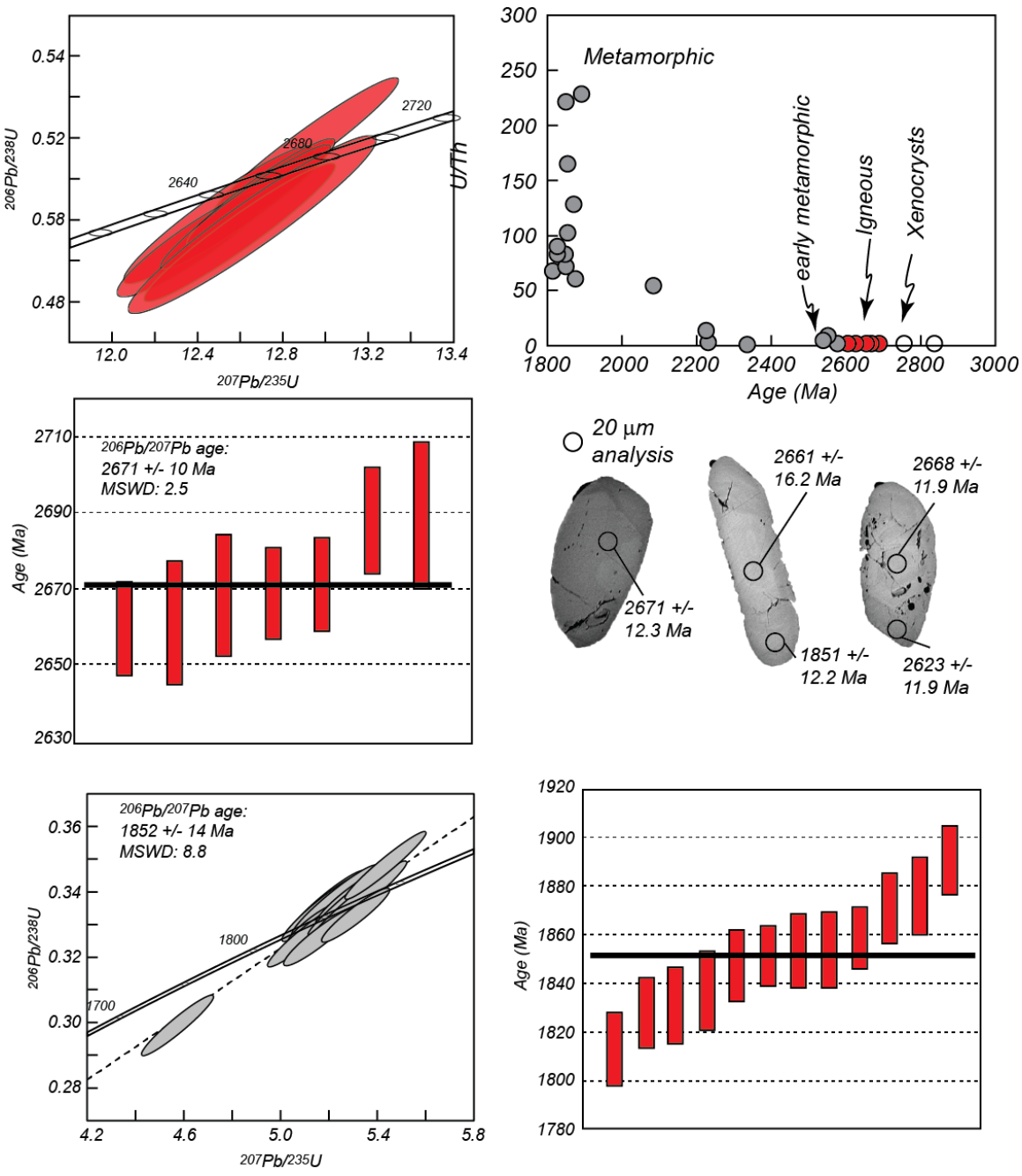

Figure 50: Zircon U-Th-Pb results for sample 15R-022a. Images are BSE.

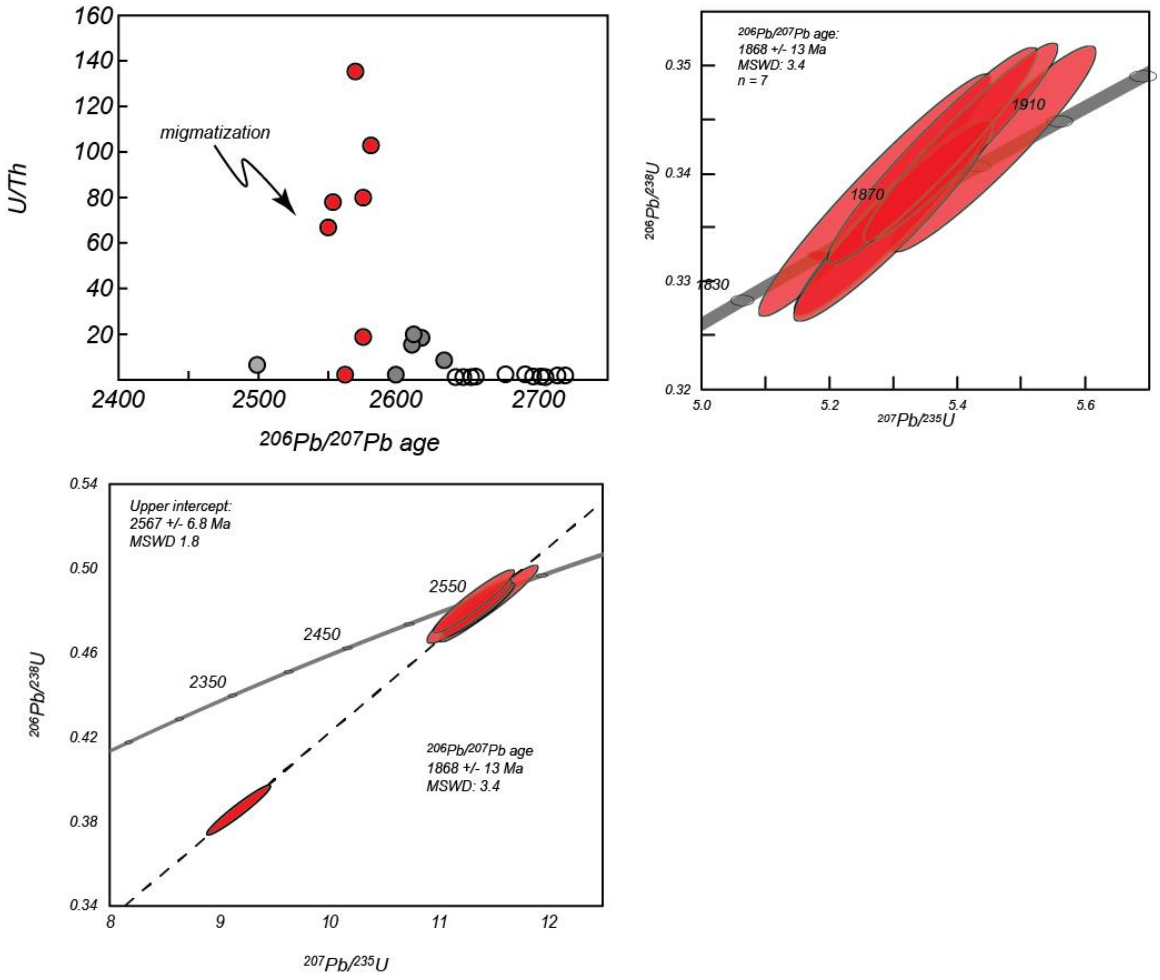

Figure 51: Zircon U-Th-Pb results for sample 15R-037. Upper right is U/Th ratio's vs time with concordant analyses plotted below. Upper riht: concordia diagram for analyses of cross cutting pegmatite.

Table 5.1

REFERENCES

Allaz, J., Selleck, B., Williams, M.L., and Jercinovic, M.J., 2013, Microprobe analysis and dating of monazite from the Potsdam Formation, New York: A progressive record of chemical reaction and fluid interaction: American Mineralogist, ed(s) Gregory Dumond and Callum Hetherington: versatile monazite: Resolving geological ecords and solving challenges in materials science, v. 98, p. 1106 – 1119.

Andsell, K.M., 2005, Tectonic evolution of the Manitoba-Saskatchewan segment of the Paleoproterozoic Trans-Hudson Orogen, Canada: Canadian Journal of Earth Sciences, v. 42, p. 741-759.

Aranovich, L.Y., and Berman, R.G., 1997, A new garnet-orthopyroxene thermometer based on reversed Al_2O_3 solubility in FeO-Al_2O_3-SiO_2 orthopyroxene: American Mineralogists, v. 97, p. 331-342.

Ashton, K.E., Hartlaub, R.P., Heaman, L.M., Morelli, R.M., Card, C.D., Bethune, K., and Hunter, R.C., 2009, Post-Taltson sedimentary and intrusive history of the southern Rae Province along the northern margin of the Athabasca Basin, Western Canadian Shield: Precambrian Research, v. 175, p. 16-34.

Ashton, K.E., Hartlaub, R.P., Bethune, K.M., Heaman, L.M., and Niebergail, G., 2013, New depositional age constraints for the Murmac Bay group of the southern Rae Province, Canada: Precambrian Research, v. 232, p. 70-88.

Aspler, L.B., and Chiarenzelli, J.R., 2002, Mixed siliciclastic-carbonate ramp sedimentation in a rejuvenated Paleoproterozoic intracratonic basin: upper Hurwitz Group, Nunavut, Canada: In: Altermann, W., Corcoran, P., (Eds.), Precambrian Sedimentary Environments: a Modern Approach to Ancient Depositional Systems, International Association of Sedimentology Special Publication, v. 33, p. 293-321.

Aspler, L.B., Chiarenzelli, J.R., and McNicoll, V.J., 2002a, Paleoproterozoic basement-cover infolding and thick-skinned thrusting in Hearne domain, Nunavut, Canada: intracratonic response to Trans-Hudson orogen: Precambrian Research, v. 116, p. 331-354

Aspler, L.B., Cousens, B.L., and Chiarenzelli, J.R., 2002b, Long-distance intracratonic transport of mafic magmas during opening of the Manikewan ocean (Trans-Hudson orogen): Griffin gabbro sills (2.11 Ga), Hurwitz Basin, Nunavut, Canada: Precambrian Research, v. 117, p. 269-294.

Aspler, L.B., and Chiarenzelli, J.R., 1996, Stratigraphy, sedimentology and physical volcanology of the Henik Group, central Ennadai-Rankin greenstone belt, Northwest Territories, Canada: late Archean paleogeography of the Hearne Province and tectonic implications: Precambrian Research, v. 77, p. 59-89.

Aspler, L.B., anc Chiarenzelli, J.R., 1998, Two Neoarchean supercontinents? Evidence from the Paleoproterozoic: Sedimentary Geology, v. 120, p. 75-104.

Aspler, LB., Chiarenzelli, J.R., Cousens, B.L., McNicoll, V.J., and Davis, W.J., 2001, Paleoproterozoic intracratonic basin processes, from breakup of Kenorland to assembly of Laurentia: Hurwitz Basin, Nunavut, Canada: Sedimentary Geology, v. 141-142, p. 287-318.

Aspler, L.B., Chiarenzelli, J.R., Cousens, B.L., and Valentino, D., 1999, Precambrian geology, northern Angikuni Lake, and a transect across the Snowbird tectonic zone, western Angikuni Lake, Northwest Territories (Nunavut): Geological Survey of Canada open file report, p. 107-118.

Aspler, L.B., Chiarenzelli, J.R., Powis, K., and Cousens, B.L., 1998, Progress report: Precambrian geology of the Angikuni Lake area, District of Keewatin, Northwest Territories: Geologic Survey of Canada, Current Research, v. 1998-C, p. 55-66.

Baldwin, J.A., Bowring, S.A., Williams, M.L., and Williams, I.S., 2004, Eclogites of the Snowbird tectonic zone: Petrologic and U-Pb geochronological evidence for Paleoproterozoic high-pressure metamorphism in the western Canadian Shield: Contributions to Mineralogy and Petrology, v. 147, n. 5, p. 528-548, doi: 10.10007/s00410-004-0572-4.

Beaumont, C., Jameison, R.A., Nguyen, M.H., and Medvedev, S., 2004, Crustal channel flows: 1. Numerical models with applications to the tectonics of the Himalayan-Tibetan orogen: Journal of Geophysical Research, v. 109, B06406, doi:10.1029.2003JB002809.

Berman, R.G., Davis, W.J., Aspler, L.B., and Chiarenzelli, J.R., 2002, SHRIMP U-Pb ages of multiple metamorphic events in the Angikuni Lake area, western Churchill Province, Nunavut: Radiogenic Age and Isotopic Studies: Report 15; Geological Survey of Canada current research, 2002-F3, p. 1-9.

Berman, R.G., 2006, Thermobarometry with Estimation of Equilibration State (TWEEQU): An IBM Compatible Software Package: Geological Survey of Canada, Open file 5408, Ottawa.

Berman, R.G., Davis, W.J., and Pehrsson, S., 2007, Collisional Snowbird tectonic zone resurrected: Growth of Laurentia during the 1.9 Ga accretionary phase of the Hudsonian orogeny: Geology, v. 35, n. 10, p. 911-914, doi:10.1130/G23771A.1.

Berman, R.G., and Aranovich, L.Y., 1996, Optimized standard state and solution properties of minerals I. Model calibration for olivine, orthopyroxene, cordierite, garnet, and ilmenite in the system FeO-MgO-CaO-Al_2O_3-TiO_2-SiO_2: Contributions to Mineralogy and Petrology, v. 119, p. 30-42.

Berman, R.G., 1991, Thermobarometry using multi-equilibrium calculations: A new technique with petrological applications: Canadian Mineralogists, v. 29, p. 833-855.

Berman, R.G., Pehrosson, S.L., Davis, W.L., Ryan, J.J., Qui, H., Ashton, K., 2013, The Arrowsmith orogeny: geochronological and termobarometric constraints on its extent and tectonic setting in the Rae craton, with implications for pre-Nuna supercontinent reconstruction: Precambrian Research, v. 232, p. 44-68.

Bethune, K.M., Berman, R.G., Rayner, N., and Ashton, K.E., 2013, Structural, petrological and U-Pb SHRIMP geochronological study of the western Beaverlodge domain: Implications for crustal architecture, multi-stage orogenesis and the extent of the Taltson orogen in the SW Rae craton, Canadian Shield: Precambrian Research, v. 232, p. 89-118.

Bickford, M.E., Collerson, K.D., and Lewry, J.F., 1994, Crustal history of the rae and Hearne provinces, southwestern Canadian Shield, Saskatchewan: constraints from geochronologic and isotopic data: Precambrian Research, v. 68, p. 1-21.

Bowring, S.A., Williams, I.S., and Compston, W., 1989, 3.96 Ga gneisses from the Slave province, Northwest Territories, Canada: Geology v. 17, p. 871-975.

Bleeker, W., 2005 North America: Precambrian continental nucleus: *In* Encyclopedia of geology w Ed(s) R.C. Selley, L.R.M. Cocks and I.R., Plimer, Elsevier, Oxford, UK, pp. 8-21.

Bleeker, W., and Ernst, R., 2006, Short-lived mantle generated magmatic events and their dyke swarms: The key unlocking Earth's paleogeographic record back to 2.6 Ga: *In* Dyke swarms – time marker of crustal evolution w Ed(s) E. Hanski, S. Mertanen, T. Ramo, and J. Vuollo, Taylor and Francis/Balkema, London, UK, pp. 3-26.

Brown, L.L., Webber, J., Williams, M.L., Regan, S., Seaman, S., *in review*, Magnetism of the Lower Crust: observations from the Chipman Domain, Athabasca Granulite Terrain, northern Canada: Tectonophysics

Brown, M., Korhonen, F.J., and Siddoway, C.S., 2011, Organizing melt flow through the crust: Elements: When the Continental Crust Melts, Ed(s) E.W. Sawyer et al., p. 261-288.

Bryant, J.A., Yogodzinski, G.M., Hall, M.L., Lewicki, J.L., and Bailey, D.G., 2006, Geochemical constraints on the origin of volcanic rocks from the Andean northern volcanic zone, Ecuador: Journal of Petrology, V. 47, N. 6, p. 1147-1175, doi: 10.1093/petrology/eg1006

Card, C.D., 2002, New investigations of basement to the western Athabasca basin: Saskatchewan Geological Survey Summary of Investigations 2002, v. 2, p. 1-17.

Card, C.D., Bethune, K.M., Davis, W.J., Rayner, N., and Ashton, K.E., 2014, The case for a distinct Taltson orogeny: Evidence form Northwest Saskatchewan, Canada: Precambrian Research, v. 255, p. 245 – 265.

Chiarenzelli, J.R., Lupulescu, M., Cousens, B., Thern, E., Coffin, L., and Regan, S., 2010, Enriched Grenbillian lithospheric mantle as a consequence of long-lived subduction beneath Laurentia: Geology, v. 38, p. 151-154

Chiarenzelli, J.R., Aspler, L., Villeneuve, M., and Lewry, J.,1998, Early Proterozoic evolution of the Saskatchewan craton and its allochthonous cover, Trans-Hudson orogen: Journal of Geology, v. 106, p. 247-267.

Chamberlain, K.R., Schmitt, A.K., Swapp, S.M., Harrison, M., Swoboda-Colberg, N., Bleeker, W., Peterson, T.D., Jefferson, C.W., and Khuduley, A.K., 2010, In situe U-Pb SIMS (IN-SIMS) micro-baddeleyite dating of mafic rocks: Method with examples: Precambrian Research, v. 183, p. 379-387.

Chapman, D.S., and Furlong, KI.P., 1992, Thermal state of the continental crust: Continental Lower Crust, Ed(s) D.M. Fountain et al., p. 179-198, Elsevier, Berlin.

Corrigan, D., Hajnal, Z., Nemeth, B., and Lucas, S.B., 2005, Tectonic framework of a Paleoproterozoic arc-continent to continent-continent collisional zone, Trans-Hudson Orogen, from geological and seismic reflection studies: Canadian Journal of Earth Sciences, v. 42, p. 421-434, doi: 10.1139/05-025.

Corrigan, D., Pehrsson, S., Wodicka, and de Kemp, E., 2009, The Paleoproterozoic Trans-Hudson Orogen: a prototype of modern accretionary processes: in Ancient Orogens and Modern Analogues, Ed(s)
Murphy et al., Geological Society of London, Special Publications, v. 327, p. 457-479, doi:10.1144/SP327.19.

Corrigan, D., Scott, D.J., and St-Onge, M.R., 2001, Geology of the northern margin of the Trans-Hudson Orogen (Foxe-Fold Belt), central Baffin Island, Nunavut: Geological Survey of Canada Current research 2001-C23, p.1-11.

Corrigan, D., Nadeau, L., Brouillette, P., Wodika, N., Houle, M.G. Tremblay, T., Machado, G., and Keating, P., 2013, Overview of GEM Multiple Metals-Melville Peninsula project, central Melville Peninsula, Nunavut: Geological Survey of Canada, Current Research, 2013-19, p. 1 – 17.

Cousens, B.L., Aspler, L.B., Chiarenzelli, J.R., Donaldson, J.A., Sandeman, H., Peterson, R.D., LeCheminant, A.N., 2001, Enriched Archean lithospheric mantle beneath western Churchill Province tapped during Paleoproterozoic orogenesis: Geology, v. 29, n. 9, p. 827-830.

Cousens, B.L., Aspler, L.B., and Chiarenzelli, J.R., 2004, Dual sources of ensimatic magmas, Hearne domain, western Churchill Province, Nunavut, Canada: Neoarchean "infant arc" processes?: Precambrian Research, v. 134, p. 169-188.

Cousens, B.L., 1998, Geochemistry and neodymium systematics of Archean and Proterozoic igneous rocks from the Angikuni and Yathkyed lakes areas, western Churchill Province, Northwest Territories: Indian Affair and Northern Development Canada, Open File EGS 1998-6, p. 1-41

Cutts, K.A., Stevens, G., Hoffmann, E., Buick, I.S., Frei, D., and Munker, C., 2014, Paleo- to Mesoarchean polymetamorphism in the Barberton Granite-Greenstone Belt, South Africa: Constraints from U-Pb monazite and Lu-Hf garnet geochronology on the tectonic processes that shaped the belt: Geological Society of America Bulletin, v. 126, n. ¾, p. 251-270.

Davis, W.J., Hanmer, S., and Sandeman, H.A., 2004, Temporal evolution of the Neoarchean central Hearne supracrustal belt: rapid generation of juvenile crust in a suprasubduction zone setting: Precambrian Research, v. 134, p. 85-112.

deCapitani, C. and K. Petrakakis, 2010, The computation of equilibrium assemblage diagrams with Theriak/Domino software: American Mineralogist,v. 95, n. 7, p. 1006-1016.

Dumond, G., McLean, N., Williams, M.L., Jercinovic, M.J., and Bowring, S.A., 2008, High resolution dating of granite petrogeneisis and deformation in a lower crustal shear zone: Athabasca granulite terrane, western Canadian Shield: Chemical Geology, v. 16, n. 4, p. 175-196, doi:10.1016/j.chemgeo.2008.04.014.

Dumond, G., Goncalves, P., Williams, M.L., and JHercinovic, M.J., 2010, Subhorizontal fabric in exhumed continental lower crust and implication for lower crustal flow: Athabasca granulite terrane, Western Canadian Shield: Tectonics, v. 29, TC2006, doi:10.1029/2009TC002514.

Dumond, G., Mahan, K.H., Williams, M.L., and Jercinovic, M.J., 2013, Transpressive uplift and exhumation of continental lower crust revealed by synkinematic monazite reactions: Lithosphere, v. 5, n. 5, p. 507-512, doi: 10.1130/L292.1

Dumond, G., Goncalves, P, Williams, M.L., and Jercinovic, M.J., 2013, UHT-HP Metamorphism in an exhumed lower crustal hot zone: GSA abstracts and Programs.

Eade, K.E., 1986, Precambrian geology of the Tulemalu Lake-Yathkyed Lake area, District of Keewatin: Geological Survey of Canada Paper, v. 84-11, p. 1-31.

Ernst, R., and Bleeker, W., 2010, Large igneous provinces (LIPs), giant dyke swarms, and mantle plumes: significance for breakup events within Canada and adjacent regions from 2.5 Ga to the present: Canadian Journal of Earth Sciences, v. 47, p. 695-739.

Flowers, R., Bowring, S.A., Mahan, K.H., and Williams, M.L., 2006a, Timescales and significance of high pressure, high-temperature metamorphism and mafic dike anatexis, Snowbird tectonic zone, Canada: Contribution to Mineralogy and Petrology, v. 151, n. 5, p. 558-581, doi:10.1007/s00410-006-0066-7.

Flowers, R.M., Mahan, K.H., Bowring, S.A., Williams, M.L., Pringle, M.S., and Hodges, K.V., 2006b,Multistage exhumation and juxtaposition of lower continental crust in the western Canadian Shield: linking high resolution U-Pb and $^{40}Ar/^{39}Ar$ thermochronometry with pressure-temperature-deformation paths: Tectonics, v. 25, TC4003, doi:10.1029/2005TC001912.

Flowers, R.M., Bowring, S.A., Mahan, K.H., Williams, M.L., and Williams, I.S., 2008, Stabilization and reactivation of cratonic lithosphere from the lower crustal record in the western Canadian shield: Contributions to Mineralogy and Petrology, v. 156, n. 4, p. 529-549, doi:10.1007/s00410-008-0301-5.

Frost, B.R., Barnes, C.O., Collins, W.J., Arculus, R.J., Ellis, D.J., and Frost, C.D., 2001, A geochemical classification for granitic rocks: Journal of Petrology, v. 42, p. 2033 – 2048.

Frost, B.R., and Frost, C.D., 2008a, A geochemical classification for feldspathic igneous rocks: Jounral of petrology, v. 49, n. 11, p. 1955 - 1969

Frost, B.R., and Frost, C.D., 2008b, On charnockites: Gondwana Research, v. 13, p. 30-44.

Furhman, M. L. and Lindsley, D. H., 1988. Ternary-feldspar modeling and thermometry: American Mineralogist, v. 73, p. 201–216.

Gehrels, G. and Pecha, M., 2014, Detrital zircon U-Pb geochronology and Hf isotope geochemistry of Paleozoic and Triassic passive margin strata of western North America: Geosphere, v. 10 (1), p. 49-65.

Gehrels, G. and Pecha, M., 2014, Detrital zircon U-Pb geochronology and Hf isotope geochemistry of Paleozoic and Triassic passive margin strata of western North America: Geosphere, v. 10 (1), p. 49-65.)

Gerbi, C., Culshaw, N., and Marsh, J., 2010, Magnitude of weakening during crustal-scale shear zone development: Journal of Structural Geology, v. 32, p. 107-117.

Gilboy, C.F., 1980, Bedrock compilation geology: Stony Rapids area (NTS 74p)-Prelimanary geological map, scale 1:250,000, Sask. Geol. Surv., Sask. Energy and mines, Regina.

Green, D. H. and Ringwood, A. E., 1967, An experimental investigation of the gabbro to eclogite transformation and its petrological applications: Geochimica et Cosmochimica Acta, v. 31, p. 767–833

Hamilton, W.B., 2011, Plate tectonics began in Neoproterozoic time, and plumes from deep mantle have never operated: Lithos, v. 123, p. 1-20.

Hanmer, S., Bowring, S.A., Van Breeman, O., and Parrish, R.R., 1992, Great Slave Lake shear zone, northwest Canada: mylonitic record of Early Proterozoic convergence, collision, and indentation: Journal of Structural Geology, v. 14, p. 757-773.

Hanmer, S., 1994, Geology, East Athabasca mylonite triange, Saskatchewan, Map 1859A, scale 1:100,000, Geol. Surv. Of Can., Ottawa.

Hanmer, S., 1997, Geology of the Striding-Athabasca mylonite zone, northern Saskatchewan and southeastern District of Mackenzie, Northwest Territories: Pap. Geol. Surv., of Can., Ottawa.

Hanmer, S., Parrish, R., Williams, M., and Kopf, C., 1994, Striding-Athabasca Mylonite: Complex Archean deep crustal deformation in the East Athabasca mylonite triangle, N. Saskatchewan: Canadian Journal of Earth Sciences, v. 31, p. 1287-1300, doi:10.1139/e94-111.

Hanmer, S., Williams, M., and Kopf, C., 1995, Modest movements, spectacular fabrics in an intracontinental deep-crustal strike-slip fault: Striding-Athabasca mylonite zone, NW Canadian Shield: Journal of Structural Geology, v. 17, n. 4, p. 493-507, doi:10.1016/0191-8141(94)00070-G.

Hanmer, S., and Williams, M.L., 2001, Targeted fieldwork in the Daly Bay Complex, Hudson Bay, Nunavut: Geological Survey of Canada Current Research 2001-C15, p. 1-26.

Hanmer, S., Sandeman, H.A., Davis, W.J., Aspler, L.B., Rainbird, R.H., Ryan. J.J., Relt, C., Roest, W.R., Peterson, T.D., 2004, Neoarchean tectonic setting of the Central Hearne supracrustal belt, western Churchill Province, Nunavut, Canada: Precambrian Research, v. 134, p. 63-83.

Herzberg, C., and Rudnick, R., 2012, Formation of cratonic lithosphere: an integrated thermal and petrological model: Lithos, v. 149, p. 4-15.

Hildebrand, R.S., Hoffman, P.F., and Bowring, S.A., 2010, the Calderian orogeny in Wopmay orogen (1.9 Ga), northwestern Canadian Shield: Geological Society of America Bulletin, v. 122, p. 794-814, doi: 10.1130/B26521.1

Hoffman, P.F., 1988, United Plates of America, the birth of a craton: Early Proterozoic assembly and growth of Laurentia: Annual Review of Earth and Planetary Sciences, v. 16, p. 543-603, doi:10.1146/annurev.ca.16.050188.002551.

Holland, T., and Powell, R., 1998, An internally consistent thermodynamic dataset for phases of petrological interest: Journal of Metamorphic Geology, v. 16, p. 309-343.

Holland, M.E., Williams, M.L., and Regan, S.P., 2012, The mary reaction: timing deep crustal deformation and metamorphism with implications for strengthening and stabilization of flowing lower crust: NEGSA 47th abstracts with programs.

Hynes, A., 2014, How feasible was subduction in the Archean?: Canadian Journal of Earth Sciences, v. 51, n. 3, p. 286-296.

Jercinovic, M.J., Williams, M.L., and Lane, E.D., 2008, In-situ trace element analysis of monazite and other fine-grained accessory minerals by EPMA: Chemical Geology, v. 254, p. 197-215.

Karlstrom, K.E., and Bowring, S.A., 1988, Early Proterozoic assembly of tectonostratigraphic terranes in south-western North America: The Journal of Geology, v. 96, p. 561–576.

Kinny, P.D., and Maas, R.2003, Lu-Hf and Sm-Nd isotope systems in zircon: in Zircon, Hanchar, J.M., and Hoskin, P.W.O. ed(s), Zircon: Reviews of Mineralogy and Geochemistry, v. 53, p. 327-341.

Klepeis, K. A., G. L. Clarke, G. Gehrels, and J. Vervoort (2004), Processes controlling vertical coupling and decoupling between the upper and lower crust of orogens: Results from Fiordland, New Zealand, Journal of Structural Geology, v. 26, n. 4, p. 765–791, doi:10.1016/j.jsg.2003.08.012

Koteas, G.C., Williams, M.L., Seaman, S.J., and Dumond, G., 2010, Granite genesis and mafic-felsic magma interaction in the lower crust: Geology, v. 38, p. 1067-1070, doi:10.1130/G31017.1.

Krikorian, L., 2002, Geology of the Wholdaia Lake Segment of the Snowbird Tectonic Zone, Northwest Territories (Nunavut): A view of the deep crust during the assembly and stabilization of the Laurentian craton: MSc Thesis, Advisor: Michael L. Williams, University of Massachusetts, Amherst.

Leslie, S.R., Mahan, K.H., Regan, S., Williams, M.L., and Dumond, G., *in review*, Contrasts in sillimanite deformation in felsic tectonites from anhydrous granulite- and anhydrous amphibolite-facies shear zones, western Canadian Shield: submitted to Journal of Structural Geology.

Leslie, S., 2012, Contrasts in sillimanite deformation in felsic tectonites from anhydrous granulite- and hydrous amphibolite-facies shear zones, western Canadian Shield [M.S.: University of Colorado, 69 p.

Lewry, J.F., and Sibbald, T.I.I., 1980, Thermotectonic evolution of the Churchill Province in northern Saskatchewan: Tectonophysics, v. 68, p. 45-82.

Loveridge, W.D., Eade, K.E., and Sullivan, R.W., 1988, Geochronological studies from Precambrian rocks from the southern District of Keewatin: Geological Survey of Canada Paper, v. 88-18, p. 1 – 36.

Macdonald, R., 1980, New edition of the geological map of Saskatchewan, Precambrian Shield area, in Summary of Investigations, Misc. Rep. 01-4.2, p. 19-21, Sask. Geol. Surv., Sask. Ind. And Resour, Regina.

Mader, U., Percival, J.A., and Berman, R.G., 1994, Thermobarometry of garnet-clinopyroxene-hornblende granulites from the Kapuskasing structural zone: Canadian Journal of Earth Sciences, v. 31, p. 1134-1145.

MacHattie, T.G., Geochemistry and geochronology of the late Archean Prince Albert group (PAg), Nunavut, Canada: Ph.D. thesis, University of Alberta, p. 1 - 340

MacLachlan, K., Davis, W., and Relt, C., 2005, U/Pb geochronological constraints on Neoarchean tectonism: Multiple compressional events in the Northwestern Hearne domain, western Churchill Province, Canada: Canadian Journal of Earth Sciences, v. 42, p. 85-109.

MacRae, N.D., Armitage, A.E., Miller, A.R., Roddick, J.C., Jones, A.L., and Mudry, M.P., 1996, The diamondiferous Akluilak lampophyre dyke, Gibson Lake area, NWT: Geological Survey of Canada Open File, v. 3228, p. 101-107.

Mahan, K.H., Williams, M.L., and Baldwin, J.A., 2003, Contractional uplift of deep crustal rocks along the Legs Lake shear zone, western Churchill Province, Canadian Shield: Canadian Journal of Earth Sciences, v. 40, n. 8, p. 1085-1110, doi:10.1139/e03-039.

Mahan, K.H., and Williams, M.L., 2005, Reconstruction of a large deep-crustal terrane: Implication for the Snowbird tectonic zone and early growth of Laurentia: Geology, v. 33, n. 5, p. 385-388, doi:10.1130/G21273.1.

Mahan, K.H., Goncalves, P., Williams, M.L., and Jercinovic, M.J., 2006a, Dating metamorphic reactions and fluid flow: Application to exhumation of high-P granulites in a crustal-scale shear zone, western Canadian Shield: Journal of Metamorphic Geology, v. 24, n. 3, p. 193-217, doi:10.1111/j.1525-1314.2006.00633.x.

Mahan, K.H., Williams, M.L., Flowers, R.M., Jercinovic, M.J., Baldwin, J.A., and Bowring, S.A., 2006b, Geochronological constraints on the Legs Lake shear zone with implications for regional exhumation of lower continental crust, western Churchill Province, Canadian Shield: Contributions to Mineralogy and Petrology, V. 152, n. 2, p. 223-242, doi:10.1007/s00410-006-0106-3.

Mahan, K.H., Goncalves, P., Flowers, R., Williams, M.L., and Hoffman-Setka, D., 2008, The role of heterogeneous strain in the development and preservation of a polymetamorphic record in high-P granulites, western Canadian Shield: Journal of metamorphic geology, v. 26, n. 6, p. 669-694, doi:10:111/j.1525-1314.2008.00783.x.

Mahan, K.H., Smit, C.A., Williams, M.L., Dumond, G., and Van Reenan, D.D., 2011a, Heterogeneous strain and polymetamorphism in high-grade terranes: Insight into crustal processes from the Athabasca Granulite Terrane, western Canada, and the Limpopo Complex, southern Africa: in van Reenen, D.D., Kramers, J.D., McCourt, S., and Perchuk, L.L., eds., Origin and evolution of Precambrain High-Grade Gneiss terranes, with Special Emphasis on the Limpopo Complex of Southern Africa: GSA Memoir, V. 207, p. 269-287, doi:10.1130/2011.1207(14).

Mancktelow, N. S., and G. Pennacchioni (2004), Theinfluence of grain boundary fluids on the micro-structure of quartz-feldspar mylonites,Journal of Structural Geology, v. 26, n.1, p. 47–69, doi:10.1016/S0191-8141(03)00081-6

Martel, E., van Breeman, O., Berman, R.G., and Pehrsson, S., 2008, Geochronology and tectonometamorphic history of the Snowbird Lake area, Northwest Territories, Canada: New insights into the architecture and significance of the Snowbird tectonic zone: Precambrian Research, v. 161, n. 3-4, p. 201-230, doi:10.1016/j.precamres.2007.07.007.

Maxeiner, R.O., and Rayner, N., 2010, continental arc magmatism along the southeast Hearne Craton margin in Saskatchewan, Canada: Comparison of the 1.92 – 1.91 Ga Porter Bay Complex and the 1.86 – 1.85 Ga Wathaman batholith: Precambrian Research, v. 184, p. 93 – 120.

Mezger, K., 1992, Temporal evolution of regional granulite terranes: Implication for the formation of lowermost continental crust: Continental Lower Crust, Ed(s): R.M. Fountain et al., p. 447-472.

Nicolas, A., and Poirier, J.P., 1976, Crystalline plasticity and solid state flow in metamorphic rocks: Selected Topics in Geological Sciences, ed. M.H.P. Bott, John Wiley and Sons, p. 444

Pehrsson, S.J., Berman, R.G., Elington, B., and Rainbird, R., 2013, Two Neoarchean supercontinents revisited: The case for a Rae family of cratons: Precambrian Research, v. 232, p. 27-43.

Pehrsson, S.,J., Jenner, G., and Kjarsgaard, B.A., 2002, The Ketyet River Group: correlation with Paleoproterozoic supracrustal sequences of northeastern Rae and implications for Proterozoic orogenesis in the western Churchill Province: Geological Association of Canada Annual Meeting, p. 90

Percival, J.A., 1992, Exposed crustal cross sections as windows on the lower crust: in Continental Lower Crust, ed(s): D.M. Fountain et al., pp. 317-362, Elsevier, Amsterdam.

Petts, D.C., Davis, W.J., Moser, D.E., and Longstaffe, F.J., 2014, Age and evolution of the lower crust beneath the western Churchill Province: u-Pb zircon geochronology of kimberlite-hosted granulite xenoliths, Nunavut, Canada: Precambrian Research, v. 241, p. 129-145.

Pouchou, J.L., and Pichoir, F., 1984, Possibilités d'analyse en profondeur à la microsonde électronique: *Recherche Aérospatiale, v. 5, p. 349-351.*

Rainbird, R.H., Davis, W.J., Pehrsson, S.J., Wodicka, N., Rayner, N., and Skulski, T., 2010, Early Paleoproterozoic supracrustal assemblages of the Rae domain, Nunavut, Canada: intracratonic basin development during supercontinent break-up and assembly: Precambrian Research, v. 181, p. 166-186.

Regan, S.P., Williams, M.L., Leslie, S.R., Mahan, K.H., Jercinovic, M.J., and Holland, M.E., 2014, The Cora Lake shear zone, Athabasca granulite terrane (Snowbird Tectonic Zone), an intraplate response to far-field orogenic processes during the amalgamation of Laurentia: Canadian Journal of Earth Sciences

Relf, C., and Hanmer, S., 2000, A speculative and critical summary of the current state of knowledge of the western Churchill province: A NATMAP perspective: Geological Association of Canada-Mineralogical Association of Canada Abstracts, v. 25, p. 857.

Rhodes, J.M., 1996, Geochemical stratigraphy of lava flows sampled by the Hawaii Scientific Drilling Project: Journal of Geophysical Research, v. 101, n. B5, p. 11,729-11,746.

Ross, G.M., Broome, J., and Miles, W., 1994, Potential fields and basement structure – western Canada sedimentary basin: *in* Geological Atlas of the Western Canada Sedimentary Basin, G.D. Mossop and I. Shetsen (comp.), Canadian Society of Petroleum Geologists and Alberta Research Council, URL <http://www.ags.gov.ab.ca/publications/wcsb_atlas/atlas.html>, [Date last accessed online].

Ross, G.M., Eaton, D.W., Boerner, D.E., and Miles, W., 2000, Tectonic entrapment and its role in the evolution of continental sphere: an example from the Precambrian of western Canada: Tectonics, v. 19, p. 116-134.

Rudnick, R.L., and Fountain, D.M., 1995, Nature and composition of the continental crust: A lower crustal perspective: Reviews of Geophysics, v. 33, n. 3, p. 267-309.

Rutter, E.H., and Brodie, K.H., 1992, Rheology of the lower crust: Contental Lower Crust, Ed(s) D.M. Fountain et al., p. 201—267, Elsevier, Amsterdam.

Sanborn-Barrie, M., Carr, S.D., and Theriault, R., 2001, Geochronological constraints on metamorphism, magmatism, and exhumation of deep-crustal rocks of the Kramanitaur Complex with implications for the Paleoproterozoic evolution of the Archean western Churchill Province, Canada: Contributions to Mineralogy and Petrology, v. 141, p. 592-612.

Sanborn-Barrie, M., Chakungal, J., James, D., Rayner, N., and Whalen, J., 2014a, Precambrian bedrock geology, Southampton Island, Nunavut: Geological Survey of Canada Canadian Geoscience Map 132, 1:100,000

Sanborn-Barrie, M., Davis, W.J., Berman, R.G., Rayner, N., Skulski, T., and Sandeman, H., 2014b, Neoarchean-continental crust formation and Paleoproterozoic deformation of the central rae craton, Committee Bay belt, Nunavut: Canadian Journal of Earth Sciences, v. 51, p. 635 – 667.

Sandeman, H.A., Schultz, M., and Rubingh, K., 2005, Results of bedrock mapping of the Darby Lake-Arrowsmith River north map areas, central Rae Domain, Nunavut: Geological Survey of Canada, Current Research 2005-C2, p. 1-11.

Sandeman, H.A., Cousens, B.L., and Hemmingway, C.J., 2003, Continental Tholeiitic mafic rocks of the Paleoproterozoic Hurwitz Group, Central Hearne sub-domain, Nunavut: insight into the evolution of the Hearne sub-continental lithosphere: Canadian Journal of Earth Sciences, v. 40, p. 1219-1237.

Shirey, S.B., Kamber, B.S., Whitehouse, M.J., Mueller, P.A., and Basu, A.R., 2008, A review of the isotopic and trace element evidence for mantle and crustal processes in the Hadean and Achean: implications for the onset of plate tectonic subduction, *in* Condie, K.C. and Pease, V., *eds.*,When did Plate Tectonics Begin on Planet Earth?: Geological Society of America Special Paper 440, p. 1-29, doi: 10.1130/2008.2440(01).

Slimmon, W.L., 1989, Bedrock compilation geology: Fond du Lac (NTS 74-O): Saskatchewan Geological Survey, Saskatchewan Energy and Mines, Map 247A, scale 1:250,000.

Spear, F.S., 1993, Metamorphic phase equilibria and Pressure-Temperature-Time paths: 2nd edition, Mineralogical Society of America, Washington D.C., p. 799.

Tella, S., Eade, K.E., and Sullivan, R.W., 1988, Occurene and possible tectonic significance of high-pressure granulite fragments in the Tulemalu fault zone, District of Keewatin, N.W.T., Canada: Canadian Journal of Earth Sciences, v. 23, p. 1950-1962.

Van Kranendonk, 2010, Two types of Archean continentral crust: plume and plate tectonics on early earth: American Journal of Science, v. 310, p. 1187-1209.

Ward, D., 2010, The relative influence of quartz and mica on crustal seismic anisotropy [M.S.: University of Colorado, 89 p.

White, S.H., 1976, The effects of strain on the microstructures, fabrics, and deformation mechanisms in quartzites: Philosophical Transactions of the Royal Society of London A, v. 283, p. 69-86.

Whitmeyer, S.J., Karlstrom, K.E., 2007, Tectonic model for the Proterozoic growth of North America: Geosphere, v. 3, n. 4, p. 220-259.

Williams, M.L., and Hanmer, S., 2006, Structural and metamorphic processes in the lower crust: Evidence from a deep-crustal isobarically cooled terrane, Canada: Evolution and Differentiation of the Continental Crust, ed(s) M. Brown and T. Rushmer, p. 231-267, Cambridge University Press, Cambridge.

Williams, M.L., Hanmer, S., Kopf, C., and Darrach, M., 1995, Syntectonic generation and segregation of tonalitic melts from amphibolite dikes in the lower crust, Striding-Athabasca mylonite zone, northern Saskatchewan: Journal of Geophysical Research, V. 100, n. B8, p. 15,717-15,734, doi:10.1029/95JB00760.

Williams, M.L., Melis, E.A., Kopf, C.F., and Hanmer, S., 2000, Microstructural tectonometamorphic processes and the development of gneissic layering: A mechanism for metamorphic segregation: Journal of Metamorphic Geology, v. 18, p. 41-57, doi:10.1046/j.1525-1314.2000.00235.x.

Williams, M.L., and Flowers, R.M., 2008, The Chipman dyke swarm, Saskatchewan, Canada: Component of the 1.9 Ga Snowbird large igneous province in the western Canadian Shield: LIP of the Month, January, 2008: http://www.largeigneousprovinces.org/08jan

Williams, M.L., Karlstrom, K.E., Dumond, G., and Mahan, K.H., 2009, Perspectives on the architecture of continental crust from integrated field studies of exposed isobaric sections: in Miller, R.B., and Snoke, A.W., eds., Crustal Cross Sections from the Western North American Cordillera and Elsewhere: Implication for Tectonic and Petrologic Processes: GSA Special Paper 465, p. 219-241, doi:10.1130/2009.2456(08).

Williams, M.L., Mahan, K.H., Dumond, G., Jercinovic, M.J., Regan, S.P., and Leslie, S., 2011, Linking metamorphism and deformation using in-situ monazite geochronology: interpretation of multistage tectonic histories: GSA annual meeting, Minneapolis, MN.

Williams, M.L., and Jercinovic, M.J., 2012, Tectonic interpretation of metamorphic tectonites: integrating compositional mapping, microstructructural analysis and in situ monazite dating: Journal of Metamorphic Petrology, v. 30, p. 739-752

Williams, M.L., Mahan, K., Dumond, G., Regan, S., and Holland, M., in prep, Garnet-forming reactions in felsic orthogneiss: implications for strengthening and densification of the lower continental crust: to be submitted to the Journal of Metamorphic Petrology